Experimental Studies of N_2- and CO_2-Foam Properties in Relation to Enhanced Oil Recovery Applications

Jonas Stensbye Solbakken

Dissertation for the degree of Philosophiae Doctor (PhD)

University of Bergen

Norway

2015

Dissertation date: June 1

Year: 2015

Title: Experimental Studies of N_2- and CO_2-Foam Properties in Relation to Enhanced Oil Recovery Applications

Author: Jonas Stensbye Solbakken

Print: AIT OSLO AS / University of Bergen

The problem is that most complex systems are counterintuitive;

they do not behave the way we think they do.

It is the structure of the entire system that gives it the behavior.

Jay W. Forrester

Scientific Environment

This dissertation was submitted March 11, 2015, as a part of the fulfillment for the degree of Philosophiae Doctor (PhD) at the University of Bergen (UoB), department of Chemistry. The thesis is based on experimental work performed at the Centre for Integrated Petroleum Research (Uni CIPR) in the period 2010-2014. The project has been a part of a larger research effort, the PETROMAKS program (2004-2013) sponsored by the Research Council of Norway.

Supervisor:

Dr. Morten Gunnar Aarra (Uni CIPR)

…….

Co-supervisor:

Professor Arne Skauge (Uni CIPR/UoB)

…….

Acknowledgements

The last ~4.5 years have been the most exciting and challenging period in my life so far. I want to use this opportunity to thank at least some of the people who have supported me in one way or another during this period.

I wish to express my gratitude to my supervisor Dr. Morten G. Aarra; thank you for sharing your knowledge with me, for your personal encouragement, and for the many good discussions.

My co-supervisor, Professor Arne Skauge, deserves a special thank as well; thank you for scientific advice and assistance throughout the work, for giving me the opportunity to participate as a Master and PhD student at Uni CIPR, and for offering me a permanent position thereafter.

Acknowledge goes to Hege Ommedal for her support as PhD-coordinator at the department of Chemistry.

I am also thankful to other past and present colleagues at Uni CIPR who have made this time enjoyable, especially, Annette Meland Johannessen, Edin Alagic, Bartek Vik, Behruz Shaker Shiran, Abduljelil Sultan Kedir, Nematollah Zamani, Per Arne Ormehaug, Tormod Skauge, Sverre Hetland, Ketil Djurhuus, Kristine Spildo, Tore Skodvin, Reza Alikarami, Anita Torabi and Eivind Bastesen.

Thanks to my friends; Hans, Daniel, Eddy, Espen and Karl-Erik for reminding me of a world outside foam bubbles and rocks.

Finally, I would like to thank my family for all their love, patience and constant support; my dear mother and father, Berit Stensbye and Roald Solbakken, my beloved, Birthe Tvedt, my family in-law, Nina, Terje and Anette, and last but not least, my little sunshine in life, Emilie. I love you!

Abstract

Foams can do more than soften a beard or extinguish a fire. Foam also offers the oil industry better mobility control. The presence of a foaming agent in porous rocks can reduce the mobility of gas and water, stabilize the gas injection front and prevent unwanted production of gas and water. These unique properties can assist the reservoir engineer in different optimization processes to enhance oil recovery (EOR) and improve the economics of mature oil fields.

A number of factors influence the properties of foam, such as the foaming agent, gas type, rock properties, interactions with oil, injection strategies, and temperature and pressure conditions. A change in one or several of these parameters may affect the performance of the foam and, consequently, the success of the intended foam application. For that reason, it is important to understand foam on a broad experimental scale.

This thesis presents experimental studies of foam in bulk and porous media.

The studies in porous media investigated: I) CO_2-foam properties compared with those of N_2-foams and II) the impact of rock material on foam generation performance and mobility control. The experiments were performed in oil-free outcrop sandstone core samples in the range of 30-280 bar and 50-100°C using alpha-olefin sulfonate ($AOS_{C14-C16}$) surfactant.

The studies in bulk evaluated a set of foaming agents relative to: I) various experimental methods (bulk tests, core flooding), II) different gas types (CO_2, N_2, air) and III) the absence and presence of oils (crude oils, alkanes). A new bulk test was designed in the thesis to allow foams with gases other than air to be studied under low pressure. The combination of several experimental approaches was introduced to improve the evaluation and screening of surfactants.

The experimental results obtained in this thesis show that the presence of different gas types (CO_2, N_2) strongly influences the properties of foam in bulk and in porous media.

The CO_2-foams were inherently weaker than the N_2-foams. Possible reasons for the apparent weakness of the CO_2-foam compared with the N_2-foam were investigated more closely. A good correlation between the CO_2-density and the CO_2-foam strength was found; conditions where the density of CO_2 is low improved the CO_2-foam strength. Also, new foam experiments with pre-equilibrated fluids were conducted. These experiments suggested that the kinetics of the mass transfer between CO_2 and the surfactant solution could not be the main cause why the CO_2-foams were weaker than the N_2-foams. However, the use of pre-equilibrated fluids significantly improved the water-blocking capabilities of the CO_2-foams, indicating that gas dissolution into the injected water is one of the predominant mechanisms that weaken the CO_2-foams during liquid injection following generation.

N_2-foam experiments in various outcrop sandstone core samples showed that the rock material is one of the main parameters controlling the in-situ foam generation performance. The results demonstrated that foam was able to be generated and reduce mobility in all the sandstone cores used under all the conditions listed above. However, large variations in foam strength and mobility control were obtained between the different core samples. The presence of low permeability laminated heterogeneities, detected through various types of core analysis, appeared to be one of the parameters affecting the foam generation performance. The detailed interactions between the rock surface properties and the thin liquid films were beyond the scope of this thesis, but are suggested to be of central importance to in-situ foam generation performance.

The combination of several experimental techniques, including the new bulk test, was shown to be valuable for improving the evaluation and screening of foamers in the absence and presence of oil. Although certain similarities and interesting trends were observed between the experiments in bulk and porous media, the bulk foam properties of this work did not generally correlate with the foam properties in porous media. It seems difficult to predict foam properties and performance separate from the porous media by means of simpler experimental methods.

It is hoped that the laboratory-derived results presented in this dissertation will contribute to generate new insights and ideas within the field of foam, provide valuable input to reservoir models and simulations, and suggest practical considerations towards the scaling of foam processes for different EOR applications.

List of Papers

Paper 1:

Properties of CO_2- and N_2-Foams as a Function of Pressure.

Authors: Morten G. Aarra, Arne Skauge, Jonas S. Solbakken and Per A. Ormehaug.

Published manuscript, Journal of Petroleum Science and Engineering 116, 72-80, March, **2014**.

Paper 2:

Supercritical CO_2-foam - The Importance of CO_2 Density on Foams Performance.

Authors: Jonas S. Solbakken, Arne Skauge and Morten G. Aarra.

Presented at the SPE Enhanced Oil Recovery Conference, Kuala Lumpur, July, **2013**.

Paper 3:

Foam Performance in Low Permeability Laminated Sandstones.

Authors: Jonas S. Solbakken, Arne Skauge and Morten G. Aarra.

Published manuscript, Energy & Fuels, 28, 803-815, January, **2014.**

Paper 4 (Internal report):

Surfactant Evaluation and Oil Interactions with Foams under Static and Dynamic Conditions.

Author: Jonas S. Solbakken.

Research report, UniCIPR, June, **2013.**

All four papers are attached to the last part of this thesis.

Table of Contents

Scientific Environment

Acknowledgments

Abstract

List of Papers

Table of Contents

List of Tables

List of Figures

Nomenclature

Unit Conversions

Chapter 1: Introduction **p. 1-14**

1.1 Energy demand 1

1.2 Current oil recovery factors and future perspectives 2

1.3 Oil recovery maximization 2

1.4 Gas-based-EOR: current interests, advantages and limitations 5

1.5 Foam for EOR 8

1.6 Foam applications 9

1.7 Oil industry's interests in foam 9

1.8 Foam properties 11

1.9 Scope and objectives 12

1.10 Paper contents and thesis structure 12

Chapter 2: Foam Fundamentals **p. 15-26**

2.1 Basic foam properties 15

2.2 Surfactants 18

2.3 Surfactant selection 22

2.4 Choice of surfactant in this thesis 24

Chapter 3: Foam Stability **p. 27-36**
3.1 Introduction 27
3.2 Gravity drainage and capillary action 28
3.3 Film forces and disjoining pressure 29
3.4 Surface elasticity 33
3.5 Gas diffusion 34

Chapter 4: Foam in Porous Media **p. 37-58**
4.1 Rock properties 38
4.1.1 Absolute permeability 40
4.1.2 Lithology 40
4.1.3 Heterogeneity 41
4.2 In-situ foam generation mechanisms 43
4.2.1 Snap-off 43
4.2.2 Lamella division 44
4.2.3 Leave-behind 44
4.2.4 Pinch-off 46
4.3 Foam mobility control 47
4.4 Foam texture 48
4.5 Foam flow 49
4.5.1 Making and breaking vs. bubble train 49
4.5.2 Flow at the limiting capillary pressure 49
4.5.3 Flow regimes 50
4.5.4 Foam propagation 52
4.6 Foam stability to subsequent fluids 53
4.7 Foam sensitivity to rock properties 54
4.7.1 Permeability 54
4.7.2 Rock heterogeneity 54
4.7.3 Wettability/lithological effects 57

Chapter 5: Gas Characteristics and the Effect of Gas Type on Foam Properties p. 59-84
5.1 Introduction 59
5.2 Carbon dioxide 62
5.3 Nitrogen 63

5.4 Physical and chemical gas characteristics (CO_2 vs. N_2) 65
5.4.1 Gas density 65
5.4.2 Gas viscosity 67
5.4.3 Gas/water solubility 68
5.4.4 Gas compressibility 71
5.4.5 pH 72
5.4.6 pH-induced wettability shifts and chemical reactions of the porous media 73
5.4.7 Surface tension - classification and expected values 75
5.4.8 Summary of the characteristics of CO_2 79
5.5 Type of surfactant against different gas components 80
5.6 Foam mobility control with pressure and temperature 82

Chapter 6: Foam-Oil Interactions p. 85-94
6.1 Introduction 85
6.2 Foam-oil interaction theories 86
6.2.1 Spreading and entering coefficients 87
6.2.2 Bridging coefficient 88
6.2.3 Lamella number 89
6.2.4 Pseudo-emulsion film theory 91
6.3 Practical viewpoints 92

Chapter 7: Foam Experimental Methods p. 95-110
7.1 Experimental methods
95 7.2 Bulk tests 95
7.2.1 Mixer method 96
7.2.2 Filter test 97
7.3 Bulk foam properties vs. foam properties in porous media 98
7.4 Foam core flooding 99
7.4.1 Characterizing foam efficiency in corefloods 101
7.5 Experiments at HPHT (special considerations) 105
7.6 Phase equilibration 109

Chapter 8: Results and Discussions **p. 111-180**

8.1 Introduction 112

8.2 CO_2-foam properties compared with N_2-foams 113

8.2.1 Experimental strategy 113

8.2.2 Foam properties as a function of pressure 114

8.2.3 Effect of mass transfer on CO_2-foam properties 121

8.2.4 CO_2-foam strength vs. CO_2-density 126

8.2.5 Experimental observations 128

8.2.6 Summary and discussion 130

8.3 Effect of rock properties on foam 144

8.3.1 Experimental strategy 144

8.3.2 Rock core analyses 145

8.3.3 Foam generation performance in low permeability laminated sandstone cores 149

8.3.4 Summary and discussion 151

8.4 Surfactant screening and bulk foam-oil interactions 156

8.4.1 Experimental strategy 156

8.4.2 Surfactant screening in the absence of oil 157

8.4.3 Bulk foam-oil interactions 163

8.5 Summary and Conclusions 174

Appendix – Experimental Protocols **p.181-190**

A. Fluid properties 181

B. Core properties 184

C. Experimental summary – foam core flooding 187

D. Experimental history to each core 188

References **p.191-212**

Papers (1-4) **p.213-end**

List of Figures

Chapter 1:
Figure 1.1 (p. 5): The recovery efficiency from gas injections may be low due to (a) poor microscopic sweep efficiency, E_D; (b) poor volumetric (areal/vertical) sweep, E_V; (c) viscous fingering problems; (d) gas override; or (e) gas channeling through highly permeable intervals ("thief zones") (modified from Hanssen et al., 1994).

Figure 1.2 (p. 6): Evolution of CO_2 projects and oil prices in the U.S. – based on data from Oil & Gas Journal EOR Surveys 1980-2010 and U.S. EIA 2010 (adapted from Alvarado and Manrique, 2010).

Figure 1.3 (p. 8): Illustration of (a) foam components and (b) foam structures (from this thesis).

Figure 1.4 (p. 9): Applications of foam for EOR: (a) support gas injections with mobility control to combat viscous fingering, gas overrides, or excessive flow of gas through highly permeable "thief zones" in the reservoir; (b) prevent unwanted fluids from coning, cusping or channeling into the production wells (adapted from Vikingstad, 2006).

Chapter 2:
Figure 2.1 (p. 15): (a) "Boy blowing bubbles", 1867 (Édouard Manet, 1832-1883) (from www.wikiart.org); (b) bulk foam structure comprising thin liquid lamellae connected in Plateau borders (from Schramm and Wassmuth, 1994).

Figure 2.2 (p. 17): Pressure differences between bubbles (adapted from http://math.berkeley.edu).

Figure 2.3 (p. 18): Images of bulk foam structures stabilized by surfactant (from Paper 4): (a) wet foam structure with spherical bubble shapes; (b) dry foam structure with polyhedral-like geometries (mainly penta-, hexa- and heptagonal shapes). For stable foams, the bulk structure can change from (a) spherical to (b) polyhedral over time.

Figure 2.4 (p. 19): Illustration of (a) surfactant molecules and classification according to the charge of the polar head group; (b) classification of surfactant functions based on the HLB number, w = water, o = oil (adapted from Aulton and Taylor, 2013).

Figure 2.5 (p. 20): Orientation of surfactant molecules (monomers) in thin liquid films (modified from Schramm and Wassmuth, 1994).

Figure 2.6 (p. 20): Surfactant associations in thin liquid films (left image from Paper 4; right figure modified from Schramm and Wassmuth, 1994).

Figure 2.7 (p. 21): Diagram illustrating the distinct changes in solution properties that occur at the cmc (from Pashley and Karaman, 2004).

Figure 2.8 (p. 22): Micelle structures (redrawn from Evans and Wennerström, 1999).

Figure 2.9 (p. 25): Generalized molecular structure of an alkene sulfonate (Na^+ is only used as an example of a counterion in the figure) (redrawn from Enick and Olsen, 2012).

Chapter 3:

Figure 3.1 (p. 29): a) Illustration of a dry foam structure with water resided in the Plateau borders. b) A pressure gradient in the continuous liquid phase causes thinning of the lamellae due to the flow of water toward the Plateau borders (modified from Weaire and Hutzler, 1999).

Figure 3.2 (p. 30): A simplified illustration of an electrical double layer in a foam lamella (adapted from www.soft-matter.seas.harvard.edu).

Figure 3.3 (p. 31): Illustration of disjoining pressure in thin liquid films (modified from Weaire and Hutzler, 1999).

Figure 3.4 (p. 32): Illustration of an idealized disjoining pressure isotherm (bold curve) (explained in Aronson et al., 1994). Force contributions from electrostatic (π_R), van der Waals (π_A), steric forces (π_S) and two capillary pressures ($P_{C2} > P_{C1}$) are represented. The repulsive steric forces are shorter in range than the attractive van der Waals forces and the repulsive electrostatic forces (adapted from Aronson et al., 1994).

Figure 3.5 (p. 34): Surface elasticity in a foam film (modified from Schramm and Wassmuth, 1994).

Figure 3.6 (p. 36): Larger bubbles grow at the expense of smaller bubbles due to gas diffusion across liquid films and between foam bubbles. The effect causes foam coarsening or collapse of the foam structure (adapted from Paper 4).

Chapter 4:

Figure 4.1 (p. 38): a) Theoretical packing of spherical grains of uniform diameter with available pore space/porosity (in white) given as a percentage (from Selley, 1998). b) Thin section of an outcrop Berea sandstone showing grains (white/gray) and pore space (pale blue) in natural porous rocks (from Paper 3). c) Illustration of a porous core plug with an interconnected network of pore spaces from inlet to outlet (modified from Solbakken, 2010).

Figure 4.2 (p. 39): X-ray image of gas injection (yellow) into a laminated Berea rock sample saturated with water (orange). Favored gas flow is indicated by the more permeable streaks of the rock, leaving the lower permeable areas of the rock sample unswept. The illustration should be considered more illustrative than complete (modified from Paper 3).

Figure 4.3 (p. 42): X-ray image of a naturally laminated Berea rock sample. The darker regions in the sample represent the laminas, $K_h \approx 90$ mD and $K_v \approx 45$ mD (from Paper 3).

Figure 4.4 (p. 45): Schematic illustration of in-situ foam generation mechanisms: a) snap-off, b) lamella division and c) leave behind. The arrows indicate the direction of flow direction, and gas, surfactant solution and spherical rock grains are indicated by white, gray and striped shading, respectively (from Kovscek and Radke, 1994).

Figure 4.5 (p. 46): Observation of two novel in-situ foam generation mechanisms: a) the neighbor-wall pinch off mechanism and b) the neighbor-neighbor pinch off mechanism (adapted from Liontas et al., 2013).

Figure 4.6 (p. 48): Examples of foam texture observations in a sight-glass out from the core under experimental conditions, 280 bar, 50°C (from Paper 1): a) N_2-foam (finer/denser texture – mobility reduction factor ≈ 120). b) CO_2-foam (coarser texture – mobility reduction factor ≈ 3).

Figure 4.7 (p. 50): Schematic illustration of the limiting capillary pressure theory of foam flow in porous media based on the gas/water drainage capillary pressure curve (from Farajzadeh et al., 2012, a similar illustration can also found in Khatib et al., 1988).

Figure 4.8 (p. 51): Schematic illustration of the two flow regimes presented as a contour plot (from Alvarez et al., 2001).

Figure 4.9 (p. 55): Distinction between a) foam mobility-control agent and b) foam blocking agent in a layered reservoir (from Seright, 1996).

Chapter 5:

Figure 5.1 (p. 63): Phase diagram of carbon dioxide (CO_2) as a function of pressure and temperature (modified from Wolfram|Alpha knowledgebase, 2013, http://www.wolframalpha.com). The yellow dots represent the experimental conditions for CO_2 used in this project.

Figure 5.2 (p. 64): Phase diagram of nitrogen as a function of pressure and temperature (modified from Wolfram|Alpha knowledgebase, 2013, http://www.wolframalpha.com). The yellow dots represent the experimental conditions for N_2 used in this project.

Figure 5.3 (p. 65): Comparison of the CO_2 and N_2 density (data from the NIST Chemistry WebBook). The yellow dots illustrate the approximate gas densities in the experiments performed in this project.

Figure 5.4 (p. 66): CO_2 density as a function of pressure and temperature. The black dashed line illustrates the anticipated trend of the CO_2 density in the reservoirs, assuming a hydrostatic pressure gradient of ~ 80 bar/km and a geothermal gradient of 30°C/km (from Gunter et al., 2004). The yellow dots illustrate the approximate gas densities in the experiments performed in this project.

Figure 5.5 (p. 67): Comparison of the CO_2 and N_2 viscosity (data from the NIST Chemistry WebBook). The yellow dots illustrate the approximate gas viscosities in the experiments performed in this project.

Figure 5.6 (p. 69): Comparison of the CO_2 and N_2 solubility in pure water and aqueous solutions of 3.6 wt. % NaCl (data calculated from http://www0.geochem-model.org/models/co2-sea/). The inset shows the N_2 solubility in water. The yellow dots illustrate the approximate gas solubilities in brine under the experimental conditions in this project.

Figure 5.7 (p. 70): Comparison of the water solubility in a) CO_2 (from Choi and Nesic, 2009) and b) N_2 (modified from Mohammadi et al., 2005).

Figure 5.8 (p. 72): The pH of CO_2-saturated water as a function of pressure and various temperatures (from Choi and Nesic, 2009). The yellow dots indicate the typical pH levels expected from the CO_2 experiments with the pre-equilibrated fluids in this project.

Figure 5.9 (p. 74): Adhesion maps of oil and water as a function of salinity and pH. a) Buckley, (1996) illustrating three regions of tentative unstable, stable and conditionally stable water films (based on the disjoining pressure isotherms) and b) Drummond and Israelachvili, (2002) illustrating three regions of tentative intermediate, water-wet and oil-wet wettability regimes (based on the static contact angle measurements). At a low pH and at moderate salinities, both of the maps reflect conditions under which the water film could be less stable and not completely wetting.

Chapter 6:

Figure 6.1 (p. 87): Illustration of the different entering and spreading scenarios of an oil phase in contact with a lamella (from this thesis).

Figure 6.2 (p. 88): Example of a) stable oil bridge and b) unstable oil bridge (from this thesis).

Figure 6.3 (p. 90): Illustration of type A, B and C foams, as defined by the lamella number (L), in contact with an oil phase (from Schramm and Novosad, 1990).

Figure 6.4 (p. 91): Pseudo-emulsion film stability (from this thesis).

Chapter 7:

Figure 7.1 (p. 96): Experimental setup for the mixer method (adapted from Paper 4).

Figure 7.2 (p. 98): Experimental setup for the filter method (adapted from Paper 4).

Figure 7.3 (p. 100): Experimental setup for the high-pressure and high-temperature (HPHT) foam core flooding experiments (from this thesis).

Figure 7.4 (p. 100): Visualization of foam texture in HPHT foam experiments (from this thesis).

Figure 7.5 (p. 106): Core preparation (in this thesis).

Figure 7.6 (p. 106): Piston cylinder with rubber gaskets exposed to swelling by CO_2 in red (from this thesis).

Figure 7.7 (p. 107): Relationship between the pressure and volume of an ideal gas according to Boyles's law: A) at low system pressure, the change in gas volume is large for a small change in pressure (i.e., gas compressibility is large); B) at higher system pressure, the change in gas volume is much smaller for the same change in pressure; C) at high pressure, the change in gas volume is smallest for a given change in pressure (i.e., gas compressibility is small) (from in this thesis).

Chapter 8:

Figure 8.1 (p. 115): Mobility reduction factors of N_2- and CO_2-foams as a function of pressure at 50°C.

Figure 8.2 (p. 116): Average gas breakthrough times during foam core flooding under various system pressures at 50°C. The error bars are added to indicate the observed variation. Typical ranges of gas breakthroughs during baseline experiments (i.e., co-injection of 80% CO_2 or N_2 and 20% seawater without surfactant) are also included for comparison.

Figure 8.3 (p. 118): Images of foam texture from different foam experiments: (1-3) N_2-foam at 280 bar and 50°C with corresponding MRF and pore volumes injected; (4-6) N_2-foam at 30 bar and 50°C with corresponding MRF and pore volumes injected; (7-9) CO_2-foams as a function of pressure (30 bar, 120 bar and 280 bar at 50°C) with corresponding MRF after 3 PV injected. The diameter of the visual cell is 1.5 mm.

Figure 8.4 (p. 120): Apparent water relative permeabilities with pore volume seawater injected after foam generation under various system pressures and 50°C; after CO_2-foams (burgundy, yellow and purple lines, respectively); after N_2-foams (red and pale blue lines); after the baseline pressure experiment indicated in the upper blue line. The lines in the figure are drawn to guide the eye.

Figure 8.5 (p. 122): Mobility reduction factors of CO_2 foams (with and without pre-equilibrated fluids) at 30 bar and 120 bar and 50°C. The CO_2-foam experiments with pre-equilibrated fluids are shown by the green and yellow profiles (at 30 bar, 50°C) and the gray and orange profiles (at 120 bar, 50°C), respectively. The N_2-foam generation at 30 bar and 50°C is included for comparison.

Figure 8.6 (p. 123): Images of CO_2-foam textures at 30 bar and 120 bar and 50°C with corresponding MRFs after ~ 3 PV injected: (1-2) CO_2-foam textures with pre-equilibrated fluids; (3-4) CO_2-foam textures without pre-equilibrated fluids. The diameter of the visual cell is 1.5 mm.

Figure 8.7 (p. 125): Apparent water relative permeabilities with pore volume seawater injected after foam generation at 30 bar and 50°C: after CO_2-foam with pre-equilibrated fluids (black dashed lines); after CO_2-foam without phase-equilibration (red solid lines); after N_2-foam without phase-equilibration (blue dashed line). The lines in the figure are drawn to guide the eye.

Figure 8.8 (p. 125): Pressure drop histories during the early stage of seawater injection (8 ml/h) following steady-state foam generations at 30 bar and 50°C (i.e., before measurements of $k_{rw,app.}$). Seawater injection after CO_2-foam with pre-equilibrated fluids, CO_2-foam without phase-equilibration and N_2-foam are indicated by black, red and blue profiles, respectively.

Figure 8.9 (p. 127): Average MRF vs. CO_2 density. The dashed line is drawn to guide the eye.

Figure 8.10 (p. 145): X-ray images of the laminated core samples used in Paper 3. The horizontal lines in the images are noises.

Figure 8.11 (p. 148): a) 2D X-ray images of gravity-stable water injection in a low permeability laminated sandstone slab (left) versus high permeability/homogeneous sandstone slab (right). Images were taken at the tracer breakthrough in both cases. b) 2D X-ray images of gravity-stable N_2-gas injection in laminated (left) versus high permeability (right) sandstone rock material. Images were taken at close to 1 pore volume injection in both cases. c) 2D X-ray images of a regular N_2-gas injection into a brine saturated sample after 0.1 and 1.5 pore volumes with gas injection (upper left and right, respectively). N_2-gas injection into a surfactant saturated sample after 0.2 and 1.5 pore volumes with gas injection (lower left and right, respectively). All experiments in the figure were conducted under 2 bar backpressure at 25°C. The slab dimensions were constant of 10 cm (length) x 5 cm (width) x 1.5 cm (thickness). The horizontal lines in the images are noises.

Figure 8.12 (p. 149): Mobility reduction factors obtained during N_2-foam generations on three low permeability laminated core samples under different elevated pressure (30-280 bar) and temperature (50-100°C) conditions. Foam experiments in Berea-weakly laminated core (B-WL), Berea-moderately laminated core (B-ML) and Berea-strongly laminated core (B-SL) are shown by green, red and blue profiles, respectively. The first, second and last experiments on the respective cores are illustrated by orange, purple and gray dots, respectively. The N_2-foam generation at 280 bar and 50°C in a high permeability and relative homogeneous Berea sandstone core sample is included for comparison (i.e., black profile, 1Berea1000, as reported in Paper 1).

Figure 8.13 (p. 150): Average gas breakthrough times during foam flooding on the laminated core samples. The error bars are added to indicate the variation observed for repeated experiments on the respective core samples. Typical ranges in gas breakthroughs during the baseline experiments (i.e., co-injection of 80% N_2 and 20% seawater without surfactant) are included for comparison.

Figure 8.14 (p. 166): Images of bulk CO_2-foam-oil interactions in the filter test at 2 bar with 3 vol.% of crude oil C: a) AOS-foam immediately after generation. The oil spreads within the lamellae. The foam was completely broken down after less than 2 hours; b) FS-500-foam 24 hours after generation. The oil is non-spreading and primarily situated as wedges in the plateau borders. The foam was stable for more than a week; c) AOS+FS (4:1) surfactant mixture 24 hours after generation. The oil is spreading but the foam remained stable for more than a week.

Figure 8.15 (p. 172): Image of an apparently stable bulk foam structure with emulsified crude oil present within the lamellae. The calculated parameters predict unstable foam according to the theory. The image was taken 2 hours after generation in the filter test ($AOS_{C14-C16}$ surfactant, N_2-gas, 3 wt.% with crude oil C).

Appendix:

Figure B.1 (p.185): Pore throat size distribution from mercury injection measurements.

Figure B.2 (p. 185): Dispersion tests

Figure B.3 (p. 186): X-ray images of the core samples used in this thesis. Horizontal lines in the images are noises.

Figure C.1 (p. 187): Example of pressure drop during a baseline pressure experiment in Berea90/(B-ML) at 280 bar and 50°C. The average value of the pressure drop for the last 0.5 PV injected (marked in red = 228 mbar) was used as reference for calculating mobility reduction factors in subsequent foam experiment at similar conditions.

List of Tables

Chapter 1:

-

Chapter 2:

Table 2.1 (p. 16): Surface tensions of liquid solutions to air (from Paper 4)

Table 2.2 (p. 19): Major classes of different types of surfactants (adapted from Levinson, 2009)

Chapter 3:

-

Chapter 4:

Table 4.1 (p. 41): Influence of rock textural parameters on porosity and permeability (adapted from Selley, 1998)

Chapter 5:

Table 5.1 (p. 62): General properties of carbon dioxide

Table 5.2 (p. 63): General properties of nitrogen

Table 5.3 (p. 77): Surface tension data of aqueous solutions under elevated conditions

Table 5.4 (p. 79): Summary of the change in the CO_2 characteristics with pressure, temperature and salinity

Chapter 6:

-

Chapter 7:

-

Chapter 8:

Table 8.1 (p. 126): Summary of MRFs obtained from repeated CO_2-foam generation experiments in outcrop Berea sandstone cores from Papers 1-2 under different experimental conditions with/without phase-equilibration using $AOS_{C14-C16}$ surfactant. The number of experiments of the total with pre-equilibrated fluids is given in the parentheses.

Table 8.2 (p. 157): Experimental overview (Paper 4)

Table 8.3 (p. 159): Surfactant ranking summary in the absence of oil for various bulk tests and gas phases. Good, moderate and poor foamers/foaming properties are shown in green, orange and red, respectively.

Table 8.4 (p. 164): Surfactant ranking summary in the presence of oil for various bulk tests, gas phases and oils. Good, moderate and poor foamers/foaming properties are shown in green, orange and red, respectively.

Table 8.5 (p. 169): S, E, B and L - FS-500 surfactant

Table 8.6 (p. 169): S, E, B and L – $AOS_{C14-C16}$ surfactant

Table 8.7 (p. 170): S, E, B and L – $AOS_{C14-C16}$ + FS-500 (4:1) surfactant mixture

Appendix:

Table A.1 (p. 181): List of surfactants

Table A.2 (p. 182): Synthetic seawater (SSW) composition

Table A.3 (p. 182): Crude oil properties at 22°C, atmospheric pressure (values in the parentheses at 50°C, atm.)

Table A.4 (p. 183): Surface tension properties, ambient conditions (from Paper 4).

Table A.5 (p. 183): Surface/interfacial tension properties at 22°C and 50°C, atmospheric pressure (values used in Paper4 for calculation of S,E,B,L parameters).

Table B.1 (p. 184): Physical properties of core material used in different papers

Table B.2 (p. 184): XRD mineralogy measurements (% of $1cm^3$ rock sample analyzed)

Table B.3 (p. 185): Average pore throat sizes

Table D.1 (p. 188): Experimental protocol - 1Berea1000 (main results presented in Paper1)

Table D.2 (p. 189): Experimental protocol - 2Berea1000 (main results presented in Paper 2)

Table D.3 (p. 189): Experimental protocol - Berea400 (main results presented in Paper 2)

Table D.4 (p. 189): Experimental protocol - Berea weakly laminated core (B-WL) (main results presented in Paper 3)

Table D.5 (p. 190): Experimental protocol - Berea moderately laminated core (B-ML) (main results presented in Paper 3)

Table D.6 (p. 190): Experimental protocol - Berea strongly laminated core (B-SL) (main results presented in Paper 3)

Table D.7 (p. 190): Experimental protocol – Bentheimer1900 (main results presented in Paper 4)

Nomenclature

Abbreviations:

A	=	area
AOS	=	alpha-olefin sulfonate
B	=	bridging coefficient
BPR	=	back pressure regulator
BT	=	breakthrough / bubble train
B-ML	=	Berea-moderately laminated
B-SL	=	Berea-strongly laminated
B-WL	=	Berea-weakly laminated
C	=	carbon atoms in the molecule
c	=	concentration of dissolved gas in a liquid
$C_{surf.}$	=	surfactant concentration
CIPR	=	Centre for Integrated Petroleum Research
cmc	=	critical micelle concentration
CT	=	computed tomography
D	=	Darcy / diffusion coefficient / dimension
DLVO	=	Derjaguin-Landau-Verwey-Overbeek
EOR	=	enhanced oil recovery
E	=	entering coefficient
E_R	=	recovery efficiency
E_D	=	microscopic displacement efficiency
E_V	=	volumetric displacement efficiency
f	=	fractional flow
FAWAG	=	foam-assisted-water-alternating-gas
f_g^*	=	optimum foam quality
FTT	=	film trapping technique
G	=	Gibbs energy
GBT	=	gas breakthrough times
GOR	=	gas-oil ratio
h	=	film thickness
HLB	=	Hydrophile-Lipophile-Balance
HPHT	=	high pressure high temperature
ID	=	identification
IOR	=	improved oil recovery
ID	=	identification
IOR	=	improved oil recovery
J	=	diffusion flux
K	=	absolute permeability
k_H	=	Henry constant
k_r	=	relative permeability
k_w	=	effective water permeability
$k_{rw.app.}$	=	apparent water relative permeability
L	=	length / Lamella number
M	=	mobility ratio

MRF	=	mobility reduction factor
N	=	original oil in place / number of molecules/particles
n	=	mole / number of components
N_c	=	capillary number
N_p	=	oil produced
NOK	=	Norwegian Kroner
OOIP	=	original oil in place
P	=	pressure
p	=	partial pressure
P_c	=	capillary pressure
P_c^*	=	critical capillary pressure
ppm.	=	parts per million
PV	=	pore volume
PVT	=	pressure-volume-temperature
P1	=	inlet/injection pressure
P2	=	outlet/production pressure
Q	=	foam quality / volumetric flow rate
R	=	radii of curvature
r	=	radius
R_o	=	oil recovery factor
RF	=	resistance factor
S	=	saturation / spreading coefficient
SAG	=	surfactant alternating gas
SDS	=	sodium dodecyl sulfate
SMR	=	selective mobility reduction
SSW	=	synthetic seawater
S_w^*	=	critical water saturation
T	=	temperature
t	=	time
USD	=	United States Dollar
V	=	volume
WAG	=	water alternating gas
WOR	=	water-oil ratio
wt.%	=	weight percent

Greek letters:

ΔP	=	pressure difference
ΔP_{gas}	=	pressure drop to gas flow
ΔP_{water}	=	pressure drop to water flow
$\Delta P_{without\ foam}$	=	pressure drop in the absence of foam/surfactant
ΔP_{foam}	=	pressure drop in the presence of foam/surfactant
θ	=	contact angle
λ	=	mobility
μ	=	viscosity / chemical potential
v	=	superficial (Darcy) velocity
Π	=	disjoining pressure
π	=	disjoining pressure forces
ρ	=	density
σ	=	charge / interfacial (surface) tension
$\nabla\phi$	=	concentration gradient

Subscript:

A	=	attractive
app.	=	apparent
c	=	capillary / critical
C14-C16	=	14-16 carbon atoms in the molecule
g	=	gas
h	=	horizontal
i	=	component / molecule
j	=	molecule
o	=	oil
R	=	repulsive
r	=	relative
S	=	structural/steric
SSW	=	synthetic seawater
surf.	=	surfactant
surf.solu.	=	surfactant solution
v	=	vertical
w	=	water

Supercript:

*	=	critical / optimum / constant

Unit Conversions

1 atm.	=	1.01325 bar	=	101325 Pa
1 bar	=	1000 mbar	=	14.5037 Psi
°C (degree Celsius)	=	(273.15+°C) = °K (degree Kelvin)	=	(°C*1.8)+32 = °F (degree Fahrenheit)
1 meter	=	100 cm	=	3.2808 feet
1 cm	=	10 mm	=	0.3937 inch
1 liter	=	0.001 m^3	=	0.264171 gallons
1 kg	=	1000 g	=	1.0*E+6 mg
1 bbl. (reservoir barrel)	=	0.15898 m^3		
1 Darcy	=	0.9869*E-12 m^2		
1 mN/m	=	1 dyne/cm		
1 %	=	10000 ppm		
1 cP	=	0.001 Pa*s		

Chapter 1

Introduction

1.1 Energy demand	**p. 1**
1.2 Current oil recovery factors and future perspectives	**p. 2**
1.3 Oil recovery maximization	**p. 2**
1.4 Gas-based-EOR: current interests, advantages and limitations	**p. 5**
1.5 Foam for EOR	**p. 8**
1.6 Foam applications	**p. 9**
1.7 Oil industry's interests in foam	**p. 9**
1.8 Foam properties	**p. 11**
1.9 Scope and objectives	**p. 12**
1.10 Paper contents and thesis structure	**p. 12**

1.1 Energy demand

Fossil fuels (i.e., oil, gas and coal) are the world's main source of energy. Based on the long-term global energy outlook, the demand for oil-based liquids is anticipated to increase from 90 million barrels per day (2013) to approximately 115 million barrels per day by 2040 (U.S. EIA, 2013).

One of the options to meet the growing demand for energy is to increase the production of oil.

1.2 Current oil recovery factors and future perspectives

The oil recovery factor, $\mathbf{R_o}$, is defined as the ratio of oil produced, $\mathbf{N_p}$, to the original oil in place (OOIP), **N** (Lake, 1989):

$$R_o = (N_p/N)\ x\ 100\% \tag{1.1}$$

The estimated average recovery factor for mature oil fields around the world is only approximately 20-40%. The recovery factor in the United States reservoirs is approximately 39%, whereas the North Sea fields, which are among the best, average 46%. If current production rates and low recovery factors continue, the global supply of oil will be effectively exhausted within a few decades (OPEC, 2013).

However, the global recovery factor indicates that large amounts of oil remain in the reservoirs, suggesting the potential to utilize our resources better and more efficiently.

Improving oil recovery from mature oil fields could be essential for extending the economic lifetime of reservoirs, and prolonging oil availability.

1.3 Oil recovery maximization

Most oil companies want to maximize recovery from their oil fields and maintain an economic production rate. The amount of oil that is ultimately produced from an oil field depends largely on the natural conditions present (e.g., reservoir quality/geology, fluid properties/distribution), the production strategies applied, and the will and creative power to invest in new technology over the long term.

The traditional oil recovery process involves three distinct stages: primary, secondary and tertiary recovery. Primary recovery utilizes the natural energies present within the reservoirs to produce oil, primarily through the liberation and expansion of pressurized reservoir fluids, such as gas, water and oil. As a transition from pressure depletion, regular water or gas injections are usually applied as secondary recovery methods. The purposes of the secondary methods are basically to: maintain reservoir pressure and displace oil toward a producer, as illustrated in Figure 1.1. Much of the oil remaining in the reservoirs after primary and secondary recovery is a target for tertiary recovery. Tertiary recovery is often used as a synonym for Improved/Enhanced Oil Recovery (IOR/EOR) processes and technologies,

which apply to improvements in the oil recovery factor compared with the anticipated recovery in the absence of these actions.

While the IOR terminology has become all-encompassing (including improved engineering, reservoir management, change in production strategy, more efficient operations, 4D seismic methods) enhanced oil recovery (EOR) is a more specific concept. EOR defines a set of methods intended to increase the production of oil beyond what could normally be achieved using conventional oil recovery techniques. The methods involve recovery of oil using fluids and processes that are not normally present within the reservoir (e.g., injection of miscible gases, chemicals, microbial or thermal methods). Thomas, (2008) provides an overview of available EOR methods. Foam is one such method and is investigated in this thesis. The choice of solutions and expected additional recoveries from tertiary recovery depends on many considerations, both economic and technical.

The added values of applying successful measures for IOR/EOR are expected to be large: Worldwide, a one percent increase in the global recovery factor represents an extra 88 billion barrels of oil, equivalent to three years of global production (Sandrea and Sandrea, 2007). For the fields on the Norwegian Continental Shelf, a one percent increase in the oil recovery factor has been estimated to have a gross value potential of approximately 270 billion NOK (assuming 70 USD/bbl., 1 USD = 5.5 NOK) (The Norwegian Ministry of Petroleum and Energy, 2010).

From a reservoir engineering point of view, the recovery efficiency, $\mathbf{E_R}$, of any fluid displacement process is the product of the microscopic displacement efficiency, $\mathbf{E_D}$, and the volumetric sweep, $\mathbf{E_V}$, of the injected fluid(s) (Lake, 1989):

$$E_R = E_D \, x \, E_V \tag{1.2}$$

The microscopic sweep efficiency refers to how well the contacted volume of oil can be displaced by the injected fluid (Figure 1.1a). The forces with the greatest effect on the quality of oil mobilization by the displacing fluid are capillary, viscous and gravity forces. The volumetric sweep efficiency is related to how much of the oil-bearing portions of the reservoir are contacted by the injected fluid (Figure 1.1b). Displacement stability and mobility control are key factors governing the sweep of injected fluids.

Two important parameters for increasing the oil recovery efficiency during fluid displacement are the: capillary number and mobility ratio.

The capillary number, $\mathbf{N_c}$, is a dimensionless quantity used to describe the force balance between the viscous and capillary forces acting in the porous media during flooding. Various definitions of the capillary number are available (Lake, 1989), and one common definition is the following:

$$N_c = \frac{v\mu}{\sigma} \tag{1.3}$$

where **v**, is the superficial (Darcy) velocity of the displacing fluid, defined as the volumetric flow rate divided by the cross-sectional area, **μ** is the viscosity of the displacing fluid and **σ** is the interfacial/surface tension between the displacing fluid (e.g., water or gas) and the fluid being displaced (e.g., oil).

An increase in oil recovery is related to an increase in the capillary number (e.g., increasing the flow rate and/or fluid viscosity and/or reducing the tension force between the displacing and the displaced fluids).

The ability of any fluid to flow in porous media is defined by its mobility, $\boldsymbol{\lambda_1}$:

$$\lambda_1 = \frac{k_{r1}}{\mu_1} K \tag{1.4}$$

where **K** is the absolute permeability (a property of the porous media), $\mathbf{k_{r1}}$ is the relative permeability of the fluid (a function of the saturation of the fluid) and $\boldsymbol{\mu_1}$ is the viscosity (a fluid property).

The mobility ratio, **M**, defines the mobility between the displacing fluid, $\boldsymbol{\lambda_1}$, and the displaced fluid, $\boldsymbol{\lambda_2}$:

$$\mathrm{M} = \frac{\lambda_1}{\lambda_2} = \frac{k_{r1}/\mu_1}{k_{r2}/\mu_2} \tag{1.5}$$

For an efficient displacement process the mobility ratio should be equal to or less than 1. Thus, "mobility control" refers to techniques that reduce the mobility ratio by changing the fluid relative permeabilities and/or viscosities such that $M \leq 1$.

All EOR processes and technologies aim to increase the capillary number (Equation 1.3) or improve mobility control (Equation 1.5) to increase the total oil recovery efficiency (Equation 1.2). For example, miscible gas floods and surfactant flooding can lower the tension forces towards the oil and affect the microscopic displacement efficiency. Foam and polymer flooding can improve sweep efficiency through mobility control in gas and water flooding, respectively. However, each EOR method has distinct advantages and limitations that must be considered for each specific reservoir situation (Green and Willhite, 1998).

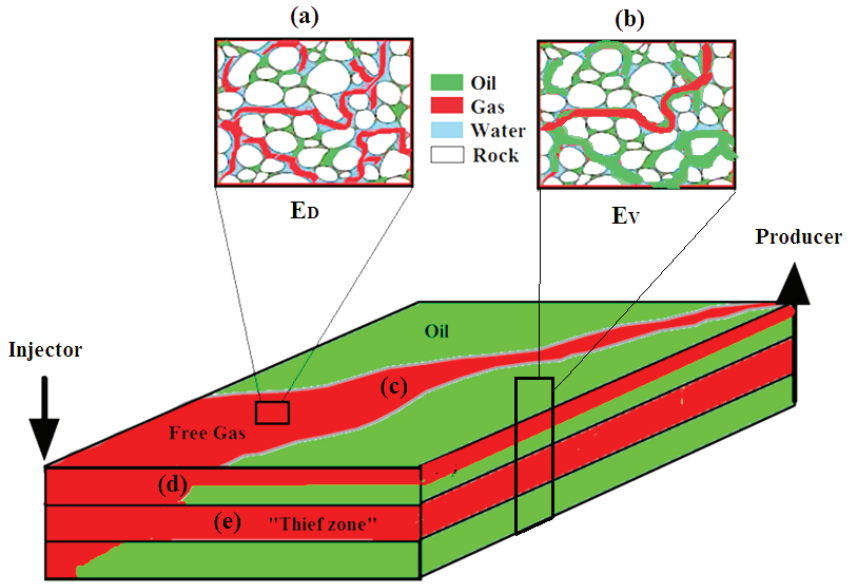

Figure 1.1: The recovery efficiency from gas injections may be low due to (a) poor microscopic sweep efficiency, E_D; (b) poor volumetric (areal/vertical) sweep, E_V; (c) viscous fingering problems; (d) gas override; or (e) gas channeling through highly permeable intervals ("thief zones") (modified from Hanssen et al., 1994).

1.4 Gas-based-EOR: current interests, advantages and limitations

EOR gas flooding has been the most widely used recovery method for light, condensate and volatile oil reservoirs. The typically used gases in EOR include CO_2, hydrocarbon gases (e.g., CH_4), N_2, air or steam. The "choice" of gas composition in a field injection situation depends

on several factors such as, gas availability, recovery conditions (miscible/immiscible) and an economic assessment of which fluid is appropriate for the field.

Over the last few years, the popularity of carbon dioxide in EOR (CO_2-EOR) has increased (Figure 1.2). This new and renewed interest in CO_2 is likely a result of the increased focus on environmental issues and the need to reduce greenhouse gas emissions (Manrique et al., 2010).

Combining CO_2 injection to enhance oil recovery with underground geological storage of CO_2 has been considered as an option to reduce greenhouse gas emissions and benefit from the total costs of carbon sequestration (Alvarado and Manrique, 2010; Energy Institute, 2010).

Outside the United States and Canada, ongoing CO_2 floods are limited (Mathiassen, 2003). The reasons for the limited application of this technique seem to be the lack of easy access to large volumes of CO_2 at an acceptable price, and various economic and technical challenges, particularly related field implementations offshore. Nevertheless, the current focus on CO_2 emissions, enhanced oil recovery, along with high oil prices, may justify long-term investments in CO_2 technology, even for several European offshore oil reservoirs (Awan et al., 2008; European Commission, 2005).

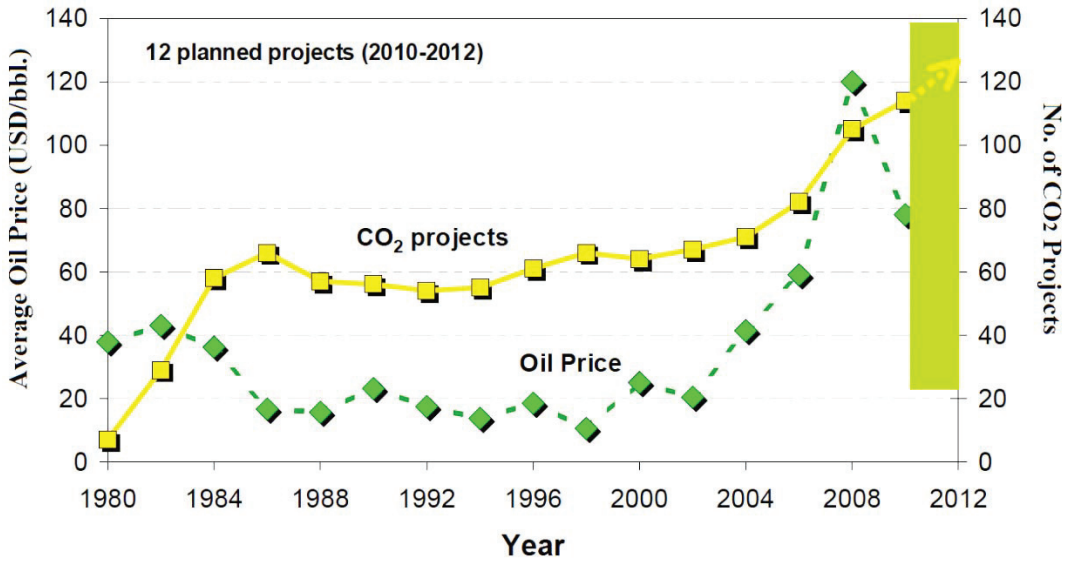

Figure 1.2: Evolution of CO_2 projects and oil prices in the U.S. – based on data from Oil & Gas Journal EOR Surveys 1980-2010 and U.S. EIA 2010 (adapted from Alvarado and Manrique, 2010).

CO_2 injection is of particular interest in EOR because of the unique effects of CO_2 on oil in place (e.g., miscibility, oil swelling, oil viscosity reduction). It is assumed that a miscible CO_2-flood can be nearly 100% effective within the reservoir in which it sweeps (Grigg and Schechter, 1997; Sanders et al., 2010; Stalkup, 1983; Talebian et al., 2013).

Actual oil recoveries from field applications injecting CO_2 or other gases are generally much lower, however, primarily due to early gas breakthrough and poor volumetric gas sweep efficiency. Thus, the injected gas only contacts a small fraction of the reservoir before being reproduced. Consequently, large volumes of oil may remain in parts of the reservoir, particularly in those locations not contacted by the injected gas (Figure 1.1).

Displacement instabilities and poor mobility control during gas injections can be traced to the low viscosity and density properties of most gases, as well as geological differences in the reservoir (Heller, 1994; Lake, 1989; Rossen, 1996):

I) A low gas viscosity (typically between 0.02 and 0.06 cP at reservoir conditions) creates a very mobile fluid in porous media (Equation 1.4), particularly compared to other reservoir fluids (e.g., oil, which has viscosities generally ranging from 0.5 cP to tens of centipoises). The resulting unfavorable mobility ratio between the displacing phase (i.e., gas) and the oil phase to be displaced could reduce the efficiency of the gas/oil displacement process (Equation 1.5). The displacement instabilities that occur when a less viscous fluid is injected to displace a more viscous fluid is often referred to as "viscous fingering" (Figure 1.1c).

II) Most gases are less dense than other reservoir liquids. Differences in the densities of the fluids in the formation could result in segregation due to buoyancy/gravity forces. Displacement instability in which a less dense fluid (e.g., gas) preferentially flows at the top in a formation, overriding the denser fluids (e.g., oil) in the lower portions, is called "gravity override". Gravity override reduces the likelihood of gas to contact and displace the oil from the lower portions of the reservoir (Figure 1.1d).

III) Similar to any other fluid injected, the gas will have a strong tendency to flow along the path of least resistance. Geological differences in the reservoir, such as layers of contrasting permeability, could therefore exert further instabilities on the gas injection front such as "gas

channeling" and excessive flow through the most permeable intervals in the formation, often referred to as "thief zones" (Figure 1.1e).

1.5 Foam for EOR

A solution to reduce gas mobility and improve gas sweep efficiency in oil reservoirs is to utilize foam. Foam is a two-phase system of gas and water, stabilized by a surfactant (e.g., soap chemicals) (Figure 1.3a). In an aqueous foam structure, the gas phase becomes discontinuous and is surrounded by continuous liquid films (Figure 1.3b).

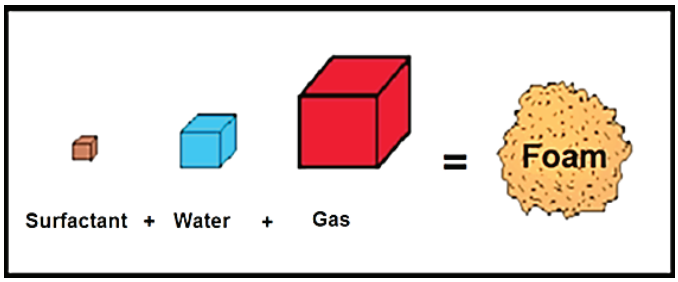

(a)

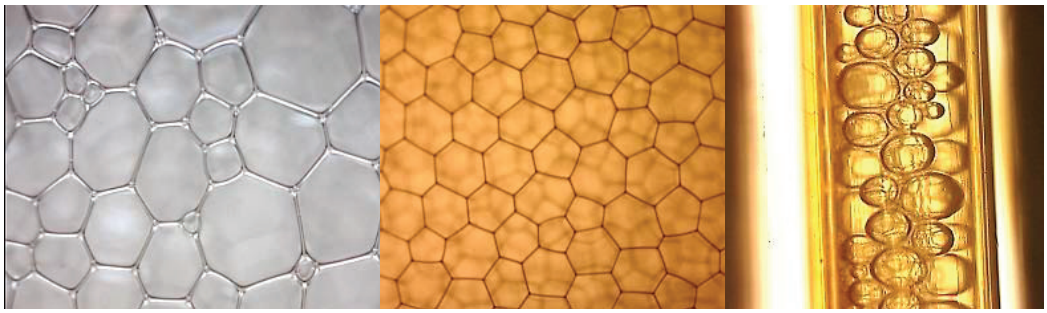

(b)

Figure 1.3: Illustration of (a) foam components and (b) foam structures (from this thesis).

In EOR applications foam has been used primarily for conformance and/or mobility control during gas injections (Figure 1.4a), or to shut off unwanted gas inflow in production well treatments (Figure 1.4b). In fact, the simultaneous combination of water, gas and surfactant to generate a foam in a reservoir can potentially overcome all three sources of poor sweep efficiency recently addressed by gas injections (Rossen, 1996; Heller, 1994).

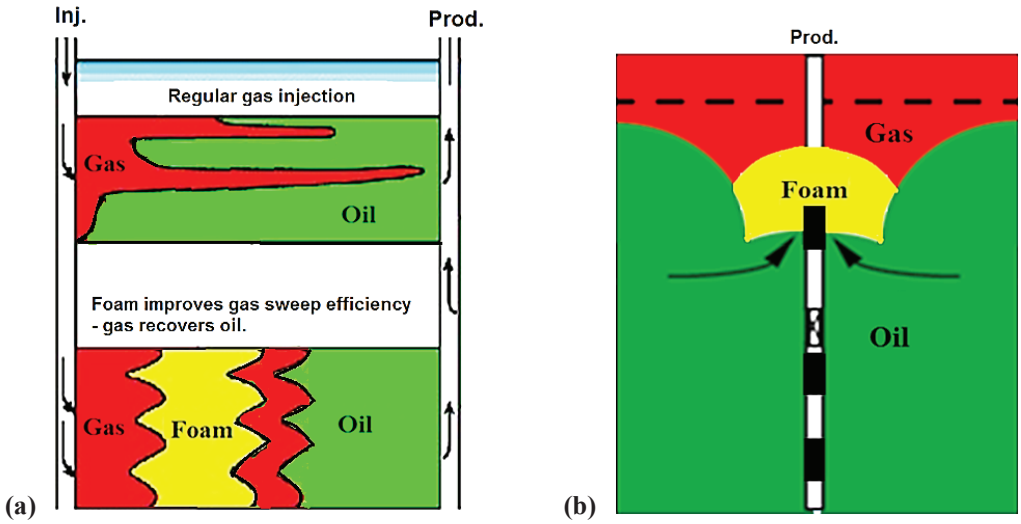

Figure 1.4: Applications of foam for EOR: (a) support gas injections with mobility control to combat viscous fingering, gas overrides, or excessive flow of gas through highly permeable "thief zones" in the reservoir; (b) prevent unwanted fluids from coning, cusping or channeling into the production wells (adapted from Vikingstad, 2006).

1.6 Foam applications

Foams are of practical interest in many chemical and industrial processes (e.g., firefighting, personal care products, food/beer industry), including several other oil field operations (e.g., well stimulation and drilling). Examples of foam applications are described in Prud'homme and Khan (1996), Schramm (1994a) and Weaire and Hutzler (1999).

For environmental purposes, foam can be used to "clean up" wastewaters. Wastewater treatment systems use foam to remove fine solids from the water stream. The fine solids are adsorbed onto the foam, which is then skimmed from the surface (Rubio et al., 2002).

Foam may also improve the "clean-up" of polluted sub-surface areas (e.g., airports, nuclear sites). For example, foam could improve the sweep efficiency of the chemicals used to displace and remove the pollutant. Lab and field demonstrations of such processes are described in (Hirasaki et al., 1997; Zhang et al., 2009).

1.7 Oil industry's interests in foam

The concept of using foam to improve gas sweep efficiency in oil reservoirs was initially patented by Bond and Holbrook, (1958). The first field application, in 1970, confirmed the laboratory-derived observations of foam as an effective method of decreasing gas and water

mobility, stopping severe gas channeling, and decreasing the produced WOR (water-oil ratio) (Holm, 1970). Several successful field projects with foam have subsequently been conducted, along with some failures (Castanier, 1987; Enick and Olsen, 2012; Turta and Singhal, 1998; Zhdanov et al., 1996). Several field trials are currently in planning or currently underway (Alvaro and Manrique, 2010; Mukherjee et al., 2014; Ocampo et al., 2013; Sanders et al., 2012).

One field example of the use of foam is the foam-assisted-water-alternating-gas (FAWAG) injection at the Snorre field in the North Sea. The application of foam for gas mobility control under difficult offshore reservoir conditions demonstrated both the technical feasibility and economical payoff of using foam at field scale. Importantly, the cost of surfactant in the foam treatment at field scale did not need to be high relative to the potential economic payoff (Aarra et al., 2002; Blaker et al., 2002; Skauge et al., 2002).

A recent report by Enick and Olsen, (2012) provides a good summary of 40 years of research and field tests of mobility and conformance control for CO_2-EOR. Despite extensive research, previous attempts to control CO_2 mobility with foam have been only partially successful and not widely accepted by the oil industry for a variety of reasons. The oil industry continues to use WAG (water alternating gas) as the technology of choice or other mechanical means (e.g., shorter well distances, horizontal wells, infield drilling, packers) to control gas floods.

Also, the positive results from the foam injection at the Snorre field using hydrocarbon gas have done little to renew interest in foam for EOR at the Norwegian Continental Shelf. A lack of plans for further implementation of this technology offshore have been reported as one of the reasons why the successful foam pilot in the late 1990s was not pursued (The Norwegian Ministry of Petroleum and Energy, 2010).

The potential economical payoff of using foam for EOR can be substantial, but the implementation of this method by the oil industry has remained somewhat elusive (Enick and Olsen, 2012; Rossen, 1996). Greater effort is therefore needed to make the technology more applicable, and to still encourage the industry to use foam in various process optimizations to enhance oil recovery and improve the economics of mature oil fields.

1.8 Foam properties

A successful foam treatment requires specific foam properties depending on the problem to be solved (Figure 1.1 and 1.3). Examples could be strong and stagnant foams for gas blocking/diverting purposes, or weaker propagating foams for mobility control deeper into the formation. A good understanding of the problem, the reservoir, and foam properties in porous media is therefore important.

The efficiency of foam to reduce gas mobility (i.e., foam strength) and its stability are key questions for all intended field applications. Various parameters have been used to determine the efficiency of foam in porous media (Schramm, 1994a), and one common parameter is the mobility reduction factor (MRF):

$$\textbf{M}\text{obility }\textbf{R}\text{eduction }\textbf{F}\text{actor }(\textbf{MRF}) = \frac{\Delta P_{foam}}{\Delta P_{without\ foam}} \tag{1.6}$$

The MRF is a dimensionless quantity expressing the magnitude in mobility reduction achieved in the presence of foam relative to that in the absence of foam. A larger MRF, indicates a stronger foam. In the laboratory, the MRF can be calculated by dividing the magnitude in pressure drop along the porous media during foam generation by the pressure drop obtained upon injection of gas and/or water (without surfactant).

The foam performance offered by a given surfactant may depend on several factors, such as surfactant type and concentration, gas composition, rock properties, foam-oil interactions, brine salinity, temperature and pressure conditions, flow rates, injection strategies and so on. Consequently, detecting and characterizing important factors governing foam properties in porous media are of great importance to achieve successful implementation of foams for EOR.

The aim of this thesis was to perform a systematic experimental approach to determine how some of the abovementioned variables affect foam properties and performance in porous media.

1.9 Scope and objectives

The foam project builds on previous experiences and foam studies at our research institution, Uni CIPR, including field experiences with the applications of foam in North Sea reservoirs, predominately the work of Aarra et al. (1994, 1996, 1997, 1998, 2002, 2011), Skauge et al. (2002) and Vikingstad et al. (2006, 2009).

The main objectives in this thesis are the following:

1. Obtain an improved understanding of CO_2-foams (compared with N_2-foams).
2. Investigate the effect of core heterogeneity on foam properties.
3. Evaluate surfactants to foam using various experimental methods and conditions.
4. Provide new data and discussions on bulk foam-oil interactions.

1.10 Paper contents and thesis structure

Experimental methods:

Dynamic core displacement experiments conducted in oil-free outcrop Berea sandstone cores under different elevated temperature and pressure conditions using alpha-olefin sulfonate (AOS) surfactant form the basis for the main studies of foam in **Papers 1-3**.

Paper 4 mainly utilizes two different bulk tests at reduced experimental conditions to evaluate a set of surfactants to foam.

Summary of paper contents:

Paper 1 (Aarra et al., 2014) investigates CO_2-foam properties in porous media as a function of pressure. The dynamic properties of CO_2-foams above and below the critical point of CO_2 were studied and compared (i.e., supercritical CO_2-foam versus gaseous CO_2-foam). New foam experiments with pre-equilibrated fluids were conducted to evaluate the influence of solubility between CO_2 and brine on foam generation performance and on foam's ability to block water. The properties of CO_2-foam were compared with those of N_2-foam under similar experimental conditions. This paper provides new insights into CO_2-foam properties compared to N_2-foams in porous media under elevated pressure and temperature conditions.

Paper 2 (Solbakken et al., 2013) builds on the results and ideas of **Paper 1** and investigates the properties of supercritical CO_2-foams of varying CO_2 densities. Physical and chemical characteristics of CO_2 (other than density) may also be important when changing experimental conditions. Properties of interest and frequently discussed in the literature related supercritical CO_2-foam were addressed. The performance of commercial AOS surfactant with dense supercritical CO_2 was compared with analogous results in the literature for other types of surfactant systems. A general lack of experimental studies of CO_2-foam properties in porous media with systematic variations in pressure and temperature was observed in the recent report by Enick and Olsen (2012). **Paper 2** attempts to contribute to this area.

Paper 3 (Solbakken et al., 2014) explores the behavior, properties and performance of foam in naturally laminated sandstone material with relatively low permeability. Laminations are common constituents in many sandstone petroleum reservoirs, where they usually occur as thin deformed layers in the formation. Several techniques were utilized to analyze the core material prior to the main foam experiments under elevated pressure and temperature conditions. This paper contributes to an improved understanding of the effects of foam in heterogeneous core material. The recognition of laminated structures in Berea sandstone and their influence on fluid flow should also be relevant to other researchers using Berea as a model rock in systematic studies of foam and other EOR processes.

Paper 4 (Solbakken, 2013) includes various approaches related to surfactant screening and foam-oil interactions. Several commercial and CO_2-recommended surfactants were evaluated and compared in two different bulk foam tests, one under ambient conditions using air as the gas phase, and one at 2 bar using CO_2 and N_2 as the gas phase. The first part of the report addresses surfactant screening in the absence of oil. Part 2 provides experimental data and discussions on bulk foam-oil interactions using the two best surfactant candidates identified in part 1. Bulk results (**Paper 4**) and foam core flooding results (**Papers 1-3)** were compared.

The four papers are found in the last part of this thesis.

Thesis structure:

The thesis is organized as follows:

Chapter 1 introduces the background and challenges that motivate this thesis. **Chapter 2** presents some basic properties of foam and surfactants, including the selection of surfactants for use in this project. **Chapter 3** describes the primary forces governing foam stability. **Chapter 4** introduces porous media and the fundamental properties of foam in it. **Chapter 5** elucidates important gas characteristics and effect of gas type on foam properties. **Chapter 6** presents the main theories for predicting foam stability in the presence of oil. **Chapter 7** includes experimental methods and procedures for studying the use of foam in EOR processes, including those used in this thesis.

Chapters 1 through **7** describe the complex interplay of the many parameters, factors and forces governing foam properties in both bulk and porous media. This background provides a basis for **Chapter 8**, which summarizes the main results and discussions of the thesis. **Chapter 9** concludes the thesis. Detailed descriptions of experimental fluids and procedures, including petrophysical properties of the core materials used are summarized in the **Appendix** (beginning on page 181).

Chapter 2

Foam Fundamentals

2.1 Basic foam properties **p. 15**

2.2 Surfactants **p. 18**

2.3 Surfactant selection **p. 22**

2.4 Choice of surfactant in this thesis **p. 24**

2.1 Basic foam properties

Foam is a dispersion of gas in a liquid in which the gas is the discontinuous (dispersed) phase and water is the continuous phase (the dispersion medium). A foam that many people have experienced is blowing single soap bubbles in the backyard (Figure 2.1a). In a bulk foam structure, numerous bubbles are separated from each other by thin liquid films, called lamella (Figure 2.1b).

a)

b)

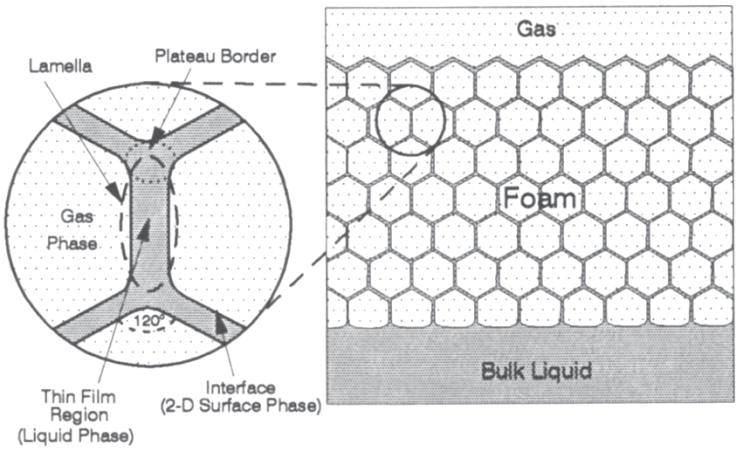

Figure 2.1: (a) "Boy blowing bubbles", 1867 (Édouard Manet, 1832-1883) (from www.wikiart.org); (b) bulk foam structure comprising thin liquid lamellae connected in Plateau borders (from Schramm and Wassmuth, 1994).

To make a foam, energy must be applied to the system to achieve dispersion. The energy (**dG**) required to increase the surface area (**dA**) is proportional to the surface tension ($\boldsymbol{\sigma_{w/g}}$) between gas and water (Atkins et al., 2005):

$$dG = dA\,\sigma_{w/g} \tag{2.1}$$

In all its simplicity, reducing the surface tension means easier foam formation for less amount of energy. Typical values of surface tension at ambient conditions are provided in Table 2.1.

Table 2.1: Surface tensions of liquid solutions to air (from Paper 4)

Liquids	**Surface tension (22°C, atm.)**
Distilled water Seawater (~ 36,000 ppm.) Different surfactant solutions (C_{surf} = 0.5 wt.% dissolved in seawater)	72.4 mN/m 70.1 mN/m ~ 16-45 mN/m

After a foam has been generated, differences in pressure on opposite sides of lamellae exist (Figure 2.2). The balance in pressure difference, $\Delta\mathbf{P}$, conforms to the law of Young-Laplace in the context of spherical bubbles or films with radii, **R**, (here, adjusted to three dimensions):

$$\Delta P = 4\sigma_{w/g}/R \tag{2.2}$$

The coefficient 4 represents a curved surface in three dimensions (Rossen, 1996; Weaire and Hutzler, 1999).

In foam, the smallest length scale is that of the surfactant molecules, which are typically on the order of nanometers. The thickness of the lamellae in dry foam is usually of colloidal dimensions (i.e., 10 μm – 1 nm). Bubble diameter can vary widely, but is normally in the colloidal range and above (Schramm and Wassmuth, 1994; Weaire and Hutzler, 1999).

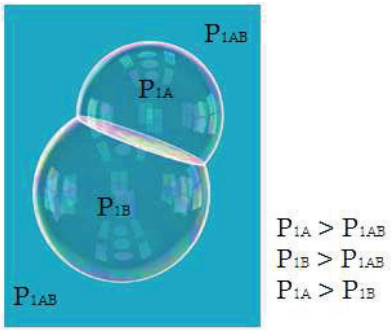

Figure 2.2: Pressure differences between bubbles (adapted from http://math.berkeley.edu/~hutching/).

The lamellae arrange themselves in discrete ways. Three lamellae must meet at an angle of 120° (Figure 2.1b), and the lamella between four bubbles (in three dimensions) form tetrahedral angles of ~ 109.5°, which is also referred to as the Maraldi angle (Schramm and Wassmuth, 1994; Weaire and Hutzler, 1999).

Foams can be characterized based on their quality **Q**, which is defined as follows:

$$Q = \frac{V_g}{V_g + V_w} x\ 100\% \tag{2.3}$$

where $\mathbf{V_g}$ is the gas volume and $\mathbf{V_w}$ is the water volume present in the foam. The unit of foam quality is percentage (%). For example, 80-quality foam contains 80 % gas by volume. Consequently, a lower quality (wetter) foam contains more liquid than a higher quality (drier) foam (Figure 2.3). Foam quality is one of many important parameters that affect foam performance and behavior in porous media (Chang and Grigg, 1999).

Immediately after the formation of the dispersion, gas and water will attempt to separate from each other. The thermodynamic drive to minimize energy leads to this spontaneous phase separation. Foams are considered unstable systems. Eventually they all collapse.

Most foams with significant lifetimes contain gas, liquid and a foam-stabilizing agent (i.e., surfactant). The surfactant molecules adsorb at the gas-liquid surface, lowering the surface tension (Table 2.1), decreasing the energy needed to create foam (Equation 2.1) and slowing down the destabilizing processes that lead to the coalescence and collapse of the foam (i.e.,

gives stability to the foam structure). The drive to minimize energy leads to the following fascinating geometric structures among foams stabilized by a surfactant (Figure 2.3):

a) 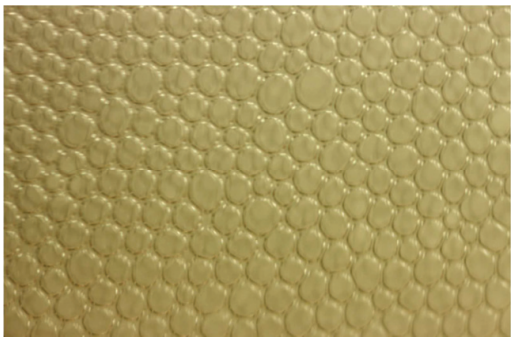 b) 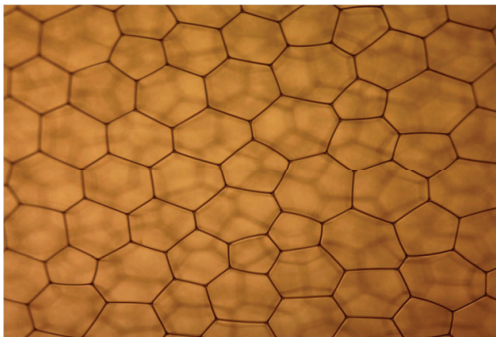

Figure 2.3: Images of bulk foam structures stabilized by surfactant (from Paper 4): (a) wet foam structure with spherical bubble shapes; (b) dry foam structure with polyhedral-like geometries (mainly penta-, hexa- and heptagonal shapes). For stable foams, the bulk structure can change from (a) spherical to (b) polyhedral over time.

2.2 Surfactants

A surface-active agent (i.e., surfactant) is typically used to improve foam stability. The efficiency of such agents is conditioned by their amphiphilic nature. The term amphiphilic indicates that the surfactant molecule is dualistic in nature, comprising a hydrophilic "water-loving" head group and a hydrophobic "water-hating" hydrocarbon tail (Figure 2.4a).

The four main classes of surfactants, as defined based on the charge and nature of their polar head groups, are as follows: anionic, cationic, nonionic and zwitterionic (Figure 2.4a). Each of these general classifications encompasses a broad range of surfactant variants (Holmberg et al., 2003; Levinson, 2009), some of which are listed in Table 2.2.

The physical and chemical properties of ionic surfactants are closely associated with the ratio between the polarity of the head group and non-polarity of the hydrocarbon chain. The ratio is affected by factors such as size, structure and position of the hydrophilic and hydrophobic moieties of the surfactant molecule, respectively. This surfactant property is commonly classified as the hydrophilic-lipophilic balance (HLB) (Griffin, 1949). The HLB number can be calculated by applying the Davies' equation (Davies, 1957). The HLB number of surfactants can be useful for determining their field of applications (Figure 2.4b).

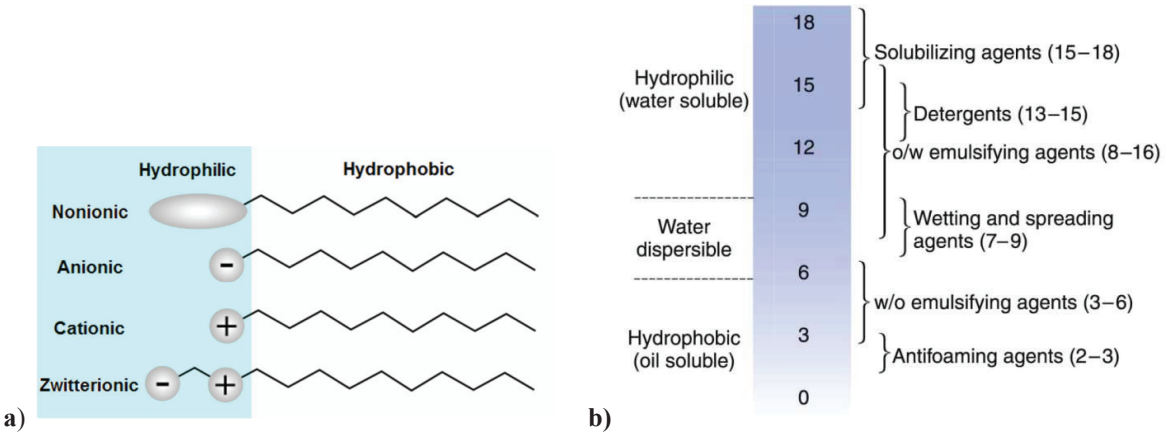

Figure 2.4: Illustration of (a) surfactant molecules and classification according to the charge of the polar head group; (b) classification of surfactant functions based on the HLB number, w = water, o = oil (adapted from Aulton and Taylor, 2013).

Table 2.2: Major classes of different types of surfactants (adapted from Levinson, 2009)

Surfactant type	Charge of polar head group	Surfactant classes
Anionic	Negative	sulfonates, sulfates, phosphates, carboxylates
Cationic	Positive	quaternary ammonium salts, amines
Nonionic	No charge	ethers, esters, ethoxy-/propoxylated alcohols, glycols, glycerin
Zwitterionic	Negative and positive	betaines, amino oxides

The most energetically favorable orientation for surfactant molecules in fluids is that in which each part of the molecule remains in the fluid in which it has the greatest affinity. At the surface of a foam lamella, the polar head groups of the surfactant are oriented and exposed to water, while the non-polar hydrocarbon chains are oriented toward the gas phase (Figure 2.5). Surfactants can therefore influence the surface and interfacial properties of a solution and stabilize thin liquid films (Lake, 1989; Schramm and Wassmuth, 1994).

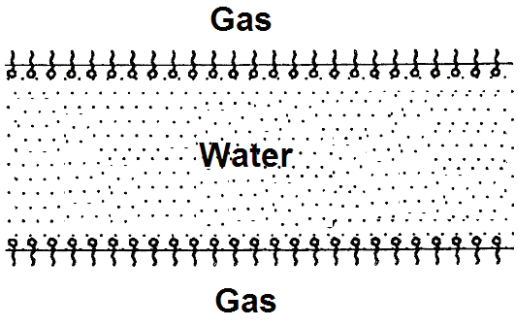

Figure 2.5: Orientation of surfactant molecules (monomers) in thin liquid films (modified from Schramm and Wassmuth, 1994).

At low concentrations, the surfactant molecules form single, dissociated monomers, preferably concentrated at the gas-water surfaces (Figure 2.5). At higher surfactant concentrations, the surface becomes saturated with surfactant molecules, and the monomers begin to aggregate into micelles. This spontaneous aggregation occurs in well-defined assemblies according to the structure and properties of the surfactant molecules. To reduce their exposure to water, the non-polar hydrocarbon chains orient their polar head groups toward water, thereby shielding the hydrocarbon chains in the interior of the micelles (Figure 2.6).

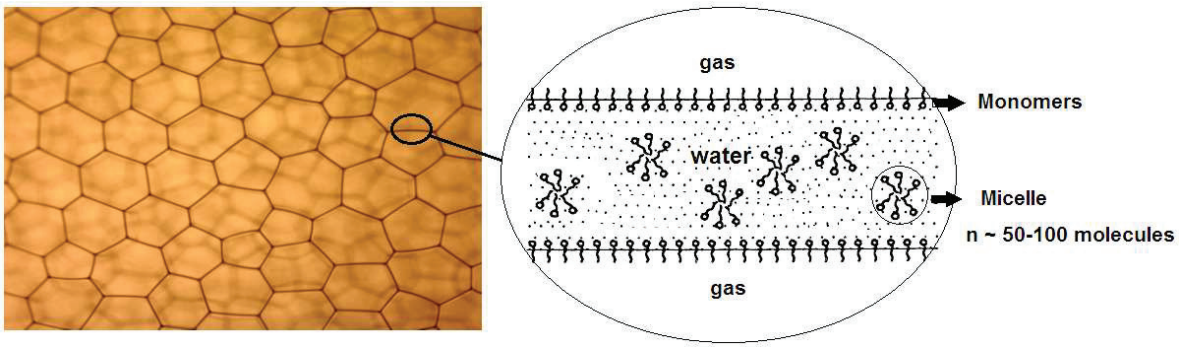

Figure 2.6: Surfactant associations in thin liquid films (left image from Paper 4; right figure modified from Schramm and Wassmuth, 1994).

The concentration at which micelles form is a characteristic of the particular surfactant and other factors (e.g., co-solutes, ionic strength, pH, temperature, pressure), and is termed the critical micelle concentration (cmc) (Barnes and Gentle, 2005; Pashley and Karaman, 2004;

Stasiuk and Schramm, 1996). Several physical and chemical properties of the solution, such as surface tension, micellar solubilization and conductivity change distinctly at the cmc (Figure 2.7). Beyond the cmc, the surface tension remains practically unchanged because reductions in surface tension are primarily attributable to the adsorption of monomers on the surface, which has now become saturated.

Foams can be generated at low surfactant concentrations, including below the surfactant's cmc (Alkan et al., 1991; Apaydin and Kovscek, 2001; Dixit et al., 1994; Fekarcha and Tazerouti, 2012; Heller, 1994; Kuhlman et al., 1992; Mannhardt and Svorstøl, 2001; Rohani et al., 2014; Sanchez and Schechter, 1989; Simjoo et al., 2013a; Tsau and Grigg, 1997; Vikingstad et al., 2006).

Beyond the cmc, uptake of otherwise sparingly soluble components (e.g., oil) may also occur in the micelles, referred to as micellar solubilization (Høiland and Blokhus, 2003). The solubilization properties of aqueous micellar solutions are relevant and important in many industries, including enhanced oil recovery, detergents and cosmetics (Christian and Scamehorn, 1995). For thin liquid films, solubilized or emulsified oil could have a vital effect on foam stability (Koczo et al., 1992; Wasan et al., 1994; see Chapter 6).

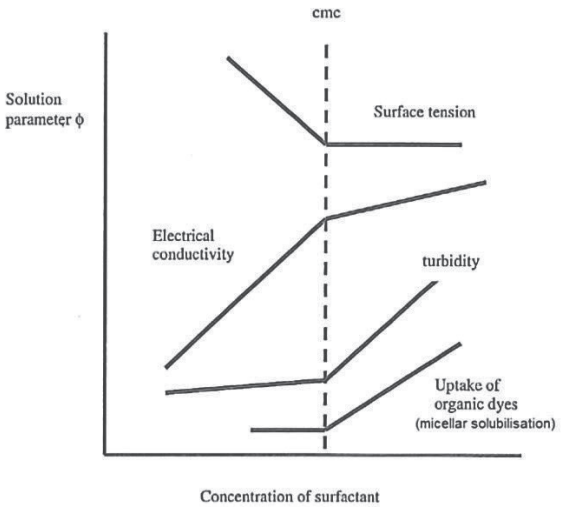

Figure 2.7: Diagram illustrating the distinct changes in solution properties that occur at the cmc (from Pashley and Karaman, 2004).

The most common micelle structure is spherical. Within a certain range above the cmc, the addition of surfactant simply increases the number of spherical micelles in the solution. Further increases in concentration may reorganize the spherical micelles into other micelle structures depending on their packing properties (Evans and Wennerström, 1999) (Figure 2.8). Increased foam stability at surfactant concentrations many times the cmc may occur due to the potential formation of such microstructures within the lamella that may oppose thinning and rupturing of foam films (Nikolov and Wasan, 1989; Wasan et al., 1994; see Chapter 3).

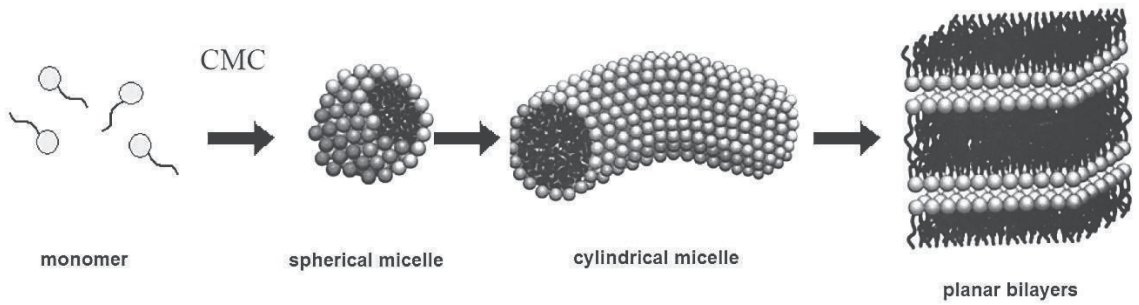

Figure 2.8: Micelle structures (redrawn from Evans and Wennerström, 1999).

Although foams can form in the presence of small amounts of surfactant, the efficient/stable foams in both bulk and porous media experiments seems to be related to a certain concentration above the cmc. In most foam field applications relevant to EOR, the surfactant is normally used in the micelle form (i.e., at surfactant concentrations above the cmc) (Enick and Olsen, 2012; Lake, 1989; Turta and Singhal, 1998).

2.3 Surfactant selection

A critical component for all foam EOR applications is the selection of surfactant. Many candidates are usually available from different vendors. However, specific I) foam properties and II) surfactant requirements are often required depending on the problem to be solved under the intended reservoir conditions, which may severely limit the number of surfactant candidates.

I) Specific foam properties could include strong and stagnant foams (i.e., very low mobility foams) for production well treatments to reduce the GOR (gas-oil ratio) (Hanssen and Dalland, 1994). Similar foam properties may also be desirable for conformance control foams to selectively block and/or divert gas flow from highly permeable thief zones to unswept parts of the reservoir. Weaker and more mobile foams (i.e., propagating foams) could be beneficial to stabilize the gas injection front with mobility control deeper into the formation without impairing injectivity (Enick and Olsen, 2012).

For CO_2-foam applications, several researchers have indicated that weaker foams could be desirable to avoid possible reservoir damage and/or large losses in injectivity. Weaker foams may also be ideal for gas mobility control in lower permeability reservoirs (Chabert et al., 2012, 2013; Bao, 2013; Holm and Garrison, 1988; Kuhlman, 1992; Mukherjee et al., 2014; Yang and Reed, 1989).

II) Specific surfactant requirements normally include thermal and chemical stability, salt tolerance/solubility, oil sensitivity, adsorption and cost.

The surfactants of interest must meet the environmental criteria and associated regulations set by the authorities (e.g., OSPAR Commission, 2009). Industrial availability for production and supply in large volumes of satisfactory quality at an acceptable price should also be confirmed with vendors and logistics.

Extensive interest in surfactant design and screening of foamers against CO_2-foams is evident in both new and older foam literature, as summarized by Enick and Olsen (2012). Early studies by Bernard et al. (1980) and Heller (1984) suggested that surfactants that are better emulsifiers (lower HLB numbers) than foamers (higher HLBs) (Figure 2.4b) might be most effective for reducing the mobility of dense CO_2. Conflicting views still appear to exist regarding whether the use of classical foaming agents can be adapted for dense CO_2 foaming (Bian et al., 2012; Chaubert et al., 2014; Sanders et al., 2010).

Examples of common surfactant types/names and their performances in laboratory studies of foam for EOR can also be found elsewhere (Borchardt, 1987; Enick and Olsen, 2012; Mannhardt et al., 2000; Preditis and Paulett, 1992; Schramm and Kutay, 2000; Tsau and Grigg, 1997; Tsau and Heller, 1992) (see Chapter 5, section 5.5).

Surfactant selection processes:

Relevant surfactants can first be tested for precipitation and solubility in reservoir brine and for thermal stability at reservoir temperature using simple, quick and inexpensive methods. Such testing will likely eliminate many candidates.

Two major experimental methods are normally utilized to evaluate surfactant formulations: bulk foam tests and foam core flooding experiments in porous media. Surfactant screening in bulk foam tests usually provides a ranking of the surfactants based on their ability to create foam (foamability) and the stability of the foam with time, both in the absence and presence of oil. The subjective ranking of foaming agents may be test dependent, and thus, test designs should be carefully evaluated. In addition, the correlation between bulk foam properties and foam properties in porous media is generally poor, i.e., surfactants that perform well in bulk foam tests may not necessarily work in porous media and vice versa (see Chapter 7, section 7.3). Bulk tests of promising candidates should therefore be followed by foam flooding experiments in porous media (preferably in reservoir core material under representative reservoir conditions). Key variables to measure and evaluate in porous media may include foam generation performance (e.g., pressure build-up profiles, mobility reduction factors, apparent viscosities), foam propagation and foam stability against subsequent injection of fluids after generation (e.g., gas/water blocking/diversion abilities) (see Chapter 7, section 7.4). Experiments in porous media should attempt to use relevant injection modes (e.g., simultaneous injection of gas and surfactant solution, surfactant alternating gas or pre-generation), flow rates, inlet foam qualities, surfactant concentrations, and gas compositions in the absence and presence of live reservoir oil for the best possible laboratory evaluation.

2.4 Choice of surfactant in this thesis

In all foam flooding experiments conducted in this thesis (**Papers 1-3**), anionic alpha-olefin sulfonate (AOS) surfactant was used. The choice of foamer was based on promising results from our earlier work, screening studies and field tests using AOS surfactants (Aarra et al., 1994, 1996, 1997, 1998, 2002, 2011; Skauge et al., 2002; Svorstøl et al., 1997; Vikingstad et al., 2006, 2009). Our positive experiences with AOS surfactants for nitrogen and methane foams under elevated pressure and temperature conditions should also make comparisons against CO_2-foams (in this thesis) interesting.

The general structure of an *n*-alkene sulfonate molecule is shown in Figure 2.9. In our work, the number of carbon atoms, n, was between 14 and 16 (C14-C16). According to the vendors, the molecular weight of the surfactants was approximately 300 g/mol. The AOS surfactants were applied in the grade of purity as received (i.e., ~ 38 and 100 % active material, respectively).

AOS are commercially available surfactants, acceptable with respect to health and environmental concerns, and can be produced in large volumes at a relatively low price. Commercial AOS formulations contain a mixture of alkene sulfonates and hydroxyalkane sulfonates. In addition, the sulfonation process of alpha-olefins may include a variety of reaction products such as trace amounts of alkene disulfonates, hydroxyalkane disulfonates and unreacted α-olefins (Blaker et al., 2002; Foster, 1997; Sivak et al., 1982; Svorstøl et al., 1997).

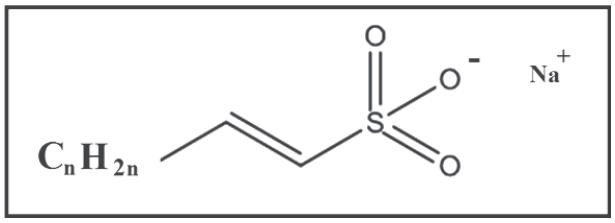

Figure 2.9: Generalized molecular structure of an alkene sulfonate (Na^+ is only used as an example of a counterion in the figure) (redrawn from Enick and Olsen, 2012).

The temperature stability of many foamers may be a major limitation on their use. AOS and other sulfonated surfactants have exhibited chemical stability and robustness in several foam tests at high temperatures, including tough North Sea reservoir conditions (280 ± 20 bar and 100 ± 20°C). The temperature stability of AOS surfactants led to the preferential use of this type of surfactant in this project (Aarra et al., 1994, 1997, 2002; Holt et al., 1996; Maini and Ma, 1986; Mannhardt and Svorstøl, 2001; McPhee et al., 1988; Tortopidis and Shallcross, 1994).

The adsorption of AOS surfactants on sandstone rock material is also reported to be quite low (often < 0.5 mg of surfactant per gram of rock) (Mannhardt et al., 1993; Mannhardt and Svorstøl, 2001; McPhee et al., 1988; ref. 35 in Simjoo et al., 2013b).

AOS surfactants with relatively long carbon chains (between C14-C18) have also frequently been used by other research institutions and oil companies, including for CO_2-foam projects (Andrianov et al., 2011; Bian et al., 2012; Chou, 1991; Enick and Olsen, 2012; Farajzadeh et al., 2009, 2010, 2011; Heller, 1984; Krause et al., 1992; Ma, 2013; Mohammadi et al., 1989; Prieditis and Paulett et al., 1992; Simjoo et al., 2013a, 2013b; Wang et al., 2014).

In **Paper 4**, different types of surfactants, including anionic, non-ionic and one zwitterionic surfactant, were evaluated and ranked based on their foam properties (i.e., foamability and foam stability) in bulk. General information about all the foamers used in this thesis is summarized in Table A.1 in the Appendix at the end of this introduction (starting on page 181).

The surfactants selected in this thesis do not represent a thoroughgoing investigation of available foamers, and surfactants that are superior to those chosen here may thus be available.

Chapter 3

Foam Stability

3.1 Introduction **p. 27**
3.2 Gravity drainage and capillary action **p. 28**
3.3 Film forces and disjoining pressure **p. 29**
3.4 Surface elasticity **p. 33**
3.5 Gas diffusion **p. 34**

3.1 Introduction

Foam stability plays a key role in most intended foam applications. Depending on its purpose, the lifetime of foam can vary from minutes and hours to days and even months. For example, a shampoo foam does not need to be stable for more than minutes, while foam for firefighting should remain stable at high temperatures for hours. Foam stability in applications related to EOR is also very important. Poor foam stability could require the foam treatment to be repeated more frequently than expected, while foams that cause injectivity problems should be easy to break if desired.

Regarding long-term foam stability, a production well at the Oseberg field in the North Sea indicated stable foam, even 6 months after treatment (Aarra et al., 1996).

The stability of foam is determined by the interplay of many different factors and forces. The mechanisms introduced in this chapter include gravity drainage, capillary suction coalescence, capillary pressure, disjoining pressure, surface elasticity and gas diffusion.

Various mechanisms to dominate foam stability in bulk and porous media have been proposed. For bulk foam, the dominating mechanisms suggested are gravity drainage and gas

diffusion (Rossen, 1996). In porous media, the important mechanisms for foam destabilization are the capillary suction coalescence, capillary pressure and the attractive van der Waals forces of the disjoining pressure (Khatib et al., 1988; Kovscek and Radke, 1994), whereas the surface elasticity and the repulsive forces of the disjoining pressure contribute to maintain their stability (Schramm and Wassmuth, 1994). The magnitude and degree of collective importance of these mechanisms remain controversial. Accordingly, there may be no generalizable theory describing the stability of all foam systems.

3.2 Gravity drainage and capillary action

Immediately after foam formation, liquid, the denser phase, tends to drain from the lamella network due to gravity. Over time, the foam structure frequently changes from wet, spherical bubbles to dry, polyhedral-like geometries as the liquid drainage process evolves (as illustrated earlier in Chapter 2, Figure 2.3). Drainage is an important phenomenon that reduces film thickness. The thinning of liquid lamellae and motion in the foam structure due to gravity drainage may lead to the sudden rupture of foam films (Schramm and Wassmuth, 1994)

In general, any factor that reduces the rate of film drainage may also increase the lifetime of the foam. Reduced drainage and improved foam stability have been reported for several polymer/gel-surfactant combinations (Aarra et al., 1997; Azdarpour et al., 2013; Cohen-Addad et al., 1994; Phillips et al., 1987; Rohani et al., 2014; Zhu et al., 1998, 2004). In addition, some mixtures of different types of surfactants enhance foam stability, possible due to the formation of a viscous surface layer (Langevin, 2000; Ross and Morrison, 1988; Schmidt, 1996).

In relatively dry foams, most of the liquid resides in the Plateau borders (Figure 3.1a). Because of its curvature, the pressure is normally lower in the Plateau borders than in liquid films. The pressure gradient leads to a flow of liquid from the lamellae toward the Plateau borders, which causes further thinning of the liquid films (Figure 3.1b). The driving force behind the movement of water toward the borders is referred to as the capillary suction coalescence (Saint-Jalmes, 2006).

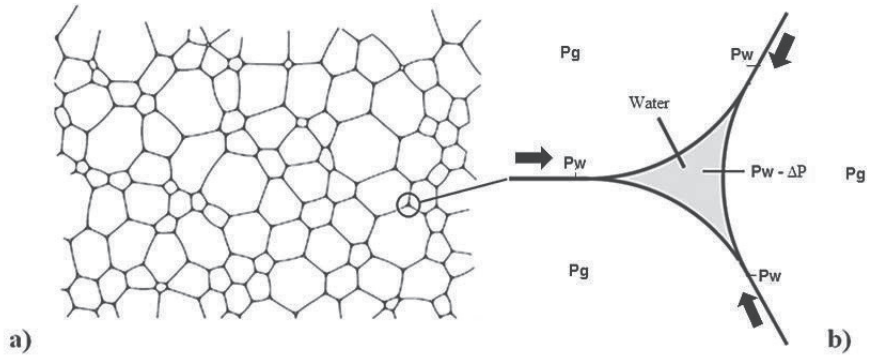

Figure 3.1: a) Illustration of a dry foam structure with water resided in the Plateau borders. b) A pressure gradient in the continuous liquid phase causes thinning of the lamellae due to the flow of water toward the Plateau borders (modified from Weaire and Hutzler, 1999).

As the foam film thins further, rupture will strongly depend on the balance between the capillary pressure, $\mathbf{P_c}$ (Equation 3.1), and the disjoining pressure (see next section).

If a foam bubble is located inside a capillary,

$$\Delta P = P_{c,g/w} = P_g - P_w = \frac{2\sigma_{g/w} \cdot cos\,(\theta)}{r} \tag{3.1}$$

for a (water-wet) gas/water system, where **r** is the radius of the capillary and **θ** is the contact angle between the solid and the gas/water surface.

Film thinning and foam coalescence by capillary actions are expected to be much stronger inside porous media with smaller pore radiuses (i.e., thinner films and larger capillary pressures) than in a bulk container. See also the theory about foam flow in porous media at the limiting capillary pressure (Chapter 4, section 4.5.2).

3.3 Film forces and disjoining pressure

According to the Derjaguin-Landau-Verwey-Overbeek (DLVO) theory, developed in the early 1940s, the total interaction energy between two colloidal particles is the result of two components: attractive and repulsive forces (Derjaguin and Churaev, 1989). This theory has also been applied to other colloidal systems, such as foams. For a foam lamella, these

intermolecular forces will be located inside the film. In other words, the stability of thin liquid films depends on the film forces that tend to disjoin or disrupt them.

The presence of ionic surfactants at the surface in a foam film will create a charged surface that induces repulsive and attractive forces. In general, ions of opposite charge are attracted to each other, whereas ions of the the same charge repel each other, resulting in the formation of an electrical double layer (Figure 3.2).

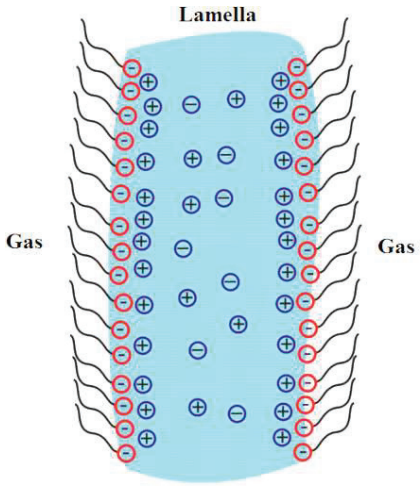

Figure 3.2: A simplified illustration of an electrical double layer in a foam lamella (adapted from www.soft-matter.seas.harvard.edu).

The net pressure operating per unit area across and perpendicular to the surfaces in thin liquid films is referred to as the disjoining pressure, Π (Figure 3.3), which can be defined as follows (Churaev and Derjagiun, 1985):

$$\Pi = \pi_A + \pi_R + \pi_S \tag{3.2}$$

where $\boldsymbol{\pi_A}$ is the attractive pressure caused by attractive molecular forces (e.g., van der Waals forces), $\boldsymbol{\pi_R}$ is the repulsive pressure from the electrostatic forces created when two charged surfaces approach each other, and $\boldsymbol{\pi_S}$ is the pressure due to structural forces as a result of the overlapping of boundary layers (e.g., repulsive steric forces, Born repulsion).

The disjoining pressure can take both positive and negative values. π_R and π_S are considered positive contributions (repulsion forces), while the attractive van der Waals forces, π_A, reduce the disjoining pressure. If Π is positive (i.e., $\pi_R + \pi_S > \pi_A + P_c$), the two surfaces separate, and the foam film may remain stable. If $\pi_R + \pi_S < \pi_A + P_c$, the film surfaces come into contact, and the lamella collapses. Hence, for a lamella in local equilibrium with no external force contributions, the capillary pressure balances the thickness of the lamella through the disjoining pressure ($P_c = \Pi$).

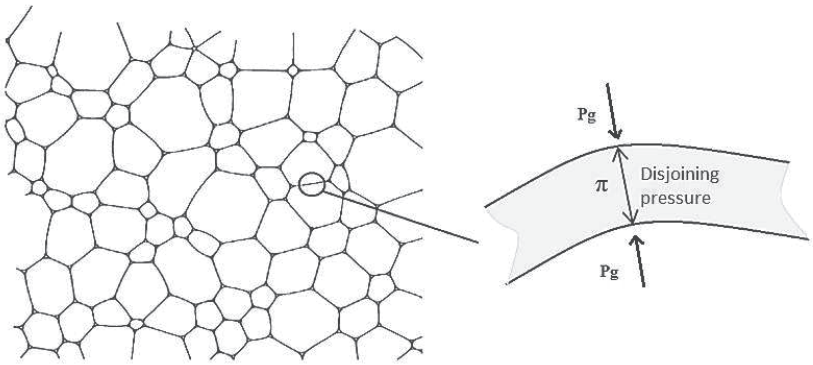

Figure 3.3: Illustration of disjoining pressure in thin liquid films (modified from Weaire and Hutzler, 1999).

The forces that contribute to the disjoining pressure are strongly dependent on the distance between the charged surfaces. Hence, for a lamella, the film thickness plays an important role. The disjoining pressure is thought to be significant only for thin films (i.e., < 100 nm). For thicker films, the disjoining pressure is not expected to be important (Schramm and Wassmuth, 1994; Wasan et al., 1994).

Figure 3.4 illustrates an idealized disjoining pressure isotherm showing how different force contributions can influence film stability at varying film thickness **h**. The disjoining pressure isotherm may vary with surfactant type, surfactant concentration, brine salinity and pH (Aronson et al., 1994; Bergeron et al., 1992, 1996).

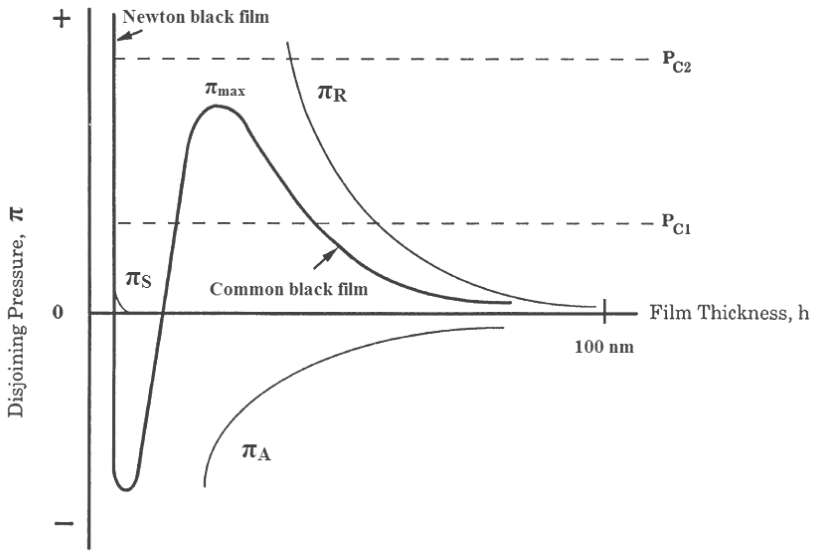

Figure 3.4: Illustration of an idealized disjoining pressure isotherm (bold curve) (explained in Aronson et al., 1994). Force contributions from electrostatic (π_R), van der Waals (π_A), steric forces (π_S) and two capillary pressures ($P_{C2} > P_{C1}$) are represented. The repulsive steric forces are shorter in range than the attractive van der Waals forces and the repulsive electrostatic forces (adapted from Aronson et al., 1994).

Recent decades have witnessed great developments in the field of surface forces. In addition to the classical DLVO components (i.e., electrostatic and van der Waals forces), several other components of different physical origins have been found to be important for stabilizing thin liquid films (e.g., steric interactions/structural forces/hydration). Kralchevsky et al. (1996) and Israelachvili (2011) explain complimentary concepts of disjoining pressure theory and non-DLVO forces in further detail.

Aronsen et al. (1994) observed a good correlation between the disjoining pressure isotherms measured for an anionic surfactant solution and its corresponding flow resistance in porous bead packs. High repulsive disjoining pressures exhibited large flow resistances (i.e., strong foam) in porous media. Increasing the surfactant concentration and salinity were even more effective for creating strong foam because they enabled even larger disjoining forces. Simjoo et al. (2013a) reported similar observations (i.e., stronger foams with increasing surfactant concentration) in a recent study in an outcrop Bentheimer sandstone using AOS C14-C16 surfactant. The authors explained that the disjoining pressure increases considerably as the surfactant concentration increases above the cmc, allowing the foam films to better withstand external forces and favoring the formation of stronger foams in porous media. Bergeron et al., (1997) found good correlation between measured disjoining pressures and gas-blocking

abilities to oil-based foams. High individual film-rupture pressures lead to strong gas-blocking foams in a porous bead pack.

Changes in the disjoining pressure isotherm with different gas types (i.e., CO_2 and N_2) have also been discussed as a possible explanation for why CO_2-foams usually are weaker then N_2-foams. Studies have indicated that both the repulsive electrostatic and the attractive van der Waals components of the disjoining pressure are smaller with CO_2 compared to N_2. A decrease in the disjoining pressure with CO_2 could result in less stable and weaker CO_2-foams (Kibodeaux, 1997; Farajzadeh, 2009).

3.4 Surface elasticity

Foams under dynamic conditions should be somewhat elastic to resist deformation without rupturing so that bubbles can withstand being bumped, compressed and deformed.

If a foam film is exposed to a sudden expansion, such as that due to an external force, the surfactant concentration in the expanded portion of the film will decrease (Figure 3.5). The non-uniform surfactant distribution along the expanded surface leads to a local increase in surface tension. The gradient in surface tension induces a spontaneous contraction of the surface, which generates flow of surfactant toward the film thinning area, while suppressing liquid flow from the film thinning area. This process attempts to resist film thinning and rupture. The surface-chemical explanation for film elasticity, which provides a resisting force to counteract film rupture, is referred to as the Gibbs-Marangoni effect (Schramm and Wassmuth, 1994).

The elasticity property may play an important role in porous media, in which the foam films traveling through the pore space are exposed repeatedly to contracting and stretching as they pass through the pore throats and bodies. Surface elasticity is expected to be less important under static conditions without external disturbances (Malysa and Lunkenheimer, 2008; Schramm and Wassmuth, 1994).

The ability of the surface to adjust and restore itself depends on properties of the surfactant and its concentration. The results have indicated that an optimum rate of change in the surface tension along the film surface is required to maintain foam stability. If the rate of change in the surface tension is too small or too fast, the film elasticity can be insufficient to prevent

rupture of the foam films (Buzzacchi et al., 2006; Eastoe et al., 2000; Georgieva et al., 2009; Huang et al., 1986; Tamura et al., 1995, 1997). For CO_2-foams with presumably low surface tension values against the liquid film at high pressures, Adkins et al. (2010) indicated that the surface tension gradient in CO_2-foams may be too small for Marangoni stabilization. Other possible influences of surface tension on foam properties are discussed in Chapter 5, section 5.4.7.

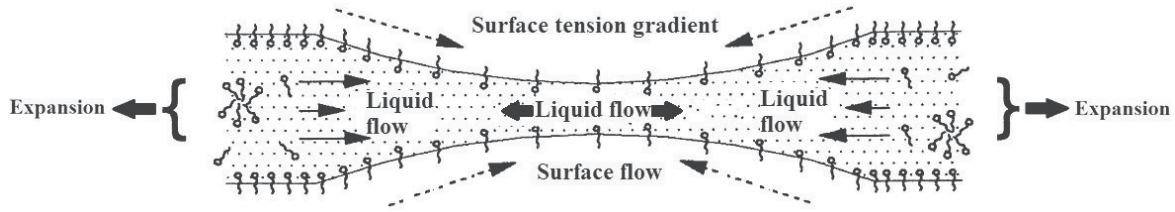

Figure 3.5: Surface elasticity in a foam film (modified from Schramm and Wassmuth, 1994).

3.5 Gas diffusion

Transport of gas across liquid films is also a well-known phenomenon affecting foam stability (Princen and Mason, 1965; Schramm and Wassmuth, 1994; Weaire and Hutzler, 1999).

Fick's laws describe the physics of diffusion (Fick, 1855). Fick's first law postulates that a substance is transported from regions of high concentrations to regions of low concentrations with a magnitude that is proportional to the concentration. In two or more dimensions, the law can be expressed as (Bird et al., 2007):

$$J = -D\nabla\phi \tag{3.3}$$

where **J** is the diffusion flux (i.e., amount of substance that will flow through a small area during a small time interval, for example ($\frac{mol}{m^2 \cdot s}$)); **D** is the diffusion coefficient (i.e., the substance's mobility) in dimensions of ($\frac{m^2}{s}$); and $\nabla\phi$, is the concentration gradient (i.e., amount of substance per unit volume), for example ($\frac{mol}{m^3}$) in the positions of ($\frac{1}{\partial x}$, $\frac{1}{\partial y}$, $\frac{1}{\partial z}$) in meter ($\frac{1}{m}$).

Fick's second law (the derivate of the first law) predicts how the diffusion changes with time, **t**. For diffusion in two or more dimensions, Fick's second law becomes the following (Bird et al., 2007):

$$\frac{\partial \phi}{\partial t} = -D\nabla^2\phi \tag{3.4}$$

In chemical systems, such as foam, the driving force for diffusion can be thermodynamically explained by the chemical potential of the system species, also known as the partial molar Gibbs free energy. Each chemical species (e.g., gas or water molecule) has its own chemical potential. At constant temperature and pressure in a system containing **n** constituent species, with the **i**-th species having $\mathbf{N_i}$ molecules, changes in the Gibbs free energy **dG** can be simplified to (Atkins et al., 2005):

$$dG = \sum_{i=1}^{n} \mu_i dN_i = \mu_1 dN_1 + \mu_2 dN_2 + .. \tag{3.5}$$

The definition of chemical potential $\boldsymbol{\mu}_i$ of the i-th species follows:

$$\mu_i = \left(\frac{\partial G}{\partial N_i}\right) T, P, N_{j \neq i} \tag{3.6}$$

At chemical equilibrium, the Gibbs free energy is at a minimum (dG = 0), and the sum of the chemical potential is also zero:

$$\mu_1 dN_1 + \mu_2 dN_2 .. = 0 \tag{3.7}$$

In foam structures, the pressure between foam bubbles of different sizes will vary (recap Equation 2.2. and Figure 2.2 in Chapter 2). These pressure gradients will act as a driving force for gas to diffuse through the liquid lamellae. The effect causes larger bubbles to grow at the expense of smaller bubbles due to gas diffusion from areas of high chemical potential to areas of low chemical potential (Figure 3.6). This foam coarsening process, also referred to as Oswald ripening, is unavoidable and may lead to instabilities and sudden collapse of the thin liquid films (Weaire and Hutzler, 1999).

The rate of mass transfer between foam bubbles is partly controlled by the nature of the gas phase used (e.g., solubility properties, diffusivity), the temperature and pressure conditions, and the ability of the surfactant at the surface to act as a barrier to gas escape (Farajzadeh et al., 2011). The greater diffusivity and solubility properties of CO_2 relative to N_2 in water have often cited as one of the reasons why CO_2-foams are usually weaker than N_2-foams in laboratory bulk and porous media experiments (Alkan et al., 1991; Du et al., 2008; Farajzadeh, 2009; Lake, 1989; Phillips et al., 1987; Wang et al., 2014).

Rossen (1996) argued that the effect of diffusion on foam stability is likely more important for bulk foams than foams in porous media, in which bubble growth may be limited by the pore walls. Similar argument was also recently reported in Nonnekes et al. (2012). Contrary to others, they therefore contended that the greater permeability of CO_2 through foam films could not be the main cause why CO_2-foams usually are weaker compared with N_2-foams during generation.

The solubility properties of CO_2 and N_2, including other possible influences of solubility on foam properties are described further in Chapter 5, section 5.4.3.

Paper 1 in this thesis examined the effect of mass transfer between fluid phases on CO_2-foam properties closer. CO_2-foam experiments with pre-saturated fluids were compared against experiments without phase-equilibration. Our results showed that the kinetics of mass transfer between CO_2 and surfactant solution cannot have been the main cause why the CO_2-foams during generation were weaker than the N_2-foams. However, mass transfer appeared to be a dominant mechanism for reduced CO_2-foam stability in porous media during liquid injection following foam generation (Chapter 8, section 8.2.3 and 8.2.6).

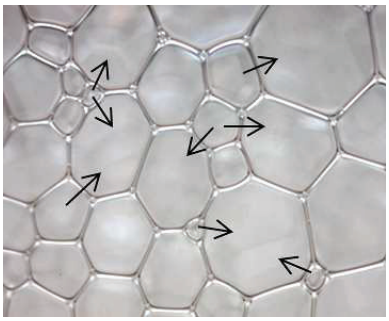

Figure 3.6: Larger bubbles grow at the expense of smaller bubbles due to gas diffusion across liquid films and between foam bubbles. The effect causes foam coarsening or collapse of the foam structure (modified from Paper 4).

Chapter 4

Foam in Porous Media

4.1 Rock properties p. 38

4.1.1 Absolute permeability p. 40

4.1.2 Lithology p. 40

4.1.3 Heterogeneity p. 41

4.2 In-situ foam generation mechanisms p. 43

4.2.1 Snap-off p. 43

4.2.2 Lamella division p. 44

4.2.3 Leave-behind p. 44

4.2.4 Pinch off p. 46

4.3 Foam mobility control p. 47

4.4 Foam texture p. 48

4.5 Foam flow p. 49

4.5.1 Making and breaking vs. bubble train p. 49

4.5.2 Flow at the limiting capillary pressure p. 49

4.5.3 Flow regimes p. 50

4.5.4 Foam propagation p. 52

4.6 Foam stability to subsequent fluids p. 53

4.7 Foam sensitivity to rock properties p. 54

4.7.1 Permeability p. 54

4.7.2 Rock heterogeneity p. 54

4.7.3 Wettability/lithological effects p. 57

4.1 Rock properties

To act as a reservoir, rocks must possess two essential properties: I) it must have pores to contain fluids (e.g., oil, gas and water); and II) the pores must be interconnected with each other to allow fluid movement and production. In other words, a rock must be both porous and permeable to serve as a profitable reservoir (Figure 4.1). The major known reserves of oil and gas are located in underground geological formations, predominantly of sandstone or carbonate rock material (Selley, 1998).

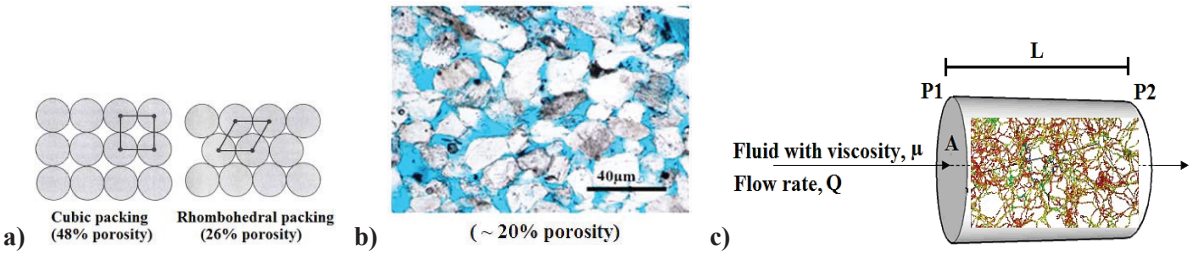

Figure 4.1: a) Theoretical packing of spherical grains of uniform diameter with available pore space/porosity (in white) given as a percentage (from Selley, 1998). b) Thin section of an outcrop Berea sandstone showing grains (white/gray) and pore space (pale blue) in natural porous rocks (from Paper 3). c) Illustration of a porous core plug with an interconnected network of pore spaces from inlet to outlet (modified from Solbakken, 2010).

This thesis investigates foam properties in outcrop Berea sandstone core material. For decades, Berea sandstone has been recognized by the petroleum industry as one of the best model rocks for use in laboratory studies of fluid flow, oil production characterization and the many variables related to different EOR processes. Other types of outcrop sandstone model rocks frequently used in laboratory studies of foam include Bentheimer, Boise and Clashach sandstones (Bernard et al., 1965; Chabert et al., 2014; Farajzadeh et al., 2009; Kim et al., 2004; Simjoo et al., 2013a). Their availability and relatively homogeneous appearance compared to many reservoir rocks have likely led to their preferential use (Churcher et al., 1991).

Theoretically, the widespread use of homogenous model rocks should facilitate comparisons between two or more cores in the same study or comparisons with other experimental studies in the literature. However, it is difficult to determine the similarity of natural rocks (i.e., with respect to physical properties, mineralogy, pore geometry, small scale heterogeneities).

Reservoir heterogeneity plays a major role in oil recovery. I) High permeability "thief zones" (e.g., layers, fractures, vugs/cavities) may permit excessive flow or segregation of fluids through these intervals, while II) low permeability structures (e.g., shale layers, faults, laminations/compaction bands) could act as barriers to fluid flow across the reservoir. Both cases (I/II) can strongly contribute to reduce sweep efficiency and lower the ultimate recovery factor from oil fields.

Although Berea sandstone is considered relatively homogenous in appearance, various degrees of heterogeneities exist within it that could influence experimental results and their subsequent interpretation (see for instance Figure 4.2).

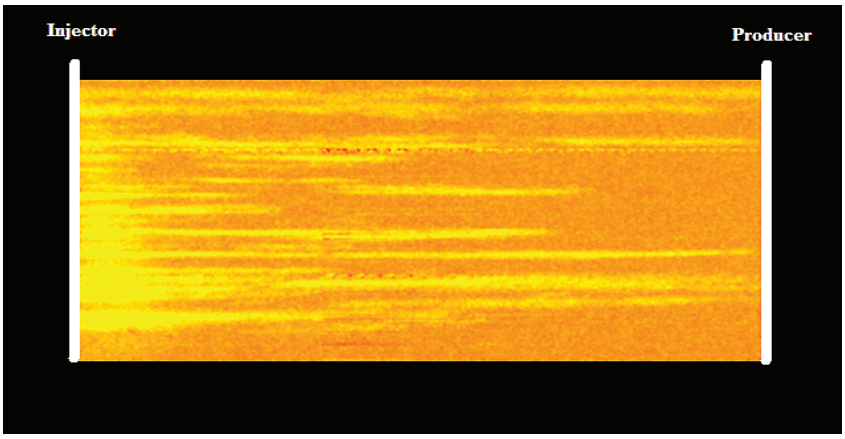

Figure 4.2: X-ray image of gas injection (yellow) into a laminated Berea rock sample saturated with water (orange). Favored gas flow is indicated by the more permeable streaks of the rock, leaving the lower permeable areas of the rock sample unswept. The illustration should be considered more illustrative than complete (modified from Paper 3).

Several papers have noted the potential for heterogeneities in Berea core material, particularly within its lower permeability ranges (i.e., < 500 mD). These studies include investigations of foam generation performance (Chou, 1991; Gauglitz et al., 2002; Solbakken et al., 2014; Zitha et al., 2003), surfactants for dense supercritical CO_2-foaming (McLendon et al., 2012), liquid injection after foam generation (Nguyen et al., 2009), foam diversion in matrix acidizing (Parlar et al., 1995), gas trapping (Zuo et al., 2012, Zhou et al., 2010, 2011), displacement experiments with CO_2 and brine (Berg et al., 2013), dispersion measurements (Menzie, 1995), EOR potential of low salinity water injection (Robertson et al., 2003; Zhang

and Morrow, 2006), EOR potential of combined low salinity and surfactant flooding (Solbakken, 2010; Spildo et al., 2012), polymer flooding (Yilmaz et al., 2009), relative permeability, capillary pressure and wettability (Corey and Rathjens, 1956; Honarpour et al., 1994; Huang et al., 1996; Oshita et al., 2000). Many of these studies indicated that their results were strongly controlled or affected by the properties and heterogeneities of the core.

4.1.1 Absolute permeability

The absolute permeability, **K**, is a property of the rock and defines its ability to transport a fluid through its interconnected network of pores. K is defined by Darcy's law, which is given by the following equation for linear one-dimensional horizontal flow in a uniform pore system occupied by a single incompressible fluid with no chemical interaction with the rock:

$$K = \frac{\mu L Q}{A \Delta P} \tag{4.1}$$

where Δ**P** is the pressure difference across the porous medium with length **L** and cross-sectional area **A** when a fluid with viscosity $\boldsymbol{\mu}$ is forced to flow through it at a constant volumetric flow rate **Q**. The SI unit of permeability is m^2, but the Darcy (D) unit has traditionally been preferred, where 1 Darcy = 0.9869 x 10^{-12} m^2 (Skarestad and Skauge, 2008).

Average permeabilities in sandstone reservoirs are typically in the range of 5-500 mD, although intervals of several Darcy's may also readily occur (Selley, 1998). Berea sandstone core material can be found in a large range of different permeabilities, typically ranging from 10 to 1200 mD (Alvarez et al., 2001; Churcher et al., 1991; Kim et al., 2004; Gauglitz et al., 2002; Siddiqui et al., 1997a, 1997b; Zhang and Morrow, 2006).

4.1.2 Lithology

The lithology of a rock is a description of its physical characteristics, such as mineralogical composition (e.g., minerals and clays) and textural parameters (e.g., grain size, grain shape, sorting, packing).

Variations in porosity and permeability are closely related to the textural parameters of a rock. A summary of the effects of different textural parameters on the magnitude of porosity and permeability in a rock is presented in Table 4.1.

Table 4.1: Influence of rock textural parameters on porosity and permeability (adapted from Selley, 1998)

Textural parameters	Influence on porosity and permeability
Grain size	Porosity is theoretically independent of grain size. Permeability decreases with decreasing grain size because pore diameter decreases.
Grain sorting	Porosity and permeability decrease as sorting becomes poorer.
Grain shape	Porosity and permeability usually decrease with decreasing grain roundness.
Grain packing	Porosity and permeability decrease with tighter packing (e.g., compaction).

Natural rocks usually contain various amounts of minerals and clays (see for instance Table B.2 in the Appendix). The chemical composition of various minerals and clays are different, and consequently, different rock-fluid interactions may be expected. As summarized by Parks (1990), the surfaces of many minerals will hydrate in the presence of water, leading to regions with distinct chemical and physical properties. In water-wet outcrop model rocks the stability of the water film along the mineral surfaces may be sensitive to different mineralogy and its distribution, as noted by Frette et al. (2009). For example, the distribution of cement and clay in Berea may not form connected phases (Bernabe and Brace, 1990), illustrating the "mineralogical heterogeneity" that can occur within a rock. Thus, rock-water interactions and water film stability may be different in various outcrop model rocks (e.g., Berea and Bentheimer).

4.1.3 Heterogeneity

Anisotropy or heterogeneity, as applied to porous rocks, indicates that some properties of the rock are not equal in all directions. For instance, pore geometry and permeability are seldom the same in all directions within a reservoir.

Micro-models, glass-bead packs and carefully prepared sand packs are examples of porous media that may yield relatively uniform pore systems. Real porous rocks (e.g., outcrop model rocks) never meet the conditions of homogeneity perfectly. Subsequent diagenetic processes

of minerals and clays in natural pore systems (e.g., cementation, compaction, dissolution, precipitation) could considerably complicate pore geometry (Figure 4.1b).

An example of rock heterogeneity is layering (Figure 4.3), such as when a less permeable layer lies parallel to a more permeable layer. For a layered case, the vertical permeability, K_v, will often be lower than the permeability horizontal to the beddings (K_h).

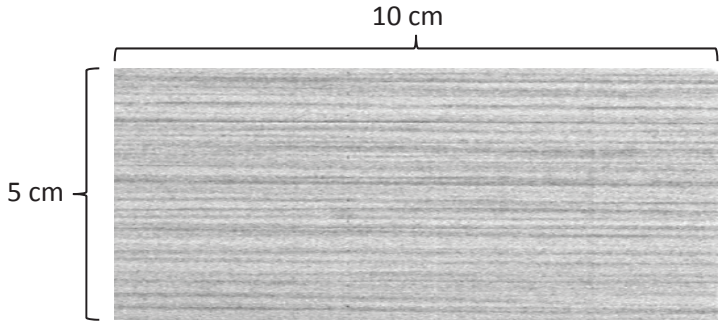

Figure 4.3: X-ray image of a naturally laminated Berea rock sample. The darker regions in the sample represent the laminas, $K_h \approx 90$ mD and $K_v \approx 45$ mD (from Paper 3).

Any deviation from uniform pore systems also decreases the accuracy of Darcy's law (Equation 4.1). Therefore, permeability measurement of core plugs in the laboratory should be carefully considered and only taken as an average quantity. Internal variations in petrophysical properties, such as millimeter-thick laminations (Figure 4.3), cannot be detected by traditional laboratory measurements (Figure 4.1c) (Torabi et al., 2008). Heterogeneities on different scales (e.g., core-scale and pore-scale) can be detected by various types of analysis (Solbakken et al., 2014). The consequences of field-management decisions based on incorrect interpretations of laboratory results and the benefits of systematic core analysis have also been stressed by other authors (e.g., Ottesen and Hjelmeland, 2008). Without more complete information concerning the geology, origin and content of natural rocks, it is impossible to precisely predict or interpret the extent to which the properties of the rock might have influenced the laboratory results.

The extent to which laminations (Figure 4.3) affect fluid flow reportedly depends on factors such as the degree of lamina relative to scale, the lamina thickness and the permeability contrast between the laminas and the more permeable layer of the rock, often referred to as the "host rock" (Fossen et al., 2007; Fossen and Bale, 2007; Lothe et al., 2002; Rotevatn et al., 2013; Torabi et al., 2008).

4.2 In-situ foam generation mechanisms

Foam studies in micro models, glass beads and capillaries identified many of the earliest recognized mechanisms of pore-level generation, destruction, trapping and flow of foam in porous media (Chambers and Radke, 1991; Hirasaki and Lawson, 1985; Mast, 1972; Ransohoff and Radke, 1988).

The three most recognized mechanisms for in-situ foam generation are snap-off, lamella division and leave-behind. These bubble-making processes are explained in detail by Ransohoff and Radke (1988), Kovscek and Radke (1994), and Rossen (1996).

4.2.1 Snap-off

The snap-off mechanism is a mechanical process that creates lamellae or bubbles when the gas phase pushes the gas-liquid surface through a pore throat and then "snaps off" (Figure 4.4a). The mechanism depends strongly on the local dynamic capillary pressure in the pore throat, the pore geometry and the aspect ratio (i.e., ratio of pore body to throat size) (Rossen, 1996).

Snap-off is regarded as the dominant mechanism for in-situ foam generation, particularly during co-injection of surfactant solution and gas (Kovscek and Radke, 1994).

Pore body radii of at least twice the pore throat radius have been suggested to be necessary to create the required drop in capillary pressure for snap-off to occur (Ransohoff and Radke, 1988).

Churcher et al. (1991) reported that the aspect ratio of Berea increased from ~5 to 11 with decreasing porosity (~26-19%) and permeability (1168-114 mD). Gauglitz et al. (2002) indicated a similar trend, with an increase in the ratio of pore body length to pore throat diameter in Berea cores from ~7 to 12 with decreasing porosity (24-19%) and permeability (780-130 mD). Interestingly, foam generation was easiest (i.e., occurred at the lowest pressure gradient applied) in the core with the lowest permeability and highest body length to throat diameter ratio. A recent study by Oughanem et al. (2013) concluded that the mean aspect ratios of four different sandstone samples, including a Berea (208 mD) and a Bentheimer (2676 mD), were relatively similar, with a value of approximately 5.

4.2.2 Lamella division

The division of a lamella or a bubble approaching a branch point with several pore throats is called lamella or bubble division (Figure 4.4b). As long as foam flow is maintained, the initial lamella or bubble can be subdivided into more lamellae or bubbles. Generating additional liquid lamellae would presumably increase the resistance to gas flow. Lamella division is thought to be favored if the bubble size is larger than the pore body, if the neighboring pores are not filled with foam, and if the lamella is stable enough to be divided (Kovscek and Radke, 1994).

4.2.3 Leave-behind

Figure 4.4c illustrates the third foam generation mechanism. The leave-behind mechanism describes the formation of stationary liquid lenses that are left behind when gas is injected into a porous medium filled with surfactant solution. The lenses created parallel to the flow direction do not offer significant resistance to gas flow. The foams generated by the leave-behind mechanism are therefore expected to be weaker than those generated by the other two generation mechanisms because the gas remains relatively continuous and mobile.

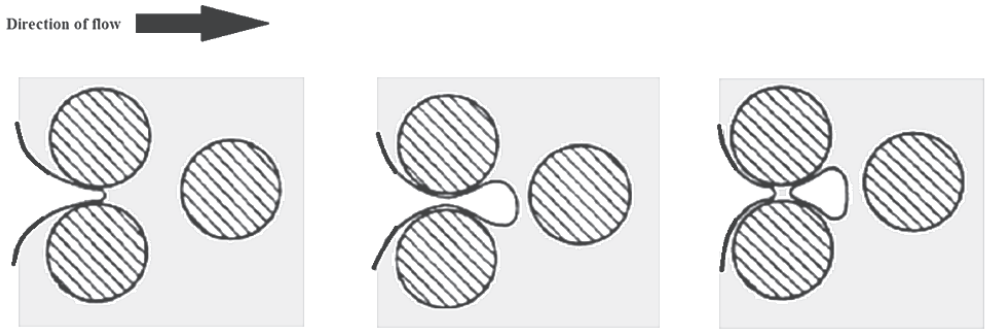

a)

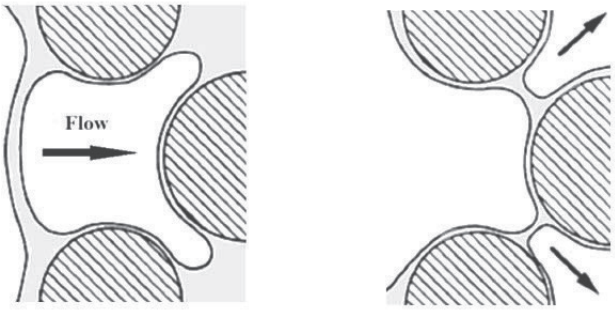

b)

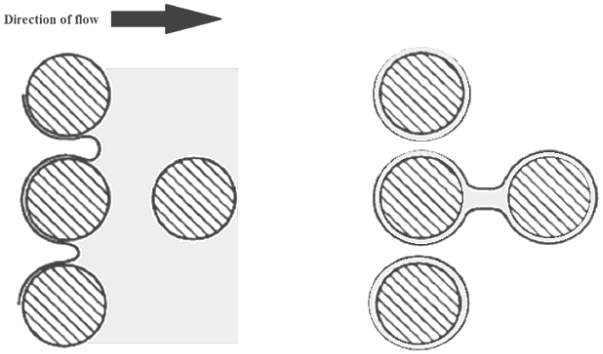

c)

Figure 4.4: Schematic illustration of in-situ foam generation mechanisms: a) snap-off, b) lamella division and c) leave behind. The arrows indicate the direction of flow direction, and gas, surfactant solution and spherical rock grains are indicated by white, gray and striped shading, respectively (from Kovscek and Radke, 1994).

4.2.4 Pinch-off

Liontas et al., (2013) recently identified two novel foam generation mechanisms in porous media: the "neighbor-neighbor pinch-off" mechanism and the "neighbor-wall pinch-off" mechanism. Foam was pre-generated and injected into a microfluidic constriction at high injection rates. A high-speed camera attached to a microscope was then used to capture the pore-level events.

In the newly observed mechanisms, additional bubbles or lamellae were formed before the gas had passed through the constriction, either by contact with neighboring bubbles or when caught between a neighboring bubble and the wall (Figure 4.5). Shear and capillary forces dictated the two pinch-off mechanisms.

Compared with the earliest proposed mechanisms of in-situ foam generation, which described the formation of foam due to contact with hard rock surfaces (Figure 4.4), the new "pinch-off" mechanisms propose that foam can also be created using neighboring bubbles to induce break-up of bubbles to generate more lamellae (Figure 4.5). The bubble sizes in this model were smaller than the pore body size, which is opposite to others who suggest the bubble size in porous media to be at least as large as the pore body (see section 4.4).

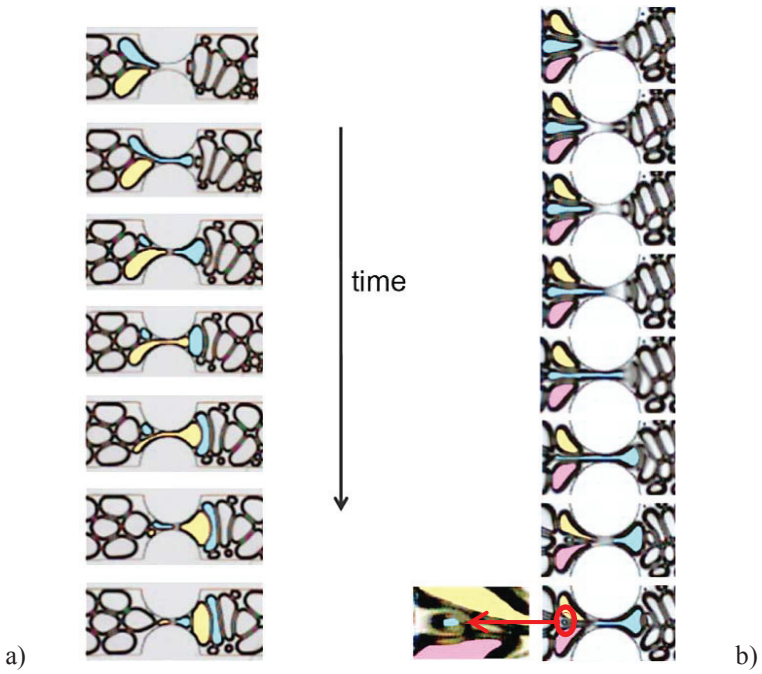

Figure 4.5: Observation of two novel in-situ foam generation mechanisms: a) the neighbor-wall pinch off mechanism and b) the neighbor-neighbor pinch off mechanism (adapted from Liontas et al., 2013).

4.3 Foam mobility control

Recall from Chapter 1 that mobility control basically refers to techniques that reduces the mobility ratio by changing fluid relative permeabilities and/or viscosities such that $M \leq 1$.

Mobility control by foam conceals the interplay of two distinct, but intimately related effects. The first is the mobility reduction of the liquid phase. The second is the mobility reduction of the gas phase. The term "foam mobility" is therefore shorthand for describing both the gas and water mobility reductions that occur in the presence of foam (Kovscek and Radke, 1994; Rossen, 1996).

It has repeatedly been reported that foam does not alter the water relative permeability function $k_{rw}(S_w)$ but changes it indirectly by increasing the gas saturation (i.e., decreasing S_w) due to the presence of foam. If liquid mobility in the presence of foam can been considered a continuous and flowing phase throughout the porous media, the liquid viscosity can be taken to be constant, and hence, the mobility reduction of the liquid phase is then reflected simply by the lowering of its relative permeability (Bernard et al., 1965; Friedmann et al., 1991; Osterloh and Jante, 1992; Rossen 1996; Sanchez and Schechter, 1989).

The effects on liquid relative permeability in the presence of foam should not be taken do mean that foam does not influence liquid mobility in porous media. Foam reduces permeability in porous media to both gas and liquid simultaneously, as stressed by Bernard et al. (1965). Nevertheless, whether liquid flows within the continuous network of lamellae, in water films along the rock surfaces or restricted to the smallest water-wet pores which do not contain gas remains controversial (Ettinger and Radke, 1992; Falls et al., 1988a; Holm, 1968; Kovscek and Radke, 1994; Mast, 1972).

Gas mobility in porous media is reduced by foam due to the formation of thin liquid films. The thin liquid lamellae can block gas flow paths or trap a portion of it, either temporarily or permanently within the porous media. Whether the gas mobility reduction caused by foam is best addressed in terms of an effective gas viscosity or as a gas relative permeability effect remains an unresolved issue as noted by several authors (Rossen, 1996; Kovscek and Radke, 1994).

4.4 Foam texture

Foam texture describes the size and distribution of bubbles. Fine/dense foams have smaller and more uniform bubble sizes (i.e., a higher number of bubbles or lamellae per unit volume) than coarser foams (Figure 4.6).

a) 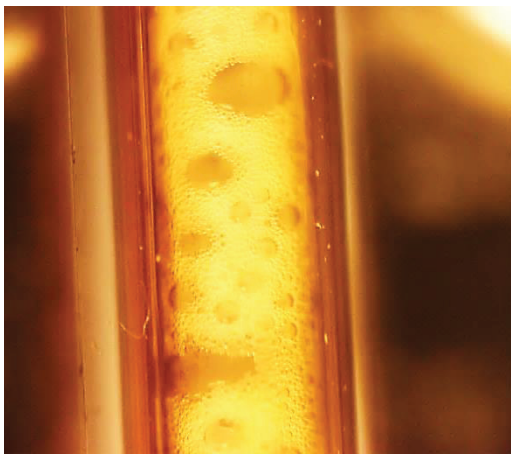 b) 

Figure 4.6: Examples of foam texture observations in a sight-glass out from the core under experimental conditions, 280 bar, 50°C (from Paper 1): a) N_2-foam (finer/denser texture – mobility reduction factor ≈ 120). b) CO_2-foam (coarser texture – mobility reduction factor ≈ 3).

The degree of mobility reduction by foam in porous media is thought to be dominated by foam texture. The idea is that smaller bubbles result in more thin liquid films and should therefore reduce gas mobility to a greater extent than larger bubbles under otherwise identical conditions. Finer foam texture is also expected to be more stable than coarser texture, which could give rise to larger pressure gradients (i.e., stronger foam) (Rossen, 1996; Kovscek and Radke, 1994).

Bubbles sizes inside natural porous media have been suggested to be at least as large as the pore body. This statement has been based on visual observations of the texture of effluent foam from porous media in laboratory experiments, assuming that the texture out of the core reflects foam texture in-situ (Ettinger and Radke, 1992; Kovscek and Radke, 1994).

It is generally expected that the foam texture will be molded and reshaped by the porous media, which makes it inherently difficult to precisely determine in-situ foam texture by any laboratory methods.

4.5 Foam flow

4.5.1 Making and breaking vs. bubble train

Two different concepts have been used to describe how foam flows in porous media: making and breaking mode (M&B) (Holm, 1968; Mast, 1972; Yang and Reed, 1989) and bubble train mode (BT) (Hirasaki and Lawson, 1985; Falls et al., 1988a; Yang and Reed, 1989).

The M&B refers to the situation in which bubbles flowing through pore constrictions are constantly breaking and reforming, whereas the BT refers to the case in which trains of bubbles can travel through several pore bodies and throats without rupturing. Consequently, BT foams are often considered stronger and more resistant to flow than M&B foams.

The differences between strong and weak foams in porous media may partially reflect differences in the way the foams are transported.

4.5.2 Flow at the limiting capillary pressure

The concept of a limiting capillary pressure to foam flow in porous media was first established by Khatib et al. (1988). Capillary pressure, P_c (defined by Equation 3.1 in Chapter 3), governs foam stability in porous media at steady state conditions for relatively high-quality foams. High capillary pressures could overwhelm the repulsive disjoining forces in foam films and possible break the lamellae. That is, if P_c is too high, the lamellae break and the foam collapse.

If the conditions in a porous rock are favorable for foam generation, large numbers of lamellae will be generated, decreasing gas mobility. As the gas mobility decreases, it displaces water (i.e., surfactant solution) to a lower saturation. A successive lowering in water saturation will result in a corresponding increase in gas/water capillary pressures (Figure 4.7). At a given saturation, the capillary pressure can be thought of as a measure of the smallest pore being entered by the non-wetting fluid, suggesting that the curvature of the drainage capillary pressure curve is a function of the pore size distribution (Lake, 1989). At some "limiting" value of capillary pressure, P_c^*, corresponding to a critical saturation of the wetting phase, S_w^*, the foam becomes unstable. That is, the rate of foam destruction becomes higher than the rate of generation, which implies a transition toward weaker foams. An increase in P_c above P_c^* is thought to initiate strong foam destruction, an increase in gas mobility, and an increase in water saturation so that the capillary pressure falls below P_c^* again. In this way,

the foam system regulates itself around steady-state conditions to maintain P_c close to P_c^*. Most theories of foam flow in porous media support the concept of the limiting capillary pressure (Rossen, 1996).

The limiting capillary pressure value for a given system has been reported to depend on factors such as surfactant type and concentration, brine salinity, rock properties (e.g., permeability), system pressure, foam quality and gas/water flow rates (Khatib et al., 1988; Holt et al., 1996; Rossen and Zhou, 1995).

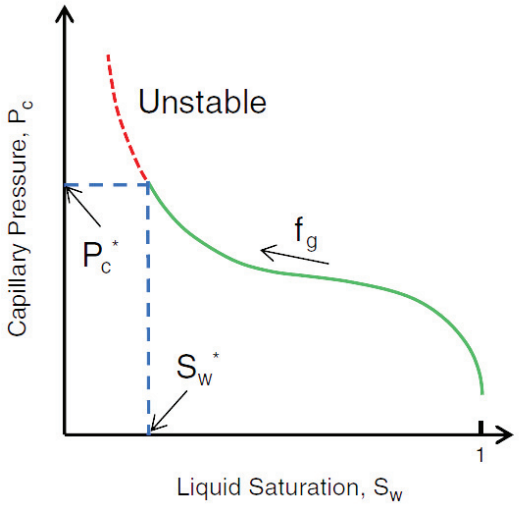

Figure 4.7: Schematic illustration of the limiting capillary pressure theory of foam flow in porous media based on the gas/water drainage capillary pressure curve (from Khatib et al., 1988).

4.5.3 Flow regimes

Two distinct regimes for describing foam flow behavior in porous media have been identified: a high-quality and a low-quality regime. The two flow regimes were first identified experimentally by Osterloh and Jante, (1992) and were later utilized and extended by other authors (e.g., Alvarez et al., 2001 and Kim et al., 2004).

The two flow regimes are primarily governed by changing the foam quality (i.e., volume fraction of gas injected) and total flow rates at steady-state conditions (Figure 4.8). The pressure gradient is nearly independent of liquid velocity in the low-quality regime, whereas nearly independent of gas velocity in the high-quality regime. A transition between the regimes occurs at a specific foam quality termed f_g^*. It is believed that the transition point

corresponds to a point at which the limiting capillary pressure, P_c^*, is obtained. Therefore, P_c^* is expected to control foam texture, and consequently, gas mobility in the high-quality regime. In the low-quality regime, it is thought that $P_c < P_c^*$ and that gas mobility depends on gas trapping and mobilization at fixed bubble texture. The optimal foam quality (i.e., highest pressure gradients at fixed total flow rates) occurs at f_g^* (Alvarez et al., 2001; Osterloh and Jante, 1992).

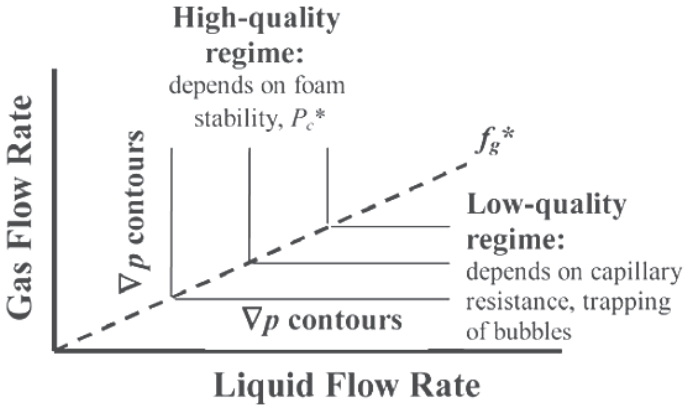

Figure 4.8: Schematic illustration of the two flow regimes presented as a contour plot (from Alvarez et al., 2001).

Contour plots of pressure gradients such as that illustrated in Figure 4.8 can provide important insights into how different injection conditions (i.e., rates and quality) could affect the apparent rheology of foam (at steady state). For example, experimental studies have used the concept of flow regimes to evaluate surfactant formulations based on different injection conditions (Chabert et al., 2013, 2014).

The apparent rheology of foam seems to be sensitive to the surfactant type and concentration and porous media used when foam quality and injection rates are changed. This sensitivity is reflected in the literature concerning whether foam is Newtonian, shear-thinning/thickening or a mixture of Newtonian and shear-thinning (as noted in the introduction by Spirov et al., 2012). Unexpected flow regimes have also been observed for dense CO_2-foams (Chabert et al., 2013; Dong, 2001; Kim et al., 2004) and polymer enhanced foams (Romero et al., 2002), compared with N_2-foams (Osterloh and Jante, 1992).

The behavior of foam in porous media with changing foam qualities and injection rates was not evaluated in this thesis.

4.5.4 Foam propagation

The ability of foam to propagate in porous media and the propagation rate are key factors for success for most foam EOR applications. In production well treatments, in which strong and stagnant foams are often desired, propagation is likely less critical, though even these processes must be able to propagate some distance into the formation (Hanssen and Dalland, 1994; Rossen, 1996).

Chou (1991) demonstrated that foam generation and propagation in the absence of oil were largely dependent on the initial state of the porous media. Pre-saturating the core with surfactant solution prior to co-injection of gas (N_2) and AOS surfactant was beneficial to obtain immediate foam generation and propagation. Without surfactant pre-flush, significantly delayed foam generation and propagation were observed. The strategy of injecting a slug of surfactant solution prior to foam generation has also been adapted in the field (Aarra et al., 1996).

In sandstone cores, strong foams using $AOS_{C14\text{-}C16}$ surfactant without oil were found to propagate close to the injection rate. These experiments were conducted under elevated pressure and temperature conditions with surfactant pre-flush using fixed injection rates (Mannhardt et al., 1999; Vikingstad and Aarra, 2009).

The presence of residual oil in laboratory corefloods greatly influences the foam propagation rate (Mannhardt and Svorstøl, 1999; Vikingstad and Aarra, 2009). Vikingstad and Aarra (2009) compared N_2-foam propagation in Berea sandstone using an AOS surfactant and a fluorinated sulfobetaine. In the absence of oil, both foams propagated close to the injection rate. In the presence of residual oil, the AOS surfactant propagated faster than in the absence of oil. Foam propagation using the fluorinated surfactant was significantly delayed by approximately 10-fold compared with the no-oil case.

With respect to foam propagation distance, Hirasaki (1989) and Patzek and Koinis (1990) reported a field steam-foam process that indicated that foam propagated and improved vertical sweep over a distance of ~ 30 m (90 ft.) from the injector.

4.6 Foam stability to subsequent fluids

Foam stability after placement should also be important to evaluate. A short lifetime of the foam after placement could require the foam process to be repeated more frequently than expected to maintain its purpose. Likewise, foams that cause injectivity problems should be evaluated for their abilities to break if desired. Foam stability to subsequent fluids can therefore be relevant to investigate in relation to production well treatments intended to prevent unwanted fluid production or in relation to conformance control processes followed by subsequent gas/liquid injections (e.g., Figure 1.4, Chapter 1).

Gas blocking abilities:

Long-lasting gas blocking abilities to foam have been demonstrated both in laboratory corefloods (Hanssen and Dalland, 1994; Aarra et al., 1994, 2011), and for significant periods in field tests (Aarra et al., 1996; Holm, 1970; Krause et al., 1992).

The critical parameters for gas-blocking foams (e.g., temperature, pressure, oil, surfactant, gas type, porous media, etc.,) were addressed and discussed in Hanssen and Dalland (1994).

In the near-well region were large volumes of gas are injected foam will dry out and collapse over time (Rossen, 1996).

Water blocking abilities:

Foams can also reduce water flow. Several authors indicate that foams can survive in laboratory corefloods, at least in a weakened form, against several pore volumes of liquid injected (Aarra et al., 2011; Bernard et al., 1965, 1980; Bhide et al., 2005; Du et al., 2007; Nguyen et al. 2009; Parlar et al., 1995; Seright, 1996; Zeilinger et al., 1995). Reduced foam stability to subsequent liquid injections has been discussed in terms of surfactant dilution, gas expansion and gas dissolution into the injected liquid phase.

4.7 Foam sensitivity to rock properties

4.7.1 Permeability

The permeability of a rock is an important parameter controlling the properties and behavior of foam in heterogeneous porous media. Despite its importance, its role is poorly known. Foam strength in laboratory core floods has for instance been reported to both increase (Bernard and Holm, 1964; Dixit et al., 1994; Lee and Heller, 1991; Mannhardt and Novosad, 1994; Yang and Reed, 1989) and decrease (Dixit et al., 1994; Marsden and Khan, 1966; Siddiqui et al., 1997a; Solbakken et al., 2014; Yang and Reed, 1989) with increasing absolute rock permeability.

Stronger foam in high permeability rocks is consistent with the theory of the critical capillary pressure to foam (section 4.5.2). Lower permeability rocks are thought to have a higher destabilizing effect on foam as they generally exert larger capillary pressures on the lamellae at any given gas saturation than higher permeability rocks (Khatib et al., 1988; Rossen and Zhou, 1995). However, several studies have demonstrated that it is possible to readily generate strong N_2-foams in Berea sandstones cores with relative low permeabilities (Chou, 1991; Gauglitz et al., 2002; Parlar et al., 1995; Solbakken et al., 2014; Vikingstad and Aarra, 2009), even as low as 9 mD (Siddiqui et al., 1997a). Thus, it is unclear whether a threshold in rock permeability to foam truly exists.

4.7.2 Rock heterogeneity

Applications of foam in heterogeneous reservoirs primarily include gas diversion and mobility control in EOR processes (Enick and Olsen, 2012), GOR control in production well treatments (Aarra et al., 1996), acid diversion in well stimulations (Thompson and Gdanski, 1993) and flow diversion in environmental remediation processes (Hirasaki 1997; Zhang et al., 2009).

Foam has been recognized as a promising method in heterogeneous porous media. A favorable property of foams is their ability to generate in target layers (i.e., preferentially in permeable layers where fluid flow is favored), diverting flow to the less permeable layers.

The distinct purposes of a foam blocking agent compared to a foam mobility control agent in heterogeneous reservoirs were stressed by Seright (1996). A mobility control agent should be able to propagate in both high permeability and low permeability zones of the reservoir to

suppress fingering, gravity override and channeling (Figure 4.9a). This foam behavior may be desirable for stabilizing the gas injection front in reservoirs with local permeability variations. In contrast to a mobility control agent, minimized penetration of foam into the lower permeable zones would be desired for a process intended to selectively block off a "thief zone" and for fluid diversion to lower permeability zones (Figure 4.9b). Any foam that enters the lower permeability areas in this case could reduce the efficiency of subsequent injected fluids (e.g., gas and water) to contact or displace oil from those zones.

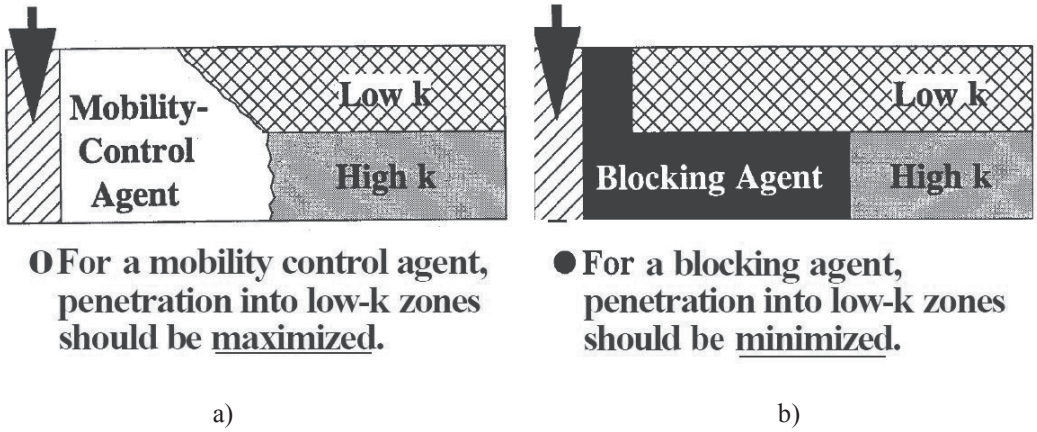

Figure 4.9: Distinction between a) foam mobility-control agent and b) foam blocking agent in a layered reservoir (from Seright, 1996).

Laboratory corefloods in heterogeneous porous media include studies of foam flow both parallel and perpendicular to permeability contrasts.

For sharp permeability boundaries arranged in series perpendicular to the flow direction, studies have demonstrated that foam can be generated as the gas passes from lower to higher permeability layers. The permeability boundaries may act as an "in-situ foam generator" favoring strong foam formation. For the reverse situation (i.e., gas flow from higher to lower permeability), only weaker foams are formed and gas mobility remains higher, suggesting that foam flows under a coalescence/coarsening regime near the critical capillary pressure (Li, 2006; Tanzil et al., 2001; Zitha et al., 2003).

For reservoir heterogeneities arranged parallel to flow direction the literature on foam distinguishes between two specific cases: I) permeability contrasts with capillary communication and II) permeability contrasts without capillary communication.

I) Selective mobility reduction (SMR) and "self-regulating" foam behaviors have been reported when capillary communication and sufficient cross-flow among layers were allowed. An ideal SMR or self-regulating behavior implies that the foam displacement front will propagate at equal velocity in each layer, independent of permeability. Such foam behavior could be desirable for a mobility control agent (Figure 4.9a) or for stabilizing the gas injection front in reservoirs with local heterogeneities, such as laminations (Figure 4.2). Gas breakthrough close to one pore volume injected has been used as a measure to indicate how efficient foam can be in heterogeneous cores (Bertin et al., 1999; Dixit et al., 1994; Heller, 1994; Yaghoobi and Heller, 1996). Recent study by Nguyen et al. (2005) in composite core with communicating layers of high permeability contrast did not reflect this ideal behavior. Non-uniform foam propagation and early gas breakthrough (~ 0.4 PV injected) in the high permeability layer was shown. A simulation study by Rossen and Lu (1997) indicated that the disruptive effects of cross-flow between layers could affect foam diversion and propagation distance negatively.

II) The diversion potential of fluids by foam from high to low permeability layers has also been repeatedly investigated in the laboratory when two cores/layers with contrasting permeabilities are arranged in parallel without capillary communication (e.g., dual core experiments) (Behenna, 1995; Bian et al., 2012; Casteel and Djabbarah, 1988; Di Julio and Emanuel, 1989; Kovscek and Bertin, 2003; Nguyen et al., 2005; Parlar et al., 1995; Siddiqui et al., 1997b). Key factors for efficient fluid diversion from higher to lower permeability layers seems to depend on the strength, stability and propagation of the foam in the target layers with respect to the permeability contrasts intended to overcome.

Recent papers have also investigated the potential of foams for fractured reservoirs (Haugen et al., 2014). The idea is to block the fractured "thief zone" with foam to divert gas flow into the surrounding matrix to achieve enhance oil recovery (EOR). Several considerations related to foam in fractures was also discussed in Farajzadeh et al. (2012a).

4.7.3 Wettability/lithological effects

Most of the literature and theories of foam in porous media are based on foam in water-wet rock material. In oil reservoirs, however, the wettability likely varies from water-wet to oil-wet, with a large degree of mixed wetting preferences in between. Each mineral or clay type may have a different affinity to various fluids, illustrating the complexity and inherent difficulties of fully describing the wetting properties of a natural rock (Abdallah et al., 2007; Anderson, 1986-1987).

Foam is generally thought to be more efficient (i.e., easier to form and more stable) in water-wet rocks than in mixed/oil-wet porous media (Farajzadeh, et al., 2012b; Rossen, 1996; Schramm et al., 1994, 1996; Suffridge et al., 1989). Though, findings supporting good CO_2-foam performance in oil-wet medium have also been reported (Haugen et al., 2014, Kuehne et al., 1992; Lescure and Claridge, 1986; Rafati and Hamidi, 2011; Romero-Zeron and Kantzas, 2007). Adsorption of surfactant at the rock interfaces that can modify or alter rock wettability to conditions favorable for foam processes and oil recovery is also frequently discussed in the literature, as summarized in Talebian et al. (2013).

The sensitivity of foam to changes in rock wettability remains unclear. Rossen (1996) stated that foams are not expected to be stable in porous media that are not strongly water-wet, suggesting that even a small reduction in water-wetness or water film stability at the rock interfaces could cause the foam to be less effective. It seems obvious that the interaction between the rock surface and the thin liquid films in the foam is of central importance on foam properties. However, in my opinion, more detailed investigations and knowledge of rock properties (e.g., mineralogy/wettability) on foam are needed.

In summary, experimental studies on foam in the literature have suggested many variables to strongly affect foam properties and performance in porous media (e.g., surfactant type and concentration, gas composition, foam-oil interactions, brine salinity, temperature and pressure conditions, flow rate, foam quality, injection strategies and so on). One of the main findings in **Paper 3** in particular, and in general in this thesis, demonstrated that foam properties and performance also can be strongly dominated by the porous media itself (see Chapter 8, section 8.3). Accordingly, it seems difficult to discuss foam properties and performance separately from the porous media in which the foam actually resides.

Chapter 5

Gas Characteristics and the Effect of Gas Type on Foam Properties

5.1 Introduction **p. 59**

5.2 Carbon dioxide **p. 62**

5.3 Nitrogen **p. 63**

5.4 Physical and chemical gas characteristics (CO_2 vs. N_2) **p. 65**

5.4.1 Gas density **p. 65**

5.4.2 Gas viscosity **p. 67**

5.4.3 Gas/water solubility **p. 68**

5.4.4 Gas compressibility **p. 71**

5.4.5 pH **p. 72**

5.4.6 pH-induced wettability shifts and chemical reactions of the porous media **p. 73**

5.4.7 Surface tension - classification and expected values **p. 75**

5.4.8 Summary of the characteristics of CO_2 **p. 79**

5.5 Type of surfactant against different gas components **p. 80**

5.6 Foam mobility control with pressure and temperature **p. 82**

5.1 Introduction

The gas phase is a primary constituent of all foams. The typically used gas types in foam include CO_2, N_2, air, hydrocarbon gases (e.g., CH_4) and steam. The "choice" of gas composition in a field situation typically depends on gas availability, the recovery conditions and an economic assessment of the appropriate fluid for the field (Aarra, 2002; Castanier 1987; Enick and Olsen, 2012; Holm and Garrison, 1988; Manrique et al., 2010; Turta and Singhal, 1998; Zhdanov et al., 1996).

Because the gas component in foam can vary, it is important to understand the influence of the different gas types on foam properties and performance.

CO_2- vs. N_2-foams: Several laboratory studies have compared the CO_2-foams with the N_2-foams in outcrop sandstone core material, without oil, using commercial anionic surfactants, under different experimental conditions. Typically the generated CO_2-foams have been significantly weaker (i.e., lower pressure gradients along the porous media) than the N_2-foams generated under similar experimental conditions (Aarra et al., 2014; Chou, 1991; Du et al., 2008; Farajzadeh et al., 2009; Gauglitz et al., 2002; Kibodeaux, 1997; Seright, 1996).

N_2-foams: Certain N_2-foams in the literature have been extraordinarily strong, reflected by very large pressure gradients along the porous media, which are often >> 50 bar/m (Chou, 1991; de Vires and Wit, 1990; Friedmann et al., 1991; Kovscek and Radke, 1994; Vikingstad and Aarra, 2009; Solbakken et al., 2014; Siddiqui et al., 1997a; Zeilinger et al. 1995).

CH_4-foams: Laboratory experiments using methane gas have also reported the formation of strong CH_4-foams. The generated methane foams have repeatedly demonstrated their robustness under high pressure and high temperature field conditions (Aarra et al., 1997, 2002, 2011; Holt et al., 1996; Mannhardt et al., 2000, 2001; Svorstøl et al., 1997).

Steam foam: Foams with vapor phases consisting of steam alone have been shown to reduce the steam mobility, improve the injection profiles and recover additional oil, but their lifetimes are often reported short. Steam foam combined with nitrogen or methane (i.e., non-condensable gases with limited solubility) has been an effective method to increase the mobility control of the steam in experimental studies and in field tests (Castanier, 1987; Falls et al., 1988b; Mohammadi et al., 1989; Sanchez and Schechter, 1989).

CO_2-foams: A summary of many studies on CO_2-foam in sandstone and in carbonate rock material in the absence of oil reveals that few surfactants can generate a CO_2-foam of similar strength and stability under elevated experimental conditions as those reported with the N_2- and CH_4-foams. However, all of the studies on CO_2-foam referenced below show that the CO_2 mobility can be lowered with a variety of surfactants, although significant differences in the degree of mobility control have been reported (Alkan et al., 1991; Bian et al., 2012; Chabert et al., 2012, 2014; Chen et al., 2012; Elhag et al., 2014; Heller, 1984, 1994; Khalil and Asghari, 2006; Kuehne et al., 1992; McLendon et al., 2012; Prieditis and Paulett, 1992; Sanders et al., 2010; Tsau and Heller, 1992; Tsau and Grigg, 1997; Yang and Reed, 1989; Xing et al., 2012).

Effect of the gas phase with/without oil: The effect of the gas composition on the foam strength has been reported as minor comparing Snorre field gas-, methane- and nitrogen-foams (Mannhardt and Svorstøl, 1999) or comparing CO_2- and methane-foams (Aarra, et al., 2011) in core flooding experiments under high pressure and high temperature conditions in the presence of residual oil. Both of the studies generated foam of a relatively similar strength using the AOS surfactant, independent of the gas composition used. However, differences in foam performance in the absence of oil have been observed comparing nitrogen-, methane-, ethane-, propane- and butane-foams (Mannhard et al., 1996), Snorre field gas- and methane-foams (Mannhardt and Svorstøl, 1999) and methane- and propane-foams (Mannhardt, 1999). The two cases above appear to reflect that an examination of actual foam properties with a changing gas phase would most likely be best achieved by excluding oil.

To reasonably explain why various gas foam systems could perform differently, a good understanding of the characteristics of the various gas types involved is required.

This chapter provides the physical and chemical characteristics of the gas phases typically used in enhanced oil recovery (EOR) processes. Particular emphasize is placed on the characteristics of CO_2 and N_2 close to the experimental conditions applied in this project. Relevant foam literature is provided within the chapter.

The gas properties relevant to this chapter were obtained from the National Institute of Standards & Technology (NIST) (data available at http://webbook.nist.gov/chemistry/fluid/). The solubilities of CO_2 and N_2 in brine were calculated from a model by Duan et al., (2003, 2006) (the model is available at http://models.kl-edi.ac.cn/models.htm).

Additional comprehensive information about CO_2 characteristics is compiled in extensive reports by the Energy Institute (2010) and Enick and Olsen (2012).

Note that, typically, the gases from natural reservoirs are not 100% pure; contaminants of other gases are anticipated in various concentrations (e.g., CO, CO_2, CH_4, H_2S, N_2, No_x, So_x, and O_2). The impurities may affect the gas characteristics, depending on the type and concentration of the contaminants (Energy Institute, 2010; Oldenburg and Benson, 2002). Impure gas phases are outside the scope of this thesis. Only industrial grade CO_2 and N_2 (> 99.5% purity) were used in this project.

5.2 Carbon dioxide

Carbon dioxide is a well-known gas present in the atmosphere, in certain oil and gas reservoirs, and is generally a chief product from the combustion of coal and hydrocarbons (Energy Institute, 2010). CO_2 comprises two oxygen atoms covalently double bonded to a single carbon atom, with an angle of 180°. Table 5.1 provides a summary of some of the general properties of CO_2.

Table 5.1: General properties of carbon dioxide

Substance:	Chemical symbol:	Mol. Weight:	Structure:	Critical point (T_c,P_c,ρ_c):
carbon dioxide	CO_2	44.01 (g/mol)	C=O=C	31.1°C, 73.8 bar, 0.468 g/cm^3

Figure 5.1 shows the phase diagram of CO_2. Under room conditions (~1 bar and 22°C), CO_2 is a gas. Above its critical point (73.8 bar and 31.1°C), CO_2 becomes supercritical. A supercritical fluid is any substance above its critical point (in terms of pressure and temperature). Supercritical fluids near their critical point cannot be easily defined as either a liquid or a gas because they can adopt properties midway between a gas and a liquid (see the subsequent descriptions of the physical properties of CO_2). The special properties of supercritical CO_2 have introduced certain advantages to several industrial processes (e.g., Johnston and da Rocha, 2009; Raventós et al., 2002).

A summary of several foam field projects indicate that most of the offshore reservoirs would attain temperature and pressure conditions at which CO_2 is a supercritical fluid. Shallow formations may represent CO_2 in the gaseous state, whereas reservoirs under liquid CO_2 conditions appear to be less frequent (Enick and Olsen, 2012; Turta and Singhal, 1998). However, during injection, the CO_2 will most likely change its phase behavior (among gas/liquid/supercritical) because of the exposure to various conditions (e.g., at the platform, in the pipe close to the seabed, or deep into the formation).

Because the reservoir condition can vary significantly with respect to pressure and temperature, it is important to understand CO_2-foam properties on a broad experimental scale. In this thesis, we studied and compared CO_2-foam properties at 2 bar and 22°C (**Paper 4**), at 30-280 bar at 50°C (**Paper 1**) and at 90-120 bar at 90°C (**Paper 2**), thus, covering the phase transition from the gaseous to the supercritical state of CO_2 (see Figure 5.1).

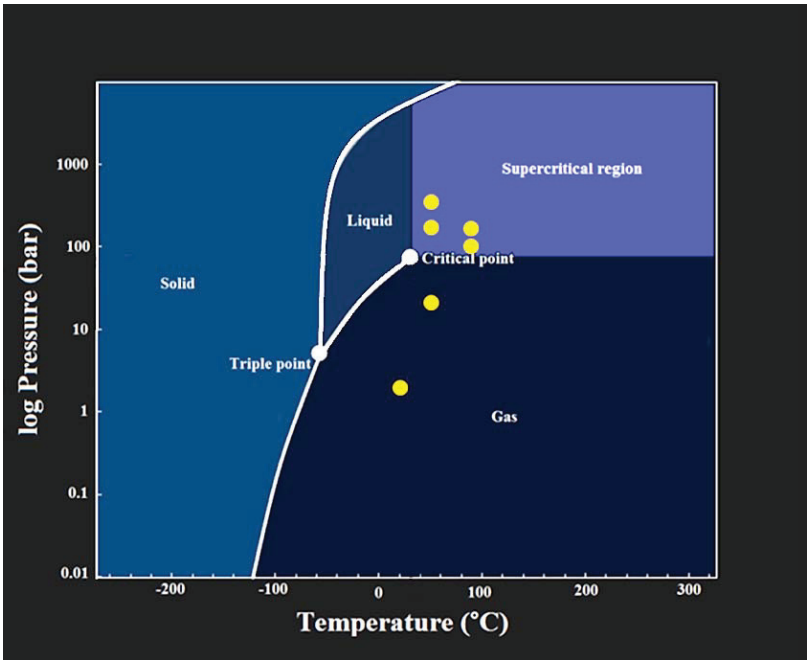

Figure 5.1: Phase diagram of carbon dioxide (CO_2) as a function of pressure and temperature (modified from Wolfram|Alpha knowledgebase, 2013, http://www.wolframalpha.com). The yellow dots represent the experimental conditions for CO_2 used in this project.

5.3 Nitrogen

Nitrogen is the largest constituent of the Earth's atmosphere (~ 78% by volume of dry air). N_2 is composed of two nitrogen atoms covalently triple bonded, with an angle of 180°. The triple bond in N_2 is one of the strongest bonds, making this gas relatively non-reactive and inert. N_2 is classified as a non-toxic, non-flammable fluid by the UN number (UN1066). Table 5.2 provides a summary of the general properties of N_2.

Table 5.2: General properties of nitrogen

Substance:	Chemical symbol:	Mol. Weight:	Structure:	Critical point (T_c,P_c,ρ_c):
(di)nitrogen	N_2	28.01 g/mol	N≡N	-146.9°C, 33.9 bar, 0.313 g/cm^3

Figure 5.2 shows the phase diagram of N_2. Under room conditions (~ 1 bar and 22°C), N_2 is a gas. At pressures and temperatures above 33.9 bar and -146.9°C, N_2 is a supercritical fluid. Generally, supercritical fluids close to their critical points exhibit properties between those of a gas and a liquid. Because N_2 under room conditions or at elevated reservoir temperatures is distant from the critical temperature (-146.9°C), it behaves as a gas and exhibits "gas-like"

properties, although it is supercritical (see the subsequent descriptions of the physical properties of N_2).

Because of its abundance in the atmosphere and its general inertness, N_2 is one of the most useful and environmentally safe gases used in the oil industry (Chambers, 1994).

The experimental conditions applied to the N_2-foam in this thesis ranged from 2 bar and 22°C (**Paper 4**) to 30-280 bar at 50°C (**Paper 1 & 3**) to 280 bar and 100°C in one experiment (**Paper 3**) (see Figure 5.2).

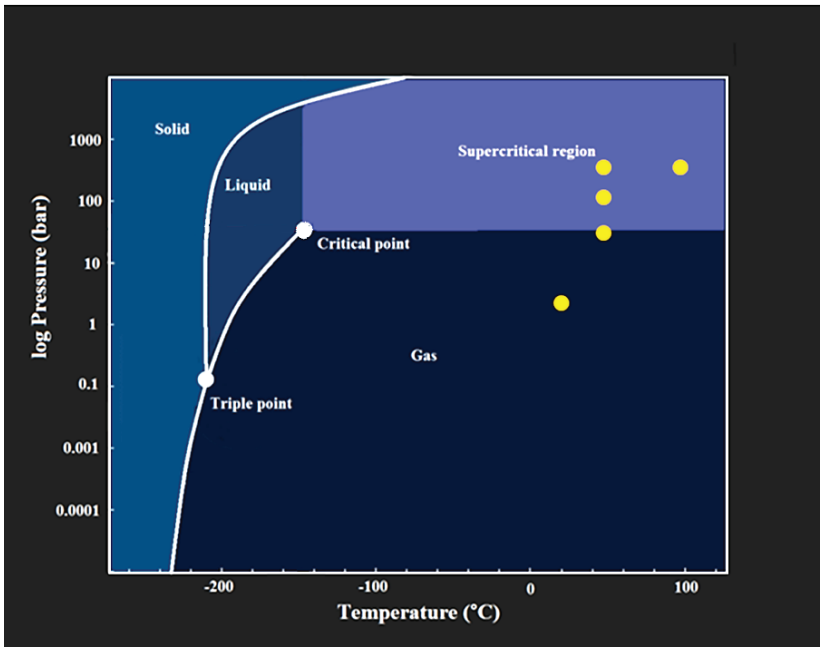

Figure 5.2: Phase diagram of nitrogen as a function of pressure and temperature (modified from Wolfram|Alpha knowledgebase, 2013, http://www.wolframalpha.com). The yellow dots represent the experimental conditions for N_2 used in this project.

5.4 Physical and chemical gas characteristics (CO_2 vs. N_2)

Several causes for the apparent weakness of the CO_2-foams compared with the N_2-foams have been suggested in the literature. The many physical and chemical differences that CO_2 possesses compared with other gas phases in foam typically used (i.e., air/N_2 and CH_4) may be a possible explanation. This section presents the characteristics of CO_2 that have been frequently suggested to have an influence on its foam properties. The characteristics of CO_2 are compared with those of N_2.

5.4.1 Gas density

Figure 5.3 compares the density of CO_2 and N_2 as a function of pressure and at temperatures relevant to this project.

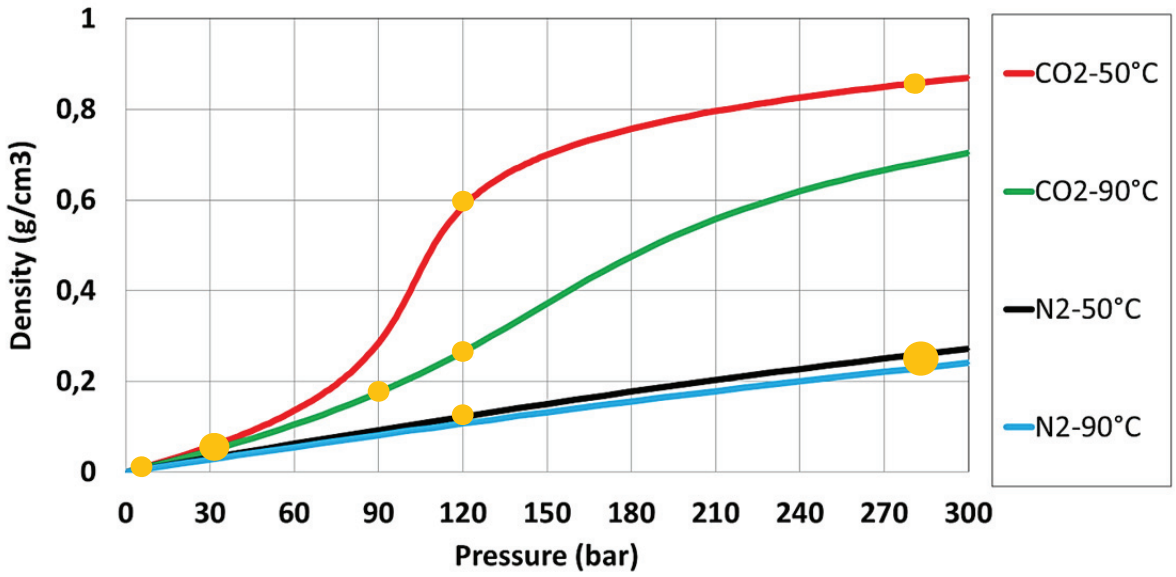

Figure 5.3: Comparison of the CO_2 and N_2 density (data from the NIST Chemistry WebBook). The yellow dots illustrate the approximate gas densities in the experiments performed in this project.

Because the temperature and pressure generally increase with the depth of the reservoir, the density of CO_2 will increase with the pressure but then level off due to the counteracting temperature effects. Figure 5.4 (the black dashed line) depicts this trend for the CO_2-density for a given geothermal/hydrostatic pressure gradient. After certain reservoir depths, depending on the geothermal/hydrostatic pressure regime, the density of CO_2 only increases

slightly with a further increase in the depth, as illustrated. The latter trend suggests a relatively similar density of supercritical CO_2 in reservoirs deeper than 2 km (Gunter et al., 2004). Under many U.S. field conditions (100-150 bar and 40-60°C), CO_2 is relatively dense (ρ_{CO2} > 0.5 g/cm^3) (Enick and Olsen, 2012). Under the North Sea reservoir conditions reported by Aarra et al., (2002) and Holt et al., (1996) (i.e., 300 bar and 90°C), density of CO_2 is most likely closer to 0.7 g/cm^3. One immediate advantage of dense CO_2 compared with gases with a low density (e.g., N_2 and CH_4) could be less critical gas injection problems associated with the gravity override.

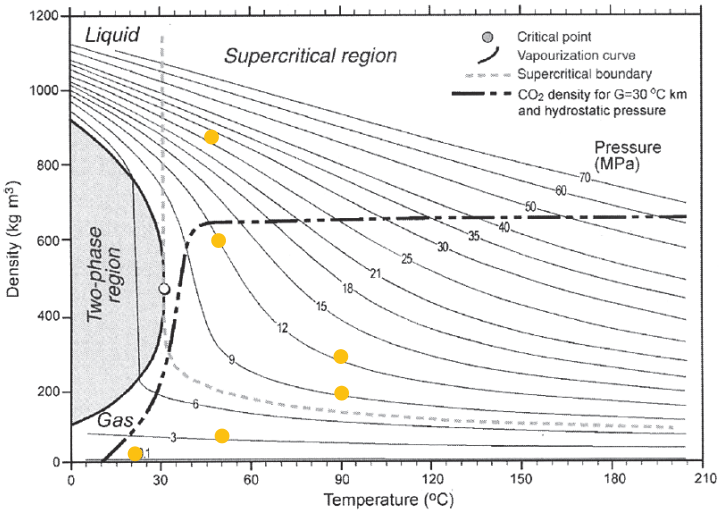

Figure 5.4: CO_2 density as a function of pressure and temperature. The black dashed line illustrates the anticipated trend of the CO_2 density in the reservoirs, assuming a hydrostatic pressure gradient of ~ 80 bar/km and a geothermal gradient of 30°C/km (from Gunter et al., 2004). The yellow dots illustrate the approximate gas densities in the experiments performed in this project.

Many surfactants appear to generate relatively weak foams with dense supercritical CO_2. In fact, mobility reduction factors and apparent viscosities of less than 15 have frequently been reported with several types of foamers in various displacement tests without oil when the density of pure CO_2 is ≥ 0.5 g/cm^3 (Aarra et al., 2014; Alkan et al., 1991; Chabert et al., 2012, 2014; Chen et al., 2012; Elhag et al., 2014; Khalil and Asghari, 2006; McLendon et al., 2012; Preditis and Paulett, 1992; Sanders et al., 2010; Xing et al., 2012).

Several researchers seem to be aware that foams formed with dense CO_2 most likely meet the definition of an emulsion (i.e., a liquid dispersed in a liquid) better than it does to the

definition of a foam (i.e., a gas dispersed in a liquid) (Bernard et al., 1980; Chambers, 1994; Chaubert, 2012, 2014; Farajzadeh et al., 2009; Heller, 1994; Kovscek and Radke 1994; Liu et al., 2005a; Reidenbach et al., 1986; Solbakken et al., 2013).

In **Paper 2** of this dissertation, CO_2-foam experiments under different experimental pressure and temperature conditions with significant variations in the CO_2 density were conducted (Figure 5.3-5.4). A good correlation between the CO_2 density and the CO_2-foam strength was found in Berea sandstone core material using commercial $AOS_{C14-C16}$ surfactant. The results showed that improved foam strength could be achieved under pressure and temperature conditions in which the density of the supercritical CO_2 is lower and more "gas-like". The results and discussion from our investigation of CO_2-foam properties with varying CO_2 density are summarized later (see Chapter 8, section 8.2).

5.4.2 Gas viscosity

For any single and multiphase flow in porous media, viscosity plays an important role regarding the displacement efficiency (Equation 1.2-1.5, Chapter 1) and flow resistance (Equation 4.1, Chapter 4). Figure 5.5 compares the viscosity of CO_2 and N_2 as a function of pressure and at temperatures relevant to this project.

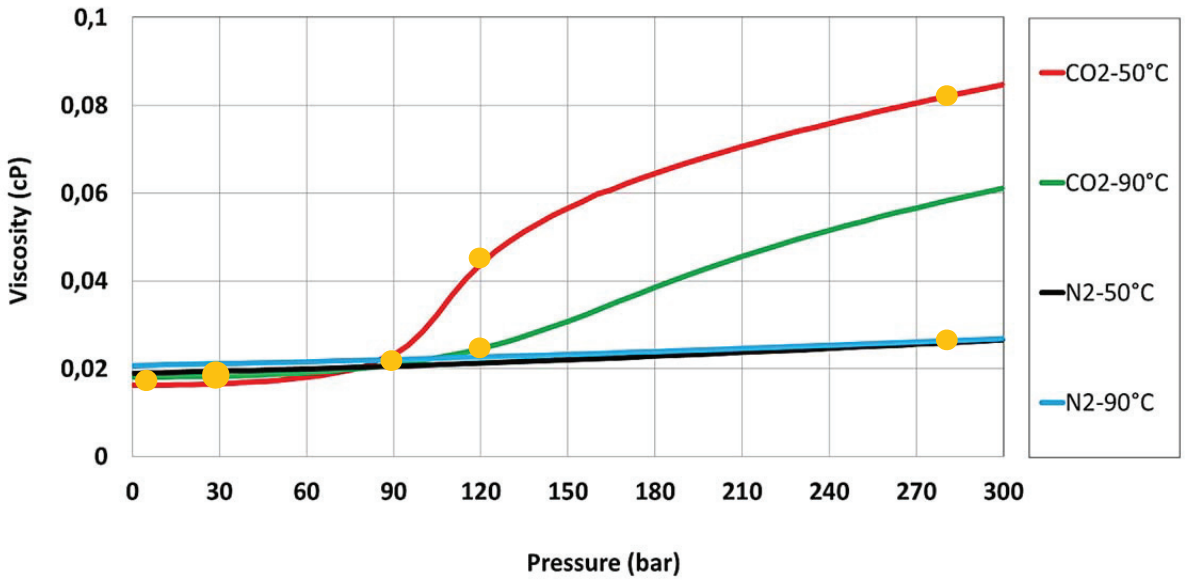

Figure 5.5: Comparison of the CO_2 and N_2 viscosity (data from the NIST Chemistry WebBook). The yellow dots illustrate the approximate gas viscosities in the experiments performed in this project.

The low gas viscosities depicted in Figure 5.5 increase the mobility of the gases in porous media. Low gas viscosity is one of the primary causes of early breakthrough and poor sweep efficiency by gas injections (see section 1.4 in Chapter 1).

The increased viscosity of dense CO_2 compared with N_2 would slightly increase the absolute level of the pressure drop across the porous media during the injection, if all else being equal. Thus, the gas viscosity alone cannot explain the apparent weakness of the CO_2-foams compared with the N_2-foams.

For the interested reader, the viscosity of CO_2 over a wider range of pressure and temperature conditions can be found in Gunter et al. (2004).

5.4.3 Gas/water solubility

Figure 5.6 compares the solubility properties of CO_2 and N_2 in pure water and saline solutions as a function of pressure and at temperatures relevant to this project.

The solubility of a gas in a liquid depends on the gas type and the liquid phase composition (e.g., ionic strength) as well on temperature, pressure and the pH of the solution (Chang et al., 1998; Gunter et al., 2004). Compared with many other gases, CO_2 is relatively soluble in water; for example, it is significantly more soluble than N_2 in water (Figure 5.6).

Henry's law can be used to quantify the solubility of gases in aqueous solutions that do not undergo speciation on dissolution. The solubility of a gas in a liquid at constant temperature is directly proportional to the partial pressure **p** of the specific gas (i.e., the thermodynamic activity of the gas molecules) above the liquid:

$$p = k_H \cdot c \tag{5.1}$$

where $\mathbf{k_H}$ is a constant (for example, 29.41 L·atm/mol for CO_2 and 1639.34 L·atm/mol for N_2 in water at 25°C) and **c** is the concentration of the dissolved gas in the liquid (mol/L) (Ebbing and Gammon, 2011).

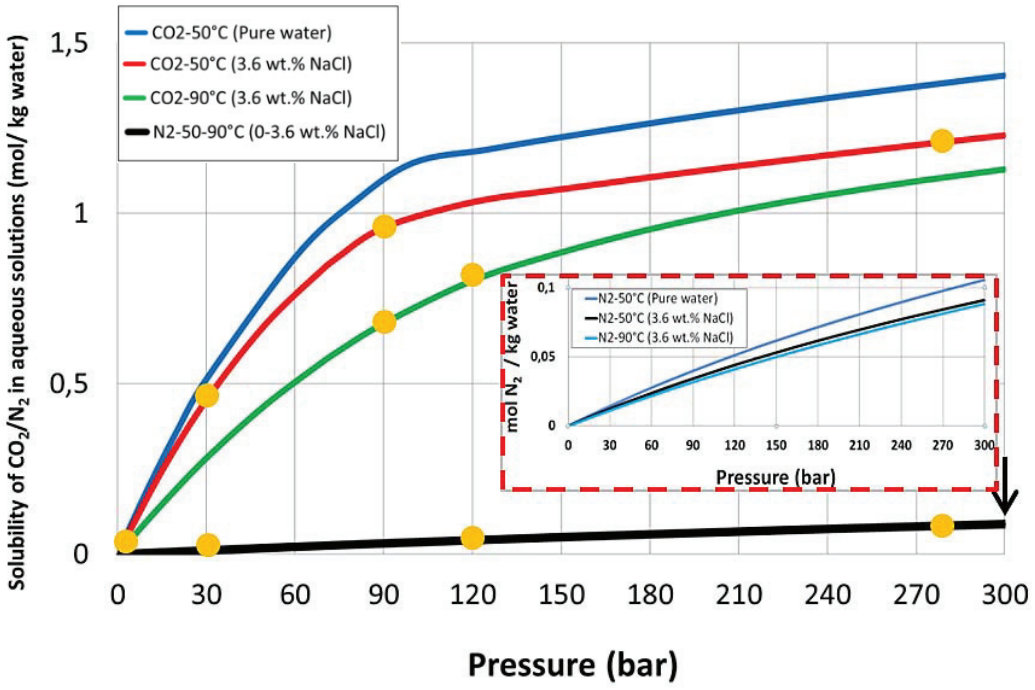

Figure 5.6: Comparison of the CO_2 and N_2 solubility in pure water and aqueous solutions of 3.6 wt. % NaCl (data calculated from http://models.kl-edi.ac.cn/models.htm). The inset shows the N_2 solubility in water. The yellow dots illustrate the approximate gas solubilities in brine under the experimental conditions in this project.

The CO_2 dissolution in water has been demonstrated experimentally in PVT cells at low and high pressures and temperatures (Yang and Gu, 2006). Farajzadeh et al., (2007) reported no measurable changes between the CO_2 dissolution in pure water and that in a surfactant solution. The rate of the reaction depends on the pressure and temperature conditions and on the degree of the CO_2-water mixing. The studies have indicated that the equilibrium concentration of CO_2 in water could be achieved within hours if CO_2 and water are well mixed.

Dissolution of gas in water is an exothermic process. This means that the process would increase the temperature in the water phase locally. The temperature rise will be larger with CO_2 than with N_2 and increases with pressure as indicated by Farajzadeh et al. (2009).

A certain amount of liquid will also dissolve into the respective gas phases. Figure 5.7 illustrates the amount of water that can be typically solubilized into CO_2 and N_2. The figures illustrate that the equilibrium concentration of water solubilized in CO_2 and N_2 at elevated temperatures and pressures is low compared with their solubilities in water.

Brine saturated with CO_2 exceeds the density and viscosity of pure brine, as noted in Ülker et al., (2007) and Islam and Carlson, (2012), respectively. No significant changes in the density or the viscosity of CO_2 when saturated with water/surfactant have been reported, possibly due to the small amounts of liquid that can be dissolved in the gas phase under elevated conditions (Choi and Nesic, 2009; King et al., 1992).

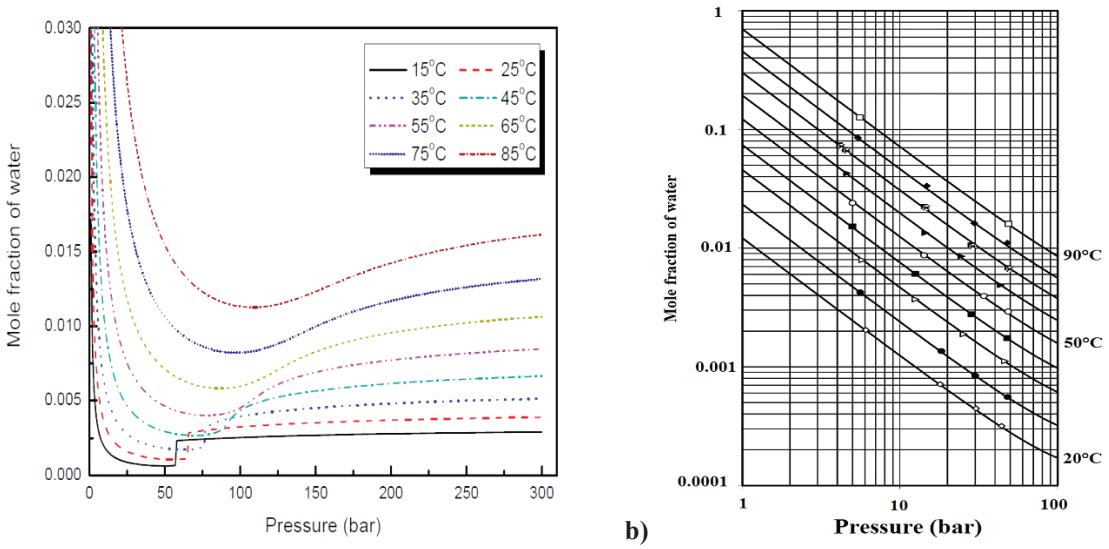

Figure 5.7: Comparison of the water solubility in a) CO_2 (from Choi and Nesic, 2009) and b) N_2 (modified from Mohammadi et al., 2005).

The transport of gas across liquid films, which is analogous to gas diffusivity, gas dissolution and solubility properties (Chapter 3, section 3.5), has been frequently cited as one of the primary reasons for the reduced stability of CO_2-foams compared with the air/N_2-foams in bulk tests (Alkan et al., 1991; Lake, 1989), the weaker CO_2-foams compared with the N_2-foams during foam generation in laboratory corefloods (Du et al., 2008; Farajzadeh et al., 2009; Wang et al., 2014), the typical shorter lifetimes and the decrease in the gas mobility reduction of steam foams compared with steam foams combined with non-condensable gases with a low solubility (e.g., N_2 and CH_4) (Castanier, 1987; Falls et al., 1988b) and the use of the combination of carbon dioxide and nitrogen to help design desirable foam stabilities in the food/drink industry (Weaire and Hutzler, 1999).

In an attempt to measure the permeation rate (i.e., the diffusion rate) of thin foam films to CO_2, Farajzadeh et al., (2011) reported that the rapid shrinkage of the CO_2-foam bubble made it impossible to quantify the permeation rate of CO_2. The foam films using the AOS surfactant and air as the dispersed phase indicated significantly lower transfer rates. It was concluded that the transport of gas across thin foam films is higher when the solubility and diffusion coefficient of the used gas phase in water are larger.

Several authors have also suggested that gas dissolution could have significant effects on the foam stability in porous media against subsequent water injection after foam generation (Bhide et al., 2005; Nguyen et al., 2009; Zeilinger et al., 1995). Comparative studies indicate that the CO_2-foams are less effective to reduce water flow compared with foams having gas components with low solubility in water (e.g., air/N_2 and CH_4) (Aarra et al., 2011, 2014; Seright, 1996).

5.4.4 Gas compressibility

Another property of gases is their compressibility. Compressibility is a measure of the relative volume change of a fluid as a response to a change in energy. Most substances expand when heated or depressurized, and contract when cooled or compressed. Gases are highly compressible and expandable fluids, whereas liquids and solids are significantly less compressible and expandable.

The compressibility of all real gases (e.g., N_2 and CO_2) is specific for the different gas phases as a function of pressure and temperature. Because changes in the density are directly related to changes in the volume, the density characteristics of the gas phase involved can be used as a measure of its compressibility. According to the gas densities presented in Figure 5.3, CO_2 will be generally less compressible than N_2 under similar elevated pressure and temperature conditions.

Foam is composed of two phases, gas and liquid. Because the gas constituent is naturally compressible, the foam is a compressible system as well.
Theoretically, the gas compressibility could be an important parameter affecting the foam flow and resistance in porous media (Rossen, 1990).

5.4.5 pH

The dissolution of CO_2 in water includes a sequence of chemical reactions as follows:

$$CO_2 \text{ (aq.)} + H_2O \leftrightarrow H_2CO_3 \text{ (Hydration of } CO_2\text{)} \quad (5.2)$$

$$H_2CO_3 \leftrightarrow H^+ + HCO_3^- \text{ (Dissociation of carbonic acid)} \quad (5.3)$$

$$HCO_3^- \leftrightarrow H^+ + CO_3^{2-} \text{ (Dissociation of bicarbonate ion)} \quad (5.4)$$

$$H_2O \leftrightarrow H^+ + OH^- \text{ (Dissociation of water)} \quad (5.5)$$

The formation of carbonic acid (H_2CO_3) lowers the pH of the aqueous phase. The hydrogen ion concentration (pH) of CO_2-saturated water as a function of pressure at various temperatures is shown in Figure 5.8.

Note from the figure that the pH level of water saturated with CO_2 is over a relatively narrow range of 3 to 4. In addition, it is possible to obtain a considerably reduced pH, even at room temperature and pressure.

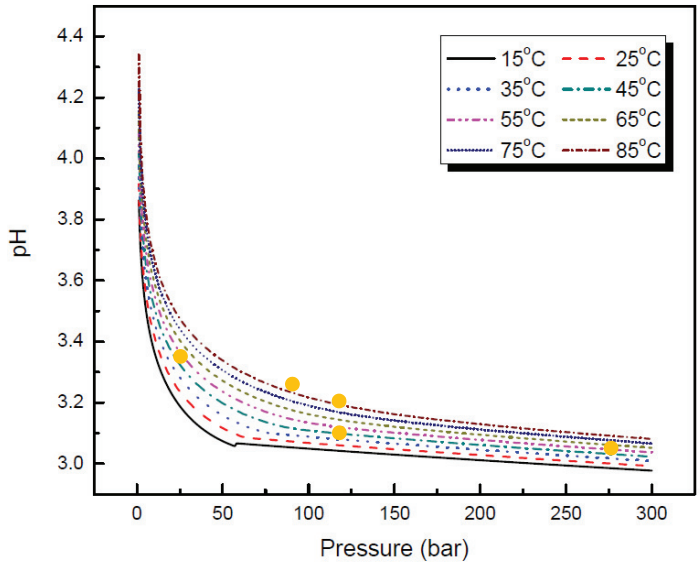

Figure 5.8: The pH of CO_2-saturated water as a function of pressure and various temperatures (from Choi and Nesic, 2009). The yellow dots indicate the typical pH levels expected from the CO_2 experiments with the pre-equilibrated fluids in this project.

Lowering the pH may affect surfactant properties in the solution or its activity at the gas-liquid surface, which may influence the electrical double layer in thin liquid films, and hence, the mechanisms thought to control foam stability (Chapter 3). In addition, dissolved HCO_3^- (bicarbonate ion) and CO_3^{2-} (carbonate ion) could increase the ionic strength of the aqueous solution due to the various salts formed from the attachment of the positively charged ions (e.g., Na^+, K+, Ca^{2+} and Mg^{2+}) to the negatively charged oxygen atoms of the ions. For particular surfactants can even a small increase in the electrolyte concentration reduce the surfactant solubility in the aqueous phase, increase the surfactant adsorption in porous media or affect the foam strength and stability (Alkan et al., 1991; Novosad and Ionescu, 1987; Tortopidis and Shallcross, 1994). A low pH environment has also been reported to impose different chemical constraints on certain foamers (Bernard et al., 1980; ref. 88 in Farajzadeh et al., 2009; Zhdanov et al., 1996).

However, based on various experimental results found in the literature, it appears that the pH values typically found with CO_2 has a small effect on the following: the long-term chemical stability of certain foamers (Alkan et al., 1991; Bernard et al., 1980; Casteel and Djabbarah, 1988), the CO_2-foam texture and rheology (Fredd et al., 2004), the bulk drainage time (Zhu et al., 1998), the stability of bulk foams made with proteins (Bolontrade et al., 2014), the bulk foamability and stability at surfactant concentrations above the cmc (Liu et al., 2005b; Solbakken, 2013) or the N_2-foam stability in bulk tests (Phillips et al., 1987; Solbakken, 2013) and porous media (Kibodeaux, 1997) where the surfactant solution has been acidified to mimic the pH environment present in the CO_2-foam systems.

No particular influence of low pH on foam properties in bulk was found in this thesis using the $AOS_{C14\text{-}C16}$ surfactant (**Paper 4**).

5.4.6 pH-induced wettability shifts and chemical reactions of the porous media

In water-wet porous media containing gas and water, the gas phase is generally expected to be the non-wetting phase. This generalization can overlook the possibilities and the consequences in which CO_2 may have to partially influence the wetting properties under varying elevated pressure and temperature conditions. Reduced water-wetness, decreased water film stability along the rock surfaces and chemical reactivity with the rock mineralogy (e.g., mineral dissolution/precipitation, particle invasion/migration, and permeability and porosity reduction/increase) are certain possibilities reported after CO_2 has been injected into

the porous media. For example, frequently discussed regarding geological sequestration of carbon dioxide (Berg et al., 2013; Czernichowski-Lauriol et al., 2006; Hildenbrand et al., 2004; Pentland, 2011; Zuo et al., 2012), and in relation to CO_2-EOR projects (Ghedan, 2009; Grigg et al., 2008; Rogers and Grigg, 2000).

Dissolution of CO_2 in water reduces the water pH (section 5.4.5). A low water pH could induce changes in the rock surface charge or influence the intermolecular forces in the wetting films (Basu and Sharma, 1996; Hirasaki, 1991). The effects of reduced water-wetness and less stable wetting films have been suggested under low pH and moderate saline environments (Figure 5.9).

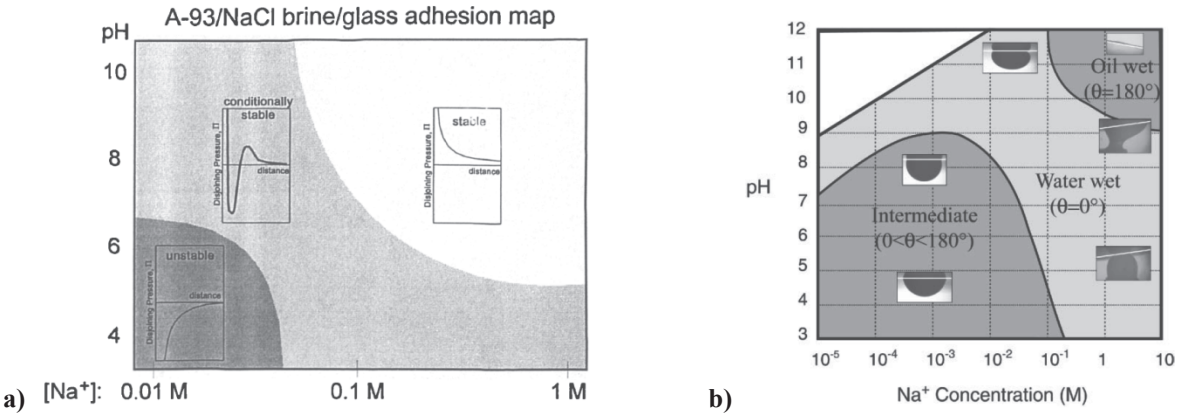

Figure 5.9: Adhesion maps of oil and water as a function of salinity and pH. a) Buckley, (1996) illustrating three regions of tentative unstable, stable and conditionally stable water films (based on the disjoining pressure isotherms) and b) Drummond and Israelachvili, (2002) illustrating three regions of tentative intermediate, water-wet and oil-wet wettability regimes (based on the static contact angle measurements). At a low pH and at moderate salinities, both of the maps reflect conditions under which the water film could be less stable and not completely wetting.

At the low pH values typically found with carbonated water at a high pressure (i.e., pH ~ 3), several rock minerals could be close to their "point of zero charge". The point of zero charge for a given mineral is the pH at which the mineral surface attains a net neutral charge. When the mineral surface has no charge, the surface has no wetting preference for either of the present phases (Railsback, 2006). Experimental results have indicated that various minerals and clays in the rock respond differently to changes in the pH (Schramm et al., 1991).

As the water pH decreases due to the dissolution of CO_2, the potential for various chemical reactions with the rock matrix may increase. The degree of reactivity between CO_2, pore-water and minerals has been indicated as a highly time-dependent and mineralogy-specific process. The reaction kinetics to quartz (i.e., the primary constituent of sandstone) in acidic environments have been found to be several orders of magnitude lower than that that of most carbonate minerals. The latter may imply that reactivity with the rock matrix could be smaller in sandstones compared with carbonate rocks (Czernichowski-Lauriol et al., 2006; Wellman et al., 2003).

Despite the growing literature on CO_2-foam in porous media, the possible wettability instabilities and chemical reactions between the injected CO_2 and the porous media have not received much attention; this is surprising considering its putative importance on the foam effectiveness in porous media (see Chapter 4, section 4.7.3). In one the few papers on foam discussing these effects, Farajzadeh et al. (2009) have indicated that the wetting preferences of the clays in their Bentheimer sandstone could have influenced by the injection of CO_2, thus, possibly playing a role in weakening the CO_2-foams compared with the N_2-foams. In addition, a reddish colored effluent from Berea sandstone core material during CO_2-foam flooding have frequently been reported, suggesting that the Berea rock mineralogy could be sensitive to environments with a low pH (Dong, 2001; Kim et al. 2004; Seright 1996; Solbakken et al., 2013).

5.4.7 Surface tension – classification and expected values

The tension force separating two immiscible fluids per unit area is thermodynamically defined in Equation 2.1 (Chapter 2). Typical values of the surface tension between various surfactant solutions and air at ambient conditions are provided in Table 2.1 (Chapter 2). A similar range for the tension properties under reduced pressure and temperature conditions have also been reported elsewhere (Dalland et al., 1992; Mannhardt et al., 2000; Rossen, 1996; Vikingstad, 2006).

The surface tension data between pure gas and water are well documented in the literature as a function of pressure, temperature and salinity (Bennion and Bachu, 2008; Hildenbrand et al., 2004; Yan et al., 2001), whereas the surface tension data between gas types and surfactant solutions under elevated pressure and temperature conditions are more limited. The surface tension under elevated conditions was not measured in this thesis. However, Table 5.3

provides an overview of the available surface tension data found in the literature. All of the values in the table with foamer refer to surfactant concentrations at or above the cmc.
An examination of the available data presented in Table 5.3 reveals the following:

I) The surface tension between CO_2 and water decreases as the:
- Pressure increases.
- Temperature decreases.
- Salinity decreases.

II) The surface tension between dense CO_2 ($\rho_{CO2} > 0.5$ g/cm^3) and many surfactant solutions appear to fall over a relatively narrow range from ~ 3-6 mN/m.

III) The surface tension between dense CO_2 and many surfactants may attain values that are up to eight times lower compared with air/N_2/CH_4 and various surfactant solutions under elevated pressure and temperature conditions.

Table 5.3: Surface tension data of aqueous solutions under elevated conditions

Aqueous solution	Gas type (phase)	Conditions (pressure, temperature)	Surface tension (mN/m)	References
Pure water	CO_2 (g)	20-60 bar, 41°C	~65→33	Bennion and Bachu, (2008)
	CO_2 (sc.)	80-270 bar, 41°C	~ 29→17	
	CO_2 (sc.)	270 bar, 41-125°C	~ 17→33	
Brine (75,780→334,008 TDS)	CO_2 (sc.)	120 bar, 41°C	~ 26→41	
Pure water	N_2 (sc.)	0-400 bar, 25°C	~ 72→63	Yan et al., (2001)
	N_2 (sc.)	400 bar, 25-100°C	~ 63→50	
Brine (12.2 wt.%)	N_2 (sc.)	69 bar, 95°C	63.9	Grigg et al., (2008)
Anionic surfactant (Witcolate 1276) in 1 wt.% brine solution	CO_2 (liq.)	103 bar, 25°C	3	Lee et al., (1991)
	CO_2 (sc.)	172 bar, 40°C	3	
Various surfactants in synthetic reservoir brine (41,238 TDS)	CO_2 (liq.)	103 bar, 25°C	3.2-5.0	Tsau and Heller, (1992)
	CO_2 (sc.)	172 bar, 40°C	3.0-4.7	
Various surfactants in 5.6 wt.% NaCl and 1.4 wt% $CaCl_2$ brine solution	CO_2 (liq.)	138 bar, 25°C	2.5-5	Tsau and Grigg, (1997)
Chaser CD 1045 surfactant in 2 wt.% brine solution ($NaCl:CaCl_2$ at ratio of 3:1)	CO_2 (g)	55 bar, 25°C	9-10	Liu et al., (2005a)
	CO_2 (liq.)	76-138 bar, 25°C	4→2.5	
	CO_2 (sc.)	103 bar, 35-75°C	4→6.5	
Various non-ionic surfactants in 2 wt.% NaCl, 0.5 wt.% $CaCl_2$ and 0.1wt.% $MgCl_2$ brine solution	CO_2 (liq.)	138 bar, 24°C	3.7-5.1	Adkins et al., (2010)
	CO_2 (sc.)	138 bar, 40°C	4.2-5.7	
	CO_2 (sc.)	138 bar, 60°C	4.5-5.5	
Various surfactants in 4 wt.% NaCl brine	CO_2 (sc.)	130 bar, 40°C	4.2-2.5	Chabert et al., (2014)
Ethoxylated amine surfactant in high salinity brine (22 %TDS)	CO_2 (sc.)	234 bar, 120°C	5	Elhag et al., (2014)
Various surfactants and surfactant mixtures in 12.2 wt.% brine solution	N_2 (sc.)	69 bar, 95°C	17-24 (single surf.) 2.7-4.3 (surf. mix)	Grigg et al., (2008)
Anionic surfactant (AOS C_{16}) in North Sea reservoir brine	CH_4 (sc.)	10-300bar, 90°C	~ 16→4	Holt et al., (1996)
Various surfactants and surfactant mixtures in synthetic seawater (35,000 TDS)	CH_4 (sc.)	138 bar, 75°C	13.2-15.4 (single surf.) 11.5-12.3 (surf. mix)	Mannhardt et al., (2000)
Anionic surfactant (AOS $C_{14/16}$) in synthetic seawater (35,000 TDS)	CH_4 (sc.)	300bar, 90°C	~ 10	Mannhardt and Svorstøl, (2001)

g = gas, liq. = liquid, sc. = supercritical
Arrows (→) indicate the trend in the surface tension with pressure, temperature or salinity.

A foam surface refers to the region that encompasses the thin film lamellae, the two surfaces on either side of the film, and part of the junction with the other lamellae (see Figure 2.1b in Chapter 2). The use of surfactants to lower the surface tension provides a well-known and important role for generating stable foams. The surface tension value relates to properties of the surfactant at the gas-water surface under specific conditions (i.e., the surfactant type and concentration, the water composition, the gas type and the pressure and temperature will be decisive factors) (see section 2.1-2.2 in Chapter 2).

The apparent weakness of CO_2-foams (compared with the N_2-foams) in porous media has also been partially attributed to the lower surface tension properties found between CO_2 and several surfactant solutions (compared with N_2 and surfactants) (Chabert et al., 2012; Chou 1991; Du et al., 2008; Kibodeaux, 1997; Kim et al., 2004; Gauglitz et al., 2002; Rossen, 1996; Rossen and Gauglitz, 1990; Farajzadeh et al., 2009).

A lower surface tension in foam could possibly result in the following:

I) Reduced capillary pressure on the lamellae at any given saturation (according to Eq. 3.1, page 29 and Figure 4.7, page 50).
II) Smaller bubble sizes (according to Eq. 2.2, page 16).
III) Lower capillary resistance per lamellae to flow (Falls et al., 1989; Hirasaki and Lawson, 1985; Rossen and Gauglitz, 1990).
IV) Higher permeation rate of the gas molecules through the foam films (Farajzadeh et al., 2008, 2011).
V) Reduced driving force for the surfactant to adsorb at the film surface (e.g., reduced surface viscosity and surface tension gradient/Marangoni stabilization) (Adkins et al., 2009, 2010; Huang et al., 1986; Tsau and Grigg, 1997; Yang and Reed, 1989).
VI) Easier foam generation at lower pressure gradients and velocities (Rossen and Gauglitz, 1990; Gauglitz et al., 2002).

Points (I-II) could possibly favor the foam stability and increase the foam strength due to the reduced capillary pressure forces on the lamellae and due to more liquid films available to reduce gas mobility. Points (III-V) could possibly make the foam appear weaker and/or less stable, whereas point (VI) could be important to achieve foam generation away from an

injection well at successive lower pressure gradients and velocities (i.e., less energy required to form the foam).

Although the surface tension is one of the contributing parameters in foam, there appears to be no straightforward relationships between gases and surfactant solution's surface tension and their performance in bulk and porous media. Stronger and more stable foams have been reported with surfactants that hold lower and higher surface tension values or vice versa (Chabert, 2014; Elhag et al., 2014; Grigg et al., 2008; Holt et al., 1996; Liu et al., 2005a). It has been reported that is seems to be difficult to predict the foam performance solely by the value of the surface tension (Grigg et al., 2008; Langvin, 2000; Liu et al., 2005a).

5.4.8 Summary of the characteristics of CO_2

Table 5.4 provides a summary of some of the main CO_2 characteristics with pressure, temperature and salinity. The trends are based on the available data presented in the preceding sections.

Table 5.4: Summary of the change in the CO_2 characteristics with pressure, temperature and salinity

CO_2 characteristics: → System parameters: ↓	Density	Viscosity	Solubility in water	Compressibility	Water pH	Surface tension to water
Pressure	increase	increase	increase	decrease	decrease	decrease
Temperature	decrease	decrease	decrease	increase	increase	increase
Salinity	-	-	decrease	-	decrease	decrease

(The table should be read as follows: the density of CO_2 increases with (increasing) pressure…the solubility of CO_2 in water decreases with (increasing) temperature… the pH value of CO_2-saturated water decreases with (increasing) water salinity… the surface tension between CO_2 and water decreases with (increasing) pressure…etc.,).

5.5 Type of surfactant against different gas components

A direct conclusive comparison of foams using different gas components may be difficult because a surfactant optimized for one gas phase may not be optimal for another phase. Therefore, a portion of the differences in foam performance could also be attributed to the type of surfactant being used.

Foamers against air/nitrogen or natural gases:

Conventional water-soluble surfactants for foam with air/nitrogen or natural gases have typically included anionic alcohol sulfates and olefin sulfonates. For saline environments, the typical surfactants have been betaines and sulfobetaines (Aarra and Skauge, 1994; Krause et al., 1992; Mannhardt et al., 2000; Mannhardt and Novosad, 1994; McPhee et al., 1988; Schramm and Kutay, 2000).

In the process of finding effective foamers against these gas types, parameters other than the gas phase itself have probably achieved more attention (e.g., good solubility in brine/ high hydropilicity, low partitioning into the oil phase/high HLB numbers, thermal stability, low adsorption onto the reservoir rock, ability to reduce gas mobility in the absence and presence of oil, etc.).

Foamers against dense CO_2 – a special case:

Several researchers have indicated the requirements for good surfactants against dense CO_2 to be very different from the good foamers typically found with other gas phases (i.e., air/nitrogen or natural gases). Conflicting views appear to exist regarding whether the use of classical foaming agents can be adapted for dense CO_2 foaming (Bian et al., 2012; Chaubert, 2012, 2014; Sanders et al., 2010). Chabert et al., (2012) have speculated that certain CO_2-foam pilots were reported as inconclusive (in contrast to the more successful foam applications in the North Sea using hydrocarbon gas), partially because the surfactants used were not specifically designed and tested against dense CO_2.

A recent report by Enick and Olsen (2012) provide a good summary of the variety of surfactants identified as viable candidates for CO_2-foam. Three distinct types of foam stabilizing agents have generally been considered: water-soluble surfactants, CO_2-soluble non-ionic surfactants and nanoparticles (Enick and Olsen, 2012).

Studies comparing the surfactant characteristics at various gas-liquid surfaces have indicated major differences between the CO_2-water and the air-water surface in terms of surfactant partitioning, adsorption kinetics, interfacial activity, surfactant packing properties and Marangoni stabilization (Adkins et al., 2009, 2010; Eastoe et al., 2000b, 2006).

According to several researchers and vendors that design and optimize surfactants for dense CO_2-foam, it appears to be possible to tailor a surfactant for good foam performance at any oil field conditions by varying its structure and hydrophilic-lipophilic balance (HLB) (Elhag et al., 2014; Heller, 1984; Sanders et al., 2010; Chabert et al., 2013). Bernard et al., (1980) suggested in an early study that surfactants that are better emulsifiers than foamers (i.e., less hydrophilic/lower HLB numbers) could be the most effective surfactants to reduce the mobility of dense CO_2.

Interestingly, many of the recommended surfactants appear to generate relatively weak foams with dense supercritical CO_2. Mobility reduction factors (MRF) and apparent viscosities ($\mu_{app.}$) less than 15 have frequently been reported with several types of foamers in various displacement tests without oil when the density of pure CO_2 is ≥ 0.5 g/cm^3 (Aarra et al., 2014; Alkan et al., 1991; Chabert et al., 2012, 2014; Chen et al., 2012; Elhag et al., 2014; Khalil and Asghari, 2006; McLendon et al., 2012; Preditis and Paulett, 1992; Sanders et al., 2010; Xing et al., 2012).

Certain dense CO_2-foams in porous media, primarily generated with commercial or proprietary water-soluble surfactant formulations, have been stronger, as reflected by the larger MRFs and $\mu_{app.}$ (Bian et al., 2012; Chabert et al., 2014; Chang and Grigg, 1999; Dong, 2001; Kuehne et al., 1992; Moradi-Araghi et al., 1997; Mukherjee et al., 2014; Tsau and Grigg, 1997; Tsau and Heller, 1992; Wellington and Vinegar, 1985).

Among the good foamers for dense supercritical CO_2, a series of commercial water-soluble surfactants and surfactant mixtures developed by Chevron Chemical Company, denoted as Chaser CD-1040, CD-1045, CD-1050 and CD-128 (see further product descriptions in Enick and Olsen, 2012), have been cited as promising. The results have been demonstrated in laboratory and field tests in sandstone and carbonate rock material, primarily under moderate temperature (40-60°C) and pressure conditions (100-150bar) (Bernard et al., 1980; Casteel and Djabbarah, 1988; Chang and Grigg, 1999; Dixit et al., 1994; Enick and Olsen, 2012;

Heller, 1994; Holm and Garrison, 1988; Kahlil and Asghari, 2006; Moradi-Araghi et al., 1997; Preditis and Paulett, 1992; Syahputra et al., 2000; Tsau and Heller, 1992; Tsau and Grigg, 1997; Wang, 1984; Yaghoobi and Heller, 1994; Yin et al., 2009).

Heller (1984) suggested in an early surfactant screening study that the most promising surfactant for CO_2-foams appeared to be commercial anionic sulfonate surfactants. Since then have several commercial AOS surfactants with relatively long carbon chains (between C14-C18) been tested and used by several research institutions and oil companies in relation to CO_2-foam projects. Mobility reduction of CO_2 have been achieved in numerous laboratory experiments using AOS surfactants (Aarra et al., 2011, 2014; Andrianov et al., 2011; Apaydin and Kovscek, 2001; Chou, 1991; Enick and Olsen, 2012; Farajzadeh et al., 2009; Kibodeaux, 1997; Kuehne et al., 1992; Ma, 2013; Prieditis and Paulett et al., 1992; Simjoo et al., 2013a, 2013b; Solbakken et al., 2013; Wang et al., 2014).

5.6 Foam mobility control with pressure and temperature

Because most of the foam field projects are typically aimed towards field-specific conditions, there are relatively few foam core flooding studies in the literature in which the pressure and temperature are varied systematically.

An important reason for considering the gas type along with the pressure and temperature is that differences in the gas density, gas viscosity, gas solubility properties, gas compressibility, water pH, gas-water surface tension and surfactant requirements may become significantly different under various experimental conditions. This phenomenon is particularly instructive when CO_2 is used as the gas phase in which many physical and chemical properties can change with relatively small changes in pressure and temperature conditions. Therefore, valuable insights into foam properties using different gas types can be gained from a comparative study of foams as a function of pressure and temperature.

In addition, the reservoir situation may vary significantly among the fields regarding pressure and temperature conditions, thus, understanding foam properties on a broad experimental scale should be educational.

Effect of pressure and temperature on the N_2- and CH_4-foams:

Several N_2-foam experiments conducted in porous media or in high pressure cells in the absence of oil using water soluble surfactants have reported N_2-foams of similar or slightly increased foam strengths with increasing system pressure (Aarra et al., 2014; Du et al., 2008; Farajzadeh et al., 2009; Friedmann and Jensen, 1987; Mani and Ma, 1986; Mannhardt et al., 1996; Sanchez and Schechter, 1989; Solbakken et al., 2014; Turta and Singhal, 1998). The positive effect of the pressure on the N_2-foam strength has been explained by: an increased rate of lamellae generation with pressure, smaller and more uniform bubble sizes at higher pressures, an improved lamellae stability due to increased adsorption of surfactant at the gas-liquid surface, an increased fraction of non-condensable component in the gas phase at high temperature with an increment in the system pressure, reduced expansion effects to weaken the foam at higher pressures, as a result of the core experimental history.

Holt et al., (1996) investigated the CH_4-foam strength as a function of pressure from 10 to 290 bar at 90°C. Two types of surfactants were used (i.e., an AOS_{C16} and a fluorinated sulfobetaine surfactant). Both of the surfactants displayed increased foam strength with increasing system pressure. The authors attributed this behavior to a reduction in surface tension, and a shift in the liquid saturation to lower values with increasing pressure. Part of the pressure effect was also explained as a possible reduction in the attractive van der Waals force component of the disjoining pressure and as a slight increase in the methane and water viscosity.

A positive dependence of increasing the system pressure on foam strength was also reported by Mannhardt et al., (1996) using different hydrocarbon solvents as the dispersed phase (i.e., methane, ethane, propane and butane).

A primary concern of foam in high temperature reservoirs is the possibility of thermal degradation of the surfactant and the consequent chances for a reduced foam effectiveness. Therefore, the temperature effects on foams and foamers are important to evaluate. Few core flooding studies of N_2- and CH_4-foams with varying temperature have been reported. However, several laboratory corefloods conducted under high pressure and high temperature (75-110°C) conditions have repeatedly shown that it is possible to generate strong foams in porous media with nitrogen and methane as the gas phase.

Foam studies under high temperatures have reported attractive foam properties with AOS surfactants (Aarra et al., 1994, 2011; Mani and Ma, 1986; Mannhardt et al., 2000; McPhee et al., 1988; Holt et al., 1996).

Effect of pressure and temperature on the CO_2-foams:

Conflicting results regarding the effects of pressure and temperature on CO_2-foam properties exist in the literature, as follows:

I) Several bulk foam studies have reported an improved CO_2-foam stability with increasing pressure, whereas increasing the temperature had the opposite effect (Alkan et al., 1991; Bernard et al., 1980; Chabert et al., 2013; Chen et al., 2012; Enick and Olsen, 2012; Lee et al, 1991; Liu et al., 2005a; Wang, 1984).

II) Laboratory corefloods of CO_2-foam have indicated the contrary effects of pressure and temperature compared with those in bulk. Reduced foam strength, stability and mobility control of CO_2 as a function of pressure (Aarra et al., 2014; Du et al., 2008; Khalil and Asghari, 2006; Kibodeaux, 1997) and improved CO_2-foam strength with increasing temperature have been reported (Khalil and Asghari, 2006; Solbakken et al., 2013; Tortopidis and Shallcross, 1994).

The reasons for the conflicting trends, as I see it, may be a general lack of correlation between foam properties in bulk and in porous media, and the general lack of systematic experimental studies of CO_2-foam properties in porous media over a wide range of pressure and temperature conditions.

Paper 1 and **Paper 2** in this thesis have investigated CO_2-foam properties in porous media with systematic variations in pressure and temperature conditions. The properties of CO_2-foam were compared against N_2-foams. The results demonstrated that the N_2-foams were stronger and more stable than the CO_2-foams under similar experimental conditions. The strength of the generated CO_2-foams was found to vary significantly under different pressure and temperature conditions. Conditions where the density of CO_2 is low improved the CO_2-foam strength (Chapter 8, section 8.2). An important reason to this behavior, as we see it, appears to lie in the many physical and chemical characteristics of carbon dioxide that change with the pressure and temperature, in which is in large contrast to nitrogen as demonstrated in this chapter.

Chapter 6

Foam-Oil Interactions

6.1 Introduction **p. 85**

6.2 Foam-oil interaction theories **p. 86**

6.2.1 Spreading and entering coefficients **p. 87**

6.2.2 Bridging coefficient **p. 88**

6.2.3 Lamella number **p. 89**

6.2.4 Pseudo-emulsion film theory **p. 91**

6.3 Practical viewpoints **p. 92**

6.1 Introduction

The effectiveness of foam in enhanced oil recovery (EOR) processes may largely depend on the stability of the foam in the presence of oil.

Most experimental data in the literature suggest that oil reduces foam efficiency (i.e., decreases foam strength, stability and mobility control). However, many studies have shown that it is possible generate relatively strong and stable foams even in the presence of high oil fractions (Aarra et al., 1994, 1997, 2002; Andrianov et al., 2011; Borchardt et al., 1987; Bhide et al., 2005; Casteel and Djabbarah, 1988; Chabert et al., 2013; Dalland et al., 1992; Friedmann and Jensen, 1986; Hanssen and Dalland, 1990; Holt et al., 1996; Maini and Ma, 1984; Mannhardt et al., 2000; Mannhardt and Svorstøl, 1999; McPhee et al., 1988; Parlar et al., 1995; Simjoo et al., 2013b; Solbakken, 2013; Strycker et al., 1987; Svorstøl et al., 1997; Tortopidis and Shallcross, 1994; Vikingstad and Aarra, 2009).

Some authors observed a significant dependence on oil saturation on foam strength (Jensen and Friedmann, 1987; Schramm, 1994b; Mannhardt and Svorstøl, 1999; Yin et al., 2009).

Others have indicated that lighter hydrocarbons/shorter chained alkanes may be the most detrimental to foam stability (Andrianov et al., 2011; Kuhlman, 1990; Schramm and Novosad, 1992; Suffridge et al., 1989; Vikingstad et al., 2006).

The sensitivity of foam to the presence of oil also depends on the type of surfactant used. Many different foams (i.e., CO_2-, CH_4- and N_2/air-foams) exhibit enhanced performance and stability in the presence of oil using different types of fluorinated surfactants (or in combinations with other surfactants, e.g., alpha-olefin sulfonates). These results have been confirmed in both static and dynamic core flooding experiments (Aarra and Skauge, 1994; Andrianov et al., 2011; Bian et al., 2012, Chabert, 2013; Dalland et al., 1992; Mannhardt et al., 1996, 2000; Raterman, 1989; Schramm and Novosad, 1990; Simjoo et al., 2013b; Solbakken, 2013; Suffridge et al., 1989; Vikingstad and Aarra, 2009).

For some foam formulations, emulsion formation appear to have reduced gas mobility in porous media and increase foam stability in bulk foam experiments, beyond that achieved in the absence of oil. Emulsification of oil may be desirable or undesirable but should not be ignored (Aarra et al., 2011; Bian et al., 2012; Bernard et al., 1980; Bhide et al., 2005; Chabert et al., 2012, 2014; Kuhlman, 1990; Mannhardt et al., 2000; Mukherjee et al.,. 2014; Vikingstad, 2006; Wassmuth et al., 2000; Yang and Reed, 1989; Yin et al., 2009).

It is generally expected that the contact between oil and foam will impair or promote some of the factors and forces responsible for keeping the foam stable (addressed in Chapter 3). Despite extensive research, no single parameter or property seems to be able to explain the complex interactions between oil and foam.

6.2 Foam-oil interaction theories

Several theories have been proposed in the literature to predict foam stability in the presence of oil. The most recognized theories are the following, which are discussed and defined in this section:

1. Spreading and entering coefficients
2. Bridging coefficient
3. Lamella number
4. Pseudo-emulsion film theory

6.2.1 Spreading and entering coefficients

The most frequently used parameters to explain the destabilization of foam by oil are the entering coefficient (**E**), defined in Equation 6.1 (Robinson and Woods, 1948; Schramm and Wassmuth, 1994):

$$E = \sigma_{w/g} - \sigma_{o/g} + \sigma_{w/o} \quad (6.1)$$

and the spreading coefficient (**S**), defined by Equation 6.2 (Harkins, 1941; Schramm and Wassmuth, 1994):

$$S = \sigma_{w/g} - \sigma_{o/g} - \sigma_{w/o} \quad (6.2)$$

where $\boldsymbol{\sigma_{w/g}}$ is the surface tension between water (i.e., surfactant solution) and gas, $\boldsymbol{\sigma_{o/g}}$ is the surface tension between oil and gas and $\boldsymbol{\sigma_{w/o}}$ is the interfacial tension between water (i.e., surfactant solution) and oil.

From a thermodynamic perspective, a stable foam in the presence of oil depend on a negative entering coefficient (E), which implies a negative spreading coefficient (S). A positive E and S, in which the oil enters into the lamellae and spreads, are usually associated with various degrees of foam destabilization, rupture or collapse (Aarra et al., 1994; Andrianov et al., 2011; Dalland et al., 1992; Mannhardt et al., 2000; Schramm and Wassmuth, 1994; Vikingstad et al., 2006).

The negative and positive scenarios of the entering and spreading coefficients are illustrated in Figure 6.1.

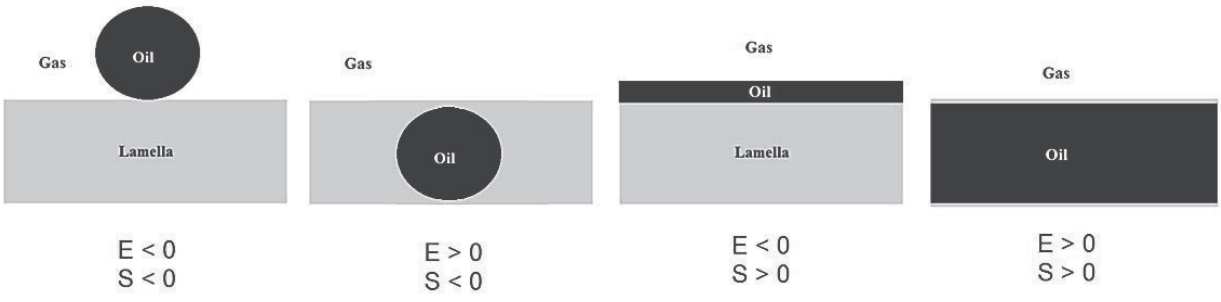

Figure 6.1: Illustration of the different entering and spreading scenarios of an oil phase in contact with a lamella (from this thesis).

6.2.2 Bridging coefficient

Another parameter often calculated when discussing the antifoam efficiency of an oil (i.e., foam breaking ability) is the bridging coefficient (**B**), defined in Equation 6.3 (Garrett, 1980; Denkov, 2004):

$$B = \sigma_{w/g}^2 - \sigma_{o/g}^2 + \sigma_{w/o}^2 \quad (6.3)$$

Once an oil drop has entered the lamella, the foam can become unstable even when the spreading coefficient is negative (i.e., $E > 0$ and $S < 0$). An oil drop that has entered the film, may lead to rupture of the lamella by separating the two film surfaces. The lamella can oppose film stretching and rupturing provided that the bridging ability is strong ($B < 0$) (Figure 6.2). For the oil to behave as an antifoaming agent (i.e., foam breaker), a positive bridging coefficient is required but not sufficient (note that if B is positive then E must also be positive, but E can still positive when B is negative). A detailed explanation of the proposed oil bridging mechanism can be found in Denkov (2004).

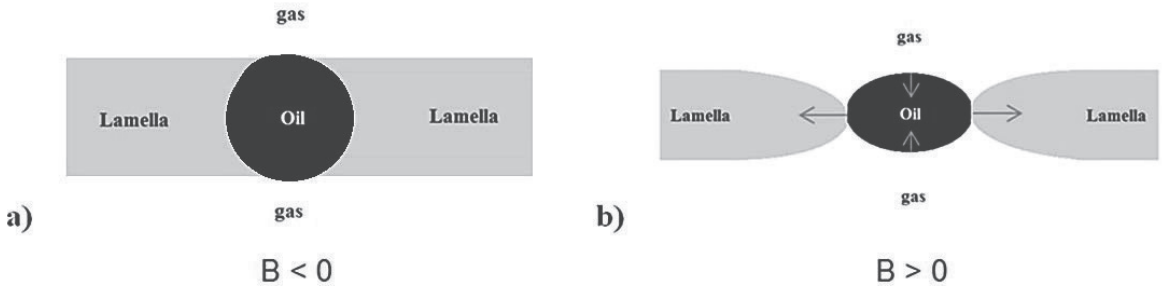

Figure 6.2: Example of a) stable oil bridge and b) unstable oil bridge (from this thesis).

It should be noted that the theories introduced thus far (i.e., E, S, and B coefficients) have primarily been developed through observations of foam films and oil under very controlled circumstances and therefore may not correlate equally well to all foam tests applied with oil present. Experimental studies indicate varying degree of correlation between foam properties in bulk and porous media in the presence of oil and the calculated coefficients (Andrianov et al., 2011; Arnaudov et al., 2001; Basheva et al., 2000; Bergeron, 1993; Bhide et al., 2005; Dalland et al., 1992; Mannhardt et al., 2000; Raterman, 1989; Rohani et al., 2014; Vikingstad

et al., 2006). Several of the abovementioned laboratory studies have also demonstrated that foam performance in the presence of oil can be strongly influenced by the particular test method, procedures and conditions applied. Thus, evaluation of foam using different experimental methods and conditions may be valuable for permitting more reliable conclusions on the oil tolerance of the foams.

6.2.3 Lamella number

Schramm and co-workers used a microvisual apparatus to study foam-oil interactions (Schramm, 1994b; Schramm et al., 1993; Schramm and Novosad, 1990, 1992). Their studies led to the definition of the lamella number. A simplified expression for the lamella number (**L**) is given as Equation 6.4:

$$L \approx 0.15 \cdot \left(\frac{\sigma_{w/g}}{\sigma_{w/o}}\right) \tag{6.4}$$

where **0.15** denotes the ratio between the radius of an oil droplet engulfed by water and the radius of the Plateau border contacting the oil surface. The value was found to be constant for all foams evaluated but might be, as noted by Schramm and Novosad (1990), dependent on the experimental system used.

The value of L determines the degree of oil emulsification within the foam lamellae. A value of $L < 1$ is believed to indicate the best foam stability in the presence of oil. A value of $L > 1$ favors uptake and transport of oil into the lamellae, which is anticipated to initiate various degree of foam destabilization.

Three types of foams (A, B and C) have been defined based on their interactions and stability with oil (Schramm and Novosad, 1990). Type A foams, indicated by $L < 1$, exhibit good stability and little interactions with the oil phase. Type B foams, indicated by $1 < L < 7$, give foams with moderate stability. Type C foams, indicated by $L > 7$, give undesirable interactions with the oil phase and foams with poor stability.

Figure 6.3 illustrates the three foam types proposed by Schramm and Novosad (1990).

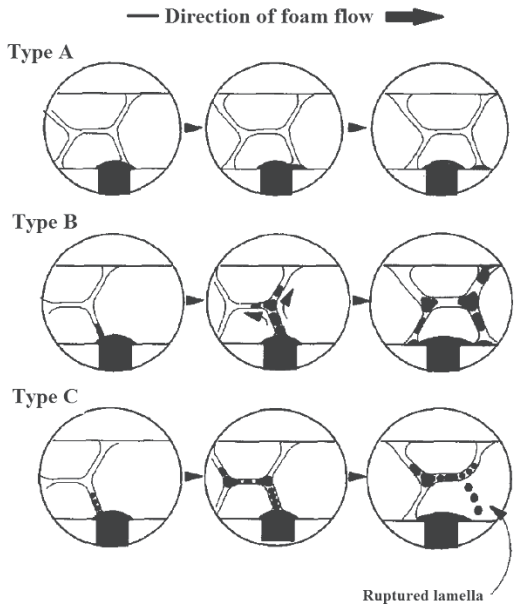

Figure 6.3: Illustration of type A, B and C foams, as defined by the lamella number (L), in contact with an oil phase (from Schramm and Novosad, 1990).

The lamella number was first introduced in an attempt to characterize and improve the understanding of foam-oil interactions in porous media. Good agreement between the calculated values of L and foam stability in porous media with residual oil saturation under reduced pressure and temperature conditions was observed by Schramm et al. (1993) and Schramm and Novosad (1990). Other studies, however, have reported the predictive power of L to be poor in both bulk and porous media experiment in the presence of different oils (Andrianov et al., 2011, Bergeron, 1993; Dalland et al., 1992; Mannhardt et al., 2000; Rohani et al., 2014; Vikingstad and Aarra, 2009).

The poor correlation between the calculated value of L and foam effectiveness in porous media in the presence of oil, may be due the assumption that the two radii of curvature (i.e., 0.15) are constant. In real porous media, this ratio would be very difficult to predict. Another limitation is that L applies to zero capillary pressure. Because most real porous rocks exert rather large capillary pressures on the liquid lamellae, this method therefore ignores the possible influence that thin film forces (e.g., disjoining pressure) can have on foam stability in the presence of oil (Bergeron, 1993).

6.2.4 Pseudo-emulsion film theory

Nikolov et al. (1986, 1989) argued that the presence of emulsified oil in a foam lamella also can have a stabilizing effect on foams, if the pseudo-emulsion film is stable. A pseudo-emulsion film is a thin film of water (i.e., surfactant solution) that separates the emulsified oil phase and the dispersed gas phase (see Figure 6.4). If the pseudo-emulsion film is stable, the oil will remain in the lamella. Otherwise, the oil can form a lens on the surface. Upon further thinning of the lamellae, the lens come into contact with the opposite film surface to form an oil bridge. An unstable oil bridge could then break down the foam.

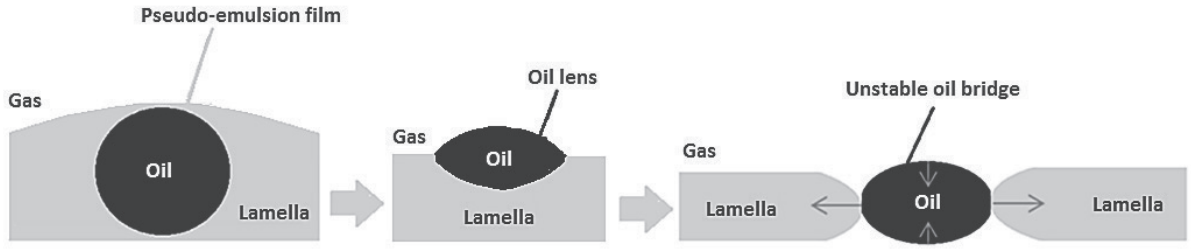

Figure 6.4: Pseudo-emulsion film stability (from this thesis).

The pseudo-emulsion film theory has been supported by several authors who find good correlations to it in both bulk and porous media experiments (Bergeron, 1993; Koczo et al., 1992; Nikolov et al., 1986; Radke and Manlowe, 1990; Raterman, 1989; Wasan et al., 1994). Measurements of the pseudo-emulsion film require complex techniques, such as the film trapping technique (FTT) described by Hadjiski et al. (2001).

The stability of a pseudo-emulsion film depends on the micellar microstructure within the film (examples of micellar structures are shown in Figure 2.8 in Chapter 2). Accordingly, the electrolyte concentration, surfactant type and concentration may influence this microstructure-stabilizing mechanism. For an oil droplet that enters the lamella, the surfactant should provide low dynamic interfacial tensions to achieve small oil droplet sizes and large interfacial tension gradients to favor Marangoni stabilization to prevent thinning of the pseudo-emulsion film (Nikolov et al., 1986).

Recent studies by Denkov and co-workers (2004, 2006) have stressed that two types of foam breakers exist: fast and slow. The fast foam breakers destroy the foam relatively rapidly, while the slow foam breakers act over many hours or longer. Fast foam breakers have been found to have low film entry barriers, while slow foam breakers have high entry barriers (i.e., high film disjoining pressures), as measured by the FFT.

Recent study by Farajzadeh et al., (2012b) suggests that the disjoining pressure in the pseudo emulsion film may be one of the underlying mechanisms of foam stability in porous media in the presence of oil.

Measurements of the pseudo-emulsion film were not performed in this thesis.

6.3 Practical viewpoints

In light of the complex foam-oil interactions, several practical viewpoints deserve some comments:

I) Despite the potential detrimental effects that oil can have on foam, several successful foam trials and field applications have been accomplished under tough reservoir conditions, which have establish foam as an EOR method (Aarra et al., 2002; Castanier, 1987; Enick and Olsen, 2012; Skauge et al., 2002; Turta and Singhal, 1998; Zhdanov et al., 1996).

II) In many reservoir situations, reservoir engineers would typically not consider a foam application until a sweep-efficiency problem is already apparent. Thus, much of the oil has likely been swept from the region near the injection well were the gas has entered before foam injection begins. This removal of oil may benefit the use of foam to reduce gas mobility in target layers already flooded by gas, namely, those with higher permeabilities and lower oil saturations (Rossen, 1996; Suffridge et al., 1989).

III) Interestingly, laboratory studies in outcrop sandstone cores seem to support point II as they indicate that foam is more stable in the presence of oil when the foam is able to form before coming into contact with oil. In these experiments, the used sandstone cores were only partly saturated with oil, leaving the first part of the core oil-free so that it could serve as an "in-situ foam generator" (Andrianov et al., 2011; Farajzadeh et al., 2010). These results also

indicate that the way the oil is introduced to foam may be an important determinant of the effectiveness of foam in the presence of oil.

IV) Foam flooding experiments performed under elevated pressure and temperature conditions in the presence of residual oil saturations have demonstrated that foam could be more efficient in porous media than in bulk tests under reduced conditions using AOS surfactant (Aarra et al., 1994; Holt et al., 1996; Mannhardt et al., 2000; Vikingstad et al., 2009).

V) Studies that have examined the diversion potential of foam in dual core experiments have reported very positive results with respect to oil recovery, particularly under miscible CO_2 conditions. The diversion potential of gas by foam from higher permeability to lower permeability core illustrates how foam might behave in heterogeneous reservoirs with varying permeability (Bian et al., 2012; Casteel and Djabbarah, 1988; Di Julio and Emanuel, 1989).

VI) The spreading, entering and bridging coefficients and lamella number (i.e., S, E, B, and L) are products from measurements of static tension values only. In reality, the surface/interfacial tension is a dynamic property that can change with time after an initial oil phase has been introduced. Thus, it is difficult to take into account the time scale of foam destabilization by oil using the theories proposed.

The latter results demonstrate that effective foams can occur even in the presence of oil. It also reflects that the design of the foam experiments should be as realistic as possible to what can happen in real oil reservoirs.

In **Paper 4** (part 2), various experimental approaches were used to study foam-oil interactions. Experiments were conducted in two different bulk tests under reduced experimental condition, and supplemented with core flooding experiments under elevated pressure and temperature conditions. The S, E, B and L parameters were calculated and evaluated for their predictive power against the bulk experiments with oil. The combination of several experimental techniques seemed valuable towards more reliable conclusions of foams tolerance to oil under different experimental conditions and scenarios (see Chapter 8, section 8.4).

Chapter 7

Foam Experimental Methods

7.1 Experimental methods **p. 95**

7.2 Bulk tests **p. 95**

7.2.1 Mixer method **p. 96**

7.2.2 Filter test **p. 97**

7.3 Bulk foam properties vs. foam properties in porous media **p. 98**

7.4 Foam core flooding **p. 99**

7.4.1 Characterizing foam efficiency in corefloods **p. 101**

7.5 Experiments at HPHT (special considerations) **p. 105**

7.6 Phase-equilibration **p. 109**

7.1 Experimental methods

The main methods used to study foam in relation to EOR processes include bulk tests, micro-model studies, core flooding and simulations.

In this thesis, foam core flooding experiments were performed in **Papers 1-3**, and two types of bulk foam tests were applied in **Paper 4**. Micro-model experiments and simulations were not used.

7.2 Bulk tests

Bulk tests are frequently used as a simple, rapid and inexpensive way of evaluating and screening surfactants to foam. The most typical and classical bulk foam tests are compiled in Bikerman (1973), Exerowa and Kruglyakov (1998) and Pugh (2005). The test methods include foam generation through various approaches such as blending, shaking, beating, blowing or sparging.

In such tests, surfactants are typically studied and compared based on their foamability and foam stability. Foamability is a dynamic property that refers to the ability of the surfactant solution to form foam under specific conditions. Foam stability is understood as a parameter describing variation in foam height or volume with time after foam generation (i.e., usually when the rate of foam formation is zero).

Bulk foam properties were studied in **Paper 4** in this thesis. The methods used involved foam generation through blending with a mixer (referred as the mixer method) and sparging, that is, injecting gas into a surfactant solution through a porous filter (referred as the filter test). The use of different experimental methods may enable an improved evaluation and selection of suitable surfactant candidates to foam.

7.2.1 Mixer method

The traditional mixer method involves foam generation in a blender under ambient conditions. Air is dispersed into the surfactant solution by continuous mixing (Figure 7.1). The foamability of the surfactant solution in this study was taken as the foam height immediately after mixing stopped. Foam height was monitored over time to evaluate foam stability. A standardized procedure was used for all experiments in this thesis to facilitate comparisons of the foaming properties of various surfactants (described in detail in **Paper 4**). The reproducibility of the foam height of identical fluid systems using the mixer method was ± 1 cm.

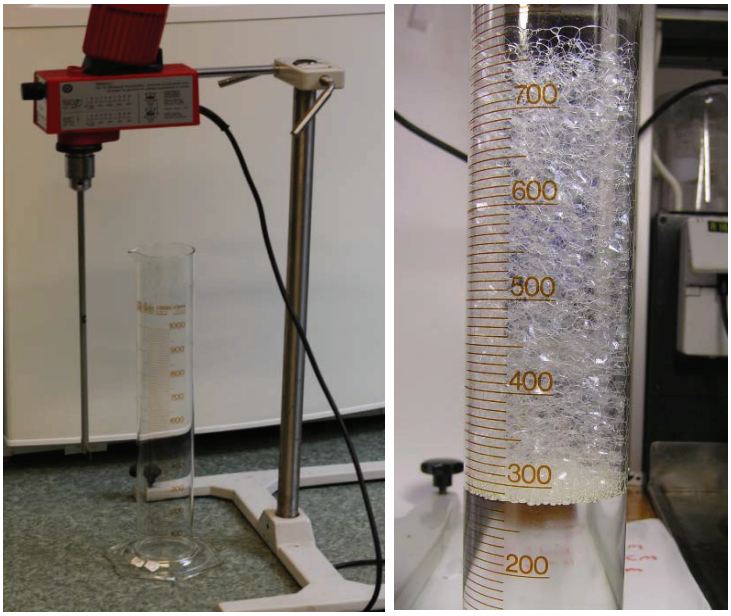

Figure 7.1: Experimental setup for the mixer method (adapted from Paper 4).

Studies in which the mixer method was utilized for foam evaluation and surfactant screening can also be found reported elsewhere (Aarra and Skauge, 1994; Andrianov et al., 2011; den Engelsen et al., 2002; Exerowa and Kruglyakov, 1998; Krasowska et al., 2005; Mannhardt et al., 2000; Rohani et al., 2014; Vikingstad, 2006; Wang, 1984).

7.2.2 Filter test

A new bulk test, the filter test, was developed in our laboratory during this project. The design of the filter test is based on concepts from the foam-rise (bubbling) method, also known as the Bikerman-test (Bikerman, 1973).

In the filter test, foam is generated through the injection of the desired gas phase through a porous filter immersed in the surfactant solution and into a column (Figure 7.2). Foamability is measured as the injected gas volume required to reach a certain foam height in the column (e.g., 10 cm was used in this thesis). After foam generation, the system is closed, and foam stability is monitored over time.

An advantage of the filter test compared with the mixer method is that it allows the study of bulk foams using gas phases other than air. Other advantages are that some pressure and temperature can be applied, the size of the bubbles can be controlled using filters of known pore sizes, and the foam generation rate (i.e., gas injection rate) can be adjusted and controlled.

In the filter test with oil present, the oil was always injected into the column before the initiation of foam generation. Foam is therefore able to generate before it comes in contact with the oil phase situated at the top of the surfactant solution in the column. In contrast, in the mixer method, the oil phase is always forced into the surfactant solution during mixing.

The repeatability of foamability using the filter test was ± 20 ml of gas phase injected at 2 barg and room temperature, and the foam stability (height) was within ± 0.5 cm. For additional experimental details, the reader is referred to **Paper 4**.

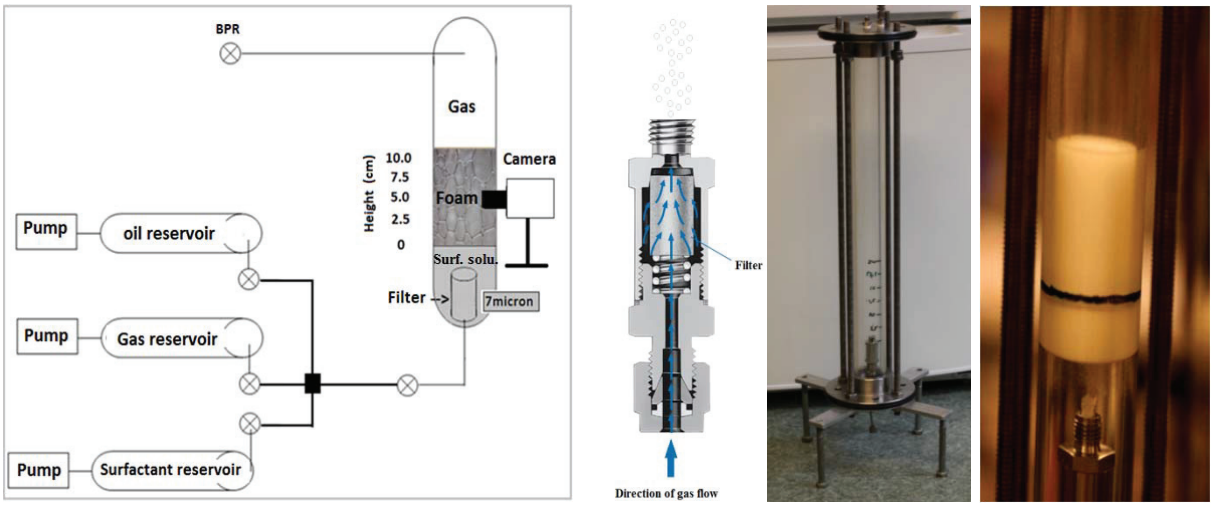

Figure 7.2: Experimental setup for the filter method (adapted from Paper 4).

7.3 Bulk foam properties vs. foam properties in porous media

A general concern with many of the experimental methods used to study foam (e.g., single film/bubble techniques, bulk foam tests, constricted tubes, micro models, glass beads packs), is how representative these methods really are to describe the conditions likely dominating in natural porous rocks. The advantages and limitations of several of the experimental methods and measurements frequently used to mimic foam events in porous media have been critically reviewed by several authors. It appears that none of the abovementioned experimental methods can predict the exact behavior of foam in porous media (Bergeron, 1993; Chambers and Radke, 1991; Denkov, 2004; Heller and Kuntamukkula, 1987; Nguyen et al., 2000; Rossen, 2003).

In the literature, both good and poor correlations between bulk foam properties and foam properties in porous media have been reported. In general, while some researchers find that good foamers in bulk foam tests also perform well in core flooding experiments, others find just the opposite. A global correlation between bulk foam properties and foam properties in porous media remains elusive (Alkan et al., 1991; Andrianov et al., 2011; Borchardt et al., 1987; Casteel and Djabbarah, 1988; Chabert et al., 2012, 2014; Dalland et al., 1992; Hanssen, 1988; Hanssen and Dalland, 1990; Kuehne et al., 1992; Lee et al., 1991; Maini and Ma, 1984; Mannhardt et al., 2000; Parlar et al., 1995; Simjoo et al., 2013a; Strycker et al., 1987; Tsau and Grigg, 1997; Vikingstad and Aarra, 2009; Wang, 1984; Yang and Reed, 1989).

Paper 4 in this thesis examined properties of foam in bulk. No obvious correlation between bulk foam properties and foam properties in porous media using $AOS_{C14-C16}$ surfactant were found (i.e., **Paper 4 vs. Papers 1-3**). Some of the main causes for this, as we saw it, are addressed in Chapter 8, section 8.4.5.

7.4 Foam core flooding

The experimental setup employed for high-pressure and high-temperature (HPHT) foam core flooding experiments in this thesis is shown in Figure 7.3. For all foam experiments, we used the co-injection method to inject surfactant solution and gas from separate reservoirs (i.e., separate piston cylinders and lines) into the core material. The co-injection method allows foam to be generated by the core material in-situ as the gas phase disperses into the surfactant solution. The total injection rate during generation was set to 40 ml/h (i.e., 32 ml/h gas and 8 ml/h surfactant solution). The constant flow rate corresponds to a superficial velocity of ~ 0.9 m/day and interstitial velocities (i.e., frontal advance rates) of 3.9-5.0 m/day for the different cores employed. Foam quality (i.e., volume fraction of gas) was 0.80 ± 0.01 at the inlet end of the core at all times. Two HTHP Quizix pumps located inside the heat cabinet were used to control the injection rates. The pumps were continuously refilled at the inlet pressure of the core, which ensured constant inflow foam quality throughout the entire experiment. Foam generation was monitored by pressure measurements at the inlet and outlet of the core (P1, P2) including measurements by an independent differential pressure meter, dP, with higher accuracy in the range of 0-20 bar. Behind the core outlet, a visual cell with inner diameter of 1.5 mm was mounted on the line to enable acquisition of images of the effluent foam from the core under experimental conditions using a Canon EOS 5D Mark II camera with an MP-E 65 mm (f/2.8 1-5x) macro lens (Figure 7.4). The visual cell was used to confirm foam generation, to detect gas/foam breakthrough times and in the visual inspection and comparison of foam textures (e.g., bubble density, size and continuity) in different foam experiments. Fluids that were produced from the core were either collected in production cylinders or produced through a back pressure regulator (BPR) at constant outlet pressure (P2). The use of production cylinders is advisable to enable accurate acquisition of pressure data with minimum noise and fluctuations often associated with back pressure regulators. The experimental setup was placed inside a heat cabinet to provide a constant elevated temperature (± 1°C).

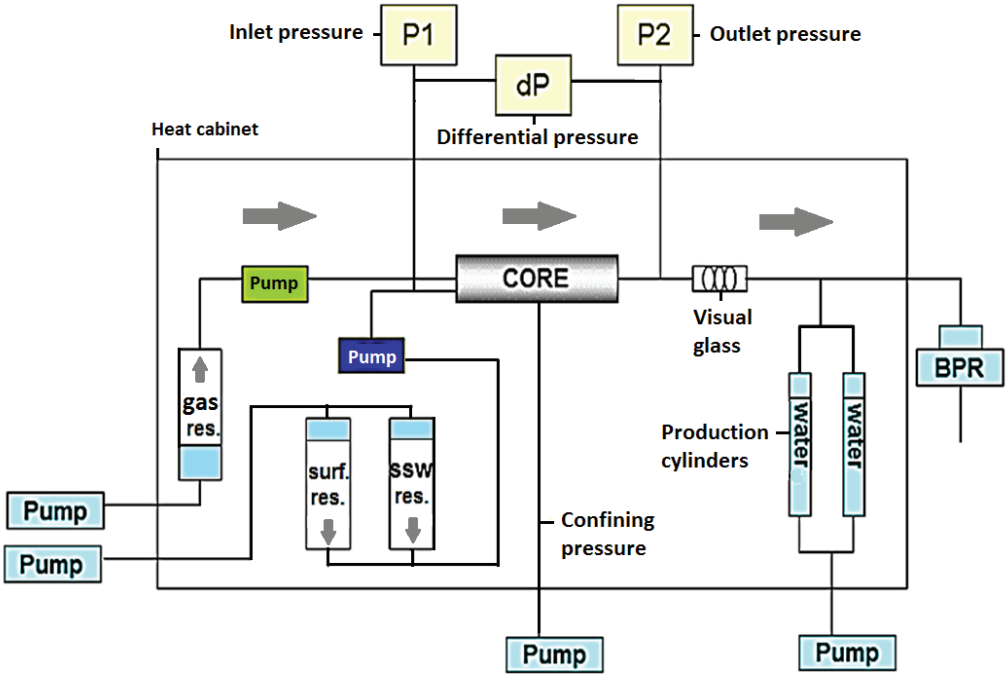

Figure 7.3: Experimental setup for the high-pressure and high-temperature (HPHT) foam core flooding experiments (from this thesis).

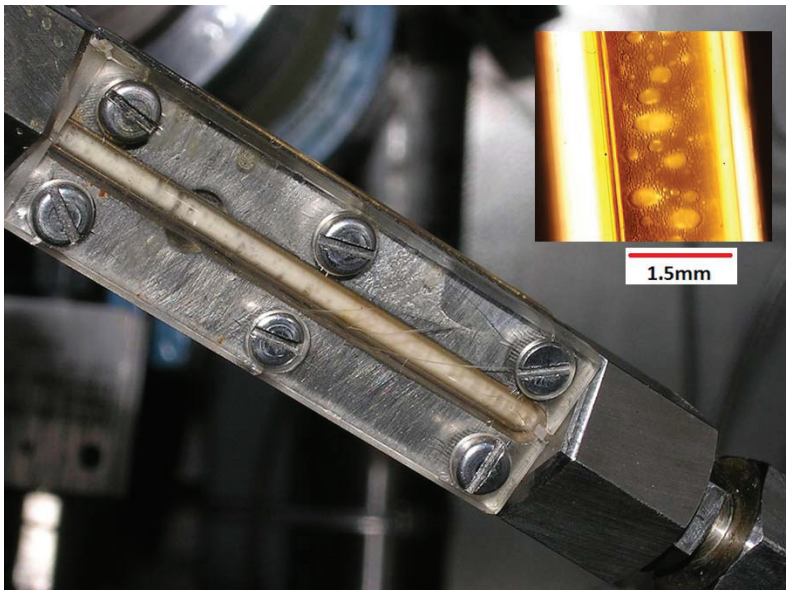

Figure 7.4: Visualization of foam texture in HPHT foam experiments (from this thesis).

Reproducibility of foam properties and performance in core flooding experiments are always important to verify to confirm actual trends on the core material employed. The repeatability of the main findings in this thesis was always evaluated, either by repeated experiments on the same core or by additional experiments using new Berea sandstone cores. For repeated experiments on the same core, the core restoration procedures included system depressurization and flooding with large volumes of seawater and brine (3 wt.% NaCl) and isopropyl alcohol (a good gas dissolver). Additional experimental details of the core flooding experiments are provided in the Appendix and in the individual papers (**Papers 1-3)**.

7.4.1 Characterizing foam efficiency in corefloods

The efficiency of foam in core flooding experiments can be characterized in many different ways. Important parameters that were measured, calculated, evaluated and compared in this project included: in-situ foam generation performance (i.e., pressure build-up profiles during simultaneous injection of gas and surfactant solution), mobility reduction factors (MRF), foam breakthrough times, visual observation and comparison of foam textures from the visual cell, and foam stability against injected brine after foam generation.

This paragraph describes how several of these parameters were characterized.

Pressure build-up profile:

The first indication of mobility control due to in-situ foam generation in porous media is an increase in the injection pressure (P1) and a corresponding increase in the differential pressure (dP = P1-P2) along the core. The characteristic pressure build-up profile of a strong foam in relatively homogeneous cores initially saturated with surfactant solution using co-injection mode usually reflects a sharp pressure build-up period following a plateau in the pressure drop after the injection of a few pore volumes. The transient pressure-build up period is attributed to a substantial reduction in liquid saturation to a constant value, front-like foam flow behavior in most of the pore space available, and significantly delayed gas breakthrough when compared with the absence of surfactant (Aarra et al., 1997; de Vries and Wit, 1990; Hanssen and Dalland, 1994; Kovscek and Radke, 1994; Osterloh and Jante, 1992; Persoff et al., 1991; Vikingstad and Aarra, 2009; Zitha et al., 2003).

Smaller and less effective pressure-build up profiles with time of generation have typically been observed in the absence of surfactant pre-flush (Simjoo et al., 2013a, 2013b), using low

surfactant concentrations (Mannhard and Svorstøl, 2001; Simjoo et al., 2013a), when comparing CO_2-foams with N_2-foams (Chou, 1991; Du et al., 2008) or with oil present in the core (Vikingstad and Aarra, 2009).

Usually, the injection of several pore volumes of gas and surfactant solution injected is sufficient to reach steady-state conditions. In some experiments, however, pressure build-ups have been significantly delayed, and occasionally stabilization is not achieved even after the injection of tens of pore volumes. The reasons for these responses are often unclear (Aarra et al., 2011; Chabert et al., 2013; Mannhard and Svorstøl, 2001; Persoff et al., 1991; Siddiqui et al., 1997a). Some authors have observed them in heterogeneous core material (Nguyen et al., 2005; Solbakken et al., 2014; Zitha et al., 2003). Some suggest these responses to be end effects (Apaydin and Kovscek, 2001; Nguyen et al., 2003; Simjoo et al., 2013a).

Foam strength:

Different methods to determine the efficiency of foam to reduce and control gas mobility in core floods have been suggested and used in the literature. The magnitude in pressure drop along the core during foam generation has been evaluated I) alone in terms of steady-state differential pressure plateau values over the full core or parts of the core with occasional extrapolation to pressure gradients (bar/m) (Aarra et al., 1997; Gauglitz et al., 2002; Osterloh and Jante, 1992; Simjoo et al., 2013b); II) as a single phase flow in terms of foam apparent viscosities, $\mu_{app.}$, and foam mobilities, λ_{foam}, based on Darcy's law (Chen et al., 2012; Mannhard and Svorstøl, 2001; Siddiqui et al., 1997a); III) compared with a measured pressure drop without foam, $\Delta P_{without\ foam}$ (i.e., no surfactant) (Aarra et al., 2011; Chabert, 2013, 2014; Chou, 1991; Mani and Ma, 1984; Mannhardt and Novosad, 1994; Siddiqui et al., 1997a).

In this thesis, mobility reduction factors (**MRF**s) were calculated to determine and compare foam strength in different experiments. The MRF was defined as the ratio of the pressure drop along the core during simultaneous injection of gas and surfactant solution, $\Delta \mathbf{P_{foam}}$, to the pressure drop value during simultaneous injection of gas and brine, under identical conditions using similar flow rates and gas/liquid ratios, $\Delta \mathbf{P_{without\ foam}}$ (Equation 7.1). The average value of steady-state pressure drop during gas/brine injection is taken as the reference "baseline pressure" (see example from Figure C.1. in the Appendix).

$$\textbf{M}\text{obility }\textbf{R}\text{eduction }\textbf{F}\text{actor }(\textbf{MRF}) = \frac{\text{dP (gas+surfactant solution)}}{\text{dP (gas+brine)}} = \frac{\Delta P_{foam}}{\Delta P_{without\ foam}} \quad (7.1)$$

The MRF is a dimensionless quantity. In general, a larger MRF value indicates a stronger foam.

Unfortunately, a precise definition of "strong" and "weak" foams does not exist in the literature, making it difficult to integrate quantitative knowledge of foam into quantitative predictions of foam performance (e.g., what MRF is "good enough", what MRF is "too strong" or "too weak"?).

In this thesis, we defined foams with MRF < 15 as weak, between 15 and 50 as moderate, and > 50 as strong.

Calculation of MRF (Equation 7.1) can be argued based on fluid saturations in the core during gas-brine injection and in the presence of foam is not the same (Mannhardt and Novosad, 1994).

Other variants of MRF have also been used. Examples include the ratio of foam (ΔP_{foam}) to single-phase water (ΔP_{water}) pressure drops (also called resistance factor, RF) (Chou, 1991; Bhide et al., 2005; Simjoo et al., 2013a) or to single-phase gas (ΔP_{gas}) pressure drops (Chabert et al., 2013).

Measurements of the baseline pressure drop in high permeability cores using single-phase water or gas may be a subject to errors due to the difficulties of accurately measuring very low differential pressures under elevated pressure and temperature conditions. MRF values calculated using single-phases will be larger in magnitude than those calculated using Equation 7.1 under identical conditions, which might complicate comparisons of different foam experiments in the literature.

Based upon information from repeated experiments, 10 to 20% variations in MRF seem to be within realistic limits of these types of measurements (Mannhardt and Novosad, 1994; Novosad and Ionescu, 1987).

Measurement of foam water blocking ability:

The stability of foams against seawater injection following generation were also evaluated in this project.

After ending the foam generation sequence, the injection of gas and surfactant solution into the core was stopped and switched to seawater (without surfactant). The seawater injection rate was set to 8 ml/h unless otherwise specified, that is, equal to the injection rate of the surfactant solution during foam generation. Usually, seawater was injected for several pore volumes before the first measurement of the effective seawater permeability, k_w. ΔP was measured at four different seawater injection rates, and k_w was calculated by Darcy's law using the viscosity of seawater at the given experimental temperature. The apparent water relative permeability, $k_{rw,app}$, was then calculated as k_w/K_w (i.e., normalized to the absolute permeability of the core, K_w, measured before the foam sequence started, where $S_w = 1$). In this method of measurement, the apparent water relative permeability represents an average value of the whole core. After each measurement, seawater injection was continued at 8 ml/h for several more pore volumes before a new measurement was performed. The foam water blocking sequence was usually stopped after the injection of a total of 10 ± 2 pore volumes of seawater. In time, this sequence corresponded to approximately 4 days of seawater injection under elevated experimental conditions.

Other methods used to characterize foam blocking abilities under elevated pressure and temperature conditions include monitoring of the gas/water injection rate as a function of time after generation at constant applied pressure gradients (Hanssen and Dalland, 1994; Aarra et al., 1997, 2011).

Insights into liquid injection after foam generation have also obtained by computed-tomography (CT) imaging under reduced experimental conditions (Du et al., 2007; Nguyen et al., 2005, 2009).

7.5 Experiments at HPHT (special considerations)

Working with fluids under HPHT conditions requires special considerations with respect to experimental equipment, setup and procedures. This section describes some of the important experimental precautions, with a particular emphasis on CO_2, considered in this project. Some of the recommendations for "best experimental practices" have been reported previously (Dong, 2001; Friedmann and Jensen, 1986; Hanssen and Dalland, 1994; Grigg et al., 2008; Kibodeaux, 1997; Kim et al., 2004; Mannhardt et al., 1996):

Corrosion:

Dry CO_2 is not corrosive to metals and alloys. In the presence of water, however, severe corrosion of the experimental equipment may occur as a result of the formation of carbonic acid (see Chapter 5, section 5.4.5). To prevent corrosion problems in this study, all lines in contact with experimental fluids were composed of corrosion-resistant Hastelloy C-276 alloys. Prevention against corrosion can reduce weakening and downtime on the experimental equipment. It can also be important for maintaining safe operations, particularly during experiments at high pressures.

Gas diffusion from the core:

The process by which fluids escape through small holes of a solid is called diffusion or effusion, depending on the hole-size of the barrier (Ebbing and Gammon, 2011). A helium balloon deflates a little bit every day as helium diffuses through the balloon. Similarly, CO_2 or N_2 can diffuse from the core and into the confining fluid in the absence of preventive measures. In the worst case, this diffusion could affect the accuracy of the flow rate and foam quality or be significant enough to create leakage problems. To minimize the effect of gas diffusion from the core in this study, the core was first surrounded by heat-shrinkable Teflon plastic tubing, then wrapped with aluminum foil, followed by an external heat-shrinkable Viton rubber sleeve (Figure 7.5). The endcaps of the core holder and the core must be wrapped together to prevent leakage at the transition where the endcaps and the ends of the core meet. The core-preparation procedures employed in this study created a good barrier to gas diffusion, as evidence by the observation of little or no dissolved gas from the confining fluid when depressurized after the experiment.

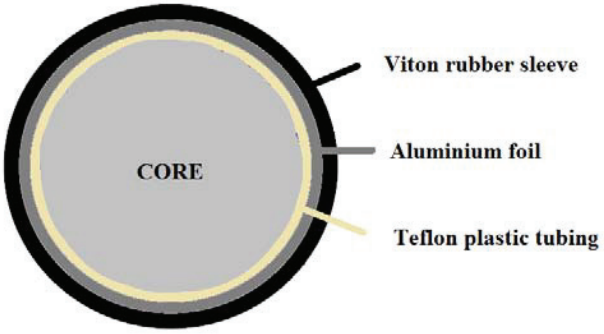

Figure 7.5: Core preparation (in this thesis).

CO_2 is also much more "soluble" in rubber than most other gases. In our studies, this effect of CO_2 was evidenced by the significant swelling of the rubber gaskets on the piston side of the cylinders containing CO_2 (Figure 7.6). Two means of avoiding leakage problems and unwanted maintenance on the equipment due to gas solubility and diffusion into the rubber gaskets are to; I) empty the cylinders filled with high-pressure CO_2 in a controlled manner (e.g., via a backpressure regulator); and II) maintain pressure on the cylinders between each CO_2 experiment (i.e., refill the CO_2 reservoirs at elevated pressure).

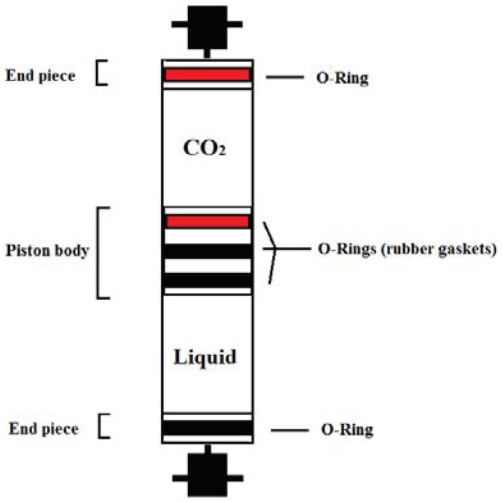

Figure 7.6: Piston cylinder with rubber gaskets exposed to swelling by CO_2 in red (from this thesis).

Gas expansion/compressibility effects:

Figure 7.7 illustrates the relationship between the pressure and volume of ideal gases when concentration and temperature are held constant (i.e., isothermal compression/expansion of gases based on Boyle's law). According to Boyle's law, the pressure and volume of ideal gases are inversely proportional. Therefore, when the gas volume is halved, the pressure is doubled, and if the volume is doubled, the pressure is halved. Consequently, changes in the gas volume for a given change in pressure will be larger when the system pressure is lower.

In most laboratory corefloods performed against a constant outlet pressure (Figure 7.3), the pressure drop arising along the core during foam generation causes the gas to expand toward the outlet end of the core. This expansion effect will be larger for the same pressure gradient when the system pressure is lower. Thus, the effect of gas expansion would be expected to be more dominant in foam experiments that are performed at low system pressure compared to high-pressure conditions.

Gas expansion could have strong effects on foam in laboratory experiments because it directly affects the flow rates and foam quality along the core.

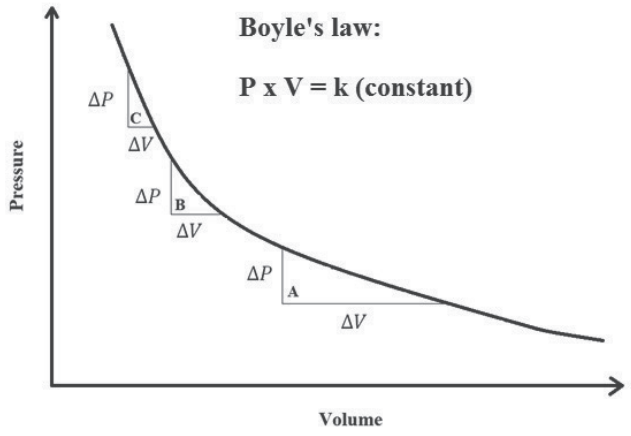

Figure 7.7: Relationship between the pressure and volume of an ideal gas according to Boyles's law: A) at low system pressure, the change in gas volume is large for a small change in pressure (i.e., gas compressibility is large); B) at higher system pressure, the change in gas volume is much smaller for the same change in pressure; C) at high pressure, the change in gas volume is smallest for a given change in pressure (i.e., gas compressibility is small) (the illustration was made in this thesis).

Our recommendation is to perform foam experiments at higher pressures to minimize gas expansion effects. We also recommend that a core material of 15 cm or longer in length to be used. A larger fraction of the core would be dominated by these effects (including capillary end effects) in shorter core samples compared with a longer core sample. For the strongest foams generated in this thesis (**Paper 3**), we could likely have limited the pressure drop during foam generation to less than 50% to minimize the potential effects from gas expansion.

Volume consideration:

The same mass of carbon dioxide can significantly vary in volume due to large changes in CO_2 density with temperature and pressure (see Figure 5.3-5.4 in Chapter 5). For example, a closed gas cylinder initially filled with 500 ml of CO_2 at 120 bar and room temperature will expand to as much as 2000 ml (i.e., factor of ~ 4) at 120 bar and 100°C due to the changes in CO_2 density. The volume of CO_2 needed under experimental conditions should therefore be carefully estimated before each experiment to avoid uncontrolled pressure build-up or other operational issues during fluid preparation under HPHT conditions.

Joule-Thomson effect:

When high-pressure CO_2 (or other non-ideal gases) is released from the BPR to atmospheric pressure, the temperature of the gas can dramatically decrease. The amount by which a gas cools on expansion (measured in °C/bar) is called the Joule-Thomson effect. Carbon dioxide has a particularly high Joule-Thomson coefficient compared with many other gases (The Energy Institute, 2010). In experiments with CO_2, this mean that the outlet end of the BPR may freeze (due to the formation of carbon dioxide snow or hydrate in the presence of water) in the absence of an additional heat source applied to the BPR. Accordingly, in this study, the inlet and outlet flow line to the BPR, including the BPR itself, were always wrapped with heating tape in addition to fiberglass insulation during all experiments. Production cylinders placed inside the heat cabinet (Figure 7.3) can also be advantageous to reduce unwanted icing associated with the Joule-Thomson effect.

7.6 Phase-equilibration

In the CO_2-foam experiments performed with pre-equilibrated fluids in this thesis (**Paper 1, 2, 4**), the surfactant solution and synthetic seawater (SSW) were saturated with CO_2, while the CO_2 reservoir was saturated with SSW. A model developed by Duan et al. (2003, 2006) was used to estimate the amount of CO_2 needed to saturate the liquids under different experimental conditions relevant to this study (i.e., 30, 90, 120 bar at 50°C and 90°C). The amount of water solubilized in CO_2 was estimated from Choi and Nesic (2009).

The following procedures were used for phase-equilibration in this thesis:

1. The respective reservoirs (i.e., gas, surfactant solution and SSW cylinders) were filled with sufficient amounts of CO_2 and SSW (i.e., more than needed) to saturate all fluids under the intended experimental conditions.

2. The reservoirs were pressurized to experimental pressure conditions using a gas booster and then shaken. A mixer ball was inserted in the cylinders to improve mixing. The shaking process was repeated until the reservoir pressure did not change with further shaking.

3. The reservoirs were then placed horizontally for further equilibration for at least 48 hours at constant experimental pressure and room temperature.

4. In the final step, the experimental temperature was applied to the reservoirs under constant experimental pressure (i.e., the solubility of CO_2 in water will decrease according to Table 5.4 in Chapter 5). After an additional 48 hours of equilibration under experimental conditions (in terms of both temperature and pressure), the baseline experiment and subsequent experimental steps according to those described in the Appendix (section C) was initiated.

5. For all foam experiments with pre-equilibrated fluids, the cylinders were oriented vertically, as illustrated in Figure 7.3 on page 100, to ensure injection of pre-equilibrated fluids only.

Chapter 8

Results and Discussions

8.1 Introduction p. 112

8.2 CO_2-foam properties compared with N_2-foams p. 113

- **8.2.1 Experimental strategy** p. 113
- **8.2.2 Foam properties as a function of pressure** p. 114
- **8.2.3 Effect of mass transfer on CO_2-foam properties** p. 121
- **8.2.4 CO_2-foam strength vs. CO_2-density** p. 126
- **8.2.5 Experimental observations** p. 128
- **8.2.6 Summary and discussion** p. 130

8.3 Effect of rock properties on foam p. 144

- **8.3.1 Experimental strategy** p. 144
- **8.3.2 Rock core analyses** p. 145
- **8.3.3 Foam generation performance in low permeability laminated sandstone cores** p. 149
- **8.3.4 Summary and discussion** p. 151

8.4 Surfactant screening and bulk foam-oil interactions p. 156

- **8.4.1 Experimental strategy** p. 156
- **8.4.2 Surfactant screening in the absence of oil** p. 157
- **8.4.3 Bulk foam-oil interactions** p. 163

8.5 Summary and Conclusions p. 174

8.1 Introduction

This chapter contains three sections that summarize and discuss the main results and observations obtained in this thesis.

Section 8.2 presents the main results from **Papers 1-2**. Our main focus was to investigate CO_2-foam properties in porous media with systematic variations in the pressure and temperature conditions. The properties of CO_2-foam were compared against those of N_2-foams under similar experimental conditions. In general, an attempt was made to achieve a better understanding of the differences between the CO_2- and N_2-foams in porous media.

Section 8.3 summarizes the main findings from **Paper 3**. The foam performance in laminated sandstones with relatively low permeability was examined. Various types of analyses were applied to characterize the laminated rock material as a supplement to the interpretation of foam flooding results under elevated pressure and temperature conditions. In general, the intent was to improve the understanding of foam generation performance relative to rock properties.

Section (8.4) provides a summary of the findings from **Paper 4** with a focus on surfactant screening and foam-oil interactions in bulk tests. Comparisons were drawn between the foam properties in bulk (**Paper 4**) and the foam properties in porous media (**Papers 1-3**).

The last section (8.5) summarizes and concludes this thesis.

Appendix (page 181):

Details of the surfactants, synthetic seawater and different oils used in this thesis are listed in the Appendix Section A. The petro-physical properties of the core materials are presented in the Appendix Section B. Descriptions of the experimental steps included in each foam core flooding experiment are given in Section C. The experimental history for each core is tabulated in Section D.

To improve readability throughout the thesis, the notation bar is used, which in reality denotes barg.

For further details, the reader is referred to **Papers 1-4**.

8.2 CO_2-foam properties compared with N_2-foams

8.2.1 Experimental strategy

Because most foam field projects are usually aimed at field-specific conditions, relatively few foam-core flooding studies exist in the literature in which the gas type, pressure and temperature are varied systematically. Because the reservoir situation can vary significantly among the fields with respect to gas composition, pressure and temperature conditions, it is important to understand the properties of foam on a broad experimental scale.

In this thesis, the CO_2-foam properties in porous media were investigated and compared at 30 bar, 120 bar and 280 bar at 50°C (**Paper 1**) and at 90 bar and 120 bar at 90°C (**Paper 2**), thus covering the phase transition from the gaseous to the supercritical state of CO_2. The properties of CO_2-foam were compared with those of N_2-foams under similar low (30 bar) and high (280 bar) pressures at 50°C. All experiments were performed in the absence of oil to reduce the number of variables and to improve characterization and comparison of foam properties in porous media.

The surfactant type ($AOS_{C14-C16}$), surfactant concentration (0.5 wt.%), synthetic seawater (~36,000 ppm TDS), outcrop Berea sandstone core material (1Berea1000 and 2Berea1000), co-injection method, inlet foam quality (80%), injection rates during foam generation (32 ml/h gas and 8 ml/h surfactant solution) and injection rate during seawater injection after generation (8 ml/h SSW) were held constant unless otherwise noted. The surfactant solution consistent of 0.5 wt.% AOS surfactant concentration dissolved in seawater.

The choice of $AOS_{C14-C16}$ surfactant was argued based on promising results from earlier work, screening studies, and field tests using AOS surfactants (Chapter 2, section 2.4). The level of concentration was chosen to compare foam properties that are well above the surfactant's critical micelle concentration (cmc). The cmc of the AOS surfactant dissolved in synthetic seawater was determined as 0.0022 wt.% via surface tension measurements at ambient conditions (Vikingstad et al., 2006). Slightly higher cmc values can be expected under elevated pressure and temperature conditions (Stasiuk and Schramm, 1996). The salinity and ionic strength of the synthetic seawater used in these experiments are comparable to the North Sea water (Mannhardt and Svorstøl, 1999).

A summary of the main findings from **Papers 1-2** with respect to foam strength, foam propagation/gas breakthrough times, foam textures and seawater injection following foam generation under various pressure and temperature conditions are provided next.

8.2.2 Foam properties as a function of pressure

In **Paper 1**, the CO_2-foam properties were investigated and compared with those of N_2-foams as a function of pressure. The CO_2-foam experiments were conducted at 30 bar, 120 bar and 280 bar and 50°C, and the N_2-foam experiments were performed at 30 bar and 280 bar and 50°C.

Foam strength:

Figure 8.1 illustrates the general trends in pressure build-up profiles obtained during foam generation under various system pressures at 50°C. The foam strength was determined through calculation of mobility reduction factors (MRF), as defined in Equation 7.1 (Chapter 7, section 7.4.1). Foams with MRF < 15 were defined as weak, between 15 and 50 as moderate, and > 50 as strong.

The foam strengths obtained under the various system pressures at 50°C are summarized as follows:

I) In general, the presence of AOS surfactant reduced the mobility of CO_2, N_2 and seawater in all experiments compared with that in absence of surfactant (MRFs in the range of 3-170 were obtained).

II) Strong N_2-foams were generated under conditions of low (30 bar) and high (280 bar) pressure and 50°C (MRF = 135 ±35).

III) The N_2-foams were stronger than the CO_2-foams.

IV) The strength of the generated CO_2-foams decreased with increasing system pressure:

- Strong CO_2-foams were generated at 30 bar and 50°C (MRF = 65 ±15).
- Weak CO_2-foams were generated at 120 bar and 50°C (MRF = 6 ±1).
- The weakest CO_2-foam was indicated at 280 bar and 50°C (MRF ≈ 3).

V) The MRFs given in parentheses represent average plateau values with variations based on repeated experiments on the same core (i.e., 1Berea1000, tabulated in the Appendix Section D).

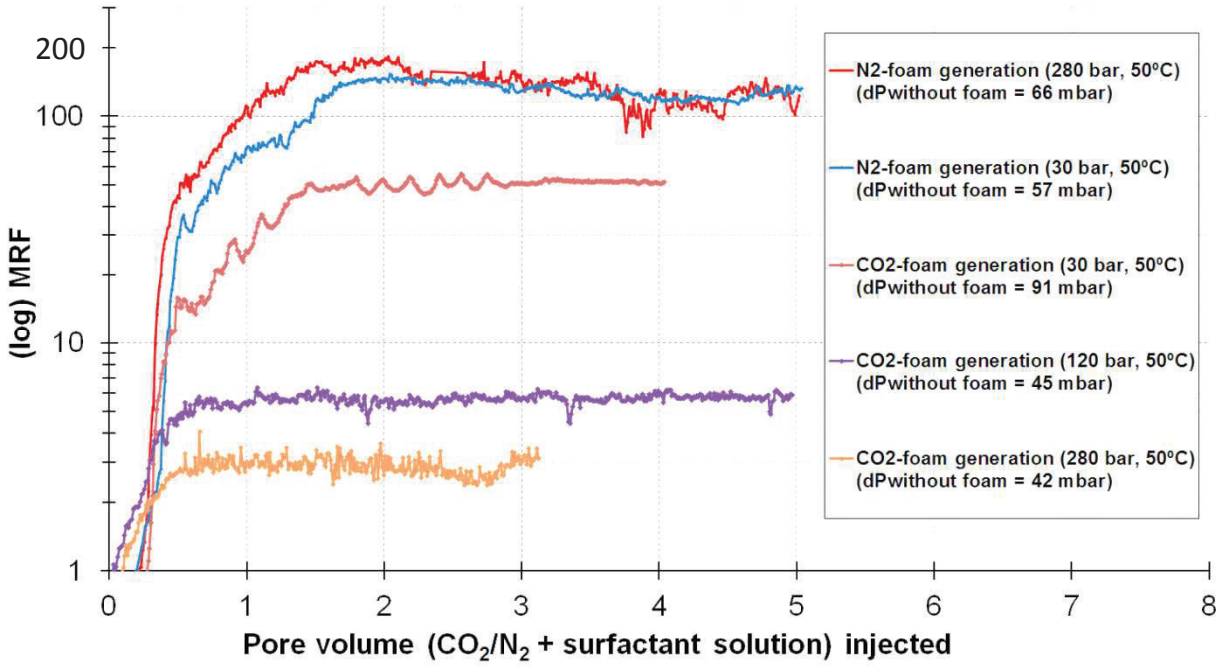

Figure 8.1: Mobility reduction factors of N_2- and CO_2-foams as a function of pressure at 50°C.

Foam/gas breakthrough times:

A visual cell was mounted on the line at the core outlet (Figure 7.3-7.4, Chapter 7). The cell was used to detect and compare the gas breakthrough (GBT) under experimental conditions in different foam experiments.

Figure 8.2 compares the average GBT obtained for repeated experiments under various system pressures at 50°C. The results of GBT can be summarized as follows:

I) In general, consistently early gas breakthroughs were observed during baseline pressure experiments in the absence of surfactant (GBT was always observed before 0.2 PV injected).
II) The presence of AOS surfactant delayed the gas breakthrough in all experiments compared with point I (GBT observed between 0.3 and 1.1 PV injected).
III) The strong N_2-foams indicated a propagation rate close to the injection rate,
GBT = 0.90 ±0.15 PV injected.
IV) The strong CO_2-foams (at 30 bar, 50°C) propagated in a manner quite similar to that of the N_2-foams, GBT = 0.9 ±0.2 PV injected.
V) The weak CO_2-foams (at 120 and 280 bar, 50°C) showed faster propagation,
GBT = 0.45 ±0.15 PV injected.

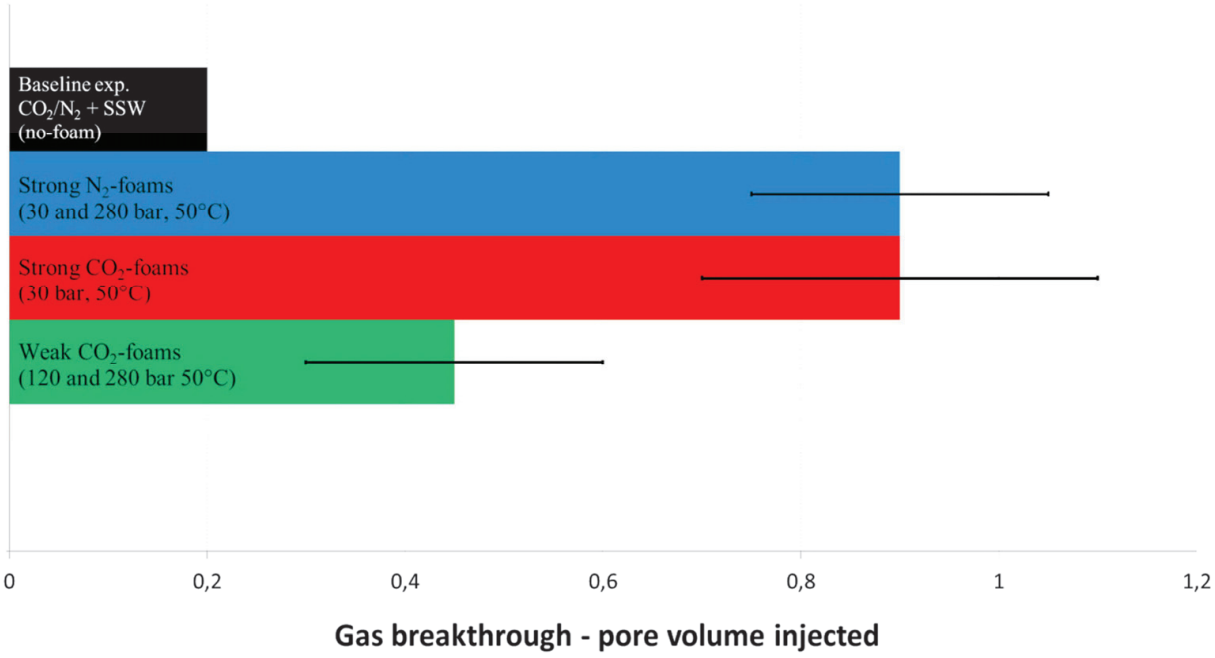

Figure 8.2: Average gas breakthrough times during foam core flooding under various system pressures at 50°C. The error bars are added to indicate the observed variation. Typical ranges of gas breakthroughs during baseline experiments (i.e., co-injection of 80% CO_2 or N_2 and 20% seawater without surfactant) are also included for comparison.

Foam textures:

The sight-glass was also used for visual observations and comparisons of foam textures leaving the core under experimental conditions in different foam experiments. Close-up images were taken with a Canon EOS 5D Mark II camera with a good lens.

Figure 8.3 on the next page shows images of typical foam textures that were observed out of the core during foam generation under various system pressures at 50°C. The observations can be summarized as follows:

I) In general, foam texture was confirmed out of the core during generation in all experiments (i.e., discontinuous CO_2/N_2 separated by liquid lamellae).

II) Three stages related were observed related to a development in the N_2-foam texture with pore volume (PV) injected:

- First stage, between ~1 and 1.5 PV injected, coarse foam texture with relatively large bubbles, lowest MRFs.
- Second stage, between ~1.5 and 2.5 PV injected, dense foam composed of small bubbles, highest MRFs.
- Third stage, from ~2.5 PV, dense foam with some larger bubbles, slightly reduced MRFs from the prior point.

III) Visual comparison of the N_2-foam texture with increments in the system pressure revealed smaller bubbles under higher pressure during the first stage (image 1 vs. 4) but little differences in the later stages.

IV) The strong N_2-foams indicated finer and denser foam textures compared with the weaker CO_2-foams. This observation supports the idea that smaller bubbles result in more liquid films, which is expected to reduce gas mobility more than larger bubbles (Chapter 4, section 4.4).

V) The CO_2-foam textures were generally coarse and composed of relatively large and non-uniform bubble sizes.

VI) Comparison of the CO_2-foam texture with increasing pressure (30 bar, 120 bar, 280 bar) indicated larger bubble sizes, less continuity in texture and more vague/diffuse CO_2/liquid surfaces (image 7 to 9).

N_2-foam textures:

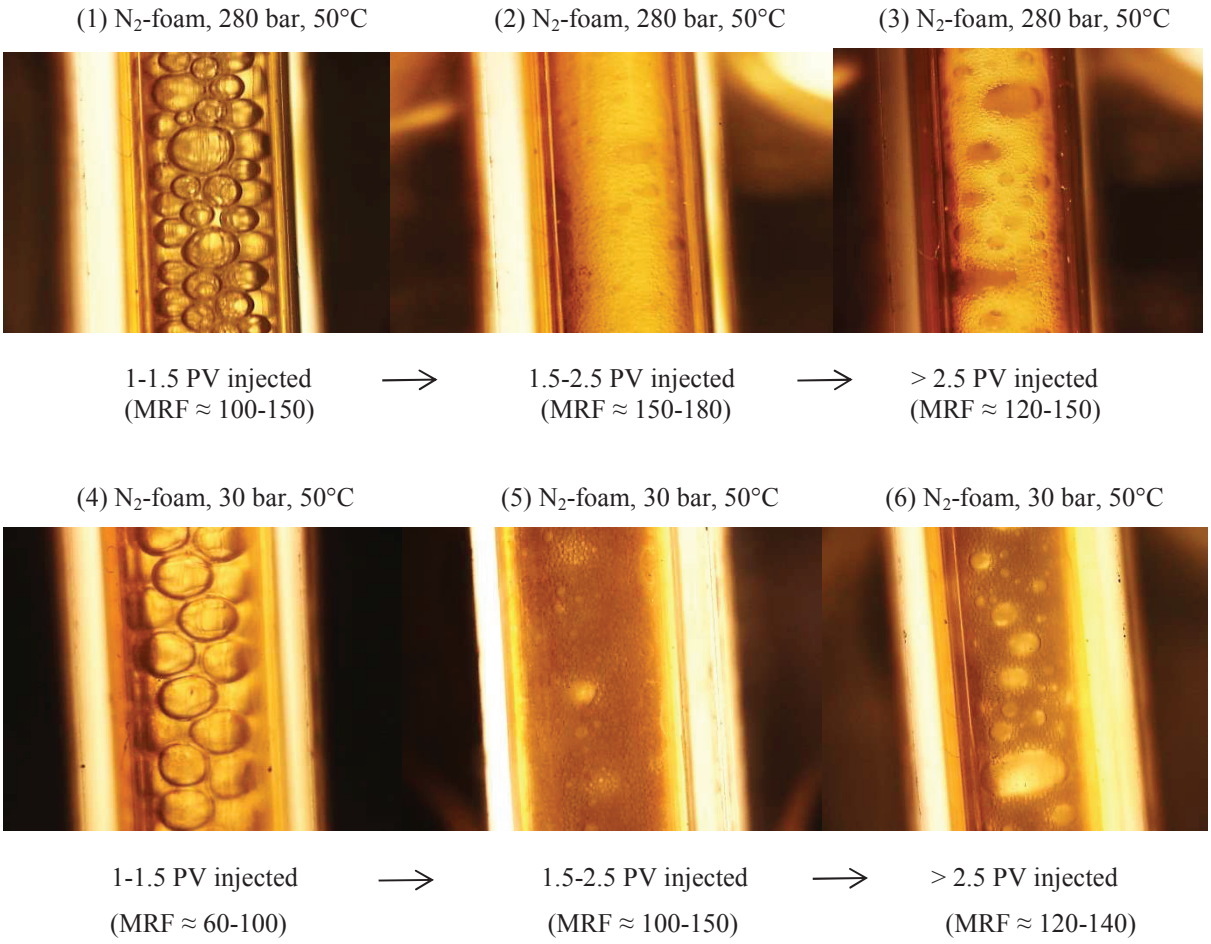

CO_2-foam textures:

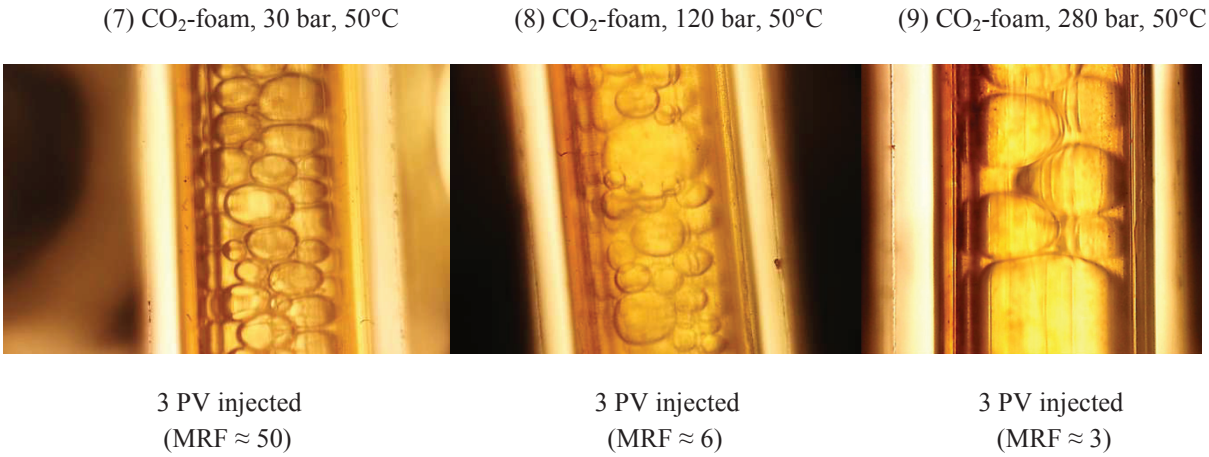

Figure 8.3: Images of foam texture from different foam experiments: (1-3) N_2-foam at 280 bar and 50°C with corresponding MRF and pore volumes injected; (4-6) N_2-foam at 30 bar and 50°C with corresponding MRF and pore volumes injected; (7-9) CO_2-foams as a function of pressure (30 bar, 120 bar and 280 bar at 50°C) with corresponding MRF after 3 PV injected. The diameter of the visual cell is 1.5 mm.

Seawater injection following foam generation:

The stability of foams against seawater injection following generation were also evaluated and compared as a function of pressure at 50°C in this thesis. After the foam generation sequence was ended, the injections of gas and surfactant solution were stopped and switched to seawater (without surfactant). A detailed description of how these measurements were conducted is provided in Chapter 7, section 7.4.1.

Figure 8.4 presents the apparent water relative permeabilities ($k_{rw,app.)}$ that were obtained with pore volume seawater injected after different foam experiments. One experiment without surfactant was also performed to better quantify the development in seawater permeability after foam generation. The $k_{rw,app.}$ value was calculated as k_w/K_w (i.e., the effective water permeability normalized to the absolute permeability). The results showed that:

I) In general, the presence of foam in the core initially reduced the seawater permeability in all experiments compared with that in the absence of surfactant.

II) Strong and long-lasting reductions in the seawater permeability were observed after the N_2-foams ($k_{rw,app.} < 0.1$ for more than 11 PV of seawater injected). Increasing the seawater injection rate in one experiment from 8 ml/h to 40 ml/h did not particularly influence the $k_{rw,app.}$ (the green dot in the figure shows $k_{rw,app.} \sim 0.06$ after 12.6 PV).

III) The stability of CO_2-foam against seawater injection was significantly poorer compared with that of the N_2-foams.

IV) Although strong CO_2-foam was generated at 30 bar and 50°C, the seawater permeability became high only after the injection of few pore volumes of seawater. Figure 8.8 illustrates the abrupt decline in pressure during the initial stage of seawater injection.

V) High seawater permeabilities were also obtained for the weak CO_2-foams under higher system pressures.

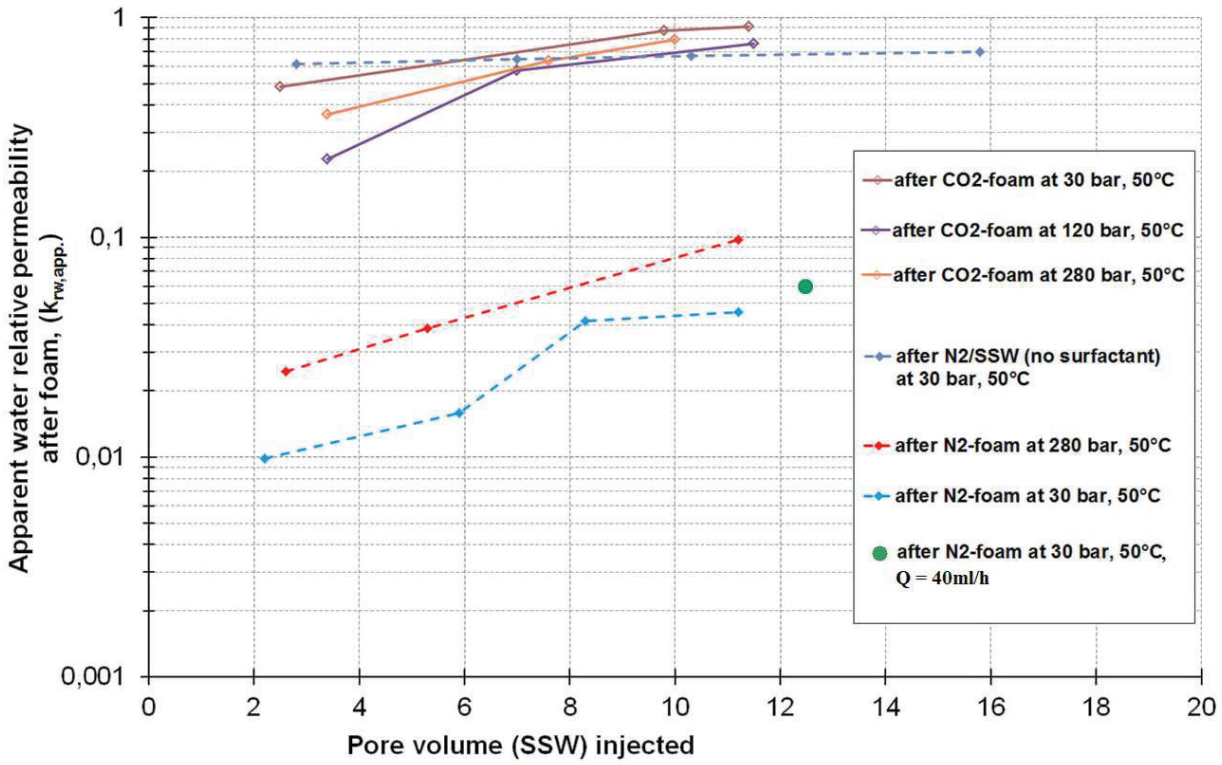

Figure 8.4: Apparent water relative permeabilities with pore volume seawater injected after foam generation under various system pressures and 50°C; after CO_2-foams (burgundy, yellow and purple lines, respectively); after N_2-foams (red and pale blue lines); after the baseline pressure experiment indicated in the upper blue line. The lines in the figure are drawn to guide the eye.

8.2.3 Effect of mass transfer on CO_2-foam properties

Several articles in the literature have discussed the difference in water solubility between CO_2 and N_2 as one of the main reasons for why the CO_2-foams are usually weaker than the N_2-foams during foam generation in laboratory core flood experiments (Du et al., 2008; Farajzadeh et al., 2009; Wang et al., 2014). In addition, several laboratory studies (e.g., Aarra et al., 2011; Bhide et al., 2005; Seright, 1996) and certain field results (e.g., Enick and Olsen, 2012; Holm and Garrison, 1988) have indicated that CO_2-foams could be less effective against subsequent liquid injection than foams containing gas components with lower solubilities in water (e.g., air/N_2, CH_4).

In **Paper 1**, the potential effects of mass transfer between the CO_2 and surfactant solution on CO_2-foam performance were investigated closer. To limit spontaneous mass transfer between the fluid phases, additional foam experiments with pre-equilibrated fluids were conducted. To our knowledge, CO_2-foam experiments with pre-equilibrated fluids at high pressure have not been previously performed in the literature.

The CO_2-foam experiments with pre-equilibrated fluids were evaluated both with respect to foam generation performance and foam stability against subsequent seawater injection after generation. The procedures used for the phase-equilibration in this thesis are described in Chapter 7, section 7.6.

<u>CO_2-foam strength with pre-equilibrated fluids:</u>

Figure 8.5 summarizes the results from CO_2-foam generation with pre-equilibrated fluids at 30 bar and 120 bar at 50°C. The results are compared with those of CO_2-foams and N_2-foam without phase-equilibration under similar pressure and temperature conditions:

I) In general, the CO_2-foams remained weaker than the N_2-foams regardless of phase-equilibration.

II) At 30 bar and 50°C, the pressure build-up profiles with pre-equilibrated fluids (compared with without pre-equilibrated fluids) indicated a more effective CO_2-foam generation and mobility reduction during the first pore volume injected and a moderately increased foam strength at the plateau (MRF 75 ± 5).

III) At 120 bar and 50°C, weak CO_2-foams of similar strengths were generated despite the phase-equilibration. One foam experiment conducted with pre-equilibrated fluids in an

analogous high permeability Berea core (i.e., 2Berea1000) indicated slightly higher MRFs though, still classified as weak foam (i.e., gray profile in the figure below).

IV) Our experimental results indicated that mass transfer between the CO_2 and surfactant solution has little influence on the overall foam strength during generation.

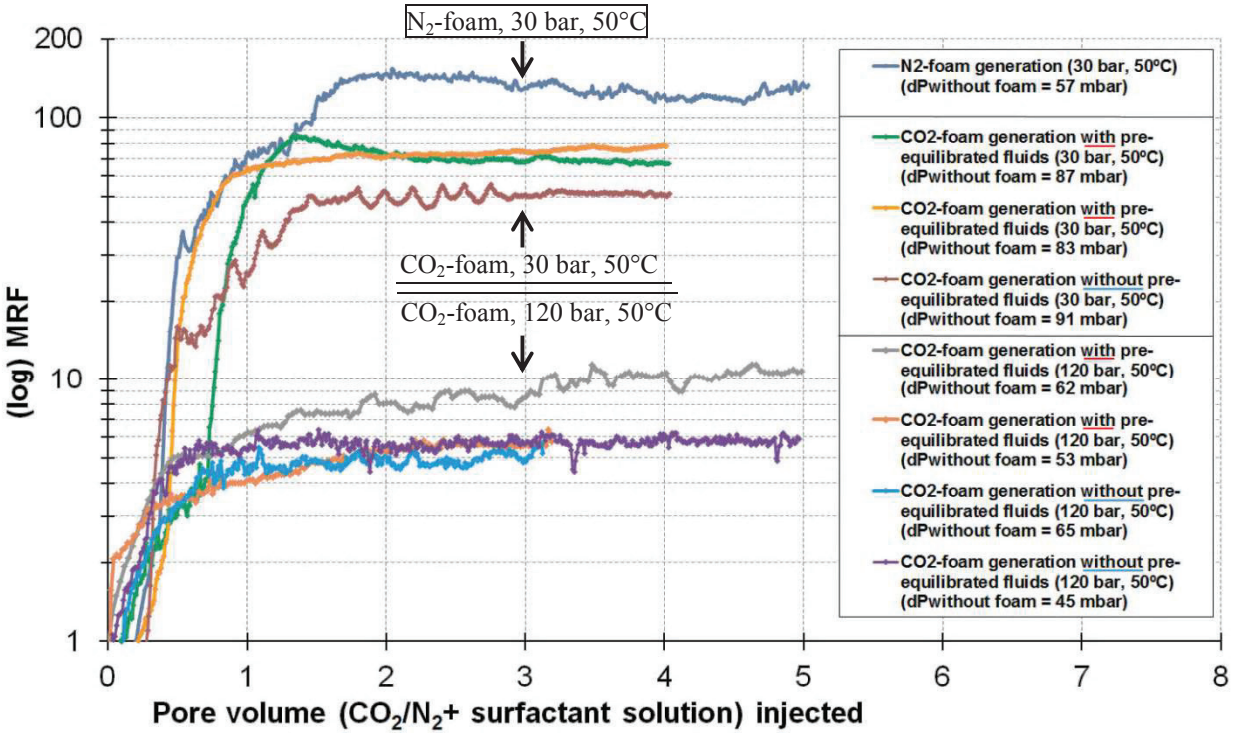

Figure 8.5: Mobility reduction factors of CO_2 foams (with and without pre-equilibrated fluids) at 30 bar and 120 bar and 50°C. The CO_2-foam experiments with pre-equilibrated fluids are shown by the green and yellow profiles (at 30 bar, 50°C) and the gray and orange profiles (at 120 bar, 50°C), respectively. The N_2-foam generation at 30 bar and 50°C is included for comparison.

Foam/gas breakthrough (GBT) with pre-equilibrated fluids:

No particular differences in CO_2 breakthrough were indicated in experiments with pre-equilibrated fluids compared with those observed without phase-equilibration in Figure 8.2. In three foam experiments with pre-equilibrated fluids at 30 bar and 50°C, the GBT were observed between ~0.8 and 1.1 PV injected. For two experiments at 120 bar and 50°C, the GBT were observed after 0.55 and 0.53 PV injected, respectively.

CO_2-foam textures with pre-equilibrated fluids:

Figure 8.6 shows images of CO_2-foam textures with pre-equilibrated fluids at 30 bar and 120 bar at 50°C. The images are compared with those of CO_2-foam textures under similar pressure and temperature conditions but without phase-equilibration. The observations showed that:

I) Slightly finer foam textures (i.e., smaller and more numerous bubbles per unit volume) were indicated with pre-equilibrated fluids compared with those without.

II) At 30 bar and 50°C, a finer textured CO_2-foam correlated with a slightly higher MRF.

III) At 120 bar and 50°C, variation in the CO_2-foam texture did not necessary reflect changes in MRF.

IV) Again, the CO_2/liquid surfaces at higher pressure (i.e., 120 bar and 50°C) appeared more vague/diffuse compared with those at lower pressure (i.e., 30 bar and 50°C). A plausible explanation for this observation might be due to a lower surface tension between the CO_2 and surfactant solution under high pressures (Chapter 5, section 5.4.7-5.4.8).

<u>CO_2-foam textures:</u>

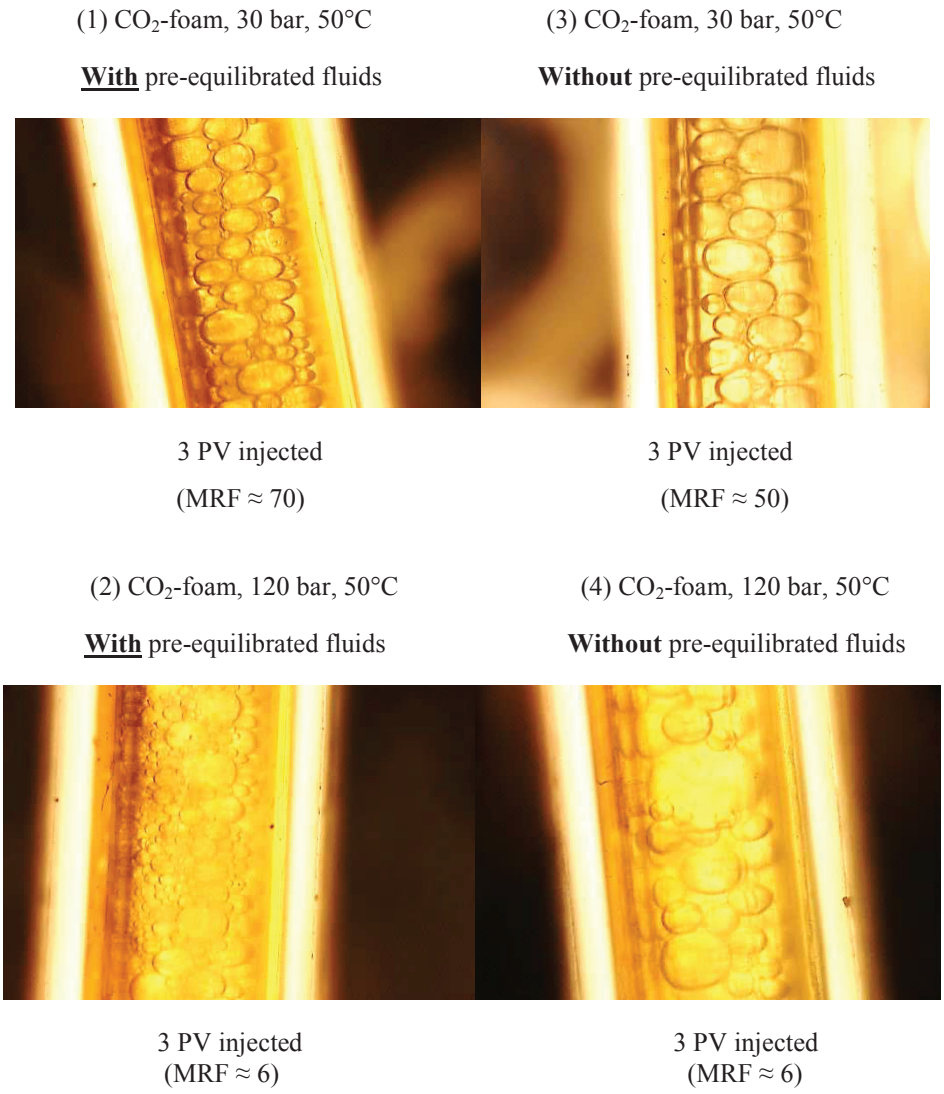

Figure 8.6: Images of CO_2-foam textures at 30 bar and 120 bar and 50°C with corresponding MRFs after ~ 3 PV injected: (1-2) CO_2-foam textures with pre-equilibrated fluids; (3-4) CO_2-foam textures without pre-equilibrated fluids. The diameter of the visual cell is 1.5 mm.

Seawater injection following CO_2-foam generation with pre-equilibrated fluids:

Seawater injection after foam generation with pre-equilibrated fluids was also investigated more closely. In these experiments, the injected seawater was pre-saturated with CO_2 under system pressure and temperature conditions.

Figure 8.7 shows the apparent water relative permeabilities ($k_{rw,app.}$) obtained during seawater injection with pre-equilibrated fluids at 30 bar and 50°C. The pressure drop response (dP) during the initial stage of seawater injection following steady-state foam is provided in Figure 8.8. The $k_{rw,app.}$ and dP values after CO_2-foam and N_2-foam without phase-equilibration are also included in the figures for comparison. The results showed that:

I) Significantly improved stability of CO_2-foam against seawater injection was demonstrated with pre-equilibrated fluids. The reduction in seawater permeability was strong and more persistent than that of the CO_2-foams without phase-equilibration.
II) The initial pressure drop histories supported improved resistance and increased foam stability with pre-equilibrated fluids, more similar to those of the N_2-foam (Figure 8.8).
III) The experimental results suggest that mass transfer between CO_2 and surfactant solution could have a significant impact on foam stability during subsequent liquid injection.

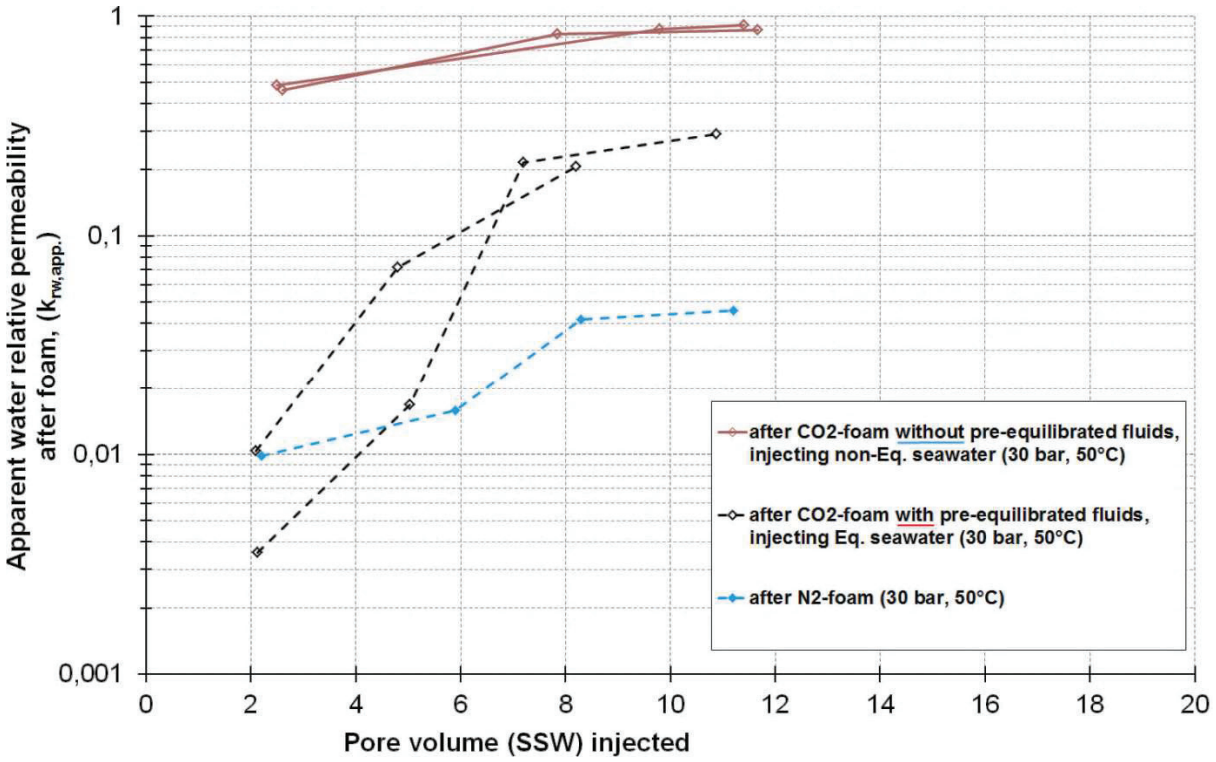

Figure 8.7: Apparent water relative permeabilities with pore volume seawater injected after foam generation at 30 bar and 50°C: after CO_2-foam with pre-equilibrated fluids (black dashed lines); after CO_2-foam without phase-equilibration (red solid lines); after N_2-foam without phase-equilibration (blue dashed line). The lines in the figure are drawn to guide the eye.

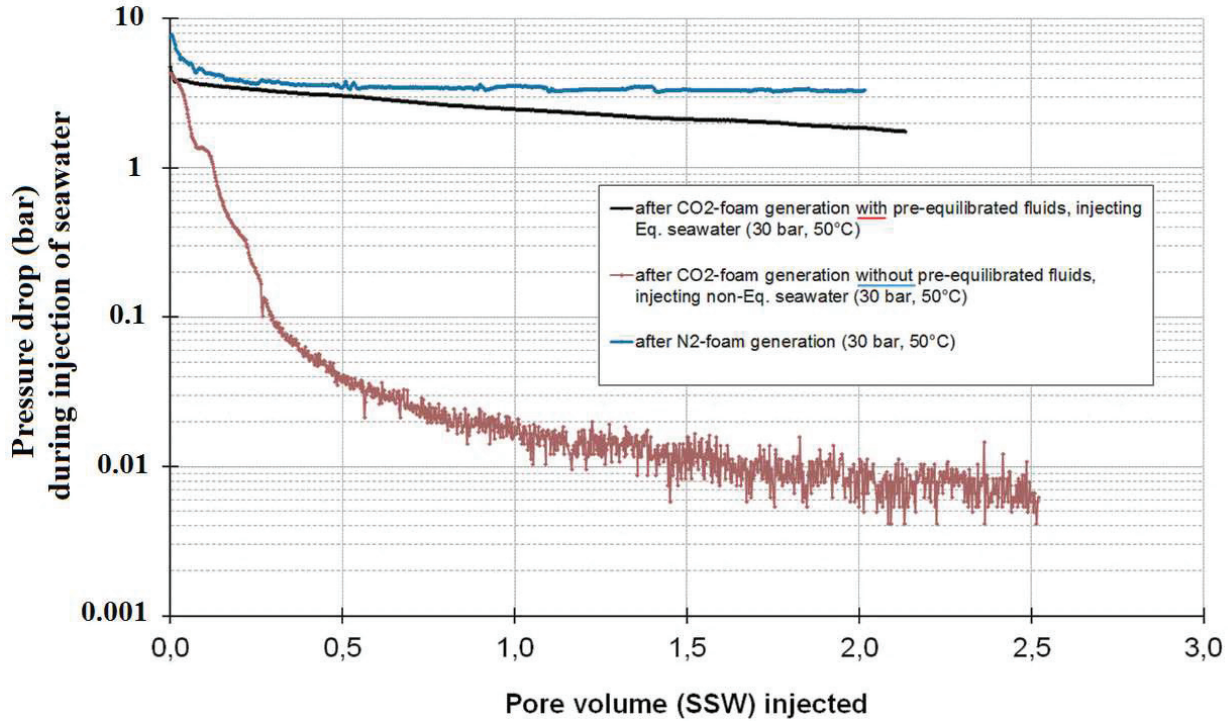

Figure 8.8: Pressure drop histories during the early stage of seawater injection (8 ml/h) following steady-state foam generations at 30 bar and 50°C (i.e., before measurements of $k_{rw,app.}$). Seawater injection after CO_2-foam with pre-equilibrated fluids, CO_2-foam without phase-equilibration and N_2-foam are indicated by black, red and blue profiles, respectively.

8.2.4 CO_2-foam strength vs. CO_2 density

In **Paper 1**, we speculated whether the decreased CO_2-foam strength with increasing system pressure (Figure 8.1) was attributable to the large variations in CO_2 density under these conditions. The dense state of supercritical CO_2 are also significantly different compared to other gas phases in foam normally used (Chapter 5).

In **Paper 2**, the CO_2-foam properties with varying CO_2 density were investigated more closely. Additional CO_2-foam experiments were conducted on an analogous high permeability Berea sandstone core (i.e., 2Berea1000) at 90 bar and 120 bar at 90°C. Under these conditions, CO_2 is supercritical but with lower and more "gas-like" densities (Figure 5.3 in Chapter 5).

Table 8.1 and Figure 8.9 summarize our portfolio of CO_2-foam experiments from **Papers 1-2** with respect to CO_2 density. The main findings showed that:

I) The CO_2-foam strength increased with:

- Decreasing absolute pressure.
- Increasing experimental temperature.

II) A good correlation between CO_2 density and MRF was shown (Figure 8.9). Conditions at which the density of CO_2 is low improved the CO_2-foam strength.

III) The additional foam experiments performed in **Paper 2** demonstrated that strong CO_2-foams could be generated even under supercritical conditions.

Table 8.1: Summary of MRFs obtained from repeated CO_2-foam generation experiments in outcrop Berea sandstone cores from Papers 1-2 under different experimental conditions with/without phase-equilibration using $AOS_{C14-C16}$ surfactant. The number of experiments of the total with pre-equilibrated fluids is given in the parentheses.

Experimental conditions (Pressure, Temperature)	CO_2 phase behavior	CO_2 density (g/cm^3)	No. of Exp.	Average MRF after 3 PV inj.
30 bar, 50°C	Gas	0.056	4 (2)	65 ± 15
90 bar, 90°C	Supercritical	0.175	2 (1)	54 ± 6
120 bar, 90°C	Supercritical	0.265	1 (1)	25
120 bar, 50°C	Supercritical	0.585	4 (2)	7 ± 2
280 bar, 50°C	Supercritical	0.857	1 (0)	3

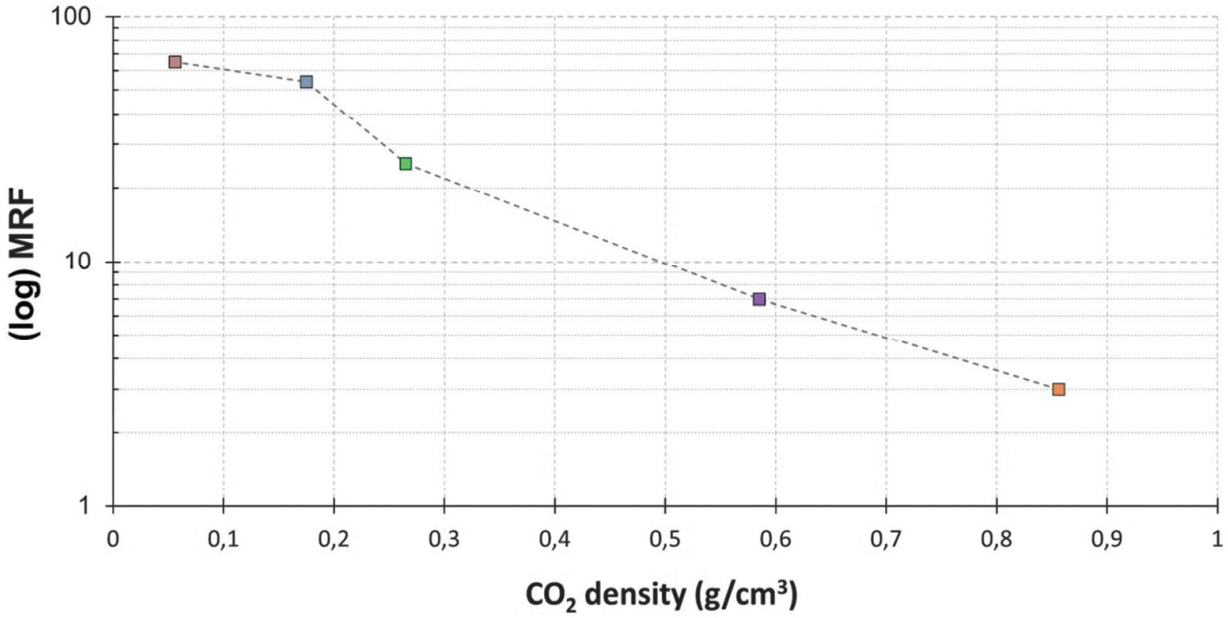

Figure 8.9: Average MRF vs. CO_2 density. The dashed line is drawn to guide the eye.

8.2.5 Experimental observations

Several experimental observations from the investigations of foam properties in porous media deserve additional comments and explanations.

Iron dissolution:

A yellow- to reddish-colored effluent was observed during all core flooding experiments with CO_2 in this thesis. Ion analysis of the effluent during foam generation indicated a maximum iron concentration of 60 ppm. Visual inspection of the experimental setup did not reveal any signs of damage or corrosion. It is known that the Berea sandstone contains a few percent iron-containing carbonate minerals and clays (Table B.2 in the Appendix). Dissolution of iron from the core in the presence of carbonic acid was therefore suggested as the cause of the iron in the effluent.

We evaluated the pH sensitivity to the core material more closely by immersing two Berea core plugs in separate beakers, one filled with seawater at pH ~ 3 (adjusted with 1 wt.% HNO_3 solution) and one filled with pure seawater. After a few days in closed beakers at room conditions, the acidic seawater had turned reddish in color with the immersed core sample, whereas a clear and colorless solution remained for the core sample in pure seawater. This observation supported our theory that Berea rock mineralogy might be sensitive to acidic environments, such as that expected during CO_2-foam flooding. Similar observations in Berea rock material were also noted by Dong (2001), Kim et al. (2004) and Seright (1996).

The influences of iron and pH on foam/surfactant were evaluated in additional detail in bulk tests in **Paper 4**. In general, the presence of 60 ppm iron ions (both Fe^{2+} and Fe^{3+}) and variable pH (between 2 and 7.5) produced notably little negative effects on foaminess and foam stability with the $AOS_{C14\text{-}C16}$ surfactant solution used in the CO_2-foam flooding experiments in **Papers 1-2**. The surfactant solution showed relatively similar bulk foam properties independent of the solution pH and iron ions added (figure 15-1, 15-2 and 15-3 in **Paper 4**). Small effects of low pH on foam have also been reported by several other researchers (Chapter 5, section 5.4.5).

Core homogeneity:

For systematic studies and comparisons of foam properties in natural porous media, relatively homogeneous rock material is preferred (Chapter 4, section 4.1).

The main foam floods in **Papers 1-2** were conducted and repeated on two high permeability Berea sandstone cores (i.e., 1Berea1000 and 2Berea1000). Several types of measurements were performed on these two cores, which supported the observation that these cores were relatively homogeneous and similar to each other for the following reasons:

I) Their petro-physical properties were relatively similar in terms of average porosity and permeability (Table B.1 in the Appendix at page 184).
II) The distribution of pore throat sizes in 1Berea1000 was relatively narrow according to data obtained from mercury injection (Figure B.1 in the Appendix).
III) Homogeneous dispersion characteristics were shown for both samples (Figure B.2 in the Appendix).
IV) Little to no visual heterogeneity was detected with the aid of X-ray imaging (Figure B.3 in the Appendix).
V) X-ray imaging of gravity stable gas and water injections in a slab of similar rock material indicated stable displacements compared with those from a laminated and heterogeneous sandstone slab (Figure 8.11 on page 148 or figure A.9. in **Paper 3**).
VI) Characteristic pressure build-up profiles of foam in homogeneous porous media saturated with surfactant using co-injection mode were shown, reflected by a sharp and efficient pressure build-up period followed by a plateau after the injection of a few pore volumes (Figure 8.1 and 8.5). The characteristic response in laboratory core flooding experiments is well documented and discussed in the literature (Chapter 7, section 7.4.1). The plateau in pressure drop is often explained by the theory of foam flow at the limiting capillary pressure (Chapter 4, section 4.5.2).
VII) Quite satisfactory reproducibility was demonstrated with respect to repeated foam experiments on the same core and compared to foam experiments on analogous high permeability outcrop Berea sandstone cores (e.g., Table 8.1 on page 126 and figure 4 in **Paper 1**). The verification of similar trends and magnitudes in foam properties strengthen the results on used core material. In addition, restored core permeabilities between 80% and 100% of the original permeability were achieved after subsequent foam experiments (Table D.1-D.2 in the Appendix). These results suggest that the potential influence of CO_2/liquid/rock reactions (e.g., iron dissolution) to have caused permanent damage on these cores must have been small.

8.2.6 Summary and discussion

This section summarizes the main findings from our investigations of CO_2-foam properties (compared with those of N_2-foams) in relatively homogeneous and high permeability outcrop Berea sandstone cores using $AOS_{C14-C16}$ surfactant. Comparisons between our results and other relevant literature are highlighted and discussed.

CO_2-foam generation performance vs. N_2-foam:

The main findings from this thesis comparing the CO_2-foam generation performance against that of N_2-foams under various experimental pressure and temperature conditions (Figure 8.1, 8.2, 8.3, 8.5, 8.6 and Table 8.1) showed that:

- N_2-foams of relatively similar strengths were generated under low and high pressures (MRF > 100).
- The CO_2-foams were weaker than the N_2-foams.
- The CO_2-foam strength was found to increase with decreasing pressure and increasing temperature; low-density conditions for CO_2 improved the CO_2-foam strength (MRF between 80-3 for ρ_{CO2} in the range of 0.056-0.857 g/cm^3).
- Strong CO_2- and N_2-foams delayed gas breakthrough significantly more than the weak CO_2-foams, though all foams reduced gas mobility and delayed gas breakthrough compared with the absence of surfactant.
- Images of foam textures at the core outlet showed denser/finer textured N_2-foams compared with coarser textured CO_2-foams.

N_2-foam strength vs. pressure:

N_2-foams of similar or slightly increased strength with increasing system pressure have also been reported by other laboratory studies (e.g., Du et al., 2008; Farajzadeh et al., 2009; Friedmann and Jensen, 1987; Mani and Ma, 1986; Mannhardt et al., 1996; Sanchez and Schechter, 1989; Solbakken et al., 2014; Turta and Singhal, 1998). The positive effect of pressure on N_2-foam strength has been hypothesized due to an increased rate of lamellae generation with pressure, smaller and more uniform bubble sizes under higher pressures, improved lamellae stability due to increased adsorption of surfactant at the gas-liquid surface, an increased fraction of non-condensable component in the gas phase at high temperature with

the increment in system pressure, and reduced expansion effects to weaken the foam under higher pressures and as a result of the core experimental history.

The slightly increased N_2-foam strength at 280 bar compared with that at 30 bar during the initial pore volumes injected, as shown in Figure 8.1, can likely be explained by several of the above-mentioned factors. For example, visual observations of the N_2-foam textures indicated smaller bubbles at 280 bar compared with those at 30 bar during the initial pore volumes injected but smaller differences at the later stages, which are in reasonable accordance with the corresponding measurements in MRFs (Figure 8.3).

Slightly increased N_2-foam strength with increasing system pressure was also noted in **Paper 3** (figure 3). In this article, the experimental history of the heterogeneous core material used was speculated to have dominated this result because successive stronger foams were generated by repeated experiments on the same core, independent of the parameters studied (figure 8 and 9 in **Paper 3**).

Based on our results, increasing pressure (in the range of 30-280 bar at 50°C) appeared to have a slightly positive effect on the N_2-foam strength.

<u>CO_2-foam strength vs. pressure and temperature:</u>

A similar dependence of pressure and temperature on the CO_2-foam strength in porous media as we obtained in this thesis, were also reported by Du et al. (2008), Khalil and Asghari (2006) and Kibodeaux (1997). Different explanations for the varying CO_2-foam strength with pressure and temperature have been proposed.

Kibodeaux (1997) argued that weaker CO_2-foam with increasing pressure was due to a possible combination of reduced disjoining pressure and lower surface tension forces. No definitive causes were identified. Kibodeaux's foam experiments were conducted in Berea sandstone cores at 4.5 bar and 138 bar at 23°C using CD-1040 (AOS) surfactant.

Khalil and Asghari (2006) attributed the pressure and temperature dependence on CO_2-foam strength to changes in the surface tension that could lead to differences in the in-situ foam texture, which directly affects foam mobility in porous media. It was hypothesized that higher absolute pressure would give rise to smaller foam bubbles that would travel more easily

through the porous media, resulting in a lower pressure drop across the core (i.e., weaker CO_2-foam). Khalil and Asghari's foam experiments were performed by injecting pre-generated foam into a carbonate sand pack at 83 bar and 103 bar at 22°C and 50°C using CD-1045 surfactant. No visual observation of the foam texture out of the core was recorded. Khalil and Asghari's interpretation contradicts our observations of the CO_2-foam textures leaving the core with increasing system pressure (Figure 8.3) and also the idea that smaller bubbles are expected to reduce gas mobility more (and not less) than larger bubbles (Chapter 4, section 4.4). Though, it may be that a lower surface tension could make the lamellae less resistant to flow, thus giving the CO_2-foam higher mobility despite of smaller bubble sizes.

Du et al. (2008) suggested that an important factor leading to the decreased CO_2-foam strength with increasing system pressure could be the increasing solubility of CO_2 in water with pressure. It was thought that the dissolved CO_2 could decrease the solubility of the surfactant in the aqueous phase and give rise to a lower surface tension that would decrease the apparent foam viscosity. Du et al.'s foam experiments were performed by injecting pre-generated foam into outcrop Bentheimer sandstone cores from atmospheric pressure to 16 bar back-pressure at 20°C using sodium dodecyl sulfate (SDS) surfactant.

An important part of the pressure and temperature dependence on CO_2-foam strength as we see it, appears to be attributed to the large changes in physical and chemical characteristics of CO_2 under the various experimental pressure and temperature conditions applied in this thesis (Chapter 5). Based on the general trends in CO_2 characteristics with pressure and temperature (summarized by Table 5.4 in Chapter 5), we imply that the increased CO_2-foam strength in this thesis appears to be generated under experimental conditions where the CO_2 is a gas, and where the characteristics of supercritical CO_2 are more "gas-like" (i.e., where the CO_2 density, viscosity and solubility properties in water are lower and where the CO_2-compressibility, water pH and likely the surface tension between CO_2 and surfactant solution are higher).

Our results with systematic variations in pressure and temperature conditions demonstrated a good correlation between the CO_2 density and the CO_2-foam strength (Table 8.1 and Figure 8.9). A possible reason for this relationship could be that the CO_2 density properties also indirectly control some of the other characteristics of CO_2 as well, which might be important for the properties of foam in porous media. For instance, the surface tension between CO_2 and several surfactant solutions in the literature appears to become consistently lower when the

density of CO_2 increases (Chapter 5, Table 5.3). A lower surface tension in foam could potentially result in both stronger and weaker foams (Chapter 5, section 5.4.7), making the significance of this parameter on CO_2-foam strength in porous media difficult to interpret accurately. In addition, the solubility of CO_2 in water increases, whereas the water pH and the gas compressibility decrease with increasing CO_2 density. The increased solubility of CO_2 in the liquid phase together with the decreased water pH could possibly influence the electrical double layer and the disjoining pressure in thin liquid films (Chapter 3, section 3.3). A decrease in the disjoining pressure could result in less stable and weaker CO_2-foams. The gas compressibility, which has a close relationship with changes in the gas density, might also affect the resistance of foam flow in porous media (Chapter 5, section 5.4.4). Accordingly, it is possible that a combination of several factors in close relationship with the changing CO_2 density is what contributes to the varying CO_2-foam strengths obtained in this project with pressure and temperature. It should be emphasized that the traditional definition of foam as a gas dispersed in a liquid is best met under pressure and temperature conditions where the CO_2 has low density. Also others have noted the correlation between the surface tension, the solubility of CO_2 in water and the CO_2 density, where the density has been postulated as the main parameter that controls the CO_2 solvation properties and the surface activity (Harrison et al., 1996; Liu et al., 2005a; Chaubert et al., 2012).

<u>CO_2-foam strength vs. N_2-foam strength:</u>

In the foam flooding experiments in this thesis, weaker CO_2-foams were observed compared with N_2-foams.

The apparent weakness of CO_2-foams compared with N_2-foams have also been reported by other comparative studies on outcrop sandstone core material in the absence of oil using commercial anionic surfactants (Chou, 1991; Du et al., 2008; Farajzadeh et al., 2009; Gauglitz et al., 2002; Kibodeaux, 1997; Seright, 1996).

Most of the previous studies ascribe the difference in foam strength between N_2- and CO_2-foams to the lower surface tension properties with CO_2 compared with N_2. However, few of these studies provide measurements of actual surface tension data. Kibodeaux, (1997) suggested a combination of lower surface tension and reduced disjoining pressure, whereas Du et al., (2008) hypothesized a combination of higher solubility in water and lower surface tension for the weaker CO_2-foams obtained. Others, such as Tsau and Grigg (1997), found the

mobility reduction factor of CO_2-foam in porous media to increase with surfactants that yielded higher surface tension gradients between the CO_2 and the aqueous phase. Adkins et al. (2009) suggested that the surface tension gradient in CO_2-foams under high pressure conditions could be too small for Marangoni stabilization. Recently, Adkins et al. (2010) indicated major differences in surfactant characteristics between the CO_2-water and air-water surfaces in terms of surfactant partitioning, adsorption kinetics, interfacial activity and surfactant packing properties.

In our opinion, the role of surface tension and surfactant characteristics at various gas-liquid surfaces may be important for why the CO_2-foams are weaker than the N_2-foams, however, this need to be investigated further by additional experimental data.

Farajzadeh et al., (2009) argued that the difference between CO_2- and N_2-foam could be due to a number of factors, primarily related to differences in the nature of the two gas phases (e.g., surface tension, solubility in water, pH effects, wettability effects and surfactant type). From these factors, the difference in solubility between CO_2 and N_2 in water was suggested as the most critical factor for the following reasons: I) a portion of the gas will be dissolved in the aqueous phase, and therefore, when the volumetric flow rate of the two gases are the same, the local gas velocities will be different, i.e., the amount of available CO_2 for foaming will be lower than that of N_2 at similar pore volume injected, and II) it could affect the gas permeability coefficient and thus the foam stability. In other words, the degree of gas escape through the foam films could be higher with CO_2 than with N_2. Contrary to Farajzadeh et al. (2009), Nonnekes et al. (2012) argued that if the foam bubbles are larger than the pores (an assumption in current foam models based on theoretical predictions and observations of the bubble sizes leaving the core in the laboratory), diffusion would not affect the bubble-size distribution for flowing bubbles, which would be limited and supported by the pore walls. A similar argument related to diffusion in porous media was also provided earlier by Rossen (1996). If this is the case, diffusion should have only a small effect on the overall foam flow resistance during foam generation and therefore, cannot explain the apparent weakness of CO_2-foam compared with N_2-foam.

In this thesis, we investigated the importance of mass transfer on CO_2-foam properties in porous media closer. CO_2-foam experiments with pre-equilibrated fluids were conducted and compared with CO_2- and N_2-foam experiments without phase-equilibration. The results with

pre-equilibrated fluids showed a slightly faster and more efficient pressure build-up period during the first pore volume injected. However, as the experiment proceeded, the use of pre-equilibrated fluids had little importance on the overall CO_2-foam strength during generation at low (30 bar) and particularly high (120 bar) system pressures (Figure 8.5). Based on our results, we contend that the kinetics of mass transfer between the CO_2 and surfactant solution (e.g., due to gas dissolution, local temperature rise and gas diffusion as hypothesized by Farajzadeh et al. (2009)) cannot be the main cause for the decreased CO_2-foam strength with increasing system pressure and does not explain why the CO_2-foams during generation (at the plateau) were weaker than the N_2-foams. Therefore, our results support the argumentation of Nonnekes et al. (2012).

During the early stage of generation, we would have anticipated the spontaneous dissolution process of CO_2 into the surfactant solution to have reduced the volumetric flow rate of CO_2 (and the foam quality) locally or exerted an immediate instability on the foam lamellae in experiments without pre-equilibrated fluids. This could have caused a delay in foam generation compared with experiments with pre-saturated fluids or compared with foams containing gas phases with low solubility in water (i.e., N_2-foams, in our case). Because the delay was not very pronounced in our experiments, the high inlet foam quality used (i.e., 80% with CO_2) may probably have saturated a good portion of the co-injected surfactant solution relatively fast as the experiment proceeded.

The outcrop Berea sandstone core material used in this thesis was classified as strongly water-wet by the Amott-Harvey and USBM indices (Shiran, 2014). For the possible wettability/chemical effects with the injected CO_2 and the porous media (Chapter 5, section 5.4.6), relevant experimental results suggest that CO_2 will not wet the rock surface over brine if the media is originally water-wet. This is coherent with the wettability indices deduced by Egermann et al. (2006) in outcrop limestone cores, Chalbaud et al. (2007) using micro-models, contact angle measurements by Chiquet et al. (2007) and Espinoza and Santamarina, (2010) and capillary trapping/relative permeability characteristics of CO_2 in Berea sandstone and other water-wet rocks by Berg et al. (2013), Hildenbrand et al. (2004), Pentland et al. (2011), Krevor et al. (2012), Silin et al. (2011) and Suekane et al. (2008). Although support exist that water remains the wetting phase, an indication appears in several of the abovementioned studies that water-wet surfaces might attain a slightly less hydrophilic character in the presence of carbon dioxide (i.e., less water-wetness but still on the water-wet side). The sensitivity of the foam to subtle changes in the wettability of the porous media is

unknown at the present, and more detailed investigations of the wettability importance on foam properties in the presence of CO_2 are required to answer this question properly. Hence, we cannot exclude the possibility that a portion of the differences between the N_2- and CO_2-foams in Berea sandstone in this project also might have been attributed to a change in the water-wetness and/or stability of the wetting liquid film during experiments with carbon dioxide compared with nitrogen. However, Kibodeaux (1997) indicated little difference in the N_2-foam performance in Berea sandstone when the AOS surfactant solution was acidified in advance to mimic the pH environments present within the CO_2-foam system. From this study, it was argued that low pH does not affect CO_2-foam strength in porous media. Future studies should use a similar experimental approach to evaluate the possible wettability/chemical effects on foam in porous media in greater detail.

The foam performance observed against various gas phases may be surfactant dependent. We are aware of the ongoing and extensive work in the literature related to finding/designing optimal foamers against the dense phase of CO_2 (Chapter 5, section 5.5). Our results showed that commercial AOS surfactant were able to reduce the mobility and delay the breakthrough of dense supercritical CO_2 (i.e., $\rho_{CO2} > 0.5$ g/cm^3) in all experiments compared with those in the absence of surfactant. However, based on the foam strengths obtained under these conditions (i.e., MRF of $\sim 7 \pm 4$) and compared with the other foams in this project, we classified the dense supercritical CO_2-foams as weak foams. Similar magnitude (i.e., MRF < 15) in foam strength as we reported in this work with dense CO_2 has also been reported elsewhere with other types of surfactant systems (Alkan et al., 1991; Chabert et al., 2012, 2014; Chen et al., 2012; Elhag et al., 2014; Khalil and Asghari, 2006; McLendon et al., 2012; Preditis and Paulett, 1992; Sanders et al., 2010; Xing et al., 2012). Accordingly, it appears to be a more general phenomenon that many types of foamers do not generate CO_2-foam of similar strengths in porous media as those reported with N_2- and CH_4-foams when the density of CO_2 is high.

Various field applications will have different demands with regard to foam properties (Chapter 1, section 1.8 and Chapter 2, section 2.3). If CO_2-foams are inherently weaker than other foams, as indicated, then this information should be important to the reservoir engineers for the scaling of foam processes in different situations. Unfortunately, precise definitions of "strong" and "weak" foams do not exist in the literature, making it difficult to integrate quantitative knowledge of foam in the laboratory into quantitative predictions of foam

performance in the field (e.g., what foam strength is "good enough?", what foam strength is "too strong?" or "too weak?"). Future studies should evaluate the potential and applications of weaker foams (e.g., MRF < 15) more carefully. If weaker foams propagate faster in addition to give gas mobility control, they may propagate deeper into the reservoir without impairing injectivity. For instance, relative to enhanced oil recovery, the diversion power of these weak supercritical CO_2-foams must be investigated more closely. If foams with lower MRFs are sufficient, foam for EOR might have great potential because nearly all surfactants in the literature appear to provide at least some degree of mobility reduction compared with the absence of surfactant.

Seawater injection following CO_2-foam vs. N_2-foam:

The main findings from this thesis comparing seawater injection after foam generations (Figure 8.4, 8.7 and 8.8) showed that:

- The N_2-foams provided greater resistance and stability against seawater flow compared with the CO_2-foams.
- Strong and long-lasting reductions in seawater permeability were obtained after N_2-foams, whereas seawater permeability following CO_2-foam generation was high only after the injection of a few pore volumes of seawater.
- The use of pre-saturated fluids significantly improved the resistance and stability to CO_2-foam against seawater injection.

Water injection following foam generations in single core experiments have also been investigated and discussed by several others (e.g., Aarra et al., 2011; Bernard et al., 1965, 1980; Bhide et al., 2005; Du et al., 2007; Kibodeaux, 1997; Nguyen et al., 2009; Parlar et al., 1995; Seright, 1996; Zeilinger et al., 1995). Their findings and observations relative to our results deserve comments and discussions.

Reasons for reduced k_{rw} in the presence of foam:

Bernard et al. (1965) concluded that foam decreases the permeability to water by developing a higher trapped gas saturation than in the absence of foam. Their N_2-foams in high permeability sand packs exhibited good stability to subsequent water injections because the permeability of water was low even after the injection of 10 to 25 pore volumes of water.

In a later paper, Bernard et al. (1980) concluded that the permeability reductions caused by CO_2-foam could be reversed by the injection of several pore volumes of brine. A rapid increase in the brine permeability was observed during the first pore volumes of surfactant-free brine injected (i.e., $k_{rw,app.} \sim 0.36$ after 4 PV of brine injected, which is relatively similar to our CO_2-foams in Figure 8.4). The increase in brine permeability was accompanied by a decrease in CO_2 saturation. The experiment was conducted in Berea sandstone core under 169 bar and 57°C. No direct comparison was made with the more persistent N_2-foams previously observed in 1965.

As we see it, the strong and long-lasting reduction in seawater permeability after N_2-foams and pre-equilibrated CO_2-foams in this thesis cannot be explained as an ordinary two-phase effect. In the absence of surfactant, the seawater relative permeability (k_{rw}) will increase until trapped gas saturation (S_{gt}) has developed. The increase in k_{rw} depends on the magnitude of S_{gt} and the seawater relative permeability curve. Based on the strong and long-lasting reduction in $k_{rw,app.}$ with N_2-foams and pre-equilibrated CO_2-foams (Figure 8.4, 8.7), we suggest these foams to exceed expected values and changes in S_{gt} with pore volume seawater injected compared with that in the absence of surfactant.

Pressure drop response during liquid injection:

Parlar et al. (1995) discussed the pressure drop response during liquid injection following N_2-foam in Berea sandstone cores. After the foam injection was stopped and the liquid injection was continued, these researchers noticed a sharp decline in the pressure drop followed by a more gradually decreasing pressure drop to a nearly constant level (i.e., a similar pressure drop response as that shown during the early stage of seawater injection following N_2-foam in this thesis in Figure 8.8). Parlar et al. explained the initial drop in pressure as a rapidly moving shock front, which resulted in only a small increase in S_w. The second decline, reflecting a larger rise in S_w, was attributed to gas dissolution into the injected liquid. The final response in pressure drop was viewed as the residual trapped gas saturation, which in reality was slowly decreasing due to gas diffusion and gas releasing (i.e., gas out of the liquid solution). Zeilinger et al. (1995) confirmed Parlar et al.'s suggestion that the second decline in pressure drop response during liquid injection was due to gas dissolution. Following N_2-foam generation, Zeilinger et al., injected surfactant solution saturated with nitrogen. The initial pressure drop response after gas shut-off and the start of liquid injection fell quickly to

roughly the same value as that without pre-saturated liquid. However, the pressure drop with pre-equilibrated liquid did not decline from this plateau for over 80 PV.

Zeilinger and Parlar et al.'s studies of liquid injection following N_2-foam with and without saturated fluids are somewhat analogous to our experimental strategy of CO_2-foam with and without phase-equilibration. However, our comparative results showed that the pressure drop during liquid injection was significantly more severe for the CO_2-foam compared to the N_2-foam. The reason for this observation appeared to be higher mass transport between the CO_2 and the injected seawater compared with N_2 and seawater because the pressure drop response with pre-equilibrated fluids was more similar to that after N_2-foam (Figure 8.8).

Mechanisms for reduced foam stability during liquid injection:

The general mechanisms for reduced foam stability during subsequent liquid injections have been discussed in terms of gas dissolution, surfactant dilution and gas expansion.

In our view, mass transfers between fluid phases and especially gas dissolution into the injected seawater appear to be the dominant mechanism for the reduced CO_2-foam stability in porous media in our experiments. We believe that the mass transfer rate could be more severe for CO_2-foam stability than for N_2-foam stability because the gas component (i.e., CO_2) is significantly more soluble in seawater than N_2 is in seawater (Chapter 5, section 5.4.3). For the CO_2-foams without phase-equilibration, the initial pressure drop response rapidly declined with the injection of small amounts of seawater (Figure 8.8). We believe that this response was dominated by a rapid and spontaneous mass transfer taking place between the CO_2 and the injected seawater (undersaturated with CO_2), which likely caused an immediate rupture of the foam lamellae and a subsequent rise in the liquid saturation and the liquid relative permeability (Figure 8.4). The use of pre-saturated seawater to limit the mass transfer changed the situation completely, even at 30 bar and 50°C, because it demonstrated CO_2-foams with significantly improved resistance and stability against the seawater injected (Figure 8.7-8.8).

The injection of 10 or more pore volumes of seawater (without surfactant) must also have reduced the concentration of AOS surfactant in the core. A reasonable suggestion is that this surfactant dilution would cause some degree of foam destabilization and gas production, thus increasing the liquid saturation and also the liquid relative permeability. Because the measured $k_{rw,app.}$ in the presence of N_2-foam remained fairly low for many pore volumes of

seawater injected, we speculate that the amount of surfactant in the core was not critically low for preserving foam stability even after extensive water injection. For instance, desorption of surfactant from the rock surfaces might be a slow process, as indicated by Bai et al. (2005). It is also well known that foams can be generated and remain stable in bulk and porous media experiments using low concentrations of surfactant (Aarra et al., 2002; Alkan et al., 1991; Apaydin and Kovscek, 2001; Dixit et al., 1994; Heller, 1994; Kuhlman et al., 1992; Liu et al., 2005a; Mannhardt and Svorstøl, 2001; Rohani et al., 2014; Sanchez and Schechter, 1989; Simjoo et al., 2013a; Tsau and Grigg, 1997; Vikingstad et al., 2006). Bhide et al., (2005) found the foam stability against water injection to increase with the use of polymeric surfactants compared with conventional surfactants, suggesting improved washout stability of polymeric surfactants at the air-water surface. In Nguyen et al. (2009), no particular difference in foam stability against liquid injection was indicated when pure brine was compared with the injection of surfactant solution, suggesting that surfactant dilution by water does not always cause the foam to become less stable.

Most of the studies discussing gas expansion as a possible foam destruction mechanism during liquid injection have been carried out under low pressure conditions where the solubility of gas in liquid is limited, but with the potential of large expansion/compressibility effects on the gas phase. As noted by Nguyen et al. (2009), it is difficult to distinguish the effects of different mechanisms during liquid injection when the compressibility effects on the gas phase are significant. Possible expansion/compressibility effects on the gas phase in our project must have been smaller because they were conducted under higher system pressures. Although N_2-foams of relatively similar strength were generated under low (30 bar) and high (280 bar) pressure, slightly higher $k_{rw,app.}$ was observed at the highest system pressure (Figure 8.4). Different development in $k_{rw,app.}$ was also observed at the later stages comparing N_2-foam and pre-equilibrated CO_2-foam at 30 bar (Figure 8.7). These prior two examples indicate that other forms of gas expansion than expansion of the free gas phase to be more important on foam stability in our experiments. It could be that gas out of the liquid solution/lamellae caused by the pressure drop during liquid injection (i.e., decreasing the solubility of gas in liquid), to have contributed to the different developments in $k_{rw,app.}$. The amount of gas out of the liquid solution depends on the solubility of the gas in the liquid. Thus, for a similar drop in pressure, it might be reasonable to believe that this mechanism will affect foam stability more in the case of high pressure N_2-foam vs. low pressure N_2-foam, and especially CO_2-foam compared to N_2-foam where the solubility of gas in liquid are higher (Chapter 5, section

5.4.3). The mechanism of gas out of the liquid solution on foam stability during subsequent liquid injection is similar to the interpretation given by Parlar et al., (1995).

Comparative studies:

In a report by Seright (1996), the water injection resistances of N_2- and CO_2-foam were tested and compared in Berea sandstone cores at 103 bar and room temperature using $AOS_{C14-C16}$ surfactant. After steady-state foam generation, brine (without surfactant) was injected. Although the N_2-foams were found to provide a certain amount of resistance even after 100 pore volumes of brine injected, the CO_2-foams were reported to be quickly "washed out" from the core because the resistance factor rapidly decreased after a few pore volumes of brine injected. Surfactant dilution was suggested as the main reason for the decreasing resistance factor with increasing brine throughput. No explanation of the huge differences in resistance factors between the CO_2- and N_2-foam was provided. To the best of our knowledge, this is the only previous investigation that quantitatively compared liquid injection after CO_2- and N_2-foam within the same study. Seright's results are similar to our initial observations of seawater injection resistances after N_2- and CO_2-foam without phase-equilibration (Figure 8.8).

Bhide et al. (2005) discusses the importance of having dissolved gases in the production water in the field together with low-solubility gas components in the foam for prolonging foam stability in production well treatments. Our results in Figure 8.7 and Figure 8.8 support Bhide et al.'s discussion.

Recently, Aarra et al. (2011) evaluated and compared the water-blocking abilities of CH_4- and CO_2-foams in outcrop limestone core material with residual oil present at 277 bar and 100°C using a similar $AOS_{C14-C16}$ surfactant and seawater composition as applied in this thesis. After foam generation, seawater was injected at different scaled pressure gradients with monitoring of the injection rate. Although CH_4- and CO_2-foams of relatively similar strength were generated (likely due to the formation of an emulsion with the dense CO_2 and the crude oil/surfactant solution), the CH_4-foam blocked water more efficiently than the CO_2-foam. At similar applied pressure gradients, a much higher water injection rate was observed after CO_2-foam. The authors argued that the higher injection rate with CO_2-foam could have been caused by a faster dissolution rate of CO_2 into the injected brine compared with methane

where the solubility in brine is low. The new CO_2-foam seawater-blocking results obtained in this thesis strongly supports this argument (Figure 8.7 and 8.8).

In summary, the comparative results obtained in this thesis confirm previous laboratory studies showing CO_2-foam to be less effective against subsequent liquid injections compared with foams having gas phases with limited solubility in liquids (e.g., Aarra et al., 2011; Seright, 1996). It is interesting to note that certain field results also appear to support the laboratory-derived results concerning poor water-blocking capabilities to CO_2-foam (Enick and Olsen, 2012 and Holm and Garrison, 1988). If CO_2-foams are less stable against subsequent water injections as indicated, this could be important information for foam field processes. An unstable foam after placement could mean that the foam treatment have to be repeated more frequently than expected to maintain its effect. Consequently, it seems instructive to compare different types of foam in the same study for an improved quantitative understanding and evaluation of the foam performance.

How is the injected liquid transported?

Parlar et al. (1995) argued that most of the injected liquid travels through only a portion of the core and that most of the gas is effectively isolated from the bulk of the injected liquid.

Du et al. (2007) imaged surfactant injection following CO_2-foam generation with the aid of X-ray CT scanning and showed strong fingering behavior of the liquid throughout the core sample. A rapid decline in the pressure drop over the entire core was accompanied with the liquid injection. Du et al.'s experiments were performed in a Bentheimer sandstone core at a back-pressure of 0-5 bar and 20°C using SDS surfactant.

Nguyen et al. (2009) extended the investigations of liquid displacing foam in outcrop sandstone cores with the aid of X-ray CT scanning. Following N_2-foam generation under ambient conditions, brine injection (with and without SDS surfactant) was monitored. The observed water fingering behavior throughout the core with CO_2-foam in Du et al. (2007) was also confirmed with N_2-foam by Nguyen et al. Gas expansion and gas dissolution into the injected liquid were expected to have strong effects on the water fingering.

Parlar et al. (1995) found that the liquid injection rate following N_2-foam did not affect the final pressure drop across the core. Similar observations with a doubling in the liquid injection

rate (from 60 ml/h to 120 ml/h) were also reported by Nguyen et al. (2009). In this thesis, a seawater injection rate of 8 ml/h versus 40 ml/h following N_2-foam generation showed relatively similar $k_{rw,app.}$ after the injection of more than 10 pore volumes of seawater (Figure 8.4).

An important but difficult question that still remains to be answered from our studies of foam's seawater-blocking abilities under high pressure and elevated temperature conditions is how the seawater is transported when injected. This might offer vital information for better evaluating the overall performance of the liquid-blocking/diversion-process. However, it is inherently difficult to gain knowledge of foam and water transport at the pore-level in porous media. Whether liquid flows within the continuous network of lamellae, in the water films along the rock surfaces or is restricted to the smallest water-wet pores that do not contain gas remains controversial (Ettinger and Radke, 1992; Falls et al., 1988a; Holm, 1968; Kovscek and Radke, 1994; Mast, 1972). We cannot exclude the possibility that the water fingering phenomena through the foam and the core reported in Du et al. (2007) and Nguyen et al. (2009) under reduced experimental conditions also might have occurred in our experiments. Future studies investigating the liquid injection following foam should be extended to single and dual core experiments under high pressure with the aid of in-situ saturation monitoring and imaging to evaluate the behavior and power of the foam-liquid-blocking/diversion-process more closely.

8.3 Effect of rock properties on foam

8.3.1 Experimental strategy

Most laboratory studies on foam have been conducted on relatively homogeneous and high permeable porous media. As the reservoir situation is rather heterogeneous with respect to permeability and layering, foam properties in relation to layered rock material with lower permeabilities are also important to understand, but this issue has received less attention.

In **Paper 3**, foam experiments were performed on three outcrop Berea sandstone cores with average permeabilities in the range of 70-130 mD and with visible layered structures (i.e., laminas) parallel to the flow direction (Figure 8.10).

During flooding experiments, most parameters were held constant, and the core material was changed.

The surfactant type ($AOS_{C14-C16}$), surfactant concentration (0.5 wt.%), gas phase (nitrogen), synthetic seawater (~36,000 ppm TDS), experimental temperature (50°C), co-injection method, inlet foam quality (80%) and injection rates during foam generation (32 ml/h gas and 8 ml/h surfactant solution) were held constant unless otherwise mentioned. The system pressure varied among 30 bar, 120 bar and 280 bar. All experiments were conducted without oil to improve the understanding of foam relative to the rock properties.

Various types of analyses were applied to characterize the laminated rock material. The results from the analyses were used as a supplement to improve understanding and interpretation of the foam results in laminated rock material under elevated pressure and temperature conditions. The experimental strategy of using different core analyses was based on previous suggestions and experiences from similar type of rock material but with another EOR method (Solbakken, 2010).

A summary of the main findings from **Paper 3** with respect to rock core analyses and foam generation performance in naturally laminated sandstone material with relatively low permeability is presented next.

8.3.2 Rock core analyses

The core analyses that were applied on the laminated rock material are provided in the appendix in **Paper 3**.

In general, five types of analyses were applied:

I) Combined X-ray diffraction (XRD)/X-ray fluorescence (XRF) spectrometry to determine the element, mineral and clay constituents in the laminated portions compared with those of the surrounding matrix (i.e., the host rock).
II) Mercury injection to estimate the distribution of pore throat sizes.
III) Data processing of thin section images to estimate the porosity and permeability values in the laminas versus the host rock.
IV) Dispersion measurements to improve understanding of the fluid transport properties.
V) 2D X-ray scanning to visualize the laminas and their potential influence on foam and fluid flow.

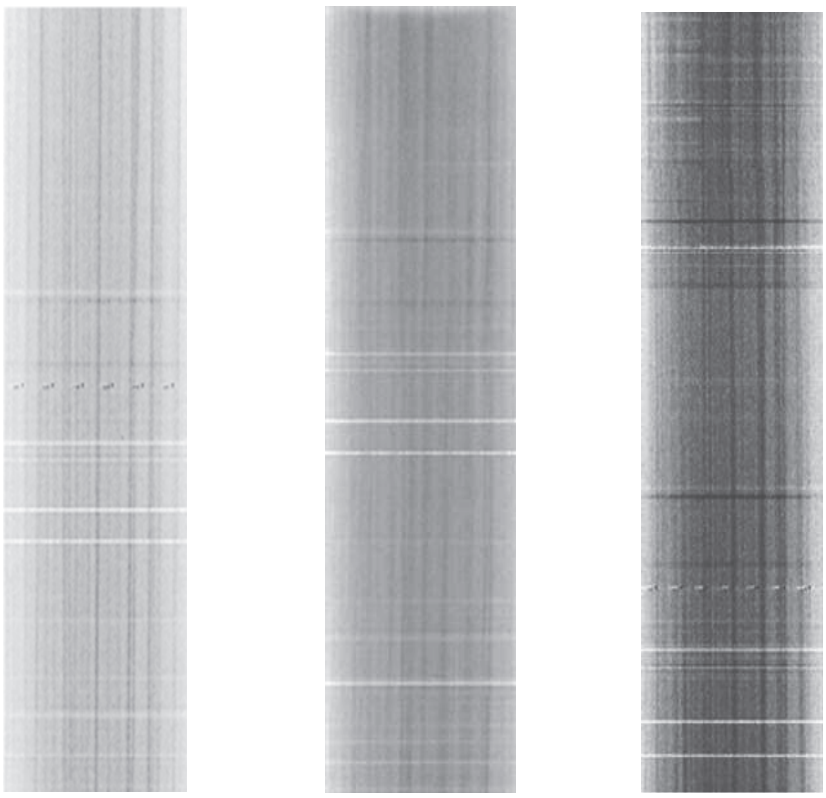

Weakly laminated core (B-WL) | Moderately laminated core (B-ML) | Strongly laminated core (B-SL)

Figure 8.10: X-ray images of the laminated core samples used in Paper 3. The horizontal lines in the images are noises.

The main findings and observations from analyses on the laminated rock material are summarized as follows:

Type of heterogeneity: Evidence of laminated rock heterogeneity was confirmed using several types of analyses on different scales: visual inspection, 2D X-ray scanning and different microscopy techniques (figure A.1, A.4 and A.5 in **Paper 3**). The laminas were classified as deformation bands according to their constituents, appearances and alignments perpendicular to the direction of compaction/overburden pressure.

Degree of heterogeneity: Different degrees of lamination were detected in each of the three cores used during foam flooding. The cores were thereafter named according to their degree of laminated heterogeneities present, i.e., Berea-weakly laminated core (B-WL), Berea-moderately laminated core (B-ML) and Berea-strongly laminated core (B-SL) (Figure 8.10).

Mineralogy: Quartz and iron-containing carbonate minerals such as siderite ($FeCO_3$) were indicated as the predominant constituents of the lamina. The host rock in general contained all of the minerals and clays detected by the XRD measurements (table A.1 in **Paper 3**).

Petro-physical properties: The laminas were observed through-going in all of the cores with various thicknesses and densities indicating internal variations in the petro-physical properties (Figure 8.10). Permeability measurements perpendicular to the lamina (using a mini-permeameter) indicated roughly half of the permeability compared with that of the parallel alignment (i.e., 45 mD vs. 90 mD). Data processing of thin-section images showed that the laminated structures generally exhibited lower porosity and permeability compared with that of the host rock (the appendix in **Paper 3** provides quantitative data on the petro-physical properties of the lamina versus the host rock). Certain portions of the lamina were observed as clusters of cementation, whereas others formed thin single structures, thus supporting internal variations in petro-physical properties along the laminas (figure A.4 in **Paper 3**). Mercury injection indicated a wider pore size distribution and a larger fraction of smaller pore throats in laminated Berea compared with those in the higher permeability outcrop sandstone samples used in this thesis (Figure B.1 and Table B.3 in the Appendix).

Fluid flow: Gravity stable water and gas injections into laminated slabs (10 cm x 5 cm x 1.5 cm) demonstrated that the presence and orientation of the laminas could act as barriers to fluid

flow and result in compartmentalization (Figure 8.11a-b). It was easier for both water and gas to flow through the more permeable regions than the laminated portions of the rock sample. Unstable displacements, earlier fluid breakthroughs and reduced sweep in the laminated samples were observed compared with a relatively homogenous and high permeability rock sample (Figure 8.11a-b). Dispersion tests in the laminated sandstone cores used during the main foam experiments showed earlier tracer breakthroughs and tailing of the tracer concentration compared with the more homogeneous outcrop sandstone core samples used in this thesis (Figure B.2 in the Appendix on page 185). The results suggested that portions of the pore volume in the laminated cores contributed less to brine flow. The gravity-stable water injection supported that the laminated areas might have potential for slow fluid contact and brine exchange (Figure 8.11a).

Foam flow: Visual observations demonstrated that the presence of surfactant was able to reduce gas mobility and improve gas sweep efficiency in laminated rock material compared with gas injection in the absence of surfactant (Figure 8.11c).

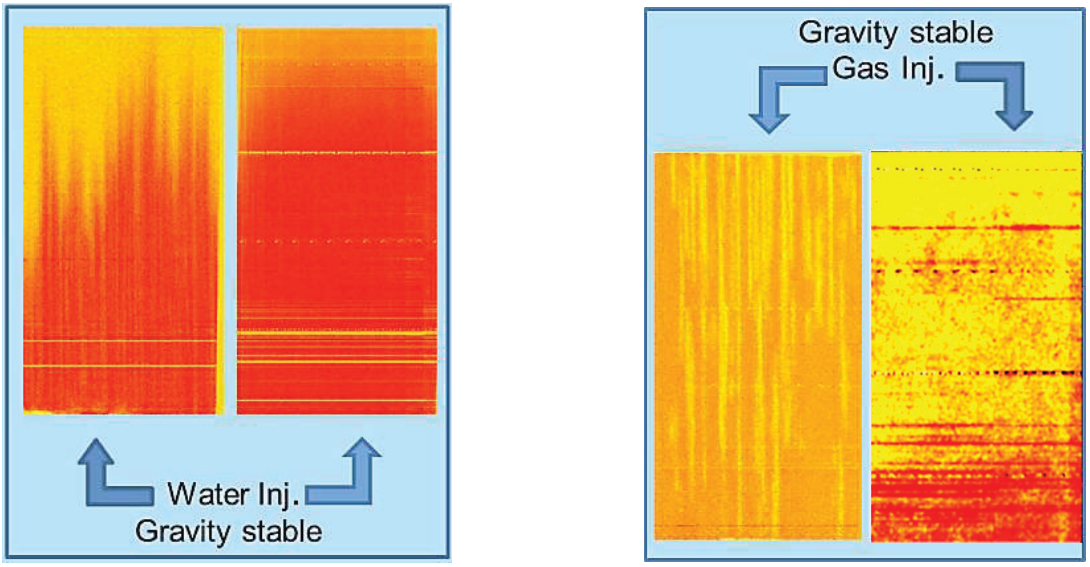

a) b)

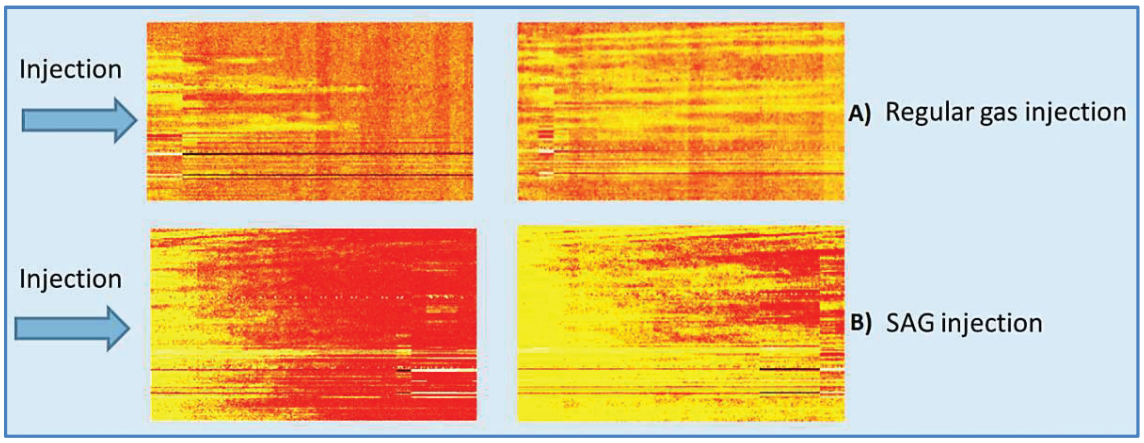

c)

Figure 8.11: a) 2D X-ray images of gravity-stable water injection in a low permeability laminated sandstone slab (left) versus high permeability/homogeneous sandstone slab (right). Images were taken at the tracer breakthrough in both cases. b) 2D X-ray images of gravity-stable N_2-gas injection in laminated (left) versus high permeability (right) sandstone rock material. Images were taken at close to 1 pore volume injection in both cases. c) 2D X-ray images of a regular N_2-gas injection into a brine saturated sample after 0.1 and 1.5 pore volumes with gas injection (upper left and right, respectively). N_2-gas injection into a surfactant saturated sample after 0.2 and 1.5 pore volumes with gas injection (lower left and right, respectively). All experiments in the figure were conducted under 2 bar backpressure at 25°C. The slab dimensions were constant of 10 cm (length) x 5 cm (width) x 1.5 cm (thickness). The horizontal lines in the images are noises.

8.3.3 Foam generation performance in low permeability laminated sandstone cores

The performance of foam in naturally laminated sandstones with low permeability was examined in core flooding experiments under high pressure and temperature conditions. The effects of the core material on the foam were evaluated by the comparing pressure build-up profiles, calculated mobility reduction factors (MRF) and gas breakthroughs (GBT) during foam generation in three laminated Berea sandstone cores. The three applied core samples had similar physical properties as measured by conventional laboratory measurements (Table B.1 in the Appendix), but as previously mentioned, they contained different degrees of laminated structures parallel to the flow direction (Figure 8.10).

Pressure build-up profiles and MRFs:

Figure 8.12 summarizes all pressure build-up profiles obtained from repeated experiments on the three laminated core samples. The details for each experiment are provided in the Appendix (Table D.4-D.6) or in **Paper 3**. Foam strength was determined by calculation of mobility reduction factors (MRF), as defined by Equation 7.1 (Chapter 7, section 7.4.1).

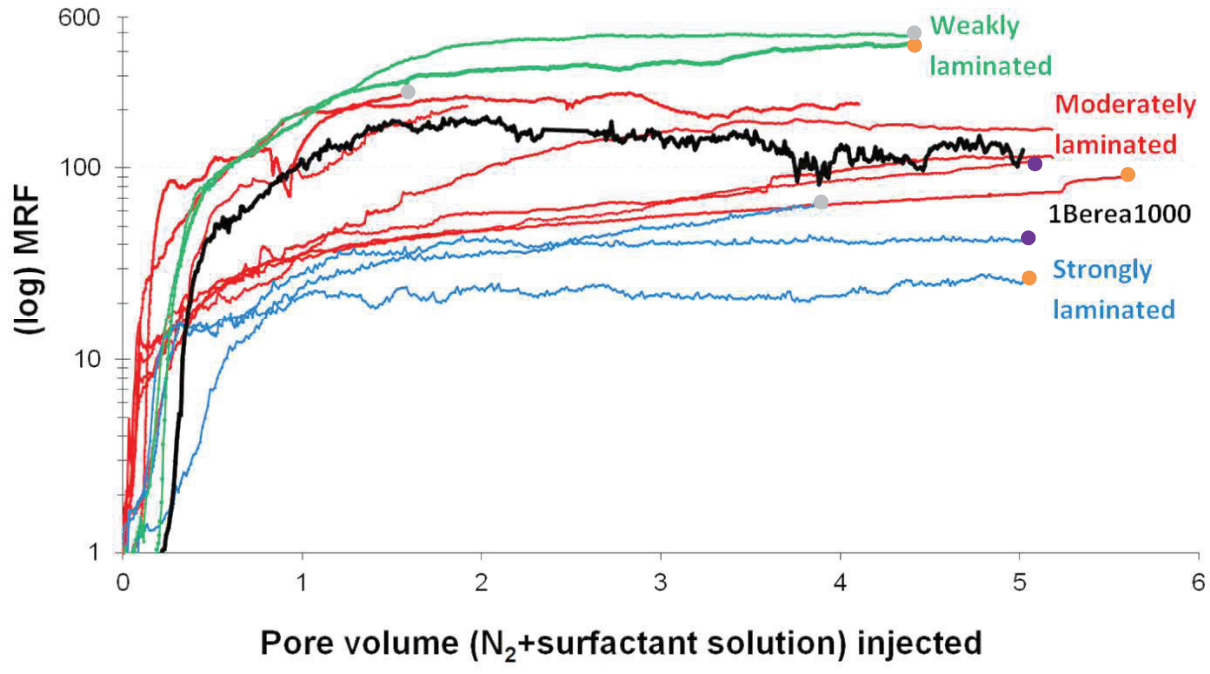

Figure 8.12: Mobility reduction factors obtained during N_2-foam generations on three low permeability laminated core samples under different elevated pressure (30-280 bar) and temperature (50-100°C) conditions. Foam experiments in Berea-weakly laminated core (B-WL), Berea-moderately laminated core (B-ML) and Berea-strongly laminated core (B-SL) are shown by green, red and blue profiles, respectively. The first, second and last experiments on the respective cores are illustrated by orange, purple and gray dots, respectively. The N_2-foam generation at 280 bar and 50°C in a high permeability and relative homogeneous Berea sandstone core sample is included for comparison (i.e., black profile, 1Berea1000, as reported in Paper 1).

Foam/gas breakthrough times:

Figure 8.13 compares the average gas breakthroughs (GBT) observed at the core outlet during the foam generation experiments on the laminated sandstone cores.

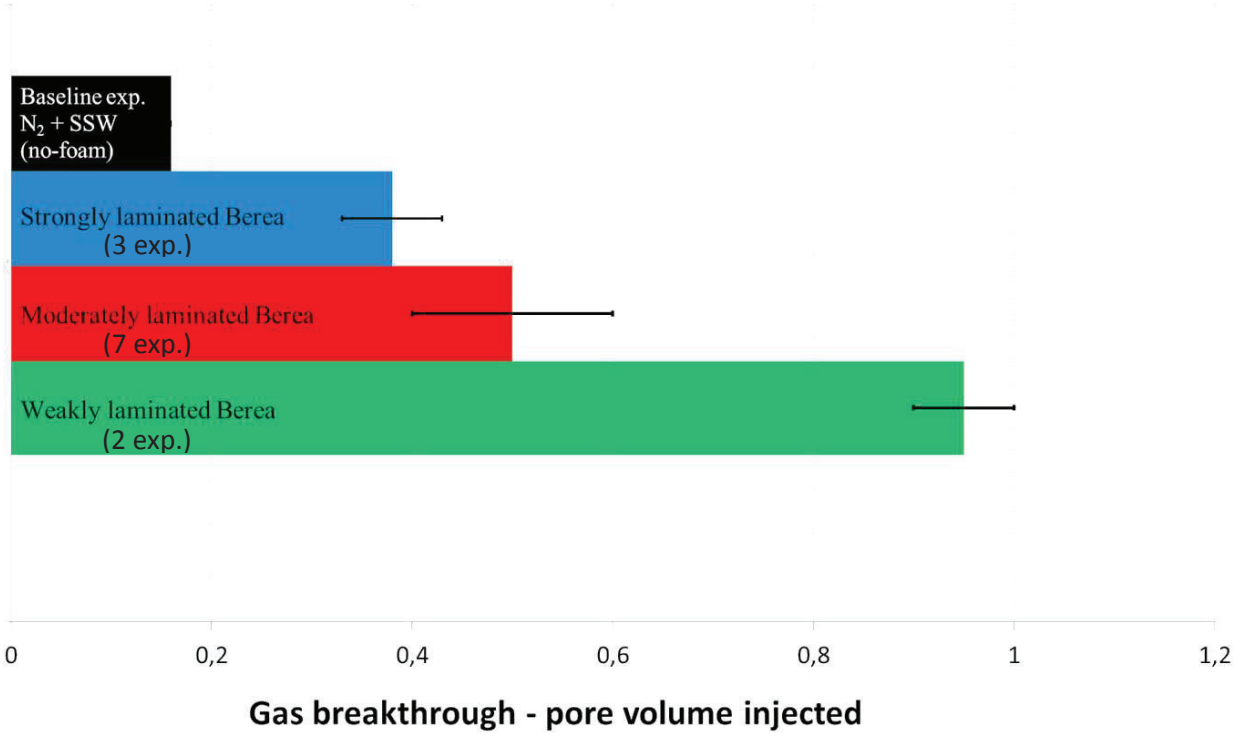

Figure 8.13: Average gas breakthrough times during foam flooding on the laminated core samples. The error bars are added to indicate the variation observed for repeated experiments on the respective core samples. Typical ranges in gas breakthroughs during the baseline experiments (i.e., co-injection of 80% N_2 and 20% seawater without surfactant) are included for comparison.

The main results and observations of foam generation performance in naturally laminated sandstone cores with low permeability under elevated pressure (30-280 bar) and temperature (50-100°C) conditions using AOS surfactant (Figure 8.12-8.13) showed that:

I) In-situ N_2-foam was generated in all the flooded laminated sandstone cores.
II) Large differences in mobility reduction factors (MRF ~ 20-500) and gas breakthrough times (GBT ~ 0.35-1.0 PV injected) were obtained from the three laminated core samples.
III) The presence and the degree of low permeability laminated heterogeneities appeared to be an important parameter that affected the performance of foam for mobility control.

IV) Increased core laminations (B-SL > B-ML > B-WL) resulted in weaker N_2-foams and reduced mobility control as reflected by:

- Less effective pressure build-up profiles (Figure 8.12).
- Lower mobility reduction factors (Figure 8.12).
- Earlier foam/gas breakthrough times (Figure 8.13).

V) Successive stronger foams and poor experimental reproducibility were observed in repeated experiments on the laminated core samples. This behavior was most evident on the core samples with a higher degree of laminations (i.e., B-ML and B-SL). The behavior was also observed regardless of changing experimental parameters (see details and discussion in section 5.5 and 6.2 in **Paper 3**).

VI) In-situ foam generation and strength did not appear to be limited by the low core permeability compared with similar foam generation experiments in Berea sandstone core material with higher permeability. In fact, the steady state MRF value in Berea cores with homogeneous flow behavior and satisfactory experimental reproducibility was higher for the lower permeability core samples (Figure 8.12 and section 6.3 in **Paper 3**).

8.3.4 Summary and discussion

This section summarizes and discusses the main learning outcomes of **Paper 3**:

- The main findings demonstrated that foam properties and performance could be strongly dominated by the rock material used.

The large variations in foam strength and foam performance observed among three laminated heterogeneous cores should motivate more research to improve understanding of foam relative to rock type and internal rock properties. Based on our foam experiments in different outcrop sandstone core material in this thesis, the mobility reduction factors were found to depend on the core material used (e.g., Figure 8.12, figure 6 in **Paper 3** and figure 16 in **Paper 4**). Varying foam properties and performance may reflect the reality in heterogeneous reservoir rock material. Accordingly, it appears to be difficult to discuss foam properties and performance separately from the porous media in which the foam actually resides. Consequently, systematic measurements and comparisons of foam relative to different rock lithologies (e.g., sandstone versus carbonate rock material, or outcrop Bentheimer sandstone versus outcrop Berea sandstone) should be an interesting topic in future studies.

- The main results recognized laminations in the outcrop Berea sandstone cores as a possible parameter that affects the performance of foam for mobility control.

Our results showed reduced mobility control (i.e., less effective pressure build-ups, lower mobility reduction factors and earlier gas breakthroughs) in cores with increased lamination (Figure 8.12-8.13). The rock core analyses demonstrated that the low permeability laminas could serve as barriers to and compartmentalization of foam and fluid flow (Figure 8.11). Based on the rock core analyses, we speculated that decreased cross flow occurs across the low permeability laminas (i.e., increased compartmentalization of foam flow) and faster foam propagation through the more permeable regions of the core with increasing lamination. The degree of cross flow is determined presumably by the permeability contrast (i.e., capillary entry pressure in the lamina) and the foam strength development in the host rock. In the cores with a higher degree of low permeability lamination (i.e., B-ML and B-SL), foam strength development in each compartmentalization might have been too slow/weak to allow foam or gas to enter all of the laminas, which could have led to successive faster foam propagation and reduced foam strength with increasing core lamination.

In the strongly laminated core, 20 pore volumes of surfactant solution were injected prior to foam generation to test whether the foam generation performance could be influenced by the surfactant throughput. The results showed a somewhat faster increase in pressure build-up when 20 instead of 2 pore volumes of surfactant solution were injected prior to foam generation, and the MRF at steady state doubled from ~20 to ~40 (i.e., B-SL, exp. 1 vs. exp. 2 in Figure 8.12). Therefore, a portion of the reduced foam strength and faster foam propagation with increasing lamination could be due to the possibility that surfactant concentration in the lamina was not sufficient because of slow fluid contact.

Efficient generation and uniform foam propagation were indicated in the weakly laminated core. The responses from B-WL are similar to those reported in homogeneous core material, where foam flow in most of the pore space has been observed to occur (Chapter 7, section 7.4.1). The responses from B-WL might indicate selective mobility reduction and "self-regulating" foam behavior (Chapter 4, section 4.7.2).

The mechanisms by which the laminas could have influenced the foam behavior under elevated pressure and temperature conditions in **Paper 3** were not confirmed. Nevertheless,

the recognition of geological structures commonly present in many sandstone petroleum reservoirs to affect foam performance could be relevant to scaling of foam mobility control in field applications, and their physical properties could provide valuable input for realistic reservoir models and simulation. The observation of laminated heterogeneities in the outcrop Berea sandstone should also be relevant to others using similar type of rock material for systematic studies of foam parameters and other enhanced oil recovery (EOR) processes because the laboratory results appear to be strongly controlled or influenced by the particular rock properties and heterogeneities present (see also Chapter 4, section 4.1).

- Foam was not limited in low permeability porous media.

Similar to other work in low permeability porous media, our results confirmed that foam performance was not limited by low permeability. Our results, however, showed that the effectiveness of foam for mobility control in three sandstone cores with similar average permeabilities might be significantly different (Figure 8.12-8.13).

Conflicting results and views exist with respect to foam's dependence on permeability (Chapter 4, section 4.7.1).
A portion of the contradiction in laboratory core flooding findings might be that the foam's dependence on rock permeability is simultaneously sensitive to other parameter as well (e.g., surfactant type, concentration, injection mode, flow rates, foam quality, gas phase, experimental conditions, etc.). In addition, the interaction between rock surface properties (e.g., mineralogy, wettability, pore geometry, small scale heterogeneities, etc.) and the lamellae might be of central importance, but this topic is often complex and difficult to address. Accordingly, it appears to be difficult to isolate the permeability as the only effective and operative parameter, especially in natural porous rocks. Thus, mixing of different rock types to compare the dependence of foam strength on permeability as reported in Bernard and Holm (1964), Lee and Heller (1991), Mannhardt and Novosad (1994) and Yang and Reed (1989) might add extra uncertainty. Interestingly, in studies comparing foam strength as a function of permeability in similar rock type (i.e., Berea sandstone) for fixed surfactant chemistry, stronger foams with decreasing core permeability (in the range of 1200-9 mD) have been indicated (Siddiqui et al., 1997a, Parlar et al., 1995). A similar trend was also noted in this thesis when we compared our previous and recent laboratory results with AOS stabilized N_2-foams in Berea sandstone cores with varying permeability, homogeneous flow

behavior and good experimental reproducibility (i.e., MRF 70 mD > 300 mD > 1000 mD) (**Paper 3**).

Experimental studies on foam flow resistance in smooth capillary tubes have investigated the relationship among gas mobility, foam texture and capillary radius (Hirasaki and Lawson 1985; Falls et al., 1989). Both studies demonstrated increased flow resistance to gas as the bubble radius decreased for a given capillary radius. However, at a fixed bubble radius, the gas flow resistance decreased as the capillary radius decreased (Hirasaki and Lawson 1985). The latter result might make sense considering that the injection of a fixed bubble size could mean that the larger capillaries would contain more bubbles per unit volume than the smaller ones and therefore display increased resistance to gas flow. Unfortunately, these capillaries are normally limited to relatively large capillaries compared with the typical pore sizes found in natural rocks (e.g., Figure B.1 and Table B.3 in the Appendix), and thus, their relevance to porous media may be questioned.

Because foam texture is expected to directly affect the gas mobility in porous media (Chapter 4, section 4.4), a plausible explanation for strong foam in low permeability Berea sandstone cores could be that the bubble sizes decrease with decreasing permeability. Finer textured foam contains more lamellae per unit volume, which might impose a greater resistance for gas to flow. Another explanation could be the trend in aspect ratio indicated for the Berea sandstone, which appears to increase with decreasing permeability (Chapter 4, section 4.2.1). Stronger snap-off events or additional generation sites per unit volume of rock may create more lamellae, which may yield added resistance to gas flow.

Another issue related to the permeability discussion of foam, relates to foam in heterogeneous porous media. The characteristic behavior of foams in heterogeneous reservoirs is their ability to generate and reduce fluid mobility in target layers where fluid flow is favored (i.e., preferentially those with higher permeabilities) (Chapter 4, section 4.7.2). As a consequence of the preferential flow and distribution of fluids in porous media, foam generation must take place in the higher permeability layers before the lower permeability layers; however, this does not mean that foam cannot be generated in the lower permeability layers.

We caution that strong foam in low permeability porous media could be undesirable for the success of foam processes in EOR. Strong foam in low permeability reservoirs might also exert potential risk of reduced injectivity and permanent damage to the formation.

- Detection of rock properties via different types of rock core analyses is important for improved understanding of foam and fluid flow in natural porous media.

Without more complete information concerning the geology, origin and content of natural rocks, it is impossible to precisely predict or interpret the extent to which the properties of the rock might have influenced the laboratory results. Although accurate descriptions of natural rocks require significant effort from several technical disciplines, systematic rock core analysis is necessary to gain insight into the complex system that determines fluid distribution and flow. The outcome of geological information could for instance lead to better interpretation of laboratory measurements and robust flow models. Therefore, close collaboration between geologists and reservoir engineers definitely would be advantageous.

To obtain important information about the rock with a minimum combination of analysis techniques, X-ray CT is recommended. This method is able to detect rock heterogeneities (such as millimeter-thick laminations) and provide visual information about their potential implications for foam and fluid flow.

8.4 Surfactant screening and bulk foam-oil interactions

8.4.1 Experimental strategy

In **Paper 4**, different experimental methods were applied to evaluate and screen a set of surfactants to foam.

The main experiments were conducted in two different bulk tests:
I) The mixer method under ambient conditions (Chapter 7, section 7.2.1).
II) The filter test at 2 bar and room temperature (Chapter 7, section 7.2.2).

Promising bulk results were supplemented with:
III) Core flooding experiments under elevated pressure and temperature conditions (Chapter 7, section 7.4).

The combination of several experimental approaches was introduced to improve the evaluation and selection of suitable foamers.

Standardized experimental procedures were applied in each method to facilitate comparison among different foamers with acceptable reproducibility (detailed experimental descriptions are provided in **Paper 4**). Synthetic seawater (~36,000 ppm TDS) was used as the reference brine in all experiments. The surfactants were used as received and the concentration of surfactant (dissolved in SSW) was held constant at 0.5 wt. % unless otherwise noted.

Table 8.2 provides an experimental overview of **Paper 4**. In summary, the surfactant evaluation included testing both in the absence and presence of oil. A set of surfactants was first evaluated and ranked in the absence of oil. The two best surfactants observed in the absence of oil in part 1 were examined further in the presence of oil in part 2. The particular surfactants that were used in the core flooding experiments passed the two bulk tests with promising results. From surface and interfacial tension measurements, proposed correlating parameters to foam stability in the presence of oil were calculated (i.e., entering (E), spreading (S), and bridging (B) coefficients and lamella (L) numbers), and their predictive abilities against the bulk experiments with oil were evaluated.

Table 8.2: Experimental overview (Paper 4)

Experimental methods:	Part 1 – Without oil:	Part 2 – With oil:
Mixer method (ambient conditions)	12 surfactants tested with air	2 surfactants tested against 5 crude oils (1-5 wt.%) and 4 alkanes (3 wt.%) - air
Filter test (2 bar)	8 surfactants tested with N_2 8 surfactants tested with CO_2	2 surf. tested - 4 crude oils/4 alkanes (3 vol.%) - N_2 2 surf. tested - 4 crude oils (3 vol.%) - CO_2 1 surf. mix - 2 crude oils (3 vol.%) - CO_2
Foam core flooding (HPHT)	1 surfactant tested against CO_2 and N_2, varying pressure, temperature and in different core material (**Papers 1-4**).	2 surfactants tested against 3 crude oils (S_{orw}) - N_2 (Vikingstad et al., 2009)
Surface/interfacial tension properties	Surface tension to air: 8 surfactants - air (22°C, atm.) 2 surfactants - air (50°C, atm.)	Calculation of S, E, B and L: 2 surfactants - 5 crude oils – air (22 and 50°C, atm.) 1 surf. mix - 2 crude oils - air (22°C, atm.)

8.4.2 Surfactant screening in the absence of oil

The first section of the **Paper 4** (i.e., page 16-33) focused on surfactant screening in the absence of oil. The main objectives involved evaluation and comparison of surfactant/foam properties and performance related to:

I) Various bulk foam tests (i.e., mixer method vs. filter test).
II) Different gas phases (i.e., air- vs. N_2- vs. CO_2-foams).
III) Bulk foam properties versus foam properties in porous media (i.e., **Paper 4** vs. **Papers 1-3**).

A total of 12 surfactants from six different manufacturers were tested initially (see Table A.1 in the Appendix at page 181 or table 1 in the **Paper 4**). Most of the surfactants were recommended by their vendors or reported in the literature as viable candidates for foaming relative to different EOR applications (e.g., mobility control of CO_2).

All surfactants were evaluated and ranked in bulk tests based on their foamability and foam stability properties (defined in Chapter 7, section 7.2).

The following criteria were used to rank surfactants in the mixer method:

Good foamability:	Foam height, h ≥ 15 cm after mixing.
Good stability:	Foam height, h ≥ 10 cm for more than 24 hours.
Moderate foamability:	Foam height, 15 cm > h ≥ 10 cm after mixing.
Moderate stability:	Foam height, 10 cm > h > 5 cm at 12-24 hours.
Poor foamability:	Foam height, h < 10 cm after mixing.
Poor stability:	Foam height, h ≤ 5 cm at 0-12 hours.

The following criteria were used to rank surfactants in the filter method:

Good foamability:	< 350 ml of gas injected to reach a 10 cm (100%) foam height.
Good stability:	Foam height, h ≥ 7 cm for more than 24 hours.
Moderate foamability:	In the range of 350-650 ml of gas injected to reach 10 cm
Moderate stability:	Foam height, 7 cm > h > 5 cm at 12-24 hours.
Poor foamability:	> 600 ml of gas injected to reach 10 cm.
Poor stability:	Foam height, h ≤ 5 cm at 0-12 hours.

The listed criteria were defined in this thesis based on earlier experiences and other surfactant screening studies using similar test methods/procedures (Aarra and Skauge, 1994; Andrianov et al., 2011; Mannhardt et al., 2000; Rohani et al., 2014; Vikingstad, 2006). The time scale for monitoring of foam stability in **Paper 4** (i.e., 24 hours) was somewhat extended compared with the time scale normally reported (i.e., usually less than 6 hours).

Surfactant ranking:

Table 8.3 provides a ranked summary of the selected surfactants based on their performances in the various bulk tests. The specific experimental results are reported in **Paper 4** (starting on page 16).

Table 8.3: Surfactant ranking summary in the absence of oil for various bulk tests and gas phases. Good, moderate and poor foamers/foaming properties are shown in green, orange and red, respectively.

Mixer method – air (ambient)		**Filter test - N_2 (2 bar)**		**Filter test - CO_2 (2 bar)**	
Foamability	**Stability**	**Foamability**	**Stability**	**Foamability**	**Stability**
1) AOS C14-16	1) FS-500	1) AOS C14-16	1) FS-500	1) FS-500	1) FS-500
2) AOS C12-14	2) AOS C14-16	2) Witcolate	2) AOS C14-16	2) AOS C14-16	2) AOS C14-16
3) FS-500	3) AOS C12-14	3) FS-500	3) Witcolate	3) AOS C12-14	3) AOS C12-14
4) Witcolate	4) Neodol 25-7	4) AOS C12-14	4) AOS C12-14	4) Witcolate	4) N-120
5) Neodol 25-7	5) Neodol 23-12	5) N-150	5) N-120	5) N-120	5) Witcolate
6) Neodol 23-12	6) Witcolate	6) N-120	6) J771	6) N-150	6) N-150
7) N-120	7) N-120	7) J771	7) N-150	7) J771	7) J771
8) N-150	8) N-150	*8) Novomer	*8) Novomer	*8) Novomer	*8) Novomer
9) J771	9) J771				
*10) Novomer	*10) Novomer				

* No foam generated

The AOS $_{C14-C16}$ surfactant (delivered as powder) and the fluorinated FS-500 surfactant were observed as the two best foamers overall. The foams generated with these surfactants exhibited good foamability and long-term foam stability in both bulk tests and against all three different gas phases (see experimental results in figure 5-10 in **Paper 4**). Good

performance in bulk tests with similar types of surfactants was also reported in Aarra and Skauge, (1994) Andrianov et al., (2011) Mannhardt et al., (2000) and Vikingstad (2006).

General observations:

I) All surfactants (except one) were able to generate foam in both bulk tests and against all three different gas phases (i.e., air, N_2 and CO_2). It was observed that certain foamers produced more foam than others and that the generated foams exhibited different stabilities. Visual observations indicated that the different foam stabilities could be related to different rates of liquid drainage, bubble coarsening and film rupture over time. However, these factors were not examined further in detail.

II) Foam stability with same type of alpha-olefin sulfonate (AOS) surfactant but from different batches or manufacturers were observed to vary. Because all surfactants were applied in the grade of purity received, it is possible that they could contain residual traces of surface active impurities that could influence the performance of the surfactant. This might also influence the properties of the foams generated. It is known that the sulfonation process of alpha-olefins could include a variety of reaction products, i.e., trace amounts of alkene disulfonates, hydroxyalkane disulfonates and unreacted alpha olefins (Foster, 1997; Sivak, 1982).

III) None of the evaluated surfactants produced better foam properties with CO_2 as the gas phase than with N_2 (g). Thus, this result supports the general characterization of CO_2-foam in porous media as "weaker" compared with N_2-foam (**Paper 1-3**, Chapter 5).

Effect of gas phase:

I) Surfactants that were specifically recommended for CO_2-foam performed poorer with CO_2 (g) than the conventional surfactants (figure 9-10 in **Paper 4**). In fact, none of the evaluated surfactants performed better with CO_2 as the gas phase compared with N_2 (g), which is consistent with the bulk experiments and observations reported by Phillips et al. (1987) and Alkan et al. (1991).

II) Additional bulk tests were conducted to investigate whether poorer bulk foam properties in the presence of CO_2 could be attributed to the lower pH environment or higher solubility between CO_2 and water compared with that of N_2 and water. Surface tension values were also

discussed. It appeared that none of these parameters were able to solely predict the difference between CO_2-foam and N_2-foam in bulk under reduced experimental conditions (page 21-28 in **Paper 4**). The consistent trend observed by varying the gas phase using various types of surfactants suggests that the apparent weakness of CO_2-foam compared with N_2-foam could be related to a fundamental difference in surfactant characteristics at the various gas-liquid surfaces.

III) The use of air versus nitrogen did not appear to have any significance to the surfactant performance in bulk under the experimental conditions because the rankings (i.e., air-foams vs. N2-foams in Table 8.3) were quite similar.

Mixer method vs. filter test:

I) Comparing the two types of bulk foam tests, relatively similar surfactant rankings were observed (i.e., air-foams vs. N_2-foams in Table 8.3). This result provides a positive confirmation with respect to bulk screening decisions in the absence of oil and a validation of the new test method (i.e., filter test) applied.

II) A significant advantage of the filter test compared with the mixer method is that it allows the study of foam with gas phases other than air. This option is important because surfactant requirements against CO_2 and other gas phases might be different from those of good foamers found with air.

Bulk foam properties compared with foam properties in porous media:

The bulk tests applied in this thesis yield two types of foam properties, i.e., foamability under dynamic conditions and stability of static foam. Intuitively, both properties could also be relevant to foam in porous media where the ease of foam generation (a dynamic process) and foam stability after placement (under more static conditions) are usually key properties in the assessment of in-situ foam performance. Interesting observations of the studies of bulk foam properties (**Paper 4**) and foam properties in porous media (**Papers 1-3**) in this thesis showed that:

I) The characterization of CO_2-foam as "weaker" compared with N_2-foam was observed both in porous media under elevated pressure and temperature conditions and in the filter test at a pressure of 2 bar.

II) The $AOS_{C14-C16}$ surfactant exhibited good and robust N_2/air-foam properties in the absence of oil from basic surfactant screening in two different bulk tests, to core flooding experiments under elevated pressure and temperature.

Although certain similarities and trends were observed between experiments in bulk and porous media using AOS $_{C14-C16}$ surfactant, the foam performance in the core floods of this thesis did not generally correlate with the foam performance in bulk. Possible reasons for this observation are described as follows:

III) The measured bulk foam properties (i.e., foamability and foam stability) provide little information about foam generation performance, foam strength, foam propagation or gas/water blocking abilities in porous media. Part of this might be due to the fact that different mechanisms dominate foam in bulk and in porous media (Chapters 3-4). Another reason appears to be the complexity and diversity of natural porous rocks (e.g., lithology, wettability, pore geometry, capillarity and heterogeneity), which cannot be satisfactorily imitated by any of the bulk tests that are currently available, according to our knowledge. From the foam experiments performed in different outcrop sandstone core materials in this thesis, the dependence of the rock material on foam performance was demonstrated (e.g., Figure 8.12 in section 8.3.3, **Paper 3** and figure 16 in **Paper 4**). Accordingly, it appears difficult to predict foam properties and performance separately from the actual porous media.

IV) The low pressure bulk tests cannot reflect the special properties and features of CO_2 under elevated pressure and temperature conditions (Chapter 5, section 5.4), which appear to be important in explaining the varying CO_2-foam performance obtained in porous media in **Papers 1-2** with pressure and temperature. Additionally, conflicting results on the effects of pressure and temperature on CO_2-foam properties exist between bulk studies and laboratory core floods in the literature (Chapter 5, section 5.6). Thus, another reason for believing that there is fundamental differences between foam properties in bulk and in porous media.

V) Based on our current experience with foam using different experimental approaches, we recommend that surfactant screening should be performed in porous media under elevated pressure and temperature conditions (e.g., with representative CO_2 characteristics) for a better evaluation of surfactants. However, note that the porous media used for surfactant screening should be carefully selected. A subjective ranking of surfactants in natural porous media (e.g.,

solely based on the MRF) could be misleading because foam performance in natural rocks may depend on parameters other than just the surfactant intended to test. Ultimately, to evaluate foamers/foams for field applications, it is necessary to perform experiments under reservoir conditions on rock material taken directly from the target reservoir.

8.4.3 Bulk foam-oil interactions

In the second part of **Paper 4** (i.e., page 34-56), we investigated the effect of oil on bulk foam. The main objectives included evaluation and comparison of bulk foam-oil interactions relative to:

I) Various bulk tests (i.e., mixer method vs. filter test with oils).
II) Different gas phases (i.e., air-, N_2 and CO_2-foam in the presence of oil).
III) Various types of oils and concentrations (i.e., crude oils and alkanes).
IV) Proposed correlating parameters to foam stability in the presence of oil (i.e., entering (E), spreading (S), and bridging (B) coefficients and lamella (L) numbers).
V) Earlier bulk foam-oil interaction studies performed at UniCIPR (i.e., **Paper 4** vs. Vikingstad, (2006)) and other relevant literature.

The oils that were applied in the experiments included five crude oils taken from five different oil reservoirs in the North Sea (denoted A-E), and the alkanes pentane (C_5H_{12}), octane (C_8H_{18}), decane ($C_{10}H_{22}$) and hexadecane ($C_{16}H_{34}$). The physical properties of the crude oils are summarized in the Appendix section A.

The evaluated surfactants were $AOS_{C14\text{-}C16}$ and fluorinated FS-500. The choice of foamers was based on their positive results in the absence of oil (Table 8.3). The same criteria as defined in the previous section (8.4.2) were used to evaluate and rank the foamers in the presence of oil.

Surfactant ranking:

Table 8.4 provides a ranked summary of the $AOS_{C14\text{-}C16}$ and the fluorinated FS-500 surfactants based on their general performance in the different bulk tests in the presence of various oils and gas phases. A combination of 0.4 wt.% $AOS_{C14\text{-}C16}$ and 0.1 wt.% FS-500 surfactant was also tested specifically against CO_2 gas (i.e., AOS+FS (4:1) in the table). The

experimental results that support the summary in Table 8.4 are reported in figure 17-27 (mixer method) and figure 28-43 (filter test) in **Paper 4**.

Table 8.4: Surfactant ranking summary in the presence of oil for various bulk tests, gas phases and oils. Good, moderate and poor foamers/foaming properties are shown in green, orange and red, respectively.

Mixer method - air/oils (ambient)		**Filter test - N_2/oils (2 bar)**		**Filter test - CO_2/oils (2bar)**	
Foamability	**Stability**	**Foamability**	**Stability**	**Foamability**	**Stability**
1) FS-500 2) AOS C14-16	1) FS-500 2) AOS C14-16	1) FS-500 2) AOS C14-16	1) FS-500 2) AOS C14-16	1) FS-500 2) AOS+FS (4:1) 3) AOS C14-16	1) FS-500 2) AOS+FS (4:1) 3) AOS C14-16

I) The overall ranking of the surfactants from the two different bulk tests were found to be consistent: 1) FS-500, 2) $AOS_{C14-C16}$.

II) The mixture of $AOS_{C14-C16}$ and FS-500 surfactant demonstrated improved bulk foam properties against two crude oils and CO_2 gas compared with that of 0.5 wt.% AOS surfactant only (figures 41 and 42 in **Paper 4**).

Enhanced foam performance in the presence of oil using different types of fluorinated surfactants (or in combination with other surfactants, e.g., alpha-olefin sulfonates) has also been demonstrated by several other researchers, both in bulk tests and in laboratory corefloods under different experimental conditions (Aarra and Skauge, 1994; Andrianov et al., 2011; Basheva et al., 2000; Bian et al., 2012, Chabert, 2013; Dalland et al., 1992;

Mannhardt et al., 1996, 2000; Raterman, 1989; Schramm and Novosad, 1990; Simjoo et al., 2013b; Suffridge et al., 1989; Vikingstad, 2006; Vikingstad and Aarra, 2009).

General observations:

I) In general, the presence of oil was shown to reduce the surfactant performance compared with that in the absence of oil (i.e., reduced foamability and foam stability). The influence of oil ranged from unaffected (in the case of the fluorinated surfactant) to oil-sensitive (in the case of the AOS surfactant). Nevertheless, both surfactants were able to generate (at least some) foam in the presence of all oils under all of the different experimental conditions applied.

II) The FS-500 foams showed robustness in all tests in the presence of oil, consistent with the calculated S, E and B coefficients and L numbers (discussed later in Table 8.5).

III) The bulk foam properties with the AOS surfactant showed sensitivity to the various bulk tests, gas phases, oil types and concentrations applied. Correlations between the bulk foam stability and the calculated S, E, B and L values for the AOS surfactant were ambiguous (discussed in Table 8.6).

IV) Improved oil tolerance with the AOS surfactant was shown in the filter test (compared with the mixer method, Table 8.4) using N_2-gas (compared with CO_2, Table 8.4), when mixed with FS-500 surfactant (AOS+FS (4:1), Table 8.4 and 8.7), under elevated temperature (in terms of the calculated S, E, B and L parameters at 50 vs. 22°C, Table 8.6) and in foam flooding experiments under elevated pressure and temperature (compared with the mixer method under ambient conditions; see details in **Paper 4** page 53). This improved performance, especially from the latter two conditions, should gain further attention for this surfactant in applications under reservoir conditions.

V) The oil configurations in the foam varied between the glass boundary and the interior of the foam (i.e., in the lamellae not anchored to the glass wall). At the glass, thick oil-filled liquid films were observed independent of the oil phase and surfactant type used. In the interior, most oils indicated a greater tendency to enter and spread the foam films stabilized with $AOS_{C14\text{-}C16}$ surfactant compared with those with the FS-500 surfactant (Figure 8.14a vs. 8.14b). In general, the foams were more stable when the oils did not spread, but foams with

spreading oils could also be very stable (Figure 8.14c). Therefore, spreading of oil alone did not appear to be an adequate reason for detrimental foam stability in the presence of oil (see also figure 22, 26, 32, 35, 40, 43 in **Paper 4**). The pseudo-emulsion film theory has been used as an explanation for stable foam in the presence of emulsified/spreading oils (Chapter 6, section 6.2.4). Because measurements on this film were not performed in this thesis, it is possible that the properties of this film might have played an important role on foam stability using the AOS surfactant and the AOS+FS surfactant mixture.

VI) The general trends found in **Paper 4** (part 2) confirm analogous work by Vikingstad, (2006) using similar surfactants, solutions and oils with a new set of results and experimental approaches.

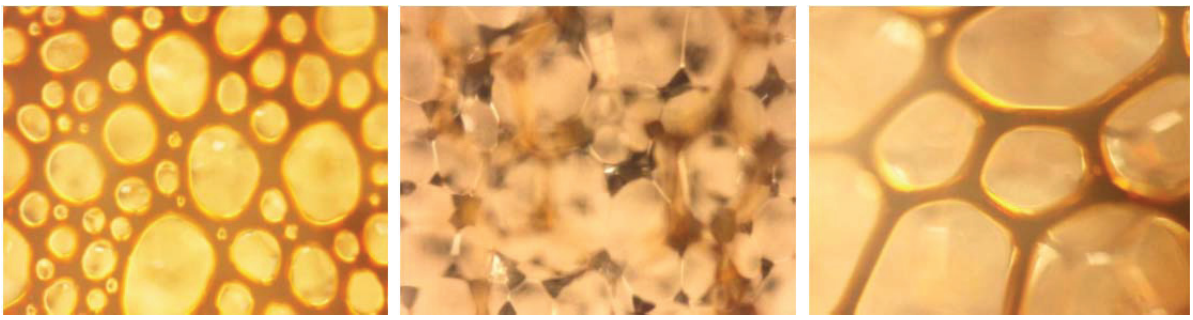

a) b) c)

Figure 8.14: Images of bulk CO_2-foam-oil interactions in the filter test at 2 bar with 3 vol.% of crude oil C: a) AOS-foam immediately after generation. The oil spreads within the lamellae. The foam was completely broken down after less than 2 hours; b) FS-500-foam 24 hours after generation. The oil is non-spreading and primarily situated as wedges in the plateau borders. The foam was stable for more than a week; c) AOS+FS (4:1) surfactant mixture 24 hours after generation. The oil is spreading but the foam remained stable for more than a week.

Effect of alkanes:

AOS surfactant: Short-chained alkanes (i.e., heptane, octane and decane) tended to inhibit foamability to a greater extent and display stronger destabilizing effects on foams than the longer-chained alkanes (i.e., hexadecane) (figure 23, 30 and 31 in **Paper 4**). All foams with alkanes were broken down within 15 hours. This trend was indicated in both bulk tests and is consistent with the observations from other bulk foam studies using anionic surfactants (e.g., Andrianov et al. (2011), Arnaudov et al. (2001), Aveyard et al. (1993), Ceglie et al., (1987);

Denkov (2004), Kuhlman (1990), Rohani et al. (2014), Suffridge et al. (1989) and Vikingstad et al. (2005), (2006)).

FS-500 surfactant: Similar bulk foam properties were obtained in the presence and absence of alkanes (figure 27 in **Paper 4**). With pentane, the foam height was twice as high as that in the absence of oil. Similar general observations from pentane and alkanes were also reported by Vikingstad (2006).

Effect of crude oils:

AOS surfactant: Foamability in the mixer method appeared to be dominated by the amount and type of crude oil present (figure 17-21 in **Paper 4**). The results with 1 wt.% crude oil showed the best foamability, although most of the foams were broken down within 10 hours. In similar experiments with 3-5 wt.% crude oil, foam heights of 2-4 cm were typically observed. With crude oil A, which was the most viscous oil, poor foamability was observed regardless of the amount of oil added. However, the low foam heights remained in the cylinder for many hours. We found it reasonable to describe all of the AOS foams with crude oils in the mixer method as quite unstable, despite the observation that the relative change in foam height with time for 3-5 wt.% crude oil was not always significant.

Foamability with the AOS surfactant in the filter test also appeared to be influenced by the type of oil (figure 28 and 33 in **Paper 4**). The amount of crude oil in this test was held constant at 3 vol.%. Compared with the mixer method, the results from the filter test using nitrogen as the gas phase demonstrated good foamability with all crude oils. Moderate to poor foaming abilities were observed for the same crude oils and CO_2. Interestingly, the oil type with AOS foams also appeared to depend on the gas phase present. In our case, reduced foaming and foam stability were observed for all the crude oils with CO_2-gas compared with N_2 (figure 28 and 29 vs. figure 33 and 34 in **Paper 4**). The oil type on foam was generally more sensitive using CO_2-gas, as reflected by a larger scatter in the bulk foam properties with CO_2 versus N_2. We found it reasonable to describe the AOS foams in the filter test with crude oils as moderately stable with nitrogen gas but unstable with carbon dioxide (Table 8.4). However, AOS foams with crude oil A and E showed good stability with nitrogen (> 24 hours), and the foam height with crude oil C and CO_2 was only halved after 16 hours (i.e., moderate stability according to our ranking criteria on page 158).

FS-500 surfactant: The generated FS-500-foams demonstrated good foaming and stability properties in both bulk tests in the presence of various crude oils and concentrations. In fact, the results in the presence of oil were usually quite similar to those in the absence of oil (figure 24, 25, 36, 37, 38, 39 in **Paper 4**). Even a reduction in the surfactant concentration to 0.1 wt.% appeared to have only minimal effects on foaming and foam stability with the FS-500 surfactant in the presence of one crude oil (figure 25 in **Paper 4**).

The reasons for the differences due to alkanes and crude oils were not investigated further, but it is evident that the type of oil can strongly affect bulk foam properties.

Effect of gas phase:

The AOS surfactant showed decreased foamability and foam stability with the same oils if CO_2 was used as the gas phase instead of N_2 (figure 28 vs. 33 and figure 29 vs. 34 in **Paper 4**).

For the FS-500 surfactant, the foamability was somewhat decreased with CO_2 compared with that using N_2, but the foam stabilities were quite similar regardless of the gas phase (figure 36 vs. 38 and figure 37 vs. 39 in **Paper 4**).

The reasons for the different effects of the gas phase on the bulk foam properties in the presence of oil were not investigated further, but evidently the gas type can also affect the foam-oil interactions. Accordingly, to improve surfactant evaluation/screening with oil, it is advisable to use the intended gas phase, even in bulk tests under reduced experimental conditions.

S, E, B and L:

The calculated spreading, entering and bridging coefficients and lamella numbers (i.e., S, E, B and L, respectively) for all crude oils are summarized in Table 8.5 for the fluorinated FS-500 surfactant, in Table 8.6 for the $AOS_{C14-C16}$ surfactant and in Table 8.7 for the AOS+FS surfactant mixture. The measured surface/interfacial tension properties used in these calculations are tabulated in Table A.4 in the Appendix. Air was always used as the gas phase. The equations for calculation of S, E, B and L and the theory behind these parameters are described in Chapter 6 (Eq. 6.1-6.4).

Table 8.5: S, E, B and L - FS-500 surfactant

Crude oil	Spreading (S)	Entering (E)	Bridging (B)	Lamella (L)
A	**- 16.6** (- 21.9) - 16.3	**- 12.6** (-10.1) - 11.7	**- 676** (- 776) - 600	**1.2** (0.4) 1.0
B	**- 14.8** (- 8.3) - 12.3	**- 4.2** (- 1.7) - 2.6	**- 362** (- 164) - 245	**0.4** (0.7) 0.4
C	**- 16.5** (- 15.0) - 15.7	**- 4.9** (- 5.4) - 5.1	**- 423** (- 403) - 384	**0.4** (0.5) 0.4
D	**- 12.0** (- 6.3) - 11.2	**- 7.6** (3.1) - 6.6	**- 405** (- 29) - 334	**1.1** (0.5) 0.9
E	**- 14.4** (- 8.9) - 12.6	**- 5.6** (- 2.9) - 5.6	**- 401** (- 204) - 336	**0.5** (0.8) 0.6

Values in black represent the calculated parameters at 22°C and atmospheric pressure from this thesis.
Values in (grey) denote the calculated parameters from Vikingstad, (2006) at 22°C and atm. pressure using a similar surfactant solution and crude oils but from different batches.
Values in red are the calculated parameters at 50°C and atmospheric pressure from this thesis.

FS-500 surfactant: All of the calculated parameters for the fluorinated surfactant indicated stable foam according to the theory, as reflected by large negative coefficients and lamella numbers close to or less than 1. The bulk foam experiments were consistent with the calculated parameters, thus demonstrating long-term foam stability (> 24 h) in both test methods with all crude oils (Table 8.4). The oil configurations in the foam texture in bulk were clearly non-spreading in all tests (e.g., Figure 8.14b). Accordingly, a good correlation between the theory and the bulk foam experiments with oil was shown with this surfactant. The trends and values are consistent with those from similar experiments by Vikingstad (2006). Increasing the temperature from 22°C to 50°C (i.e., red values in the table) indicated a slightly negative trend in the parameters, i.e., most of the S, E, and B coefficients became less negative. However, the values were still clearly in line with the theory of stable foam.

Table 8.6: S, E, B and L – $AOS_{C14-C16}$ surfactant

Crude oil	Spreading (S)	Entering (E)	Bridging (B)	Lamella (L)
A	**- 2.0** (- 5.9) - 6.6	**- 1.6** (- 5.0) - 6.1	**- 107** (- 337) - 321	**22.7** (9.5) 13.4
B	**2.7** (4.6) - 0.5	**3.7** (5.6) 1.1	**172** (250) 16	**8.4** (8.1) 5.1
C	**1.6** (- 3.2) - 3.4	**2.6** (- 0.4) - 2.0	**117** (- 85) -127	**8.2** (2.5) 5.0
D	**2.5** (4.7) - 1.9	**3.5** (7.9) - 0.5	**164** (303) - 54	**9.0** (2.5) 4.5
E	**2.2** (4.2) 2.3	**3.4** (5.6) - 0.5	**154** (241) - 64	**7.4** (5.8) 7.4

Values in black represent the calculated parameters at 22°C and atmospheric pressure from this thesis.
Values in (grey) denote the calculated parameters from Vikingstad, (2006) at 22°C and atm. pressure using a similar surfactant solution and crude oils but from different batches.
Values in red are the calculated parameters at 50°C and atmospheric pressure from this thesis.

AOS surfactant: Correlations between the calculated parameters and bulk foam stability using the $AOS_{C14-C16}$ surfactant were not as evident. Most coefficients were positive for most of the crude oils, and the high lamella numbers indicated foams with poor stability. The AOS foam with crude oil A predicted the best compatibility with reference to negative S, E and B coefficients, but in contrast, the lamella number with this oil was the highest of all the crude oils used. Based on the calculated parameters, (at best) moderate to unstable foams were expected with the AOS surfactant in the presence of these crude oils. From the experiments in the mixer method, low foam heights (i.e., h < 5 cm) were displayed with all of the crude oils and different concentrations after less than 6 hours (figure 17-21 in **Paper 4**). The oil configurations in foam showed clear spreading in all experiments (e.g., figure 22 in **Paper 4**). The low bulk foam heights experienced with the crude oils compared with those in the absence of oil were therefore in line with the calculated S, E, B, and L values (i.e., blue values in Table 8.6).

Similar to the results from the mixer method, the filter test using nitrogen gas also indicated poor foam stability with crude oil C and D. However, good foam stability was shown with crude oil A and E (figure 29 in Paper 4), which was not consistent with the calculated values.

An interesting and opposite effect on the calculated parameters occurred when the temperature was increased from 22°C to 50°C with the AOS surfactant compared with that of the FS-500 surfactant (i.e., red values in Table 8.6). The improved performance for the AOS surfactant, which turned the S, E, B and L values towards lower and more negative values with increasing temperature, should garner further attention for this surfactant for applications under reservoir conditions.

Table 8.7: S, E, B and L – $AOS_{C14-C16}$ + FS-500 (4:1) surfactant mixture

Crude oil	Spreading (S)	Entering (E)	Bridging (B)	Lamella (L)
A	**- 11.9** (-2.0)	**- 11.7** (-1.6)	**- 583** (-107)	**23.5** (22.7)
C	**- 8.2** (1.6)	**- 7.6** (2.6)	**- 359** (117)	**9.4** (8.2)

Values in black are the calculated parameters for the surfactant mixture at 22°C and atmospheric pressure from this thesis. Values in (blue) are the calculated parameters for the AOS surfactant only (from Table 8.6).

AOS+FS (4:1) surfactant mixture: The improved CO_2-foam stabilities that were demonstrated with the surfactant mixture against two crude oils and CO_2 (g) were consistent with the calculated S, E and B coefficients, indicating large negative values (although air was used as the gas phase in Table 8.7). However, the high lamella numbers predicted strongly emulsifying oils, an indicator of poor foam stability according to the lamella number theory (Chapter 6, section 6.2.3). Emulsifying/spreading oils in the bulk experiments were clearly observed (Figure 8.14c), but the foam remained stable for more than a week. Consequently (and generally in this study), the lamella number was found to have poor predictive power because good foam stability was observed with values ranging from 0.4 to 23.5. The improved oil tolerance was questioned with respect to the pseudo-emulsion film theory (Chapter 6, section 6.2.4) and the degree of collective contribution from the two surfactants (because 0.1 wt.% FS-500 surfactant performed equally well alone compared with higher surfactant concentration and without the AOS surfactant). The combination of surfactants with positive foam properties should be an interesting topic for future studies, e.g., against dense supercritical CO_2.

General remarks about the S, E, B and L parameters:

I) The variation in the spreading, entering and bridging coefficients among the AOS and the FS-500 surfactant were basically caused by the differences in surface tension (ST) between these two surfactants. The surface tension between the AOS solution and air at ambient conditions was 28.8 mN/m, while it was 16.0 mN/m for the FS-500 solution and air (Table A.4 in the Appendix). Due to the perfluoroalkyl-group, fluorinated surfactants can have a greater potential for reducing the surface tension of water than commonly used surfactants, as noted by Dalland et al. (1992), Mannhardt et al. (2000) and Vikingstad et al. (2006). The higher lamella numbers that were observed with the AOS surfactant compared with the FS-500 surfactant were mainly a result of the consistent lower interfacial tension (IFT) values measured between the AOS solution and oils (i.e., $\sigma_{w/o\ (AOS/oils)}$ = 0.19-0.86 mN/m compared with $\sigma_{w/o\ (FS\text{-}500/oils)}$ = 2.02-5.83 mN/m, from Table A.5 in the Appendix). The greater tendency for oils to be emulsified/spread into the lamellae in AOS foams compared with the FS-500 foams might be due to the prior differences in IFT values between the two surfactants and the crudes.

II) Small variations in the surface/interfacial tension values cause large differences in these parameters. Hence, the accuracy of these measurements is important. It therefore may seem

especially challenging to predict the foam stability in the presence of oil when the coefficients are close to zero (± 3).

III) The proposed parameters that are evaluated in the literature are usually based on measurements of static tension values. From a practical viewpoint, the surface/interfacial tensions can change with time after an initial oil phase has been introduced. Because of this, it is difficult to predict how active the oil could be (i.e., degree of foam destabilization with time) solely based on the static values. Foam experiments with oil should therefore be considered more carefully in terms of the time scale. The time scale of foam stability monitored in **Paper 4** (i.e., 24 hours) was somewhat extended compared with that normally reported for similar bulk studies (i.e., usually less than 6 hours) (Aarra and Skauge, 1994; Andrianov et al., 2011; Mannhardt et al., 2000; Rohani et al., 2014; Vikingstad, 2006). The additional duration of the bulk foam experiments in this study demonstrated, among others, that the foam stability can vary significantly even when the oil was measured to be thermodynamically capable of breaking the films (i.e., E, S and B > 0 and L > 1). The bulk foam structure illustrated in Figure 8.15 was, for instance, completely broken down after 10 hours. The time scale of foam stability should also be an important parameter to consider in reservoir applications.

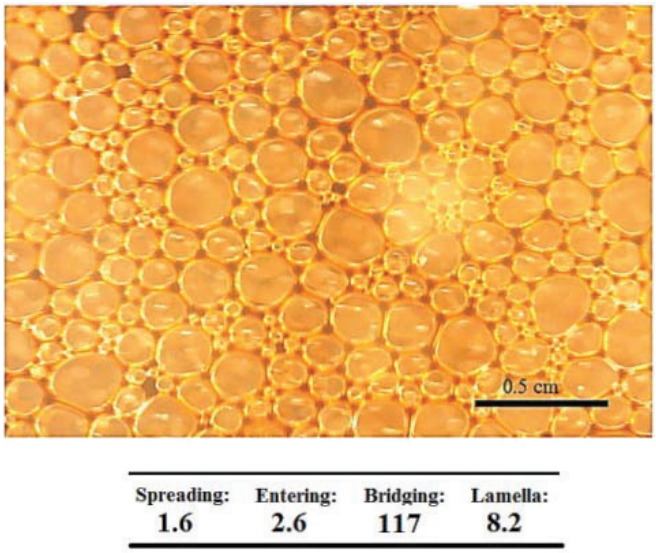

Figure 8.15: Image of an apparently stable bulk foam structure with emulsified crude oil present within the lamellae. The calculated parameters predict unstable foam according to the theory. The image was taken 2 hours after generation in the filter test ($AOS_{C14-C16}$ surfactant, N_2-gas, 3 wt.% with crude oil C).

Mixer method vs. filter test (vs. porous media):

I) In the two bulk tests used in **Paper 4**, the oil was introduced to the foam in different ways. In the mixer method, the oil phase was dispersed into the foam during mixing. In the filter test, the foam was generated before contact with the oil phase. The results indicate that for similar oils, the oils were less harmful to foam in the filter test than in the mixer method.

II) A concrete example related to point I was demonstrated with the AOS surfactant. The mixer method indicated poor foaming in the presence of more than 1 wt. % with any of the crude oils (figure 17-21 in **Paper 4**), while the filter test showed that the max foam height (i.e., 10 cm) could be achieved in virtually all bulk foam experiments with the same crude oils (figure 28 and 33 in **Paper 4**). The results of the varying foamability observed from the two bulk tests are interesting because it suggest that the foam performance in the presence of oil could be dependent on the way the foam and oil come into contact.

III) The dependence of how the foam and oil come into contact on bulk foam properties may also have relevance to foam-oil contact in porous media. For instance, foam studies in porous media have indicated foam to be more efficient when generated; in oil-free parts of the core before contact with oil (Andrianov et al., 2011; Farajzadeh et al., 2010); after miscible CO_2-flooding in dual core floods (Bian et al., 2012; Casteel and Djabbarah, 1988; Di Julio and Emanuel, 1989); and in HPHT core flooding experiments with residual oil compared to the mixer method (Aarra et al., 1994; Holt et al., 1996; Mannhardt et al., 2000; Vikingstad et al., 2009).

The latter results indicate that the mixer method at ambient conditions is not a representative method for describing foam-oil interactions in porous media under elevated experimental conditions.

VI) The combination of several experimental techniques seems to be valuable for permitting more reliable conclusions of foam tolerance to oil under different experimental conditions and scenarios. However, to thoroughly evaluate the influence of oil on the foam relative to EOR processes, the design of the experiments should be based on information from the actual reservoir situation so that the foam behavior could be reflected as realistically as possible (Chapter 6, section 6.3).

8.5 Summary and Conclusions

Experimental studies of foam have been performed in this thesis to investigate various aspects related to this EOR method. The studies have investigated: I) CO_2-foam properties compared with those of N_2-foams, II) the impact of rock properties on foam generation performance and mobility control, and III) surfactant screening and bulk foam-oil interactions.

CO_2-foam properties compared with N_2-foams

CO_2-foam properties were investigated in oil-free outcrop Berea sandstone core material with systematic variations in pressure and temperature conditions and in bulk under low pressure using alpha-olefin sulfonate ($AOS_{C14-C16}$) surfactant. The properties of CO_2-foam were compared with those of N_2-foams under similar experimental conditions. The experimental results and observations obtained in this thesis showed that:

- The presence of different gas types (CO_2, N_2) strongly influenced the properties of the foam in bulk and porous media.

The experiments in porous media demonstrated large variations in foam strength, mobility reduction factors, gas breakthrough times, outlet foam textures and foam resistance/stability against seawater injection when foam experiments using CO_2 were compared against those using N_2 in the range of 30-280 bar and 50-100°C.

The use of different gas types (CO_2, N_2) in bulk at 2 bar and ambient temperature showed variations in the surfactant foamability and foam stability.

- Different effects on the N_2- and CO_2-foam properties in porous media with pressure and temperature were obtained.

N_2-foams of relatively similar properties were obtained at 30 bar and 280 bar system pressure and 50°C (i.e., strong foam, MRF > 100, gas breakthrough close to the injection rate, fine/dense foam textures at the core outlet and strong and long-lasting reductions in water permeability during seawater injection following the foam generation.

The CO_2-foam strength was observed to increase with decreasing system pressure and increasing experimental temperature. Low-density conditions for CO_2 improved the CO_2-foam strength (MRF between 80-3 for ρ_{CO2} in the range of 0.056-0.857 g/cm^3).

The CO_2 breakthrough varied with the CO_2-foam strength. The strongest CO_2-foams delayed the gas breakthrough to a similar degree to the N_2-foams, while the weakest CO_2-foams showed lower gas mobility reduction. However, all CO_2-foams were able to reduce gas mobility and delay gas breakthrough compared with that in the absence of surfactant.

Images of the CO_2-foams at the core outlet showed coarser textures than those of the N_2-foams. The CO_2-foams with increasing pressure (30 bar, 120 bar, 280 bar) exhibited larger bubble sizes, less continuity in texture and more vague/diffuse CO_2/liquid surfaces. Smaller bubbles were observed in CO_2-foams with pre-equilibrated fluids compared to experiments without pre-equilibrated fluids at 30 bar and 120 bar system pressure and 50°C. The variation in foam texture upon using pre-equilibrated fluids did not reflect particular changes in the foam strength and mobility reduction factors. The observed textures out of the core in this thesis correlated to a certain degree with the idea that smaller bubbles reduce gas mobility more than larger bubbles and that a finer foam texture is more stable than a coarser texture. However, it remains inherently difficult to determine the extent to which the outlet foam texture reflects foam texture in-situ.

The CO_2-foam stability and resistance against seawater injection following the CO_2-foam generation were poor/less effective compared with the N_2-foams. The water permeability was high only after the injection of a few pore volumes of seawater regardless of the foam strength during generation. The use of pre-equilibrated fluids significantly improved the CO_2-foam resistance and stability against seawater injection. The experimental results indicate mass transfer, and especially, gas dissolution into the injected seawater to be one of the predominant mechanisms for the reduced CO_2-foam stability in porous media during subsequent liquid injection.

- The CO_2-foams were inherently weaker than the N_2-foams in bulk and porous media.

The apparent weakness in the strength of the CO_2-foam compared with that of the N_2-foam confirm analogous laboratory studies in oil-free outcrop sandstone core material using

commercial anionic surfactants, over a wider range of pressure and temperature conditions than normally reported (Chou, 1991; Seright, 1996; Kibodeaux, 1997; Gauglitz et al., 2002; Du et al., 2008; Farajzadeh et al., 2009).

The comparative results obtained in this thesis support earlier laboratory studies, discussions and field tests reporting CO_2-foam to exhibit poor/less effective water-blocking capabilities compared to foams consisting of gases with lower solubility in liquids (Holm and Garrison, 1988; Seright, 1996; Bhide et al. 2005; Aarra et al., 2011; Enick and Olsen, 2012).

The characterization of CO_2-foam as weaker than N_2-foam was also observed in bulk under low pressure. From a set of 12 different foamers, including the $AOS_{C14-C16}$ surfactant, none of the foaming agents tested performed better with CO_2 as the gas phase than with N_2-gas. The use of nitrogen-gas versus air did not appear to have any significance on the bulk foam properties (i.e., foamability and foam stability) because the ranking of surfactants with these gas types (i.e., N_2-foams vs. air-foams) were quite similar. The observations of the foam properties in bulk with different gas types are consistent with earlier bulk experiments (Phillips et al., 1987; Alkan et al., 1991).

The differences in performance observed between the CO_2- and N_2-foams could be due to a number of factors, which primarily appear to originate from the differences in the natures of the two gas types (described in Chapter 5). While no definitive explanation was found to explain the apparent weakness of CO_2-foams in this thesis, some possible causes were investigated, eliminated and proposed:

The results from CO_2-foam experiments in porous media with pre-equilibrated fluids indicate that the kinetics of mass transfer between the CO_2 and the surfactant solution (e.g., due to gas dissolution, local temperature rise and gas diffusion) could not be the main cause for the decreased CO_2-foam strength with increasing system pressure and why the CO_2-foams were weaker than the N_2-foams during generation.

A good correlation between the CO_2-density and the CO_2-foam strength was obtained in porous media; conditions where the density of CO_2 is low improved the CO_2-foam strength. A possible reason for this relationship could be that the CO_2 density properties also indirectly could control some of the other characteristics of CO_2 as well (e.g., surface tension, pH,

solubility, gas compressibility), which might be important to the foam properties in porous media. Accordingly, it is possible that a combination of several factors in close relation with the change in CO_2 density is what contributed to the varying CO_2-foam strength obtained in this thesis with pressure and temperature. The role of surfactant characteristics at various gas-liquid surfaces might be fundamentally different, as recently indicated by Adkins et al. (2010), and thus could be important to the weakness of the CO_2-foams. From the literature, there appears to be a general phenomenon that many types of foamers cannot generate CO_2-foams of similar strengths in porous media as those reported with N_2- and CH_4-foams, especially when the density of CO_2 is high.

Additional bulk experiments were also conducted to investigate if the poorer bulk foam properties in the presence of CO_2 could be attributed to the lower pH environment or higher solubility between the CO_2 and surfactant solution compared with that of N_2 and surfactant. Typical surface tension values from the literature were also discussed. It appears that none of these parameters were able to solely predict the difference between CO_2-foams and N_2-foams in bulk under low pressure.

The mechanisms and potential of "weak" CO_2-foams should be examined further by more experimental data.

Effect of rock properties on foam

In-situ foam generation performance was studied in naturally laminated sandstone cores with relative low permeability. During flooding experiments, most parameters were held constant, and the core material was changed. Based on the experimental results and observations that were obtained in the low permeability laminated cores and in different oil-free outcrop sandstone core materials used in this thesis in general, the following conclusion can be drawn:

- The results obtained in this thesis points out the rock material as one of the main parameters controlling the in-situ foam generation performance.

Large variations in pressure build-up profiles, foam strength, mobility reduction factors and gas breakthrough times were observed between three laminated heterogeneous cores with relatively similar physical properties.

The presence and the degree of low permeability laminated heterogeneities, detected through various types of core analysis, appears to be one of the parameters affecting the foam generation performance. Increased core lamination resulted in weaker N_2-foams and reduced gas mobility control.

Similar to any other fluid injected, the gas will have a strong tendency to flow along the path of least resistance. As a consequence of the preferential flow and distribution of fluids, foam generation must take place in the higher permeability layers before in the lower permeability layers; however, this does not mean that foam cannot be generated in lower permeability layers. In this thesis, foam generation performance was not limited by the low core permeability. In fact, the steady state MRF values in Berea core samples with homogeneous flow behavior and satisfactory experimental reproducibility were larger in lower permeability cores than in higher permeability cores. The results, however, show that the effectiveness of foam to control mobility in sandstone cores with internal variations in permeability might be significantly different.

Summarizing similar N_2-foam experiments in different outcrop sandstone core material, the magnitude in the mobility reduction factors appears to depend on the core material used. Stronger N_2-foam was, for instance, generated in outcrop Berea sandstone cores than in an outcrop Bentheimer sandstone core. The detailed interactions between rock surface properties (e.g., mineralogy, wettability, pore geometry, small scale heterogeneities, etc.) and thin liquid films were beyond the scope of this thesis, but should be investigated further.

Systematic measurements and comparisons of foam relative to different rock lithologies should be an interesting topic to consider for future studies.

Surfactant screening and bulk foam-oil interactions

A new bulk test was designed in this thesis to allow gases other than air to be studied under low pressure. The new test method was used in combination with other experimental techniques to evaluate and screen a set of foamers in the absence and presence of oil. Generally, the combination of several experimental techniques seemed valuable for improving the evaluation and screening of foamers. An advantage of the new filter test compared with the more traditional mixer method is that it allows the study of foam with gas phases other than air. The option of using the intended gas type in surfactant evaluation/screening was

observed to be important even at reduced experimental conditions. The bulk foam properties (i.e., foamability and foam stability) using CO_2-gas were often different and generally reduced relative to those against N_2-gas/air, indicating that the requirements for foaming agents against CO_2 could be different from those of good foamers found with other gas types. This observation applied both with and without oil present.

Out of 12 the surfactants that were evaluated in the absence of oil, an $AOS_{C14-C16}$ surfactant and a fluorinated sulfobetaine surfactant (FS-500) were found to be the two best foamers overall. Both surfactants exhibited good foamability and long-term foam stability (> 24 hours) in two different bulk tests (i.e., filter test and mixer method) and against the three different gas types applied (i.e., CO_2, N_2 and air). Surfactants that were specifically recommended for CO_2-foam performed poorer than most of the conventional surfactants.

The $AOS_{C14-C16}$ and fluorinated FS-500 surfactant were evaluated further against various types of oils present (i.e., crude oils and alkanes). The fluorinated FS-500 surfactant generated more stable foams in the presence of oil compared with the AOS surfactant. The overall ranking of the two surfactants in the presence of oil were confirmed by both bulk tests: 1) FS-500 and, 2) $AOS_{C14-C16}$.

The FS-500 foams showed good foamability and long-term foam stability (> 24 hours) in all bulk tests with oil present, consistent with the calculated parameters that have been proposed to predict foam stability in presence of oil (i.e., entering (E), spreading (S), and bridging (B) coefficients and lamella (L) numbers according to Chapter 6).

The AOS foams were more oil-sensitive. Additionally, the correlation between the bulk foam stability and the calculated S, E, B and L values was difficult to clearly predict because most of the calculated coefficients were close to zero. The lamella number was, in general, found to have poor predictive power because good foam stability was observed with values ranging from 0.4 to 23.5. Improved oil tolerance using the AOS surfactant was shown in the filter test (compared with the mixer method) using N_2-gas (compared with CO_2), when mixed with FS-500 surfactant (AOS+FS (4:1), under elevated temperature (in terms of the calculated S, E, B and L parameters at 50 vs. 22°C) and in foam flooding experiments under elevated pressure and temperature with residual oil saturation (compared to the mixer method with oil).

General observations from the bulk foam texture with oil present indicated that the foams were more stable when the oils did not spread, but foams with spreading oils could also be very stable. Therefore, the spreading of oil alone did not appear to be an adequate reason for detrimental foam stability in the presence of oil. The stability of the pseudo-emulsion film was beyond the scope of this thesis, but the properties of this film might have played an important role in foam stability using the AOS surfactant and the AOS+FS surfactant mixture.

Although certain similarities and interesting trends were observed between the experiments in bulk and porous media, the bulk foam properties of this work did not generally correlate with the foam properties in porous media. It is inherently difficult to predict foam properties and performance separately from the porous media.

In spite of the existing uncertainties about the microscopic mechanisms of foam in porous media, we would always recommend foam experiments to be conducted in reservoir rock material at the intended reservoir conditions for the closest possible evaluation of the foam project performance at lab-scale. Although core flooding experiments under elevated conditions are more difficult, time-consuming and expensive to perform, these types of experiments are more realistic towards a foam field application than bulk foam tests under reduced experimental conditions.

Appendix – Experimental Protocols

A. Fluid properties:

Surfactants:

The following surfactants were used in this thesis (Table A.1).

Table A.1: List of surfactants

Surfactant ID:	Type:	% Active:	Description:	Manufacturer:
AOS C14-C16	Anionic	~100 %	α-olefin sulfonate, C14-C16 (Delivered as white powder) (Good solubility in SSW, clear solution) (Used in core flooding exp. in **Papers 1-3**) (Evaluated in bulk tests in **Paper 4**)	Shell
Sulframin AOS 38	Anionic	37.6 %	α-olefin sulfonate, C14-C16 (Delivered as clear transparent liquid) (Good solubility in SSW, clear solution) (Used in core flooding exp. in **Papers 1-3**) (Evaluated in bulk tests in **Paper 4**)	Witco
Enordet O122 #1	Anionic	31 %	α-olefin sulfonate, C12-C14 (Evaluated in bulk tests in **Paper 4**)	Shell
Enordet O122 #2	Anionic	33 %	α-olefin sulfonate, C12-C14 (Evaluated in bulk tests in **Paper 4**)	Shell
Witcolate 1247H	Anionic	60 %	Ammonium salt of etoxylated sulfated alcohol, C6-C10 (Evaluated in bulk tests in **Paper 4**)	AkzoNobel
Enordet J771	Anionic	32 %	Propoxylated sulfate, C12-C13, 7 PO groups (Evaluated in bulk tests in **Paper 4**)	Shell
(Zonyl) FS-500	Zwitterionic	27 %	Perfluoralkyl sulfobetaine (Evaluated in bulk tests in **Paper 4**)	DuPont
Neodol 25-7	Non-ionic	17 %	Linear alcohol ethoxylate, C12-C15, 7 EO groups (Evaluated in bulk tests in **Paper 4**)	Shell
Neodol 23-12	Non-ionic	24 %	Linear alcohol ethoxylate, C12-C13, 12 EO groups (Evaluated in bulk tests in **Paper 4**)	Shell
Surfonic N-120	Non-ionic	100 %	Branced nonylphenol etoxylate, 12 EO groups (Evaluated in bulk tests in **Paper 4**)	Huntsman
Surfonic N-150	Non-ionic	100 %	Branced nonylphenol etoxylate, 15 EO groups (Evaluated in bulk tests in **Paper 4**)	Huntsman
Novomer	Non-ionic	100 %	Poly(propylene) carbonates (Evaluated in bulk tests in **Paper 4**)	NOVOMER

Brine:

The composition of the synthetic seawater used in this thesis is listed in Table A.2.

Table A.2: Synthetic seawater (SSW) composition

Salt	NaCl	Na_2SO_4	$NaHCO_3$	KCl	$MgCl_2$	$CaCl_2$
[wt.%]	2.489	0.406	0.019	0.068	0.521	0.131

TDS = 36,340 ppm
Ionic strength = 0.724 M.
Viscosity = 1.07 cP (22°C, atm.), 0.56 cP (50°C, atm.), 0.34 cP (90°C, atm.).
Density = 1.029 g/ml (22°C, atm.), 1.015 g/ml (50°C, atm.).
The brine was always filtered through a 0.45 µm filter before use.

Gases:

Carbon dioxide (used in **Papers 1-2** and **4**) was delivered by Yara Industrial, > 99.5% purity.

Nitrogen (used in **Papers 1-4**) was delivered by Yara Praxair, > 99.5% purity.

Air was used as gas phase in one of the bulk tests in **Paper 4**. The main constituents in dry air are;

Nitrogen (≈ 78%), Oxygen (≈ 21%) and Argon (≈ 1%).

Oils:

Five different crude oils from five oil reservoirs in the North Sea were used in **Paper 4** (denoted A-E). Some of their physical properties are provided in Table A.3.

Table A.3: Crude oil properties at 22°C, atmospheric pressure (values in the parentheses at 50°C, atm.)

Crude oil ID	**Density (g/cm^3)**	**Viscosity (cP)**	**API gravity (°API)**
A	0.941 (0.932)	272 (62)	18
B	0.860 (0.833)	11.0 (2.9)	32
C	0.848 (0.796)	22.8 (7.5)	35
D	0.837 (0.823)	10.7 (4.3)	37
E	0.821 (0.809)	8.4 (2.7)	40

In addition, the following alkanes were used in **Paper 4**: pentane (C_5H_{12}), octane (C_8H_{18}), decane ($C_{10}H_{22}$) and hexadecane ($C_{16}H_{34}$).

Surface/interfacial tension properties:

Table A.4: Surface tension properties, ambient conditions (from Paper 4).

Aqueous solutions	Surface tension to air, $\sigma_{w/g}$, 22°C, atm. (± 0.5 mN/m)
Distilled water (no Surf.)	72.4
Synthetic seawater (SSW) (no Surf.)	70.1
Surfactant solutions (0.5 wt. % in SSW)	
FS-500	16.0
AOS C14-C16	28.8
AOS C12-C14	29.1
N-120	30.4
Witcolate 1247H	31.7
N-150	32.9
J771	36.4
Novomer	44.8

Table A.5: Surface/interfacial tension properties at 22°C and 50°C, atmospheric pressure (values used in Paper4 for calculation of S,E,B,L parameters).

Surface/Interfacial tension:	22°C, atm.	50°C, atm.
Method	du Noüy ring method	du Noüy ring method
$AOS_{C14-C16}$ surfactant solution against air	28.8 mN/m	22.3 mN/m
FS 500 surfactant solution against air	16.0 mN/m	14.6 mN/m
$AOS_{C14-C16}$ + FS 500 surfactant mix (4:1) against air	18.8 mN/m	-
Crude oils (A-E) against air	30.6-25.5-26.7-25.8-26.0 mN/m	28.6-22.0-25.0-23.5-23.7 mN/m
Method	Spinning drop method	Spinning drop method
$AOS_{C14-C16}$ surfactant solution against crude oils (A-E)	0.19-0.50-0.53-0.48-0.58 mN/m	0.25-0.67-0.67-0.74-0.86 mN/m
FS 500 surfactant solution against crude oils (A-E)	2.02-5.40-5.83- 2.22-4.40 mN/m	2.29-5.00-5.32-2.32-3.48 mN/m
$AOS_{C14-C16}$ + FS 500 surfactant mix (4:1) - crude oils (A&C)	0.12 & 0.30 mN/m	

B. Core properties:

Physical properties of the outcrop sandstone core material used are given in Table B.1.

Table B.1: Physical properties of core material used in different papers

Core ID	Length [cm]	Diameter [cm]	Cross sec. area [cm^2]	Pore Volume [ml]	Average Porosity [%]	Average Absolute Permeability [K_w]	Main results presented in Paper #
Berea70/(B-WL*)	29.9	3.75	11.04	57.0	17.3	67	3
Berea90/(B-ML*)	30.0	3.76	11.10	58.5	17.6	93	3
Berea130/(B-SL*)	23.5	3.76	11.10	49.3	18.9	130	3
Berea400	30.5	3.82	11.46	74.9	21.5	425	2
1Berea1000	26.4	3.77	11.16	65.7	22.3	1011	1
2Berea1000	19.4	3.71	10.81	45.2	21.6	1049	2
Bentheimer1900	25.4	3.75	11.04	60.4	21.5	1900	4

* Core IDs used in **Paper 3**: (B-WL) = Berea-weakly laminated core, (B-ML) = Berea-moderately laminated core, (B-SL) = Berea-strongly laminated core.

A summary of the mineralogy to used core material are tabulated in Table B.2.

Table B.2: XRD mineralogy measurements (% of $1cm^3$ rock sample analyzed)

Core ID	Illite/Smectite	Illite/Mica	Kaolinite	Chlorite	Quartz	K-Feldspar
Berea130/(B-SL)	0	3.0	3.2	1.7	87.5	1.9
Berea400	0	3.8	3.6	0.2	88.7	2.5
1Berea1000	0.2	2.7	6.0	1.1	82.7	5.1
Bentheimer1900	Trace amounts	3.2	0	0	90.6	4.6

...→

Core ID	Plagioclase	Calcite	Dolomite	Siderite	Pyrite
Berea130/(B-SL)	0.9	Trace amounts	0.9	0.9	0
Berea400	0.4	0	0.8	0	Trace amounts
1Berea1000	0.4	0.4	1.5	0	0
Bentheimer1900	0	0.6	0	1.0	Trace amounts

Information of typical pore sizes and their distribution in some of the core material used are given in Figure B.1 and Table B.3.

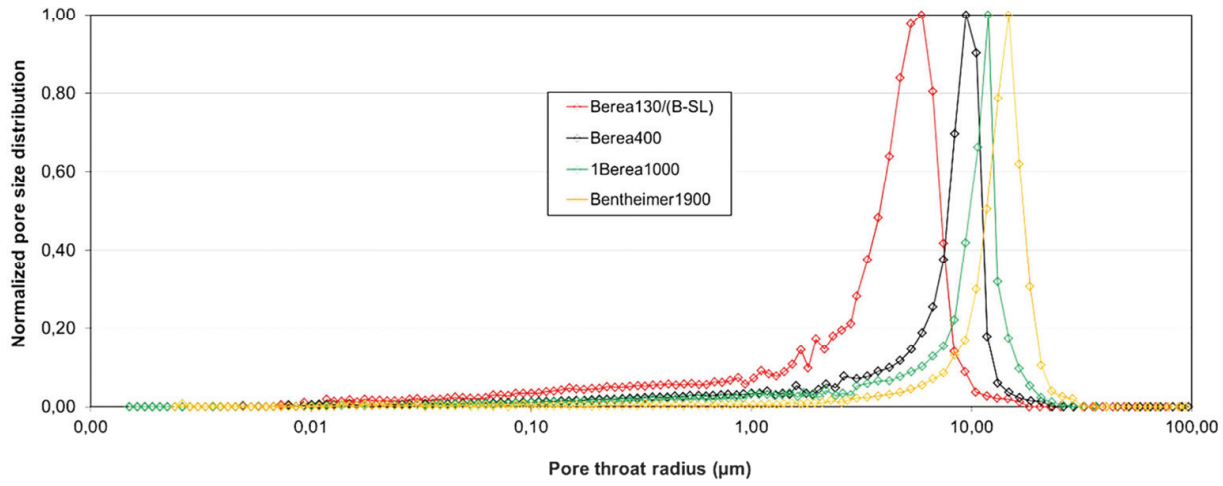

Figure B.1: Pore throat size distribution from mercury injection measurements.

Table B.3: Average pore throat sizes

Core ID	Average pore throat radiuses (ref. Figure B.1) (µm)
Berea130/(B-SL)	6
Berea400	9
1Berea1000	12
Bentheimer1900	15

Figure B.2 shows dispersion profiles for most of the core samples used. The details of these tests are better described in the appendix in **Paper 3**.

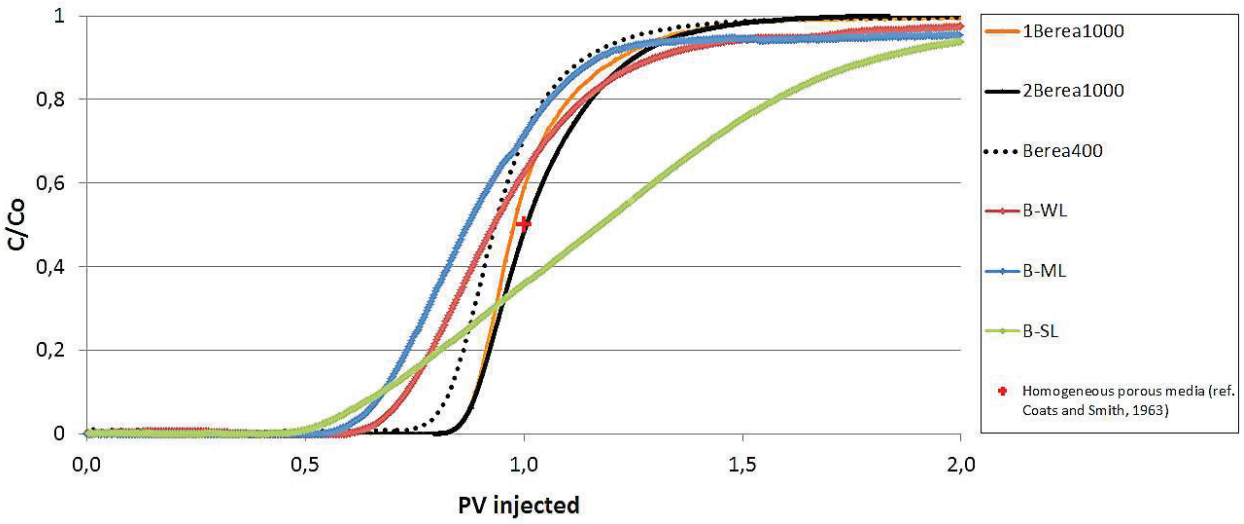

Figure B.2: Dispersion tests

The core materials were sliced lengthwise after experiments and imaged with the aid of X-ray scanning to indicate possible anomalies in the rock samples used (see Figure B.3).

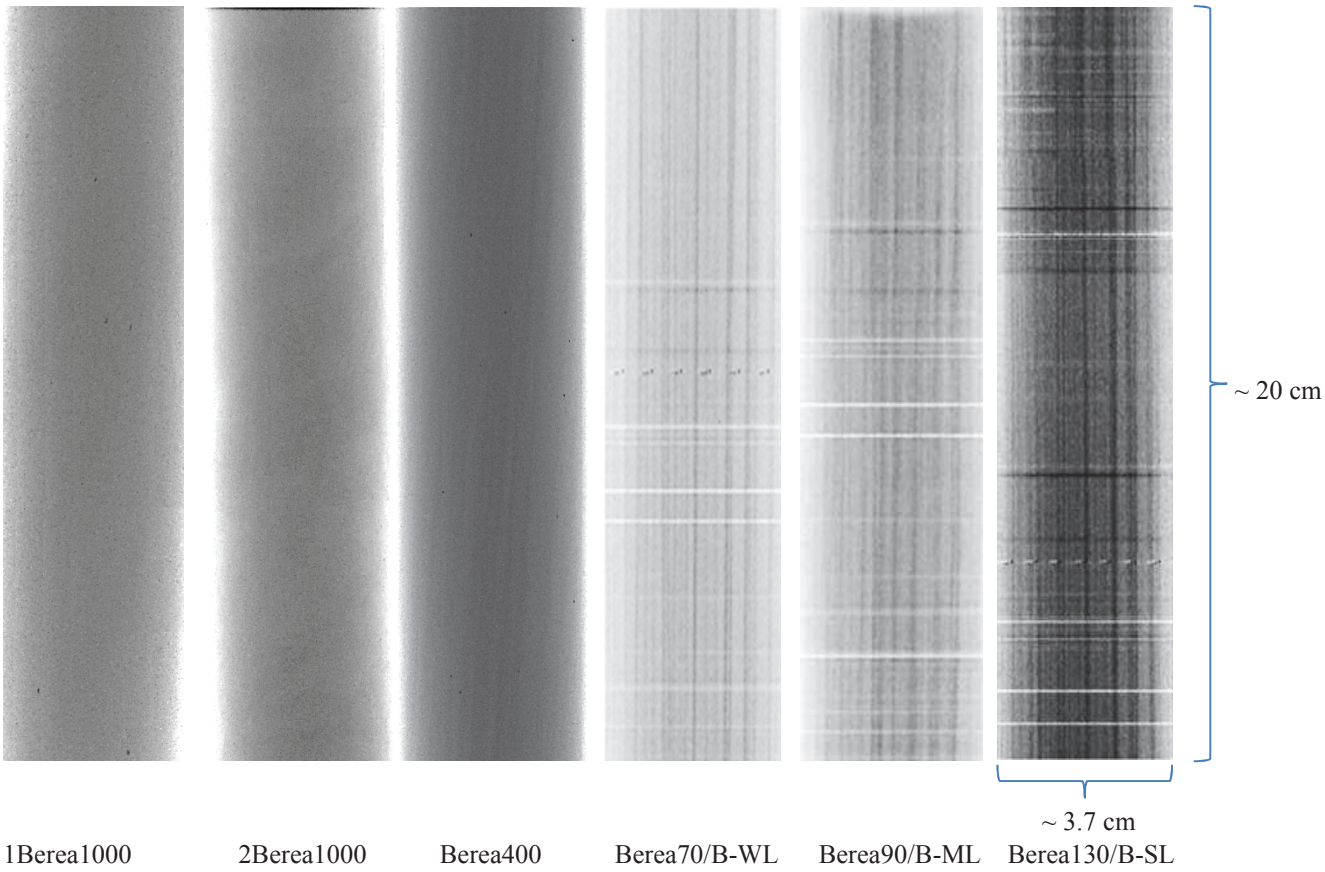

Figure B.3: X-ray images of the core samples used in this thesis. Horizontal lines in the images are noises.

C. Experimental summary – foam core flooding:

The following steps included in each foam core flooding experiment in this thesis:

(1) Baseline pressure measurements; simultaneous injection of gas and seawater at 80% gas fraction, Q_{tot} = 40 mL/h (i.e. 32 mL/h with gas and 8 mL/h with seawater).

For the baseline pressure ($dP_{without\ foam}$), the average value of the steady state pressure drop during baseline pressure measurement was used as reference for calculating mobility reduction factors (MRF) (see Figure C.1).

(2) Adsorption coverage; injection of two pore volumes of surfactant solution prior to foam generation, $Q_{surf.solu.}$ = 8 mL/h.

(3) Foam generation experiment; simultaneous injection of gas and surfactant solution at 80% foam quality, Q_{tot} = 40 mL/h (i.e. 32 mL/h with gas and 8 mL/h with surfactant solution).

(4) Foam water blocking; injection of seawater only (i.e. no surfactant), Q_{SSW} = 8 mL/h.

(5) Core restoration; cleaning of the core back to absolute water permeability (K_w). The core restoration procedures included depressurization and flooding with large volumes of seawater and brine (3 wt.% NaCl) and isopropyl alcohol (a good gas dissolver).

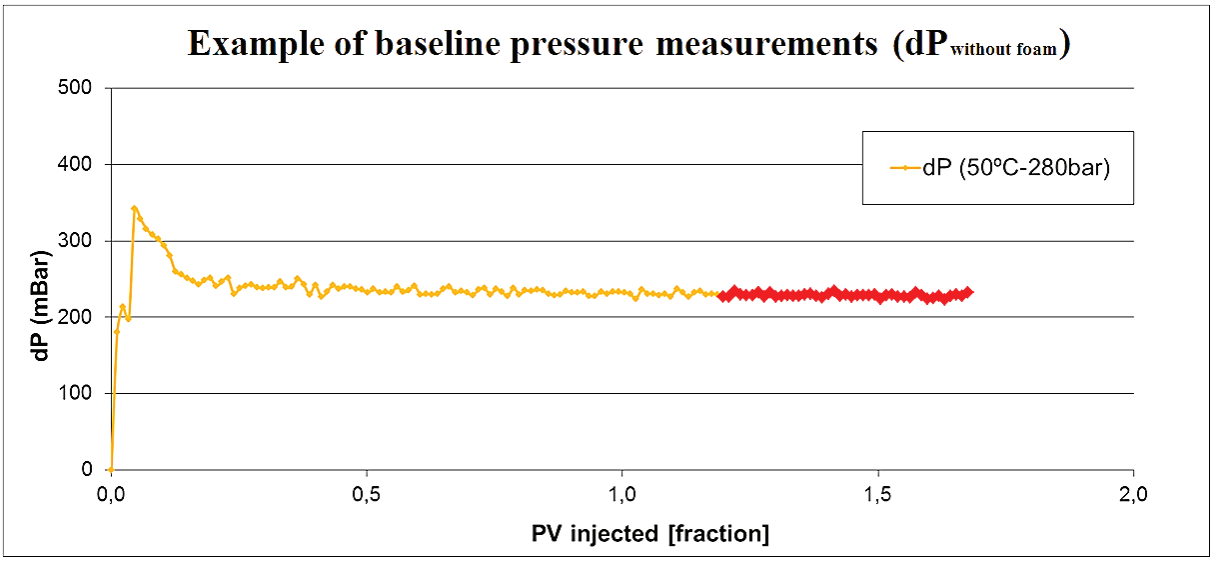

Figure C.1: Example of pressure drop during a baseline pressure experiment in Berea90/(B-ML) at 280 bar and 50°C. The average value of the pressure drop for the last 0.5 PV injected (marked in red = 228 mbar) was used as reference for calculating mobility reduction factors in subsequent foam experiment at similar conditions.

D. Experimental history to each core:

Table D.1: Experimental protocol - 1Berea1000 (main results presented in Paper1)

Core ID	Experiment no. (in same core)	Experimental conditions (gas phase, pressure, temp.)	Basline pressure $dP_{without\ foam}$ (bar)	Foam generation $dP_{foam\ (at\ the\ end\ of\ exp.)}$ (bar)	Core restoration after foam exp. (% of K_w)
1Berea1000	1.	N_2, 30 bar, 50°C	0.057	7.8	~ 100
1Berea1000	2.	N_2, 280 bar, 50°C	0.066	8.7	~ 100
1Berea1000	3.	CO_2, 280 bar, 50°C	0.042	0.13	92
1Berea1000	4.	CO_2, 30 bar, 50°C	0.065	5.0	~ 100
1Berea1000	5.	CO_2, 120 bar, 50°C	0.045	0.26	79
1Berea1000	6.*	N_2, 30 bar, 50°C	0.103	0.17	~ 100
1Berea1000	7.**	N_2, 30 bar, 50°C	0.108	18.3	~ 100
1Berea1000	8.	N_2, 30 bar, 50°C	0.106	12.4	97
1Berea1000	9.	CO_2, 30 bar, 50°C	0.091	4.7	~ 100
1Berea1000	10.	CO_2, 120 bar, 50°C	0.065	0.35	83
1Berea1000	11.	N_2, 30 bar, 50°C	0.101	15.1	93
1Berea1000	12.***	N_2, 30 bar, 50°C	0.094	-	79
1Berea1000	13.	CO_2, 30 bar, 50°C (Pre-equilibrated fluids)	0.087	6.0	84
1Berea1000	14.****	CO_2, 30 bar, 50°C (Pre-equilibrated fluids)	0.084	-	84
1Berea1000	15.	CO_2, 30 bar, 50°C (Pre-equilibrated fluids)	0.083	6.5	82
1Berea1000	16.	CO_2, 120 bar, 50°C (Pre-equilibrated fluids)	0.053	0.30	-

* Poor reproducibility (reason unknown).

** Reversed injection direction.

*** Baseline pressure measurement (N_2 and SSW without surfactant).

**** Experiment failed due to leakage during foam generation.

Table D.2: Experimental protocol - 2Berea1000 (main results presented in Paper 2)

Core ID	Experiment no. (in same core)	Experimental conditions (gas phase, pressure, temp.)	Basline pressure $dP_{without\ foam}$ (bar)	Foam generation $dP_{foam\ (at\ the\ end\ of\ exp.)}$ (bar)	Core restoration after foam exp. (% of K_w)
2Berea1000	1.	CO_2, 120 bar, 90°C (Pre-equilibrated fluids)	0.052	1.3	91
2Berea1000	2.	CO_2, 120 bar, 50°C (Pre-equilibrated fluids)	0.062	0.68	85
2Berea1000	3.	CO_2, 90 bar, 90°C (Pre-equilibrated fluids)	0.065	3.7	-

Table D.3: Experimental protocol - Berea400 (main results presented in Paper 2)

Core ID	Experiment no. (in same core)	Experimental conditions (gas phase, pressure, temp.)	Basline pressure $dP_{without\ foam}$ (bar)	Foam generation $dP_{foam\ (at\ the\ end\ of\ exp.)}$ (bar)	Core restoration after foam exp. (% of K_w)
Berea400	1.*	CO_2, 90 bar, 90°C	0.075	-	94
Berea400	2.	CO_2, 90 bar, 90°C	0.082	4.5	-

***** Experiment failed due to leakage during foam generation.

Table D.4: Experimental protocol - Berea weakly laminated core (B-WL) (main results presented in Paper 3)

Core ID	Experiment no. (in same core)	Experimental conditions (gas phase, pressure, temp.)	Basline pressure $dP_{without\ foam}$ (bar)	Foam generation $dP_{foam\ (at\ the\ end\ of\ exp.)}$ (bar)	Core restoration after foam exp. (% of K_w)
B-WL	1.	N_2, 120 bar, 50°C	0.270	117.7	~ 100
B-WL	2.	N_2, 120 bar, 50°C	0.273	129.9	-

Table D.5: Experimental protocol - Berea moderately laminated core (B-ML) (main results presented in Paper 3)

Core ID	Experiment no. (in same core)	Experimental conditions (gas phase, pressure, temp.)	Basline pressure $dP_{without\ foam}$ (bar)	Foam generation $dP_{foam\ (at\ the\ end\ of\ exp.)}$ (bar)	Core restoration after foam exp. (% of K_w)
B-ML	1.	N_2, 30 bar, 50°C	0.217	19.7	~ 100
B-ML	2.	N_2, 120 bar, 50°C	0.227	25.4	~ 100
B-ML	3.	N_2, 280 bar, 50°C	0.228	26.2	~ 100
B-ML	4.	N_2, 280 bar, 100°C	0.177	28.1	95
B-ML	5.	N_2, 280 bar, 50°C (Q_{tot} = 8 ml/h at 80% foam quality)	0.178	38.3	91
B-ML	6.	N_2, 30 bar, 50°C	0.250	52.3	91
B-ML	7.	N_2, 120 bar, 50°C	0.257	61.4	85

Table D.6: Experimental protocol - Berea strongly laminated core (B-SL) (main results presented in Paper 3)

Core ID	Experiment no. (in same core)	Experimental conditions (gas phase, pressure, temp.)	Basline pressure $dP_{without\ foam}$ (bar)	Foam generation $dP_{foam\ (at\ the\ end\ of\ exp.)}$ (bar)	Core restoration after foam exp. (% of K_w)
B-SL	1.	N_2, 30 bar, 50°C	0.165	4.3	97
B-SL	2.	N_2, 30 bar, 50°C	0.165	7.1	98
B-SL	3.	N_2, 30 bar, 50°C	0.165	10.4	-

Table D.7: Experimental protocol – Bentheimer1900 (main results presented in Paper 4)

Core ID	Experiment no. (in same core)	Experimental conditions (gas phase, pressure, temp.)	Basline pressure $dP_{without\ foam}$ (bar)	Foam generation $dP_{foam\ (at\ the\ end\ of\ exp.)}$ (bar)	Core restoration after foam exp. (% of K_w)
Bentheimer1900	1.	N_2, 30 bar, 50°C	0.045	0.27	~ 100

References

Aarra, M.G. *Properties of Microemulsions and Foams in Relation to Improved Oil Recovery*, PhD dissertation, University of Bergen, **1998**.

Aarra, M.G., Ormehaug, P.A., Skauge, A., and Masalmeh, S.K. *Experimental Study of CO_2- and Methane-Foam Using Carbonate Core Material at Reservoir Conditions*, Presented at the SPE Middle East Oil and Gas Show and Conference, Manama, Bahrain, 20-23. March **2011**. Paper SPE 141614.

Aarra, M.G., Ormehaug, P.A., and Skauge, A. *Foams for GOR Control: Improved Stability by Polymer Additives*, Presented at the 9th EAGE European Symposium on Improved Oil Recovery, The Hague, The Netherlands, 20-22. October, **1997**.

Aarra, M.G., and Skauge, A. *A Foam Pilot in a North Sea Oil Reservoir: Preparation for a Production Well Treatment*, Presented at the 69th Annual Technical Conference and Exhibition, New Orleans, LA, 25-28. September, **1994**. Paper SPE 28599.

Aarra, M.G., Skauge, A., and Martinsen, H.A. *A Breakthrough for EOR in the North Sea*, Presented at SPE Annual Technical Conference and Exhibition, San Antonio, Texas, 29. Sep.-2. Oct., **2002**. Paper SPE 77695.

Aarra, M.G., Skauge, A., Solbakken, J., and Ormehaug, P.A. *Properties of N_2- and CO_2-Foams as a Function of Pressure*, JPSE, Vol. 116, April, **2014**, pp. 72-89.

Aarra, M.G., Skauge, A., Søgnestad, S., and Stenhaug, M. *A Foam Pilot Test Aimed at Reducing Gas Inflow in a Production Well at the Oseberg Field*, Presented at the 8th European Symposium on Improved Oil Recovery, Vienna, Austria, 15-17. May, **1996**.

Abdallah, W., Buckley, J.S., Carnegie, A., Herold, J.E.B., Fordham, E., Graue, A., Habashy, T., Seleznev, N., Signer, C., Hussain, H., Montaron, B., and Ziauddin, M. *Fundamentals of Wettability*, Oilfield Review, Schlumberger Wettability Workshop, Bahrain, May, **2007**, pp. 44-61.

Adkins, S.S., Chen, X., Chan, I., Torino, E., Nguyen, Q.P., Sanders, A.W., and Johnston, K.P. *Morphology and Stability of CO_2-in-Water Foams with Nonionic Hydrocarbon Surfactants*, Am. Chem. Soc., Langmuir, 26(8), **2009**, pp. 5335-5348.

Adkins, S.S., Chen, X., Nguyen, Q.P., Sanders, A.W., and Johnston, K. *Effect of Branching on the Interfacial Properties of Nonionic Hydrocarbon Surfactants at the Air-Water and Carbon Dioxide-Water Interfaces*, Journal of Colloid and Int. Sci. 346, **2010**, 455-463.

Alkan, H., Goktekin, A., and Satman, A. *A Laboratory Study of CO_2-Foam Process for Bati Raman Field, Turkey*, Presented at the SPE Middle East Oil Show, Bahrain, 16-19. November, **1991**. Paper SPE 21409.

Alvarado, D., and Manrique, E. *Enhanced Oil Recovery: An Update Review*, Energies, 3, **2010**, pp. 1529-1575.

Alvarez, J.M., Rivas, H.J., and Rossen, W.R. *Unified Model of Steady-State Foam Behaviour at High and Low Foam Qualities*, SPEJ, September, **2001**, pp. 325-333.

Anderson, W.G. *Wettability Literature Survey-Part 1-5*, Journal of Petroleum Technology, October **1986** – November **1987** (5 separate articles).

Andrianov, A., Farajzadeh, R., Nick, M.M., Talanana, M., and Zitha, P.L.J. *Immiscible Foam for Enhancing Oil Recovery: Bulk and Porous Media Experiments*, Presented at the SPE Oil Recovery Conference, Kuala Lumpur, Malaysia, 19-21. July, **2011**. Paper SPE 143578.

Apaydin, O.G., and Kovscek, A.R. *Surfactant Concentration and End Effects on Foam Flow in Porous Media*, Transport in Porous Media, 43, **2001**, pp. 511-536.

Arnaudov, L., Denkov, N.D., Surcheva, I., Durbut, P, Broze, G., and Mehreteab, A. *Effect of Oily Additives on Foamability and Foam Stability. 1. Role of Interfacial Properties*, Langmuir, Vol. 17, No. 22, **2001**, pp. 6999-7010.

Aronsen, A.S., Bergeron, B., Fagan, M.E., and Radke, C.J. *The Influence of Disjoining Pressure on Foam Stability and Flow in Porous Media*, Colloids and Sur. A: Phys. Chem. Eng. Aspects, Vol. 83, **1994**, pp.109-120.

Atkins, P.W., and Paula, J. de. *Elements of Physical Chemistry*, 4th ed., Oxford University Press, New York, **2005**.

Aulton, M.E., and Taylor, K.M.G. *Aulton's Pharmaceutics: The Design and Manufacture of Medicines*, 4th edition, Elsevier, **2013**, Chapter 5.

Awan, A.R., Teigland, R., and Kleppe, J. *A Survey of North Sea Enhanced-Oil-Recovery Projects Initiated During the Years 1975 to 2005*, SPE Reservoir Evaluation & Engineering, June, **2008**. pp. 497-512.

Azdarpour, A., Rahmani, O., Mohammadian, E., Parak, M., Daud, A.R.M., and Junin, R. *The Effects of Polymer and Surfactant on Polymer Enhanced Foam Stability*, IEEE Business Engineering and Industrial Applications Colloquium, **2013**, pp. 97-102.

Bai, B., Grigg, R.B., Liu, Y., and Zeng, Z. *Adsorption Kinetics of Surfactant Used in CO_2-Foam Flooding onto Berea Sandstone*, Presented at the 2005 SPE Annual Technical Conference and Exhibition, Dallas, Texas, 9-12. October, **2005**. Paper SPE 95920.

Bao, Y. *Field Test of Carbon Dioxide Gas Channeling Foam Plugging*, Applied Mechanics and Materials Vols. 316-317, **2013**, pp. 769-772.

Basheva, E.S., Ganchev, D., Denkov, N.D., Kasuga, K., Satoh, N., and Tsujii, K. *Role of Betaine as Foam Booster in the Presence of Silicone Oil Drops*, Langmuir, 16, **2000**, pp. 1000-1013.

Behenna, F.R. *Acid Diversion from an Undamaged to a Damaged Core Using Multiple Foam Slugs*, Presented at the SPE European Formation Damage Symposium, Hague, the Netherlands, 15−16. May, **1995**. Paper SPE 30121.

Bennion, D.B., and Bachu, S. *A Correlation of the Interfacial tension between Supercritical Phase CO_2 and Equilibrium Brines as a Function of Salinity, Temperature and Pressure*, Presented at the 2008 SPE Annual Technical Conference and Exhibition, Denver, Colorado, 21-24. September, **2008**. Paper SPE 114479

Berg, S., Oedai, S., and Ott, H. *Displacement and Mass Transfer between Saturated and Unsaturated CO_2-Brine Systems in Sandstone*, International Journal of Greenhouse Gas Control, 12, **2013**, pp. 479-492.

Bergeron, V. *Disjoining Pressure Measurements for Foam Films Stabilized by a Nonionic Sugar-Based Surfactant*, Langmuir, 12, **1996**, pp. 1336-1342.

Bergeron, V., Fagan, M.E., and Radke, C.J. *Generalized Entering Coefficients: A Criterion for Foam Stability against oil in Porous Media*, Langmuir, 9, **1993**, pp. 1704-1713.

Bergeron, V., Hanssen, J.E., and Shoghl, F.N. *Thin-Film Forces in Hydrocarbon Foam Films and Their Application to Gas-Blocking Foams in Enhanced Oil Recovery*, Colloids and Surfaces A: Physicochemical and Engineering Aspects, 123-124, **1997**, pp. 609-622.

Bergeron, V., and Radke, C.J. *Equilibrium Measurements of Oscillatory Disjoining Pressures in Aqueous Foam Films*, Langmuir, 8, **1992**, pp. 3020-3026.

Barnes, G.T., and Gentle, I.R. *Interfacial Science – An Introduction*, 1st edition, Oxford University Press, New York, **2005**, Chapter 3.

Basu, S., and Sharma, M.M. *Measurements of Critical Disjoining Pressure for Dewetting of Solid Surfaces*, Journal of Colloid and Interface Science, 181, **1996**, pp. 443-455.

Bernabe, Y., and Brace, W.F. *Deformation and Fracture of Berea Sandstone*, Geophysical Monograph, Vol. 56, **1990**, pp. 91-101.

Bernard, G.G., Holm, L.W. *Effect of Foam on Permeability of Porous Media to Gas*, SPEJ, Vol. 4, Issue 3, September, **1964**, pp. 267–274.

Bernard, G.G., Holm, L.W., and Harvey, C.P. *Use of Surfactant to Reduce CO_2 Mobility in Oil Displacement*, SPERE, August **1980.**

Bernard, G.G., Holm, L.W., and Jacobs, W.L. *Effect of Foam on Trapped Gas Saturation and on Permeability of Porous Media to Water*, SPEJ, Vol. 5, Issue 4, December, **1965**, pp. 267–300.

Bertin, H.J., Apaydin, O.G., Castanier, L.M., and Kovscek, A.R. *Foam Flow in Heterogeneous Porous Media: Effect of Cross Flow*, SPEJ, Vol. 4, Issue, 2, June, **1999**, pp. 75-82.

Bhide, V., Hirasaki, G., Miller, C., and Puerto, M. *Foams for Controlling Water Production*, Presented at the 2005 SPE International Symposium on Oilfield Chemistry, Houston, Texas, 2-4. February, **2005**. Paper SPE 93273.

Bian, Y., Penny, G., and Sheppard, N.C. *Surfactant Formulation Evaluation for Carbon Dioxide Foam Flooding in Heterogeneous Sandstone Reservoirs*, Presented at the SPE Improved Oil Recovery Symposium, Tulsa, Oklahoma, 14-18. April, **2012**. Paper SPE 154018.

Bikerman, J.J. *Foams*, Berlin Heidelberg, Springer-Verlag, **1973**.

Bird, B.R., Stewart, W.E., and Lightfoot, E.N. *Transport Phenomena*, John Wiley and Sons, USA, 2nd edition, **2007**, pp. 513-542.

Blaker, T., Aarra, M.G., Skauge, A., Rasmussen, L., Celius, H.K., Martinsen, H.A., and Vassenden, F. *Foam for Gas Mobility Control in the Snorre Field: The FAWAG Project*, SPERE, Vol. 5, No. 4, August, **2002**, pp. 317-323.

Bolontrade, A.J., Scilingo, A.A., and Añón, M.C. *Amaranth Proteins Foaming Properties: Film Rheology and Foam Stability – Part 2*, Colloids and Surfaces B: Biointerfaces, http://dx.doi.org/10.1016/j.colsurfb.2014.10.061, **2014**.

Bond, D.C., and Holbrook, O.C. *Gas Drive Oil Recovery Process*, U.S. Patent 2,866,507, **1958**.

Borchardt, J.K. *Foaming Agents for EOR: Correlation of Surfactant Performance Properties with Chemical Structure*, Presented at the SPE International Symposium on oilfield Chemistry, San Antonio, Texas, 4-6. February, **1987**. Paper SPE 16279.

Buckley, J.S. *Mechanisms and Consequences of Wettability Alteration by Crude Oils*, PhD dissertation, Heriot-Watt University, Edinburgh, United Kingdom, **1996**.

Buzzacchi, M., Schmiedel, P., and Rybinski, W. *Dynamic Surface Tension of Surfactant Systems and its Relation to Foam Formation and Liquid Film Drainage on Solid Surfaces*, Colloid and Surfaces: Phys. Chem. Eng. Asp., Vol. 273, Issue 1-3, **2006**, pp.47-54.

Castanier, L.M. *Steam with Additives: Field Projects of the Eighties*, J. Pet. Sci. Eng., 2, **1989**, pp. 193-206

Casteel, J.F., and Djabbarah, *N.F. Sweep Improvements in CO_2 Flooding by Use of Foaming Agents*, SPERE, Vol. 3, No. 4, November **1988**, pp. 1186-1192.

Chabert, M., Morvan, M., and Nabzar, L. *Advanced Screening Technologies for the Selection of Dense CO_2 Foaming Surfactants*, Presented at the 18th SPE Improved Oil Recovery Symposium, Tulsa, Oklahoma, 14-18. April, **2012**. Paper SPE 154147.

Chabert, M., Nabzar, L., Rohaida, S., Hamid, P., Sedaralit, F., and Darman, N. *An Integrated Laboratory Workflow for the Design of a Foam Pilot in Malaysia*, Presented at the 17th European Symposium on Improved Oil Recovery, St. Petersburg, Russia, 16-18. April, **2013**.

Chabert, M., Nabzar, L., Beunat, V., Lacombe, E., and Cuenca, A. *Impact of Surfactant Structure and Oil Saturation on the Behaviour of Dense CO_2 Foams in Porous Media*, Presented at the SPE Improved Oil Recovery Symposium, Tulsa, Oklahoma, 12-16. April, **2014**. Paper SPE 169116.

Chalbaud, C., Robin, M., Bekri, S., and Egermann P. *Wettability Impact on CO_2 Storage in Aquifers: Visualisation and Quantification Using Micromodel Tests, Pore Network Model and Reservoir Simulations*, Presented at the International Symposium of the Society of Core Analysts, Calgary, Canada, 10-12. September, **2007**. Paper SCA2007-09.

Chambers, D.J. *Foams for Well Stimulation*, in Foams: Fundamentals and Application in the Petroleum Industry (ed. Schramm, L.L.), American Chemical Society, Washington DC, **1994**, pp. 355-404.

Chambers, K.T., and Radke, C.J. *Capillary Phenomena in Foam Flow Through Porous Media*, in Interfacial Phenomena in Petroleum Recovery (ed. Morrow, N.M.), Marcel Dekker, New York, **1991**, pp. 191-255.

Chang, S.H., and Grigg, R.B. *Effects of Foam Quality and Flow Rate on CO_2-Foam Behaviour at Reservoir Temperature and Pressure*, SPE Reservoir Eval. & Eng., Vol. 2, No. 3, June, **1999**, pp. 248-254.

Chang, Y., Coats, B.K., and Nolen, J.S. *A Compositional Model for CO_2 Floods Including CO_2 Solubility in Water*, Society of Petroleum Engineers, **1998**, pp. 155-160.

Chen, Y., Elhag, A.S., Poon, B.M., Cui, L., Ma, K., Liao, S.Y., Omar, A., Worthen, A.J., Hirasaki, G.J., Nguyen, Q., and Johnston, K.P. *Ethoxylated Cationic Surfactants for CO_2 EOR in High Temperature, High Salinity Reservoirs*, Presented at the SPE Improved Oil Recovery Symposium, Tulsa, Oklahoma, 14-18. April, **2012**. Paper SPE 154222.

Chiquet, P., Broseta, D., and Thibeau, S. *Wettability Alteration of Caprock Minerals by Carbon Dioxide*, Geofluids, 7, **2007**, pp. 112–122.

Choi, Y.S., and Nesic, S. *Corrosion Behaviour of Carbon Steel in Supercritical CO_2-Water Environments*, Paper No. 09256, NACE International, Houston, Texas, **2009**.

Chou, S.I. *Conditions for Generating Foams in Porous Media*, Presented at the 66th Annual Technical Conference and Exhibition of SPE, Dallas, Texas, 6-9. October, **1991**. Paper SPE 22628.

Christian, S.D., and Scamehorn, J.F. *Solubilization in Surfactant Aggregates*, Marcel Dekker, Inc., New York, **1995**.

Churaev, N.V and Derjaguin, B.V. *Inclusion of Structural Forces in the Theory of Stability of Colloids and Films*, Journal of Colloids and Interface Science, Vol. 103, No. 2, **1985**, pp. 542-553.

Churcher, P.L., French, P.R, Shaw, J.C., and Schramm, L.L. *Rock Properties of Berea Sandstone, Baker Dolomite, and Indiana Limestone*, Presented at the SPE International Symposium on Oilfield Chemistry, Anaheim, California, 20-22. February, **1991**. Paper SPE 21044.

Cohen-Addad, S., and di Meglio, J.M. *Stabilization of Aqueous Foam by Hydrosoluble Polymers. 2. Role of Polymer/Surfactant Interactions*. Langmuir, 10, **1994**, pp. 773-778.

Corey, A.T., and Rathjens, C.H. *Effect of Stratification on Relative Permeability*, JPT, December, **1956**, pp. 69-71.

Czernichowski-Lauriol, I., Rochelle, C., Gaus, I., Azaroual, M., Pearce, J., and Durst, P. *Geochemical Interactions Between CO_2, Pore-Waters and Reservoir Rocks*, Advances in the Geological Storage of Carbon Dioxide, Nato Science Series IV: Earth and Environmental Series, Vol. 65, **2006**, pp. 157-174.

Dalland, M., Hanssen, J.E., and Kristiansen T.S. *Oil Properties with Foams at Static and Flowing Conditions in Porous Media*, Presented at the 13th IEA Collaborative Project on Enhanced Oil Recovery Symposium, Banff, Canada, 27-30. September, **1992**.

Davies, J.T. pp. *A Quantitative Kinetic Theory of Emulsion Type. I. Physical Chemistry of the Emulsifying Agent*, Gas/Liquid and Liquid/Liquid Interfaces, Proceedings of 2nd International Congress Surface Activity, Butterworths, London, **1957**, 426-438.

den Engelsen, C.W., Isarin, J.C., Gooijer, H., Warmoeskeren, M.M.C.G., and Wassink, J.G. *Bubble Size Distribution of Foam*, AUTEX Research Journal, Vol. 2, No. 1, March, **2002**, pp. 14-27.

Denkov, N.D. *Mechanisms of Foam Destruction by Oil-Based Antifoams*, Am. Chem. Soc. Langmuir, 20, **2004**, pp. 9463-9505.

Denkov, N.D., and Marinova, K.G. *Antifoam effects of solid particles, oil drops and oil-solid compounds in aqueous foams*, in Colloidal Particles at Liquid Interfaces (Ed. Binks, B.P., and Horozov, T.S), Cambridge University Press, Cambridge, UK, **2006**, pp. 383-444.

Derjaguin, B.V., and Churaev, N.V. *The Current State of the Theory of Long-Range Surface Forces*, Colloids and Surfaces, Vol. 41, **1989**, pp. 223-237.

de Vries, A.S., and Wit, K. *Rheology of Gas/Water Foam in the Quality Range Relevant to Steam Foam*, SPERE, May, **1990**, pp. 185-192.

Di Julio, S.S., and Emanuel, A.S. *Laboratory Study of Foaming Surfactant for CO_2 Mobility Control*, SPERE, May, **1989**, pp. 136-142.

Dixit, A., Tsau, J.S., and Heller, J.P. *Laboratory Study on Surfactant-Based Selective Mobility Control*, Presented at the 1994 SPE Permian Basin Oil & Gas Recovery Conference, Midland, Texas, 16-18. March, **1994**. Paper SPE 27729.

Dong, Y. *Experimental Study of CO_2 Foam Flow in Porous Media and Application of Fractional-Flow Method to Foam Flow*, MS Thesis, University of Texas at Austin, **2001**.

Drummond, C., and Israelachvili, J. *Surface Forces and Wettability*, JPSE, 33, **2002**, pp. 123-133.

Du, D.X., Beni, A.N., Farajzadeh, R., and Zitha, P.L.J. *Effect of Water Solubility on Carbon Dioxide Foam Flow in Porous Media: An X-ray Computed Tomography Study*, Ind. Eng. Chem. Res., 47, **2008**, pp. 6298-6306.

Du, D.X., Zitha, P.L.J., and Uijttenhout, M.G.H. *Carbon Dioxide Foam Rheology in Porous Media: A CT Scan Study*, SPEJ, June, **2007**, pp. 245-252.

Duan, Z.H., and Sun, R. *An Improved Model Calculating CO_2 Solubility in Pure Water and Aqueous NaCl Solutions from 273 to 533 K and from 0 to 2000 bar*, Chem. Geol. 193 (3-4), **2003**, pp. 257-271.

Duan, Z.H., Sun, R., Zhu, C., and Chou, I.M. *An Improved Model for the Calculation of CO_2 Solubility in Aqueous Solutions Containing Na^+, K^+, Ca^{2+}, Mg^{2+}, Cl^-, and SO_4^{2-}*, Marine Chem**.** 98 (2-4), **2006**, pp. 131-139.

Eastoe, J., and Dalton, J.S. *Dynamic Surface Tension and Adsorption Mechanisms of Surfactants at the Air-Water Interface*, Adv. in Colloid and Int. Sci., 85, **2000**, pp. 103-144.

Eastoe, J., Dower, A., Paul, A., Steytler, D.C., Rumsey, E., Penfold, J., and Heean R.K. *Fluoro-Surfactants at Air/Water and Water/CO_2 Interfaces*, Phys. Chem. Chem. Phys., 2, **2000b**, pp. 5235-5242.

Eastoe, J., Gold, S., and Steytler, D.C. *Surfactants for CO_2*, Langmuir, 22, **2006**, pp. 9832-9842.

Ebbing, D.D., and Gammon, S.D. *General Chemistry*, 9th edition, Brooks/Cole, Cengage Learning, USA **2011**, pp. 175-222 (Part 1.5).

Egermann, P., Chalbaud, C., Duquerroix, J.P., and Le Gallo, Y. *An Integrated Approach to Parameterize Reservoir Models for CO_2 Injection in Aquifers*, Paper presented at the SPE Annual Technical Conference and Exhibition, San Antonio, Texas, 24-27. September, **2006**. Paper SPE 102308.

Elhag, A.S., Chen, Y., Chen, H., Reddy, P.P., Cui, L., Worthen, A.J., Ma, M., Hirasaki, G.J., Nguyen, Q.P., Biswal, S.L., and Johnston, K.P. *Switchable Amine Surfactants for Stable CO_2/Brine Foams in High Temperature, High Saline Reservoirs,* Paper presented at the SPE Improved Oil Recovery Symposium, Tulsa, Oklahoma, 12-16. April, **2014**. Paper SPE 169041.

Energy Institute. *Good Plant Design and Operation for Onshore Carbon Capture Installations and Onshore Pipelines*, first edition, London, September, **2010**.

Enick, R.M. and Olsen, D.K. *Mobility and Conformance Control for Carbon Dioxide Enhanced Oil Recovery (CO_2-EOR) via Thickeners, Foams, and Gels – A Detailed Literature Review of 40 Years of Research*, DOE/NETL – 2012/1540; Activity 4003.200.01, Report prepared for the U.S. Department of Energy, **2012**.

Espinoza, D.N., and Santamarina J.C. *Water-CO_2-Mineral Systems: Interfacial Tension, Contact Angle, and Diffusion-Implications to CO_2 Geological Storage*, Water Resources Research, Vol. 46, W07537**, 2010**, pp. 1-10.

Ettinger, R.E., and Radke, C.J. *Influence on Foam Texture on Steady Foam Flow in Berea Sandstone*, SPERE, 7, **1992**, pp. 83-90.

European Commission. *Enhanced Oil Recovery using Carbon Dioxide in the European Energy System*, **2005**. Report EUR 21895 EN – DG JRC – Institute for Energy.

Evans, D.F., and Wennerström, H. *The Colloidal Domain, Where Physics, Chemistry, Biology and Technology Meet*, 2nd edition, Wiley-VCH, New York, **1999**.

Exerowa, D., and Kruglyakov P.M. *Foam and Foam Films: Theory, Experiment, Application*, Elsevier: Amsterdam, **1998**.

Falls, A.H. Hirasaki, G.J., Patzek, T.W., Gauglitz, D.A., Miller, D.D., and Ratulowski, T. *Development of a Mechanistic Foam Simulator: The Population Balance Approach and a Description of Generation by Capillary Snap-off*, SPERE, August, **1988a**, pp. 884-892.

Falls, A.H., Lawson, J.B., and Hirasaki, G.J. *The Role of Noncondensable Gas in Steam Foams*, JPT, Vol. 40, Issue 1, **1988b**, pp. 95-104.

Falls, A.H., Musters, J.J., and Ratulowski, J. *The Apparent Viscosity of Foams in Homogeneous Bead Packs*, SPERE, May, **1989**, pp. 155-164.

Farajzadeh, R., Andrianov, A., Bruining, H., and Zitha, P.L.J. *Comparative Study of CO_2 and N_2 Foams in Porous Media at Low and High Pressure-Temperatures*, Ind. Eng. Chem., 48, **2009**, pp. 4542-4552.

Farajzadeh, R., Andrianov, and Zitha, P.L.J. *Investigation of Immiscible and Miscible Foam for Enhancing Oil Recovery*, Ind. Eng. Chem., 49, **2010**, pp. 1910-1919.

Farajzadeh, R., Barati, A., Delil, H.A., Bruining, H., and Zitha, P.L.J. *Mass Transfer of CO_2 Into Water and Surfactant Solutions*, 25, **2007**, pp. 1493-1511.

Farajzadeh, R., Krastev, R. and Zitha, P.C.J. *Foam film permeability: Theory and Experiment*, Adv. Colloid Int. Sci., 137, **2008**, pp. 27-44.

Farajzadeh, R., Muruganathan, R.M., Krastev, R. and Rossen, W.R. *Effect of Gas Type on Foam Film Permeability and its Implications for Foam Flow in Porous Media*, Adv. Colloid Int. Sci., 168, **2011**, pp. 71-78.

Farajzadeh, R., Wassing, B.M., and Boerrigter, P.M. *Foam Assisted Gas-Oil Gravity Drainage in Naturally-Fractured* Reservoirs, Jour. Pet. Sci. Eng., 94-95, **2012a**, pp. 112-122.

Farajzadeh, R., Andrianov, A., Krastev, R., Hirasaki, G.J., and Rossen, W.R. *Foam–Oil Interaction in Porous Media: Implications for Foam Assisted Enhanced Oil Recovery*, Adv. Colloid Int. Sci., 183-184, **2012b**, pp. 1-13.

Fekarcha, L., and Tazerouti, A. *Surface Activities, Foam Properties, HLB, and Krafft Point of Some n-Alkanesulfonates (C14-C18) with Different Isometric Distributions*, Journal of Surfactant Detergents, 15, DOI 10.1007/s11743-012-1335-2, **2012**, pp. 419-431.

Fick, A. *Ueber Diffusion*, Annalen der Physik (German), Vol. 170, Issue 1, **1855**, pp. 59-86.

Fossen, H., and Bale, A. *Deformation Bands and Their Influence on Fluid Flow*, Am. Assoc. Pet. Geol. Bull., 91, **2007**, pp. 1685−1700.

Fossen, H., Schultz, R. A., Shipton, Z. K., and Mair, K. *Deformation Bands in Sandstone - A Review*, J. Geol. Soc., 164, **2007**, pp. 755−769.

Foster, N.C. *Sulfonation and Sulfation Processes*, The Chemithon Corporation, report, **1997**, pp. 1-36.

Fredd, C.N., Miller, M.J., and Quintero, B.W. *Impact of Water-Based Polymer Fluid Characteristics on CO_2 Foam Rheology*, Presented at the SPE International Symposium and Exhibition on Formation Damage Control, Lafayette, Louisiana, 18-20. February, **2004**. Paper SPE 86493.

Frette, O.I., Virnovsky, G., and Hildebrand-Habel, T. *Modelling the Stability of Thin Water Films Using SEM Images*, Presented at the 2009 SPE EUROPEC/EAGE Annual Conference and Exhibition, Amsterdam, The Netherlands, 8-11. June, **2009**. Paper SPE 121250.

Friedmann, F., and Jensen, J.A. *Some Parameters Influencing the Formation and Propagation of Foams in Porous Media*, Presented at the SPE California Regional Meeting, Oakland, California, 2-4. April, **1986**. Paper SPE 15087.

Friedmann, F., Chen, W.H., and Gauglitz, P.A. *Experimental and Simulation Study of High-Temperature Foam Displacement in Porous Media*, SPERE, February, **1991**, pp. 37-45.

Garrett, P.R. *Preliminary Considerations Concerning the Stability of a Liquid Heterogeneity in a Plane Parallel Liquid Film*, J. Colloid Interface Sci., 76, **1980**, 587-590.

Gauglitz, P.A., Friedmann, F., Kam, S.I., and Rossen W.R. *Foam Generation in Homogeneous Porous Media*, Chem. Eng. Sci., Vol. 57, Issue 19, October, **2002**, pp. 4037-4052.

Georgieva, D., Cagna, A., and Langevin, D. *Link between Surface Elasticity and Foam Stability*, Soft Matter, 5, **2009**, pp. 2063-2071.

Ghedan, S. *Global Laboratory Experience of CO_2-EOR Flooding*, Presented at the SPE/EAGE Reservoir Characterization & Simulation Conference, Abu Dhabi, UAE, 19-21. October, **2009**. Paper SPE 125581.

Green, D.W., and Willhite, G.P. *Enhanced Oil Recovery*, Richardson, Texas: Henry L. Doherty Memorial of AIME, Society of Petroleum Engineers, **1998**.

Griffin, W.C. *Classification of Surface-Active Agents by "HLB"*, JSCC, 1, 5, **1949**, pp. 311-326.

Grigg, R.B., and Schechter, D.S. *State of the Industry in CO_2 Floods*, Presented at the SPE Annual Technical Conference, San Antonio, Texas, 5-8. October, **1997**. Paper SPE 38849.

Grigg, R.B., Svec, R.K., Zeng, Z.W., Mikhalin, A., Liu, Y., Yin, G., Ampir, S., and Kassim, R. *Improving Gas Flooding Efficiency*, final report submitted by New Mexico Petroleum Recovery Research Center, report prepared for U.S. Department of Energy, August, **2008**. DOE Award No.: DE-FC26-04NT15532.

Gunter, W.D., Bachu, S., and Benson, S. *The Role of Hydrogeological and Geochemical Trapping in Sedimentary Basins for Secure Geological Storage of Carbon Dioxide*, Geological Society, London, 233, **2004**, pp.129-145.

Hadjiiski, A., Tcholakova, S., Denkov. N.D., Durbut, P., Broze, G., and Mehreteab, A. *Effect of Oily Additives on Foamability and Foam Stability. 2. Entry Barriers*, Langmuir, 17, **2001**, pp. 7011-7021.

Hanssen, J.E., and Dalland, M. *Foams for Effective Gas Blockage in the Presence of Crude Oil at Reservoir Temperature*, Presented at the 7th SPE/DOE Symposium on Enhanced Oil Recovery, Tulsa, Oklahoma, **1990**. Paper SPE/DOE 20193.

Hanssen, J.E., and Dalland, M. *Gas-Blocking Foams*, in Foams: Fundamentals and Application in the Petroleum Industry (ed. Schramm, L.L.), American Chemical Society, Washington DC, **1994**, pp. 319-353.

Hanssen, J.E., Holt, T., and Surguchev, L.M. *Foam Processes: An Assessment of Their Potential in North Sea Reservoirs Based on a Critical Evaluation of Current Field Experience*, Presented at the SPE/DOE ninth Symposium on Improved oil Recovery, Tulsa, Oklahoma, 17-20. April, **1994**. Paper SPE/DOE 27768.

Harkins, W.D. *A General Thermodynamic Theory of Spreading of Liquids to Form Duplex Films and of Liquids or Solids to Form Monolayers*, J. Chem. Phys., 9, **1941**, pp. 552-568.

Harrison, K.L., Johnston, K.P., and Sanchez, I.C. *Effect of Surfactants on the Interfacial Tension between Supercritical Carbon Dioxide and Polyethylene Glycol*, Langmuir, 12, **1996**, pp. 2637-2644.

Haugen, Å., Mani, N., Svenningsen, S., Brattekås, B., Graue, A., Ersland., and Fernø, M.A. *Miscible and Immiscible Foam Injection for Mobility Control in EOR in Fractured Oil-Wet Carbonate Rocks*, Transport in Porous Media, 104, **2014**, 109-131.

Heller, J.P. *Reservoir Application of Mobility Control Foams in CO_2 Floods*, Presented at the SPE/DOE Fourth Symposium on Enhanced Oil Recovery, Tulsa, Oklahoma, 15-18. April **1984**. Paper SPE/DOE 12644.

Heller, J.P. *CO_2 Foams in Enhanced Oil Recovery*, in Foams: Fundamentals and Application in the Petroleum Industry (ed. Schramm, L.L.), American Chemical Society, Washington DC, **1994**, pp. 201-234.

Heller, J.P., and Kuntamukkula, M.S. *Critical Review of the Foam Rheology Literature*, Ind. Eng. Chem. Res., 26, 2, **1987**, pp. 318-325.

Hildenbrand, A., Schlömer, S., Krooss, B.M., and Littke, R. *Gas Breakthrough Experiments on Peltic Rocks: Comparative Study with N_2, CO_2 and CH_4*, Geofluids, 4, **2004**, pp. 61-80.

Hirasaki, G.J. *The Steam-Foam Process*, JPT, May, **1989**, pp. 449-456.

Hirasaki, G.J. *Wettability Fundamentals and Surface Forces*, SPE Formation Evaluation, June, **1991**.

Hirasaki, G.J., Miller, C.A., Szafranski, R., Lawson, L.B., Tanzil, D., Jackson, R.E., Londergan, J., and Meinardus, H. *Field Demonstration of the Surfactant/Foam Process for Aquifer Remediation*, Paper presented at the 1997 SPE Annual Technical Conference and Exhibition in San Antonio, Texas, 5-8. October, **1997.** Paper SPE 39292.

Hirasaki, G.J., and Lawson, J.B. *Mechanisms of Foam Flow in Porous Media: Apparent Viscosity in Smooth Capillaries*, SPEJ, Vol. 25, Issue 2, **1985**, pp. 176–190.

Holm, L.W. *Foam Injection Test in the Siggins Field, Illinois*, JPT, December **1970**, pp. 1499-1506.

Holm, L.W. *The Mechanism of Gas and Liquid Flow Through Porous Media in the Presence of Foam*, SPEJ, December, **1968**, pp. 359-369.

Holm, L.W., and Garrison, W.H. *CO_2 Diversion With Foam in an Immiscible CO_2-Field Project*, SPERE, February, **1988**, pp. 112-118.

Holmberg, K. *Novel Surfactants: Preparation, Applications, and Biodegradability*, Marcel Dekker, New York, Second edition, **2003**.

Honarpour, M.M., Cullick, A.S., and Saad, N. *Influence of Small-Scale Rock Laminations on Core Plug Oil/Water Relative Permeabilities and Capillary Pressure*, Presented at the University of Tulsa Centennial Petroleum Engineering Symposium, Tulsa, Oklahoma, 29-31. August, **1994**. Paper SPE 27968.

Holt, T., Vassenden, F., and Svorstøl, I. *Effect of Pressure on Foam Stability; Implications for Foam Screening*, Presented at the 1996 SPE/DOE 10th Symposium on Improved Oil Recovery, Tulsa, Oklahoma, 21-24. April, **1996**. Paper SPE 35398.

Huang, D.D., Nikolov, A., and Wasan, D.T. *Foams: Basic Properties with Application to Porous Media*, Langmuir, Vol. 2, No. 5, **1986**, pp. 672-677.

Huang, Y., Ringrose, P.S., Sorbie, K.S., and Larter, S.R., *The Effects of Heterogeneity and Wettability on Oil Recovery from Laminated Sedimentary Structures*, SPE Journal, December, **1996**. Paper SPE 30781.

Høiland, H., and Blokhus, A.M. *Solubilization in Aqueous Surfactant Systems,* in Handbook of Surface and Colloid Chemistry, 2nd edition, (ed. Birdi, K.S.), CRC Press, Boca Raton, **2003**, Chapter 8.

Islam, A.W., and Carlson, E.S. *Viscosity Models and Effects of Dissolved CO_2*, Energy and Fuels, 26, 8, **2012**, pp. 5530-5336.

Israelachvili, J.N. *Intermolecular and Surface Forces*, 3rd edition, Elsevier, USA, **2011**, pp. 341-497

Jensen, J.A., and Friedmann, F. *Physical and Chemical Effects of an Oil Phase on the Propagation of Foam in Porous Media*, Presented at the SPE California Regional Meeting, Ventura, California, 8-10. April, **1987**. Paper SPE 16375.

Johnston, K.P., and da Rocha, S.R.P. *Colloids in Supercritical Fluids over the last 20 Years and Future Directions*, The Journal of Supercritical Fluids, Vol. 47, Issue 3, January, **2009**, pp. 523-530.

Khalil, F., and Asghari, K. *Application of CO_2-Foam as a Means of Reducing Carbon Dioxide Mobility*, JCPT, Vol. 45, No. 5, May **2006**, pp. 37-42.

Khatib, Z.I., Hirasaki, G. J., and Falls, A.H. *Effects of Capillary Pressure on Coalescence and Phase Mobilities in Foams Flowing Through Porous Media*, SPERE, August, **1988**, pp. 919-926.

Kibodeaux, K.R. *Experimental and Theoretical Studies of Foam Mechanisms in Enhanced Oil Recovery and Matrix Acidization Applications*, PhD dissertation, The University of Texas at Austin, **1997**.

Kim, J.S., Dong, Y, and Rossen, W.R. *Steady-State Flow Behavior of CO_2 Foam*, Presented at the SPE/DOE Fourteenth Symposium on Improved Oil Recovery, Tulsa, Oklahoma, 17-21. April, **2004**. Paper SPE 89351.

King, M.B. *The Mutual Solubilities of Water with Supercritical and Liquid Carbon Dioxide*, Journal of Supercritical Fluids, 5, **1992**, pp. 296-302.

Koczo, K., Lobo, L., and Wasan, D.T. *Effect of Oil on Foam Stability: Aqueous Foams Stabilized by Emulsions*, J. Colloid Interface Sci., 150, **1992**, pp. 492-506.

Kovscek, A.R., and Bertin, H.J. *Foam Mobility in Heterogeneous Porous Media (II: Experimental Observations)*, Transport in Porous Media, 52, **2003**, pp. 37-49.

Kovscek, A.R., and Radke, C.J. *Fundamentals of Foam Transport in Porous Media*, in Foams: Fundamentals and Application in the Petroleum Industry (ed. Schramm, L.L.), American Chemical Society, Washington DC, **1994**, pp.115-163.

Kralchevsky, P.A., Danov, K.D., and Ivanov, I.B. *Thin Liquid Film Physics*, in Foams: Theory, Measurements, and Applications, (ed. Prud'homme, R.K., and Khan, S.A.), Surf. Sci. Series, Vol. 57, Marcel Dekker, New York, **1996**, pp. 1-98.

Krasowska, M., Hristova, E., Khristov, K., Malysa, K., and Exerowa, D. *Isoelectric State and Stability of Foam Films, Bubbles and Foams from PEO-PPO-PEO Triblock Copolymer (P-85*). Colloid Polym., Sci., 284, **2006**, pp. 475–81.

Krause, R.E., Lane, R.H., Kuehne, D.L., and Bain, G.F. *Foam Treatment of Producing Wells To Increase Oil Production at Prudhoe Bay*, Presented at the SPE/DOE Eighth Symposium on Enhanced Oil Recovery, Tulsa, Oklahoma, 22-24. April, **1992**. Paper SPE/DOE 21191.

Krevor, S.C.M., Pini, R., Zuo, L. and Benson, S.M. *Relative Permeability and Trapping of CO_2 and Water in Sandstone Rocks at Reservoir Conditions*, Water Resources Research, Vol. 48, W02532, **2012**.

Kuehne, D.L., Frazier, R.H., Cantor, J., and Horn, W. *Evaluation of Surfactants for CO_2 Mobility Control in Dolomite Reservoirs*, Presented at the SPE/DOE Eighth Symposium on Enhanced Oil Recovery, Tulsa, Oklahoma, 22-24. April, **1992**. Paper SPE/DOE 24177.

Kuhlman, M.I. *Visualizing the Effect of Light Oil on CO_2 Foams*, JPT, Vol. 42, No. 7, July, **1990**, pp. 902-908.

Kuhlman, M.I., Falls, A.H., Hara, S.K., Monger-McClure, T.G., and Borchardt J.K. *CO_2 Foam With Surfactants Used Below Their Critical Micelle Concentrations*, SPERE, Vol. 7, No. 4, November, **1992**, pp. 445-452.

Lake, L.W. *Enhanced Oil Recovery*, Prentice Hall, New Jersey, **1989**.

Langevin, D. *Influence of Interfacial Rheology on Foam and Emulsion Properties*, Advances in Colloid and Interface Science, Vol. 88, Issue 1-2, December, **2000**, pp. 209-222.

Lee, H.O., Heller, J.P., and Hoefer, A.M.W. *Change in Apparent Viscosity of CO_2 foam With Rock Permeability*, SPERE, November, **1991**, pp. 421-428.

Lescure, B.M., and Claridge, E.L. *CO_2 Foam Flooding vs. Rock Wettability*, Presented at the SPE Annual Technical Conference and Exhibition, New Orleans, U.S.A., 5-8. October, **1986**. Paper SPE 15445.

Levinson, M.I. *Surfactant Production: Present Realities and Future Perspectives*, in Handbook of Detergents, Part F: Production (ed. Zoller, U.), Taylor & Francis Group, Florida, **2009**, pp. 1-37.

Li, Q. *Foam Generation and Propagation in Homogeneous and Heterogeneous Porous Media*, PhD dissertation, University of Texas at Austin, **2006**.

Liontas, R., Ma, K., Hirasaki, G.J., and Biswal, S.L. *Neighbor-Induced Bubble Pinch-Off: Novel Mechanisms of In Situ Foam Generation in Microfluidic Channels*, Soft Matter, 9, **2013**, pp. 10971–10984.

Liu, Y., Griegg, R.B., and Svec, R.K. *CO_2 Foam Behaviour: Influence of Temperature, Pressure, and Concentration of Surfactant*, Presented at the SPE Production Operations Symposium, Oklahoma City, Oklahoma, 16-19. April, **2005a**. Paper SPE 94307.

Liu, Y., Griegg, R.B., and Bai, B. *Salinity, pH, and Surfactant Concentration Effects on CO_2-foam*, Presented at the SPE International Symposium on Oilfield Chemistry, The Woodlands, Texas, 2-4. February, **2005b**. Paper SPE 93095.

Lothe, A. E., Gabrielsen, R. H., Larsen, N., and Bjørnevoll, B. T. *An Experimental Study of the Texture of Deformation Bands: Effects on Porosity and Permeability of Sandstones*, Pet. Geosci., 8, **2002**, pp. 195-207.

Ma, K. *Transport of Surfactant and Foam in Porous Media for Enhanced Oil Recovery Processes*, PhD dissertation, Rice University, **2013**.

Maini, B.B., and Ma, V. *Relationship Between Foam Stability Measured in Static Tests and Flow Behaviour of Foams in Porous Media*, Presented at the 59th Annual Technical Conference and Exhibition, Houston, Texas, 16-19. September, **1984**. Paper SPE 13073.

Maini, B.B., and Ma, V. *Laboratory Evaluation of Foaming Agents for High-Temperature Applications- I. Measurements of Foam Stability at Elevated Temperatures and Pressures*, JCPT, December, **1986**, pp. 65-69.

Malysa, K., and Lunkenheimer, K. *Foams under Dynamic Conditions*, Curr. Opinion in Colloid and Int. Sci., 13, **2008**, pp. 150-162.

Mannhardt, K., *Core Flood Evaluation of Solvent Compositional and Wettability Effects on Hydrocarbon Solvent Foam Performance* JCPT, Vol. 38, No. 13, **1999**, pp. 1-12.

Mannhardt, K., and Novosad, J.J. *Adsorption of Foam-Forming Surfactants for Hydrocarbon-Miscible Flooding at High Salinities*, in Foams: Fundamentals and Application in the Petroleum Industry (ed. Schramm, L.L.), American Chemical Society, Washington DC, **1994**, pp. 259-316 (Chapter 7).

Mannhardt, K., Novosad, J.J., and Schramm, L.L. *Core Flood Evaluation of Hydrocarbon Solvents Foams*, JPSE, Vol. 14, **1996**, pp. 183-195.

Mannhardt, K., Novosad, J.J., and Schramm, L.L. *Comparative Evaluation of Foam Stability to Oil*, SPE Reservoir Eval. & Eng. 3 (1), February **2000**, pp. 23-34.

Mannhardt, K., Schramm, L.L., and Novosad, J.J. *Effect of Rock Type and Brine Compositions on Adsorption of Two Foam Forming Surfactants*, SPE Advanced Technology Series, Vol. 1, No. 1, **1993**, pp. 212-218.

Mannhardt, K., and Svorstøl, I., *Effect of Oil Saturation on Propagation in Snorre Reservoir Core*, JPSE, Vol. 23, Issue 3-4, October, **1999**, pp. 189-200.

Mannhardt, K., and Svorstøl, I., *Surfactant Concentration for Foam Formation and Propagation in Snorre Reservoir Core*, JPSE, Vol. 30, Issue 2, July, **2001**, pp.105-119.

Manrique, E., Thomas, C., Ravikiran, R., Izadi, M., Lantz, M., Romero, J., and Alvardo, V. *EOR: Current Status and Opportunities*, Presented at the SPE Improved Oil Recovery Symposium, Tulsa, Oklahoma, 24-28. April, **2010.** Paper SPE 130113.

Marsden, S.S., and Kahn, S.A. *The Flow of Foam Through Short Porous Media and Apparent Viscosity Measurements*, SPEJ, March, **1966**, pp. 17-25.

Mast, R.F. *Microscopic Behavior of Foam in Porous Media*, SPE, **1972**. Paper SPE 3997.

Mathiassen, O.M. *CO_2 as Injection Gas for Enhanced Oil Recovery and Estimation of the Potential on the Norwegian Continental Shelf*, PhD dissertation, Norwegian University of Science and Technology (NTNU), **2003**.

Menzie, D.E. *Dispersion Measurement as a Method of Quantifying Geologic Characterization and Defining Reservoir Heterogeneity*, Report prepared for the U.S. Department of Energy, May, **1995.**

McPhee, C.A., Tehrain, A.D.H., and Jolly, R.P.S. *Foam Flooding of Cores Under North Sea Reservoir Conditions*, Presented at the SPE/DOE Enhanced Oil Recovery Symposium, Tulsa, Oklahoma, 17-20. April, **1988**. Paper SPE/DOE 17360.

McLendon, W.J., Koronaios, P., McNulty, S., Enick, R.M., Biesmans, G., Miller, A., Salazar, L., Soong, Y., Romanov, V., and Crandall, D. *Assessment of CO_2-Soluble Surfactants for Mobility Reduction using Mobility Measurements and CT Imaging*, Presented at the SPE Improved Oil Recovery Symposium, Tulsa, Oklahoma, 14-18. April, **2012**. Paper SPE 154205.

Mohammadi, A.H., Chapoy, A., Tohidi, B., and Richin, D. *Water Content Measurement and Modeling in the Nitrogen + Water System*, J. Chem. Eng. Data., 50, 2, **2005**, pp. 541-545.

Mohammadi, S.S., Slyke, D.C., and Ganong, B.L. *Steam-Foam Pilot Project in Dome-Tumbador, Midway-Sunset Field*, SPERE, February, **1989**, pp. 7-16.

Moradi-Araghi, A., Johnston, E.L., Zornes, D.R., and Harpole, K.J. *Laboratory Evaluation of Surfactants for CO_2-Foam Applications at the South Cowden Unit*, Presented at the International Symposium on Oilfield Chemistry, Houston, Texas, 18-21. February, **1997**. Paper SPE 37218.

Mukherjee, J., Norris, S.O., Nguyen, Q.P., Scherlin, J.M., Vanderwal, P.G., and Abbas, S. *CO_2 Foam Pilot in Salt Creek Field, Natrona County, WY: Phase I: Laboratory Work, Reservoir Simulation, and Initial Design*, Presented at the SPE Improved Oil Recovery Symposium, Tulsa, Oklahoma, 12-16. April, **2014**. Paper SPE 169166.

Nguyen, Q.P., Alexandrov, A., Zitha, P.L.J., and Currie, P.K., *Experimental and Modeling Studies on Foam in Porous Media: A Review*, Presented at the 2000 SPE International Symposium on Formation Damage Control, Lafayette, Louisiana, 23-24. February, **2000**. Paper SPE 58799.

Nguyen, Q.P., Currie, P.K., and Zitha, P.L.J. *Effect of Crossflow on Foam-Induced Diversion in Layered Formations*, SPEJ, March, **2005**, pp. 54-65.

Nguyen, Q.P., Zitha, P.L.J., Currie, P.K., and Rossen, W.R. *CT Study of Liquid Diversion with Foam*, SPE Production & Operations, February, **2009**, pp. 12-21.

Nikolov, A.D., and Wasan, D.T. Huang, D.W., and Edwards, D.A. *The Effect of Oil on Foam Stability: Mechanisms and Implications for Oil Displacement by Foam in Porous Media*, Presented at the SPE Annual Technical Conference and Exhibition, New Orleans, Louisiana, 5-8. October, **1986**. Paper SPE 15443.

Nikolov, A.D., and Wasan, D.T. *Ordered Micelle Structuring in Thin Films Formed from Anionic Surfactant Solutions: I. Experimental*, J. Colloid and Interface Sci., Vol. 133, Issue 1, **1989**, pp.1-12.

Nonnekes, L.E., Cox, S.J. and Rossen, W.R. *Effect of Gas Diffusion on Mobility of Foam for EOR*, Presented at the SPE Annual Technical Conference and Exhibition, San Antonio, Texas, 8-10. October, **2012**. Paper SPE 159817.

Novosad, J.J., and Ionescu, E.F. *Foam Forming Surfactants For Beaverhill Lake Carbonates and Gilwood Sands Reservoirs*, Presented at the 38th Annual Technical Meeting of the Petroleum Society of CIM, Calgary, 7-10. June, **1987**. Paper No. 87-38-80.

Ocampo, A., Restrepo, A., Cifuentes, H., Hester, J., Orozco, N., Gil, C., Castro, E., Lopera, S., and Gonzalez, C. *Successful Foam EOR Pilot in a Mature Volatile Oil Reservoir Under Miscible Gas Injection*, Presented at the International Petroleum Technology Conference, Beijing, China, 26-28. March, **2013**. Paper IPTC 16984.

Oldenburg, C.M., and Benson, S.M. *CO_2 Injection for Enhanced Gas Production and Carbon Sequestration*, Presented at the SPE International Petroleum Conference and Exhibition, Villahermosa, Mexico, 10-12. February, **2002**. Paper SPE 74367.

Organization of the Petroleum Exporting Countries (OPEC). *World Oil Outlook 2013*, Vienna, Austria, **2013**. Report is available at www.opec.org.

Oshita, T., Okabe, H., and Namba, T. *Early Water Breakthrough – X-ray CT Visualizes How It Happens in Oil-Wet Cores*, Presented at the 2000 SPE Asia Pacific Conference on Integrated Modelling for Asset Management, Yokohama, Japan, 25-26. April, **2000**. Paper SPE 59426.

OSPAR Commission. *Assessment of Impacts of Offshore Oil and Gas Activities in the North-East Atlantic*, **2009**. Report is available at www.ospar.org.

Osterloh, W.T., and Jante, M.J. *Effects of Gas and Liquid Velocity on Steady-State Foam Flow at High Temperature*, Presented at the SPE/DOE Enhanced Oil Recovery Symposium, Tulsa, Oklahoma, 22-24. April, **1992**. Paper SPE 24179.

Ottesen, B., and Hjelmeland, O. *The Value Added From Proper Core Analysis*, Presented at the International Symposium of the Society of Core Analysts, Abu Dhabi, UAE, 29 Oct. – 2 Nov., **2008**.

Oughanem, R., Youssef, S., Peysson, Y., Bazin, B., Maire, E., and Vizika, O. *Pore-Scale to Core-Scale Study of Capillary Desaturation Curves Using Multi-Scale 3D Imaging*, Presented at the International Symposium of the Society of Core Analysts, Napa Valley, U.S.A., 16-19. September, **2013.**

Parks, G.A. *Surface Energy and Adsorption at Mineral-Water Interfaces: an Introduction*, Reviews in Mineralogy and Geochemistry, 23, **1990**, pp. 133-169.

Parlar, M., Parris, M.D., Jasinski, R.J., and Robert, J.A. *An Experimental Study of Foam Flow Through Berea Sandstone with Applications to Foam Diversion in Matrix Acidizing*, Presented at the Western Regional Meeting, Bakersfield, California, 8-10. March, **1995**. Paper SPE 29678.

Pashley, R.M., and Karaman, M.E. *Applied Colloid and Surface Chemistry*, John Wiley & Sons Ltd., England, **2004**, Chapter 4.

Patzek, T.W., and Koinis, M.T. *Kern River Steam-Foam Pilots*, JPT, April, **1990**, pp. 496-503.

Pentland, C.H. *Measurements of Non-wetting Phase Trapping in Porous Media*, PhD dissertation, Imperial College London, **2011**.

Persoff, P., Radke, C.J., Preuss, K., Benson, S.M., and Witherspoon, P.A. *A Laboratory Investigation of Foam Flow in Sandstone at Elevated Pressure*, SPERE, August, **1991**, pp. 365-372.

Phillips, A.M., Couchman, D.D., and Wilke, J.G. *Successful Field Application of High-Temperature Rheology of CO_2 Foam Fracturing Fluids*, Presented at the SPE/DOE Low Permeability Reservoirs Symposium, Denver, Colorado, 16-19. May, **1987**. Paper SPE/DOE 16416.

Prieditis, J., and Paulett, G.S. *CO_2-Foam Mobility Tests at Reservoir Conditions in San Andreas Cores*, Presented at the SPE/DOE Eighth Symposium on Enhanced Oil Recovery, Tulsa, Oklahoma, 22-24. April, **1992**. Paper SPE/DOE 24178.

Princen, H.M., and Mason, S.G. *The Permeability of Soap Films to Gases*, J. Colloid and Sci., 20, **1965**, pp. 353-375.

Prud'homme, R.K., and Kahn, S.A. *Foams: Theory, Measurements, and Applications*, Surf. Sci. Series, Vol 57, Marcel Dekker, New York, **1996**.

Pugh, R.J. *Experimental Techniques for Studying the Structure of Foams and Froths*, Adv. Colloid Interface Sci., **2005**, 114–115, 239–51.

Radke, C.J., and Manlowe, D.J. *A Pore-Level Investigation of Foam-Oil Interactions in Porous Media*, SPERE, 5, November, **1990**, pp. 495-502.

Rafati, R., and Hossein, H. *The Influence of Reservoir Rock Wettability on CO_2-Foam Stability in Porous Media*, Presented at the International Petroleum Technology Conference, Bangkok, Thailand, 15-17. November, **2011**.

Railsback, L.B. *An explanation of Point of Zero Charge*, Railsback's Some Fundamentals of Mineralogy and Geochemistry, **2006,** http://www.gly.uga.edu/railsback/Fundamentals/ (8150PointofZeroCharge).

Ransohoff, T.C., and Radke, C.J. *Mechanisms of Foam generation in Glass-Bead Packs*, SPERE, May, **1988**, pp. 573-585.

Raterman, K. *An Investigation of Oil Destabilization of Nitrogen Foam in Porous Media*, Presented at the 64th SPE Annual Technical Conference and Exhibition, San Antonio, Texas, 8-11 October, **1989**. Paper SPE 19692.

Raventós, M., Duarte, S., and Alarcón, R. *Application and Possibilities of Supercritical CO_2 Extraction in Food Processing Industry: An Overview*, Food Sci. Tech Int., 8, 5, **2002**, pp. 269-284.

Reidenbach, V.G., Harris, P.C., Lee, Y.N., and Lord, D.L. *Rheological Study of Foam Fracturing Fluids Using Nitrogen and Carbon Dioxide*, SPE Production Engineering, Vol. 1, Issue 1, **1986**, pp. 31-41.

Robertson, E.P., Thomas, C.P., Zhang, Y., and Morrow, N.R. *Improved Waterflooding through Injection-Brine Modification*, Report prepared for the U.S. Department of Energy, January, **2003**.

Robinson, J.V., and Woods, W.W. *A Method of Selecting Foam Inhibitors*, J. Soc. Chem. Ind., 67, **1948**, pp. 361-365.

Rohani, M.R., Ghotbi, C., and Badakhshan, A. *Foam Stability and Foam-oil Interactions*, Pet. Sci. Tech., 32, **2014**, pp.1843-1850.

Rogers, J.D., and Grigg, R.B., *A Literature Analysis of the WAG Injectivity Abnormalities in the CO_2 Process*, Presented at the 2000 SPE/DOE Improved Oil Recovery Symposium, Tulsa, Oklahoma, 3-5. April, **2000**. Paper SPE 59329.

Romero, C., Alvarez, J.M., and Muller, A.J. *Micromodel Studies of Polymer-Enhanced Foam Flow Through Porous Media*, Presented at the 2002 SPE/DOE Improved Oil Recovery Symposium, Tulsa, Oklahoma, 13-17. April, **2002**. Paper SPE 75179.

Romero-Zeròn, L., and Kantzas, A. *The Effect of Wettability and Pore Geometry on Foamed-Gel-Blockage Performance*, SPERE, Vol. 10, Issue 2, April, **2007**, pp. 150-163.

Ross, S., and Morrison, I.D. *Colloidal Systems and Interfaces*, John Wiley and Sons, New York, **1998**, pp. 294-325.

Rossen, W.R. *Theory of Mobilization Pressure Gradient of Flowing Foams in Porous Media, II. Effect of Compressibility*, Journal of Colloid and Interface Science, Vol. 136, No. 1, April, **1990**, pp. 17-37.

Rossen, W.R. *Foams in Enhanced Oil Recovery* in Foams: Theory, Measurements, and Applications, (ed. Prud'homme, R.K., and Khan, S.A.), Surf. Sci. Series, Vol 57, Marcel Dekker, New York, **1996**, pp. 413-464.

Rossen, W.R. *A critical review of Roof snap-off as a mechanism of steady-state foam generation in homogeneous porous media*, Colloid and Surfaces A: Physicochem. Eng. Aspects, 225, **2003**, pp. 1-24.

Rossen, W.R., and Gauglitz, P.A. *Percolation Theory of Creation and Mobilization of Foams in Porous Media*, AIChE Journal, Vol. 36, No. 8, August, **1990**, pp. 1176-1188.

Rossen, W.R., and Lu, Q. *Effect of Capillary Crossflow on Foam Improved Oil Recovery*, Presented at the 1997 SPE Western Regional Meeting, Long Beach, California, 25−27. June, **1997**. Paper SPE 38319.

Rossen, W.R., and Zhou, Z.H. *Modeling Foam Mobility at the Limiting Capillary Pressure*, SPE Advanced Technology Series, Vol. 3, No. 1, **1995**, pp. 146-153.

Rotevatn, A., Sandve, T. H., Keilegavlen, E., Kolyukhin, D., and Fossen, H. *Deformation Bands and Their Impact on Fluid Flow in Sandstone Reservoirs: The Role of Natural Thickness Variations*, Geofluids, **2013**, DOI: 10.1111/gfl.12030.

Rubio, J., Souza, M.L., and Smith, R.W. *Overview of flotation as a wastewater treatment*, Min. Eng., 15, **2002** pp. 139-155.

Saint-Jalmes, A. *Physical Chemistry in Foam Drainage and Coarsening*, Soft Matter, 2, **2006**, pp. 836-849.

Sanchez, J.M., and Schechter, R.S. *Surfactant Effects on the Two-Phase Flow of Steam-Water and Nitrogen-Water through Permeable Media*, JPSE, 3, **1989**, pp.185-199.

Sanders, A.W., Jones, R.M., Linroth, M., and Nguyen, Q.P. *Implementation of a CO_2 Foam pilot Study in the SACROC Field: Performance Evaluation*, Presented at the SPE Annual Technical Conference and Exhibition, San Antonio, Texas, 8-10. October, **2012**. Paper SPE 160016.

Sanders, A.W., Nguyen, Q.P., Nguyen, N.M., Adkins, S.S., and Johnston, K.P. *Twin-Tailed Surfactants for Creating CO_2-in-Water Macroemulsions for Sweep Enhancement in CO_2-EOR*, Presented at the Abu Dhabi International Petroleum Exhibition & Conference, Abu Dhabi, United Arabic Emirates, 1-4. November, **2010**. Paper SPE 137689.

Sandrea, I., and Sandrea, R. *Global Oil Reserves – Recovery Factors Leave Vast Target for EOR Technologies*, Oil & Gas Journal, November, **2007.**

Schmidt, D.L. *Nonaqueous Foams*, in Foams: Theory, Measurements, and Applications, (ed. Prud'homme, R.K., and Khan, S.A.), Surf. Sci. Series, Vol 57, Marcel Dekker, New York, **1996**, pp. 287-314

Schramm, L.L. *Foams: Fundamentals and Application in the Petroleum Industry*, American Chemical Society, Washington DC, **1994a**.

Schramm, L.L. *Foam Sensitivity to Crude Oil in Porous Media*, in Foams: Fundamentals and Application in the Petroleum Industry (ed. Schramm, L.L.), American Chemical Society, Washington DC, **1994b**, pp. 165-197 (Chapter 4).

Schramm, L.L., and Kutay, S.M. *Emulsions and Foams in the Petroleum Industry*, in Surfactants: Fundamentals and Application in the Petroleum Industry (ed. Schramm, L.L.), Cambridge University Press, United Kingdom, **2000**, pp. 79-120 (Chapter 3).

Schramm, L.L., and Mannhardt, K. *The Effect of Wettability on Foam Sensitivity to Crude Oil in Porous Media*, Jour. Pet. Sci. Eng., Vol. 15, Issue 1, July, **1996**, pp.101-113.

Schramm, L.L., and Mannhardt, K., and Novosad, J.J. *Electrokinetic Properties of Reservoir Rock Particles*, Colloids and Surfaces, 55, **1991**, pp. 309-331.

Schramm, L.L., and Novosad, J.J. *Micro-Visualization of Foam Interactions with a Crude Oil*, Colloids and Surfaces, 46, **1990**, pp 21-43.

Schramm, L.L., and Novosad, J.J. *The Destabilization of Foams for Improved Oil Recovery by Crude Oils: Effect of the Nature of the Oil*, J. Petr. Sci. Eng., **1992**, pp. 77-90.

Schramm, L.L., Turta, A.T., and Novosad, J.J. *Microvisual and Coreflood Studies of Foam Interactions With a Light Crude Oil*, SPERE, Vol. 8, No. 3, **1993**, pp. 201-206.

Schramm, L.L., and Wassmuth, F. *Foams: Basic Principles*, in Foams: Fundamentals and Application in the Petroleum Industry (ed. Schramm, L.L.), American Chemical Society, Washington DC, **1994**, pp. 3-45 (Chapter 1).

Shiran, B.S. *Enhanced Oil Recovery by Combined Low Salinity Water and Polymer Flooding*, PhD dissertation, University of Bergen, **2014**.

Selley, R.C. *Elements of Petroleum Geology*, Academic Press, San Diego, 2nd edition, **1998**,

Seright, R.S. *Improved Techniques for Fluid Diversion in Oil Recovery Processes*, Final report, DOE/BC/14880-15, Contract No. DE-AC22-92BC14880, U.S. DOE, January, **1996**.

Siddiqui, S., Talabani, S., Saleh, S. T., and Islam, M. R. *A Laboratory Investigation of Foam Flow in Low-Permeability Berea Sandstone Cores*, Presented at the 1997 SPE Production Operations Symposium, Oklahoma City, March 9-12. **1997a**. Paper SPE 37416.

Siddiqui, S., Talabani, S., Yang, J., Saleh, S., and Islam, M. R. *An Experimental Investigation of the Diversion Characteristics of Foam in Berea Sandstone Cores of Contrasting Permeabilities*, Presented at the 1997 SPE Production Operations Symposium, Oklahoma City, March 9-12. **1997b**. Paper SPE 37463.

Silin, D., Tomutsa, L., Benson, S.M., and Patzek, T.W. Microtomography and Pore-Scale Modeling of Two-Phase Fluid Distribution, Transp. Porous Media, 86, **2011**, pp. 495–515.

Simjoo, M., Dong, Y., Andrianov, A., Talanana, M., and Zitha, P.L.J. *Novel Insight into Foam Mobility Control*, SPE Journal, June, **2013a**, pp. 416-427.

Simjoo, M., Dong, Y., Andrianov, A., Talanana, M., and Zitha, P.L.J. *CT Scan Study of Immiscible Foam Flow in Porous Media for Enhanced Oil Recovery*, Industrial & Engineering Chemistry Research, 52, March, **2013b**, pp. 6221-6233.

Sivak, A., Goyer, M., and Perwak, J. *Environmental and Human Health Aspects of Commercially Important Surfactants*, in Solution Behavior of Surfactants, Vol. 1, (ed. Mittel, K.L., and Fandler, E.J.), Plenum Publishing Corporation, **1982**, pp. 161-188.

Skarestad, M., and Skauge, A. *PTEK 213 – Reservoarteknikk II* (Norwegian)**,** University of Bergen, **2008**.

Skauge, A., Aarra, M.G., Surguchev, L.M, Martinsen, H.A., and Rasmussen, L. *Foam Assisted WAG: Experience from the Snorre Field*, Presented at the SPE/DOE Improved Oil Recovery Symposium, Tulsa, Oklahoma, 13-17. April, **2002**. Paper SPE 75157.

Solbakken, J.S. *An Experimental Study of Low Salinity Surfactant Flooding in Low Permeability Berea Sandstone*, Master Thesis, University of Bergen, **2010**.

Solbakken, J.S., Skauge, A., and Aarra, M.G. *Supercritical CO_2-foam - The Importance of CO_2 Density on Foams Performance*, Presented at the SPE Enhanced Oil Recovery Conference, Kuala Lumpur, Malaysia, 2-4. July, **2013**. Paper SPE 165296.

Solbakken, J.S., Skauge, A., and Aarra, M.G. *Foam Performance in Low Permeability Laminated Sandstones*, Energy & Fuels, 28, **2014**, pp. 803-815.

Solbakken, J.S. *Surfactant Evaluation and Oil Interactions with Foams at Static and Dynamic Conditions*, Internal report, UniCIPR, May, **2013**.

Spildo, K., Johannessen, A.M., and Skauge, A. *Low Salinity Waterflood at Reduced Capillarity*, Presented at the Eighteen SPE Improved Oil Recovery Symposium, Tulsa, Oklahoma, 14-18. April, **2012**. Paper SPE 154236.

Spirov, P., Rudyk, S.N., and Khan, A.A. *Foam Assisted WAG, Snorre Revisit with New Foam Screening Model*, Presented at the North Africa Technichal Conference and Exhibition, Cairo, Egypt, 20-22. February, **2012**. Paper SPE 150829.

Stalkup, F.I. *Status of Miscible Displacement*, SPEJ, April, **1983**. pp. 815-826.

Stasiuk, E.N.B., and Schramm, L.L. *The Temperature Dependence of the Critical Micelle Concentrations of Foam-Forming Surfactants*, Journal of Colloid and Interface Science, Vol. 178, Issue 1, March, **1996**, pp. 324-333.

Strycker, A.R., Madden, M.P., and Sarathi, P. *Effectiveness of Screening Tests as Predictive Models for Steamflood Additives*, SPERE, November, **1987**.

Suekane, T., Nobuso, T., Hirai, S., and Kiyota, M. *Geological Storage of Carbon Dioxide by Residual Gas and Solubility Trapping*, Int. J. Greenhouse Gas Control, 2, **2008**, pp. 58–64.

Suffridge, F.E., Raterman, K.T., and Russel, G.C. *Foam Performance Under Reservoir Conditions*, Presented at the SPE Annual Technical Conference and Exhibition, San Antonio, Texas, 8-11. November, **1989**. Paper SPE 19691.

Svorstøl, I., Blaker, T., Tham, M.J., and Hjellen, A. *A Production Well Foam Pilot in The North Sea Snorre Field – Application of Foam to Control Premature Gas Breakthrough*, Presented at the 9th European Symposium on Improved Oil Recovery, The Hague, The Netherlands, 20-22. October, **1997**.

Syahputra, A.E., Tsau, J-S., and Grigg, R.B. *Laboratory Evaluation of Using Lignosulfonate and Surfactant Mixture in CO_2 Flooding*, Presented at the 2000 SPE/DOE Improved Oil Recovery Symposium, Tulsa, Oklahoma, 3-5. April, **2000**. Paper SPE 159368.

Talebian, S.H., Masoudi, R., Tan, I.M., and Zitha, P.L.J. *Foam assisted CO_2-EOR; Concepts, Challenges and Applications*, Presented at the SPE Enhanced Oil Recovery Conference, Kuala Lumpur, Malaysia, 2-4. July, **2013**. Paper SPE 165280.

Tamura, T., Kaneko, Y., and Nikaido, M. *Stability Factors of Foam Film in Contrast to Fluctuation Induced by Humidity Reduction*, Journal of Colloid and Interface Science, 190, **1997**, pp. 61-70.

Tamura, T., Kaneko, Y., and Ohyama, M. *Dynamic Surface Tension and Foaming Properties of Aqueous Polyoxyethylene n-Dodecyl Ether Solutions*, Journal of Colloid and Interface Science, Vol. 173, Issue 2, **1995**, pp. 493-499.

Tanzil, D. *Foam Generation and Propagation in Heterogeneous Porous Media*, PhD dissertation, Rice University, **2001**.

The Norwegian Ministry of Petroleum and Energy. *Report by the Government-Appointed Committee on Increased Oil Recovery on the Norwegian Continental Shelf*, **2010**.

Thomas, S. *Enhanced Oil Recovery – An Overview*, Oil & Gas Science and Technology, Vol. 63, No. 1, **2008**, pp. 9-19.

Thompson, K.E., and Gdanski, R.D. *Laboratory Study Provides Guidelines for Diverting Acid with Foam*, SPE Production and Facilities, Vol. 8, Issue 4, November, **1993**, pp. 285-290.

Torabi, A., Fossen, H., and Alaei, B. *Application of Spatial Correlation Functions in Permeability Estimation of Deformation Bands in Porous Rocks*. Journal of Geophysical Research, Vol. 113, **2008**, B08208, DOI: 10.1029/2007JB005455.

Tortopidis, S., and Shallcross, D.C. *Carbon Dioxide Foam Flood Studies Under Australian Reservoir Conditions*, Presented at the SPE Asia Pacific Oil & Gas Conference, Melbourne, Australia, 7-10. November, **1994**. Paper SPE 28811.

Tsau, J.S., and Grigg, R.B. *Assessment of Foam Properties and Effectiveness in Mobility Reduction for CO_2-foam Floods*, Presented at the SPE International Symposium on Oilfield Chemistry, Houston, Texas, 18-21. February, **1997**, Paper SPE 37221.

Tsau, J.S., and Heller, J.P. *Evaluation of Surfactants for CO_2-Foam Mobility Control*, Presented at the 1992 SPE Permian Basin Oil and Gas Conference, Midland, Texas, 18-20. March, **1992**. Paper SPE 24013.

Turta, A.T., and Singhal, A.K. *Field Foam Applications in Enhanced Oil Recovery Projects: Screening and Design Aspects*, Presented at the SPE International Oil and Gas Conference and Exhibition, Beijing, China, 2-6. November, **1998**. Paper SPE 48895.

U.S. Energy Information Administration (EIA). *International Energy Outlook 2013*, Washington, D.C., United States, July, **2013.** Report is available at www.eia.gov.

Ülker, B., Alkan, H., and Pusch, G. *Implications of the Phase-Solubility Behaviour on the Performance Predictions of the CO_2 Trapping in Depleted Gas Reservoir and Aquifers*, Presented at the 69th EAGE Conference and Exhibition, **2007**, Paper SPE 107189.

Vikingstad, A.K. *Static and Dynamic Studies of Foam and Foam-Oil Interactions*, PhD dissertation, University of Bergen, **2006**.

Vikingstad, A.K., and Aarra, M.G. *Comparing the Static and Dynamic Foam Properties of a Fluorinated and an Alpha Olefin Sulfonate Surfactant*, JPSE., Vol 65, **2009**, pp.105-111.

Vikingstad, A.K., Aarra, M.G., and Skauge, A. *Effect of Surfactant Structure on Foam-Oil Interactions Comparing Fluorinated Surfactant and Alpha Olefin Sulfonate in Static Foam Tests*, Colloids and Surfaces A: Phys. Chem. Eng. Aspects, 279, **2006**, pp. 105-112.

Wang, G.C. *A Laboratory Study of CO_2-Foam Properties and Displacement Mechanisms*, Presented at the SPE/DOE Fourth Symposium on Enhanced Oil Recovery, Tulsa, Oklahoma, 15-18. April, **1984**. Paper SPE/DOE 12645.

Wang, D., Hou, Q., Luo., Y., Zhu, Y., and Fans, H. *Feasibility Studies of CO_2 Foam Flooding EOR Technique after Polymer Flooding for Daqing Reservoirs*, Journal of Dispersion Science and Technology, DOI: 10.1080/01932691.2014.880846, **2014.**

Wasan, D.T., Koczo, K., and Nikolov, A.D. *Mechanisms of Aqueous Foam Stability and Antifoaming Action With and Without Oil*, in Foams: Fundamentals and Application in the Petroleum Industry (ed. Schramm, L.L.), American Chemical Society, Washington DC, **1994**, pp. 47-114 (Chapter 2).

Wassmuth, F., Schramm, L.L., Mannhardt, K., and Hodgins, L., *Scale-Up Evaluations and Simulations of Mobility Control Foams for Improved Oil Recovery*, in Surfactants: Fundamentals and Application in the Petroleum Industry (ed. Schramm, L.L.), Cambridge University Press, United Kingdom, **2000**, pp. 251-294 (Chapter 7).

Weaire, D., and Hutzler, S. *The Physics of Foams*, Clarendon press, Oxford, **1999**.

Wellington, S.L., and Vinegar, H.J. *CT Studies of Surfactant-Induced CO_2 Mobility Control*, Paper Presented at the 60th Annual Technical Conference and Exhibition of SPE, Las Vegas, Nevada, 22-25. September, **1985**. Paper SPE 14393.

Wellman, T.P., Grigg, R.B., McPherson, B.J., Svec, R.K., and Lichtner, P.C. *Evaluation of CO_2-Brine-Reservoir Rock Interaction with Laboratory Flow Tests and Reactive Transport Modeling*, Presented at the SPE International Symposium on Oilfield Chemistry, Houston, Texas, 5-7. February, **2003**. Paper SPE 80228.

Xing, D., Wei, B., McLendon, W., Enick, R., McNulty, S., Trickett, K., Mohamed, A., Cummings, S., Eastoe, J., Rogers, S., Crandall, D., Tennant, B., McLendon, T., Romanov, V., and Soong, Y. *CO_2-Soluble, Nonionic, Water-Soluble Surfactants That Stabilize CO_2-in-Brine Foams*, Presented at the SPE Improved Oil Recovery Symposium, Tulsa, Oklahoma, 24-28. April, **2010**. Paper SPE 129907.

Yaghoobi, H., and Heller, J.P. *Effect of Capillary Contact on CO_2-foam Mobility in Heterogeneous Core Samples*, Presented at the 1996 Permian Basin Oil and Gas Recovery Conference, Midland, U.S.A., 27−29. March, **1996**; Paper SPE 35169.

Yan, W., Zhao, G-Y., Chen, G-J., and Guo, T-M. *Interfacial Tension of (Methane + Nitrogen) + Water and (Carbon Dioxide + Nitrogen) + Water Systems*, J. Chem. Eng. Data, 46, **2001**, pp. 1544-1548.

Yang, C., and Gu, Y. *Accelerated Mass Transfer of CO2 in Reservoir Brine Due to Density-Driven Natural Convection at High Pressures and Elevated Temperatures*, Ind. Eng. Chem. Res., 45, 8, **2006**, pp. 2430-2436.

Yang, S.H., and Reed, R.L. *Mobility Control Using CO_2-Foams*, Presented at the 64th Annual Technical Conference and Exhibition of SPE, San Antonio, Texas, 8-11. October, **1989**. Paper SPE 19689.

Yilmaz, N., Bakhtiyarov, A.S., and Ibragimov, R.N. *Experimental Investigation of Newtonian and Non-Newtonian Fluid Flows in Porous Media*, Mechanics Research Communications, 39, **2009**, pp. 638-641.

Yin, G., Grigg, R.B., and Svec, Y. *Oil Recovery and Surfactant Adsorption During CO_2-Foam Flooding*, Presented at the 2009 Offshore Technology Conference, Houston, Texas, 4-7. May, **2009**. Paper OTC 19787.

Zhdanov, S.A., Amiyan, A.V., Surguchev, L.M., Castanier, L.M., and Hanssen J.E. *Application of Foam for Gas and Water Shut-off: Review of Field Experience*, Presented at the SPE European Petroleum Conference, Milan, Italy, 22-24. October, **1996**. Paper SPE 36914.

Zhang, Z.F., Freedman, V.L., and Zhong, L. *Foam Transport in Porous Media – A Review*, Report prepared for the U.S. Department of Energy, **2009**.

Zhang, Y., and Morrow, N.R. *Comparison of Secondary and Tertiary Recovery With Change in Injection Brine Composition for Crude Oil/Sandstone Combinations*, Presented at the 2006 SPE/DOE Symposium on Improved Oil Recovery, Tulsa, Oklahoma, 22-26. April, **2006**. Paper SPE 99757.

Zhou, N., Matsumoto, T., Hosokawa, T., and Suekane, T. *Pore-Scale Visualization of Gas Trapping in Porous Media by X-ray CT Scanning*, Flow Measurement and Instrumentation, 21, **2010,** pp. 262-267.

Zhou, N., Suekane, T., Hosokawa, T., Nguyen, H.T., and Wang, Q.W. *Capillary Trapping of Carbon Dioxide in Geological Storage*, Proceedings of the 2011 International Workshop on Heat Transfer Advances for Energy Conservation and Pollution Control, Xi'an, China, 17-20. October, **2011.**

Zhu, T., Ogbe, D.O., and Khataniar, S. *Improving the Foam Performance for Mobility Control and Improved Sweep Efficiency in Gas Flooding*, Industrial & Engineering Chemistry Research, 43, 15, **2004**, pp. 4413-4421.

Zhu, T., Strycker, A., Raible, C.J., and Vineyard, K. *Foams for Mobility Control and Improved Sweep Efficiency in Gas Flood*, Presented at the 1998 SPE/DOE Improved Oil Recovery Symposium, Tulsa, Oklahoma, 19-22. April, **1998**. Paper SPE 39680.

Zeilinger, S.C., Wang, M., Kibodeaux, K.R., and Rossen, W.R. *Improved Prediction of Foam Diversion in Matrix Acidization*, Presented at the Production Operations Symposium, Oklahoma City, 2-4. April, **1995**. Paper SPE 29529

Zitha, P.L.J., Nguyen, Q., and Currie, P.K. *Effect of Flow Velocity and Rock Layering on Foam Flow: an X-ray Computed Tomography Study*, Presented at the SPE Asia Pacific Oil and Gas Conference and Exhibition, Jakarta, Indonesia, 15-17. April, **2003**. Paper SPE 80530.

Zuo, L., Krevor, S., Falta, R.W., and Benson, S. *An Experimental Study of CO_2 Exsolution and Relative Permeability Measurements during CO_2 Saturated Water Depressurization*, Transport in Porous Media, 91, **2012**, pp. 459-479.